Technical Report RSC-56

(NASA-CR-14[illegible]) [illegible] MICROWAVE [illegible] N74-34773
[illegible] MOISTURE
[illegible]
(Texas A&M Univ.) [illegible] $14.[illegible] [illegible]
[illegible] G3/13 [illegible]

DUAL FREQUENCY MICROWAVE RADIOMETER MEASUREMENTS OF SOIL MOISTURE FOR BARE AND VEGETATED ROUGH SURFACES

By

SIU LIM LEE

August 1974

Supported by

National Aeronautics and Space Administration

Grant NSG 44-001-001 and Contract NAS 9-13904

TEXAS A&M UNIVERSITY
REMOTE SENSING CENTER
COLLEGE STATION, TEXAS

TECHNICAL REPORT RSC-56

DUAL FREQUENCY MICROWAVE RADIOMETER MEASUREMENTS OF SOIL MOISTURE FOR BARE AND VEGETATED ROUGH SURFACES

By

SIU LIM LEE

August 1974

Supported by

National Aeronautics and Space Administration

Grant NSG 44-001-001 and Contract NAS 9-13904

ABSTRACT

A series of controlled ground-based passive microwave radiometric measurements on soil moisture were conducted to determine the effects of terrain surface roughness and vegetation on microwave emission. A review was given to some apparent temperature models for bare and vegetated rough surfaces and theoretical predictions were made using Sibley's apparent temperature models for bare and vegetated smooth surfaces. The theoretical predictions were compared with the experimental results and with some recent airborne radiometric measurements on soil moisture. The relationship of soil moisture to the permittivity for the soil of this experiment was obtained in the laboratory.

The passive microwave radiometer used for this experiment was a dual frequency radiometer, 1.41356 GHz and 10.69 GHz, mounted on a flat bed truck with a 75-foot articulated arm serving as the sensor platform. Measurements were taken for angles between 0° and 50°, generally in 10° increments, from an altitude of about fifty feet.

Three distinct surface roughnesses were created to study the effects of surface roughness on apparent temperature measurements. With the roughness of the surfaces undisturbed, oats were later densely and uniformly planted. Vegetation effects were examined from comparisons between

vegetated and bare field measurements. Observations supporting the effects of surface roughness and vegetation were obtained through extensive ground truth.

The effects of surface roughness and vegetation were found to be highly significant and played decisive roles in regard to the capability of the passive microwave radiometer to detect soil moisture. The 1.4 GHz radiometer was less affected by the surface roughness and vegetation than the 10.6 GHz radiometer, which under vegetated conditions was incapable of detecting soil moisture. It was concluded that lower frequency band passive microwave radiometers are capable of detecting the soil moisture of bare and vegetated rough surfaces remotely.

Comparisons between the theoretical predictions and the experimental results indicated discrepancies in magnitude. Inadequacy in the bare surface theoretical model and the uncertainty concerning the absolute correctness of the permittivity of the soil measured were apparently the causes of these discrepancies. The vegetation model appeared to be a valid model, for its predictions were experimentally verified.

The concept of skin depth and the corresponding equivalent soil moisture were studied. The equivalent soil moisture was believed to be the appropriate soil moisture parameter to correlate apparent temperature with soil

moisture. Data analysis did indicate that it was a more appropriate soil moisture parameter than two other customarily used soil moisture parameters (0-2 cm average and 0-18 cm average).

ACKNOWLEDGEMENTS

Sincere gratitude is due Dr. John W. Rouse, Jr. for his continued support and helpful advice during the course of the study.

Special thanks are extended to my many colleagues of the Remote Sensing Center, Texas A & M University, particularly to Mr. Richard Newton, Mr. Jack Hill, and Mr. Parviz Babai for their helpful advice and encouragement.

Sincere appreciation is due personnel of both the NASA and Lockheed Electronics Company who worked in this experiment, especially to Dr. Jack F. Paris for his effort in data reduction and Mr. Andy Giles for his helpful assistance in the field data acquisition.

I also wish to thank Mr. Ralph E. Miller of Texas A & M University Farm Service for his service in field preparations for this study.

The financial support of this research was provided by the National Aeronautics and Space Administration under Grant NSG 44-001-001 and Contract NAS 9-13904.

TABLE OF CONTENTS

LIST OF TABLES

LIST OF FIGURES

CHAPTER I

INTRODUCTION

Remote Sensing of Soil Moisture

Soil moisture data are significant and important for agriculture, hydrology, runoff and flood forecasting, rangeland management and farming. Instruments and techniques are available for measuring soil moisture content by contact means, however, when investigating on a large land area or some remote inaccessible areas, contact methods become impractical. The techniques of remote sensing are needed to gather such information with speed and an acceptable degree of accuracy. Remote sensors that have been employed in the study of possible detection of soil moisture content include cameras, thermal infrared sensors, and microwave sensors.

Aerial photography has been a useful reconnaissance tool for hydrologic studies. Reflection at photographic wavelengths (0.4 - 0.9 nm) is sensitive to differences in the surface characteristics at the air-soil interface, and tonal contrasts can be used to infer soil moisture

conditions [1].

Thermal infrared sensors measure emittance, i.e. the self emission, of the objects. The thermal infrared region extends from approximately 4nm to 24nm. Measurements made at the regions 3 to 5 nm and 8 to 14 nm indicated the detection of variation in soil moisture is possible [2], [3].

Despite their potential as soil moisture detection remote sensors, the photographic and thermal infrared sensors have the main drawbacks that they can reveal only the very surface soil moisture information and they are inoperable in bad weather. Microwave sensors have the potential of yielding information regarding the interior characteristics of bodies. Furthermore, their performance is almost independent of weather conditions and time of day.

Microwave sensors are of two basic types: passive and active. The frequency range over which these two types of sensors operate extends from 0.1 GHz to beyond 100 GHz. Experimental and theoretical studies have confirmed that there is a high degree of correlation between the electrical properties of soil and soil moisture. This suggests that the microwave remote sensors could be applicable in the determination of soil moisture content. In 1968, Kennedy [4] and Edgerton [5] began the investi-

gation of passive microwave sensors for determination of soil moisture content. Numerous theoretical studies (Peake [6], [7], Stogryn [8], Fung et al. [9] and Johnson [10]) and experimental studies (Schmugge et al. [11], Richerson [12], Jean [13] and Kroll [14])have been conducted to measure soil moisture with microwave radiometers. The radiometric results indicated that under some conditions the soil moisture content can be determined quite accurately, and the passive microwave radiometer has high potnetial in this application. Unlike the infrared and photographic techniques which provide only surface information, the microwave radiometer can detect moisture content at considerable depth into the soil.

Another microwave remote sensor for soil moisture content detection is radar, the active microwave sensor. The application of radar on the detection of soil moisture has received less attention than the microwave radiometer, yet it has proved to be a high potential candidate. Rouse [15] has discussed the possibility of using radar scatterometers to measure soil moisture content. Moore et al. [16], Waite et al. [17], [18], and Davis et al. [19] have shown experimentally the feasibility of using radar for the determination of soil moisture content.

Past History and Inadequacies of Soil Moisture Detection by Passive Microwave Radiometer

In 1965 Kennedy et al. [20], [21] initiated a series of radiometric studies of snow and soil, from which the possible application of microwave radiometer for the detection of soil moisture content was stimulated. The first soil moisture measurements on natural terrains by microwave radiometer was conducted by Kennedy and Edgerton [22], and by Edgerton et al. [23]. The measurements were ground based. On May 21, 1968 NASA conducted a series of aircraft flights equipped with microwave radiometers over southern California for the remote determination of soil moisture [24]. The microwave radiometers (MR62/MR64) were operated at 9.3, 15.8, 22.2, and 34.0 GHz frequencies. From the results it was concluded that a moist layer more than 0.1 inch below a dry surface layer could not be detected by microwave radiometers at one to two cm wavelengths. However, using a ten cm wavelength (approximately 3 GHz) microwave radiometer, Basharinov and Skutko [25] demonstrated that soil moisture content could be inferred to within a 3% moisture content value from the radiometric data.

More recent investigators include those of Richerson [12], Jean [13], Poe et al. [26], Schmugge et al. [11],

Kroll [14] and Sibley [27]. Richerson investigated the relationship of the moisture content of smooth surface to its radiative properties and used this relationship to study the expected performance of a tower-based microwave radiometer in monitoring soil moisture. Jean reported the results of airborne radiometric measurements at 21.13, 11.15, 6.01, and 2.81 cm, 2.69, 4.99, and 10.69 GHz. Their results were generally encouraging, but the amount of data were very limited.

Poe et al. reported on a series of microwave radiometric measurements at wavelengths 0.81, 2.2, 6.0 and 21.4 cm on bare soil with a variety of moisture conditions. Their measurements compared favorably with the computed values obtained from the theory of vertically structured media [26] for moderately moist to saturated soil conditions at all wavelengths. It was concluded that a semi-quantitative understanding of the microwave emission properties of the soil has been reached.

Schmuggee et al. also reported a series of aircraft flights over bare land using microwave radiometers in the wavelength range 0.8 cm to 21 cm. The results indicated that it is possible to monitor soil moisture variations with airborne microwave radiometers, and that the emission measured is a function of the radiometer wavelength and the distribution of soil moisture. It was shown that the

longer wavelengths were more sensitive to the variation of soil moisture. Kroll analyzed airborne microwave radiometer measurements over selected sites in Chickasha, Oklahoma and Weslaco, Texas. His analysis shows that the airborne microwave radiometric monitoring of soil moisture is feasible, but noted that continued research, along with development of more reliable techniques, should be conducted.

Sibley has investigated the effects of vegetation on the detection of soil moisture content. He has developed theoretical models for the apparent temperature of vegetated terrains. However, very little experimental data were available to substantiate his models.

Examining the past investigations and experiences, a summary of the past inadequacies can be reached. It appears that the problem lies in three areas. The first area is the need for a fuller understanding of the radiative and scattering characteristics of natural surfaces, and the relation between the moisture content and the radiative characteristics of natural surfaces. The theoretical models of the apparent temperature of natural surfaces need to take into account the possible effect of vegetation, surface roughness conditions, skin depth of the soil, contribution from the atmosphere and the antenna pattern of the radiometer.

The second area in the inadequacies lies in the experimental measurement programs. In the past and at the present still, the acquisition of meaningful data has been difficult. This appears to be caused by two factors: the lack of a well controlled and cooperated experiment program, and the inadequate techniques that are available in handling and interpreting the tremendous amount of data collected. In the case of an airborne mission conducted conjunctively with a ground-based study, a well controlled and cooperative program for the overall experiment is especially important so that the airborne data and ground data are correlated. In the past experimental measurement programs, measurements have been made at various frequencies. As emission is a function of the radiometer frequency, investigations on the "optimum" frequency for monitoring soil moisture is necessary.

The third factor which has reduced the effectiveness of the passive microwave radiometer in monitoring soil moisture content has been the disjointed development of the experimental measurements and the theoretical studies. A conjunctive effort is needed to made the passive microwave radiometer a more effective remote sensing tool in the monitoring of the soil moisture. This work reports such a conjunctive effort of investigation.

Objective

The dependence of microwave emissions upon soil moisture content is recognized and has been attributed to an increase in the dielectric constant of soil with increasing moisture content. However, this emission process is affected by the surface roughness and the vegetation coverage. These and many other parameters might play important roles in the possible determination of soil moisture content by passive microwave radiometers.

The objective of this study is to examine empirically the effect of soil surface roughness and vegetation on the measurement of soil moisture by passive microwave radiometers. The experimental results are compared with the results of the theoretical models and previous work conducted by other investigators. From this experiment, an attempt is made to establish the actual potential of the passive microwave radiometer for monitoring the moisture content of natural terrains.

Scope of Report

Models of apparent temperature of natural terrain incorporating surface roughness and vegetation effects have been developed by Peake [6], Peake et al. [7], Johnson [10] and Sibley [27]. This study reports on a ground based

experiment of soil moisture detection for bare and vegetated rough surfaces by a dual frequency microwave radiometer. The results of the experiment serve to evaluate the existing theoretical models.

Chapter II discusses the basics of passive microwave radiometry and the dual frequency passive microwave radiometer system that was used in this investigation.

Chapter III begins with a background study on the theoretical modeling of microwave emission of natural terrain, considering the effects of surface roughness and vegetation. A review is given of the apparent temperature models for bare and vegetated terrains. The surface roughness conditions considered are smooth, medium rough, and rough surfaces. The study of the vegetation effect is concerned with uniform vegetation coverage on smooth and rough surfaces.

Chapter IV describes the laboratory measurements of dielectric constants of the soil used in this investigation. A report is also given on the ground-based experiment program.

Chapter V is concerned with the analysis of the experimental results and comparison with the theoretical solutions. The effects of surface roughness and vegetation on the apparent temperature measurements are observed. A review is also given to some recent research efforts.

Chapter VI gives conclusions and recommendations for further study.

CHAPTER II

PASSIVE MICROWAVE RADIOMETER

Microwave Thermal Emission

Electromagnetic radiation is emitted by all natural objects above absolute-zero temperature. This electromagnetic radiation covers a wide range of frequencies and polarizations, and both the total radiated power and the power in any spectral band increases with the temperature of the emitting object. Thermal radiation is described for an ideal radiator or "blackbody" by Planck's radiation law [28]:

$$K = \frac{hf^3}{c^2}\left[\frac{1}{\exp(hf/kT)-1}\right] \qquad \text{(II-1)}$$

where:

h = Planck's constant = 6.626×10^{-34} joule-seconds

c = speed of light = 3×10^{8} meters/second

k = Boltzmann's constant = 1.38×10^{-23} joules/°K

f = frequency of radiation

T = absolute temperature

At microwave frequencies, Planck's blackbody radiation law can be quantitatively approximated by the Rayleigh-Jeans approximation. This approximation holds in

the frequency range where

$$hf << kT \tag{II-2}$$

The approximation is given as

$$K \approx \frac{kf^2T}{c^2} = \frac{kT}{\lambda^2} \quad j/m^2 \tag{II-3}$$

where λ is the wavelength of the radiation. Considering the power density within a small frequency Δf, the radiated power can be approximated by

$$P = \frac{kT\Delta f}{\lambda^2} \tag{II-4}$$

This version of the Rayleigh-Jeans Approximation relates directly between the temperature and radiated power of a blackbody. The measure of the power of the received radiated energy is generally related to the temperature scale. The power received at the radiometer antenna is given by [29]

$$P_{ant} = \frac{kT}{\lambda^2}\int df \int A(\theta,\phi)\, d\Omega \quad \text{watts} \tag{II-5}$$

where $\int df = B$ = radiometric bandwidth in Hz

$\int A(\theta,\phi)d\Omega = \lambda^2$ = the antenna response function

If an ideal antenna is matched to a load at the same temperature T_{ant}, and a blackbody radiating source is assumed, then (II-5) can be written as

$$P_{ant} = k T_{ant} B \quad \text{watts} \tag{II-6}$$

If the radiating body is not a blackbody, as is the case in the real world, the radiance will be reduced by a factor ε, the emission coefficient. Because of (II-3) the effect of emission coefficient on radiance is comparable to that of temperature. This leads to the concept of apparent radiation temperature, or simply apparent temperature (T_a):

$$T_a = \varepsilon T \tag{II-7}$$

which would cause a blackbody to yield the same radiance as that of the real world radiating body at temperature T. Emissivity, which is defined as

$$\text{emissivity} = \frac{\text{Power emitted at a particular polarization by a unit area of surface into an element of solid angle } d\Omega_o \text{ in the direction } \Theta_o, \phi_o.}{\text{Power emitted at the same polarization by a unit area of blackbody at the same temperature into the same element of solid angle in the same direction}}$$

is the correction factor and the key to the understanding of the radiometric data from natural terrain. It is a function of the permittivity, surface roughness, and vegetation cover of the terrain, and of the polarization, viewing angle, and frequency of the radiometer sensor. For real world radiometric measurements, the radiated

power received at the antenna is

$$P_{ant} = kB\epsilon T_{ant} = kBT_a \quad \text{watts} \qquad \text{(II-8)}$$

where T_a = apparent antenna temperature induced by the source in degree Kelvin (°k)

Apparent Temperature

As discussed above, apparent temperature T_a as defined by (II-7) is a measure of the radiance of the real world radiator relative to a blackbody radiation. Solving (II-8) for the apparent antenna temperature, T_a, the relationship between the apparent temperature of the source in terms of its radiated power is

$$T_a = \frac{P_a}{kB} \quad \text{degree k} \qquad \text{(II-9)}$$

Considering that the target is being observed from a distance, the apparent temperature induced on the antenna would be a sum of several contributions. The most significant contributors to the apparent temperature at a particular polarization are: 1) the thermal radiation emitted by the surface, 2) the scattered diffuse radiation of the atmosphere between the antenna and the target surface, 3) the scattered radiation from quasipoint sources such as the sun, and 4) the reflected sky temperature [6], [7], [30].

Peake [6] developed a model for apparent surface temperature expressing the emissivity of a smooth surface in terms of its scattering coefficients, which he empirically derived. His expression for the apparent temperature, which is the sum of the above four major contributors, may be expressed generally as

$$T_{ai}(\theta) = T_{ground} + T_{atmosphere} + T_{quasi\text{-}point\ source} + T_{reflected\ sky\ radiation}$$

It was found that the contribution from the quasi-point source, mostly from the sun, is negligible and therefore, can usually be neglected. The contribution of the reflected sky temperature to the total apparent temperature is in the vicinity of one to two degrees, therefore, generally it can be neglected also.

Passive Microwave Radiometer System and Its Fundamentals

The microwave radiometer is essentially a high gain, low noise receiver which detects thermal radiation of objects. It is capable of detecting very small radiation power level (-90 to -100 dBm) of most natural bodies [31], [32].

The passive microwave radiometer system is composed of four basic subsystems. The four basic subsystems are (1) the spectrum surveillance subsystems, (2) the

RF subsystem, (3) the receiver subsystem, and (4) the data processing subsystem. The spectrum surveillance subsystem includes the antenna, mixers, filters, and spectrum analyzer. The RF subsystem consists of a modulator head of specific frequency band and the reference noise generators (RNG). The RF head performs RF switching between the antenna and the RNG, filtering, frequency conversion, and IF preamplification. The receiver subsystem is the key of the radiometer system. It consists of a broadband IF input, square law detector, low-noise and low-offset dc amplifier, Y-factor measurement circuitry, timing and control circuitry for Dicke switch operation and synchronism, alarm and band selector logic, and the data multiplexer. The essential part of the receiver subsystem is the Y-factor measurement circuitry. The Y-factor measure circuitry is basically a digital measurement technique (similar in operation to the AD converter) that enables the radiometer system to act as a form of a gain modulated radiometer. A detailed discussion of the Y-factor measure circuitry can be found in reference [32]. Finally, the data processing subsystem consists of the digital computer units for apparent temperature conversion, data interfacing and recording.

There are two basic types of microwave radiometers: the unmodulated type, and the modulated type (or "Dicke"

type). These two types of microwave radiometers are shown in Figure (II-1(a) and (b)) [30]. The early microwave radiometers are of the unmodulated type. They have limiting sensitivity caused mainly by internal noise of the amplifier, and the fluctuation of the amplifier gain. Modern microwave radiometers are mostly with "Dicke" type radiometer. In 1946, Dicke [33] developed the "switching radiometer" which reduces the effects of gain fluctuation at a small tradeoff with the analysis time. The "Dicke" type microwave radiometer utilizes a ferrite device which modulates the incoming antenna power against a stable reference source. The ferrite switch, or the "Dicke" switch, is driven by a reference oscillator, alternately connects the output of the antenna port and a reference source to the input of the RF amplifier. A square wave modulated signal is produced for any difference that occurs between the antenna temperature and the temperature of the matched base load. The amplitude of the modulated signal is matched to the corresponding temperature difference. This square wave modulated signal is then represented by a DC voltage proportional to the temperature difference of the apparent antenna temperature and the known reference source.

The absolute accuracy of the radiometric brightness temperature depends on the fineness of the calibration.

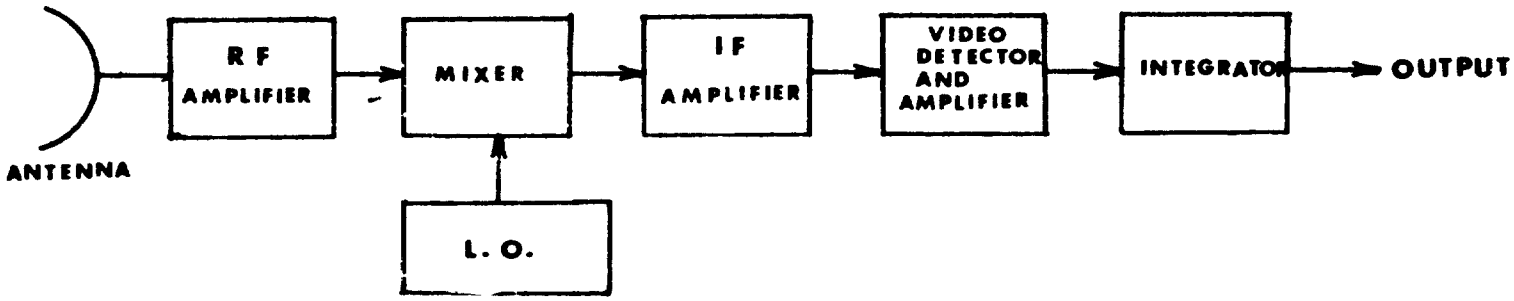

Figure II-1a. The Unmodulated Type Microwave Radiometer.

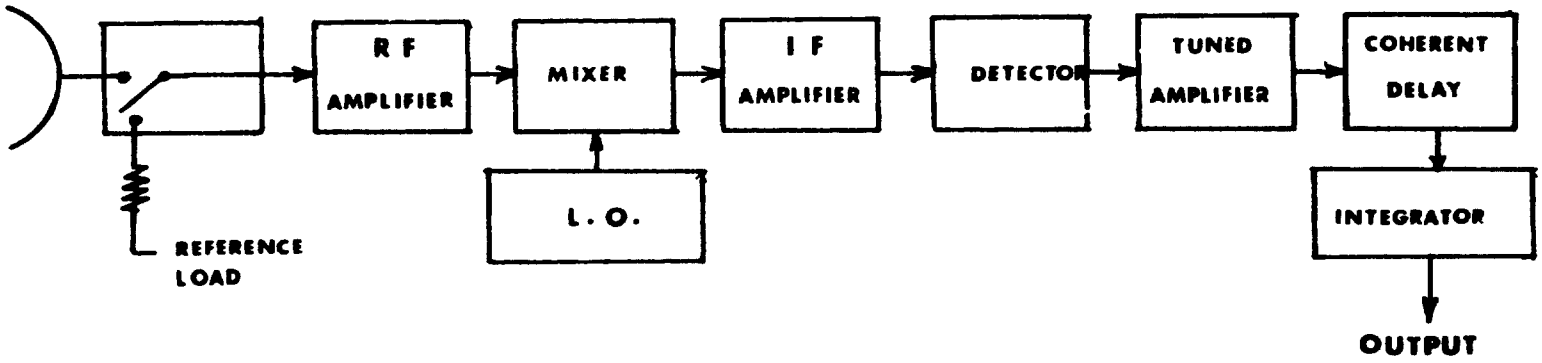

Figure II-1b. The Modulated Type ("Dicke" Type) Microwave Radiometer [30].

The reference noise generators (RNG) are the key of the calibration. Absolute accuracy of the brightness temperature is achieved by minimizing the uncertainties of the RNG thermometric temperatures.

Besides calibration, two other factors play important roles in making valid measurements of the brightness temperature of radiating objects by the microwave radiometer. These two factors are the sensitivity and the stability of the system.

The sensitivity of a radiometer can be described in terms of the equivalent rms noise (T_{rms}) at its inputs:

$$\Delta T = \frac{\sqrt{2}\, T_{op}}{\sqrt{B\tau}} \qquad \text{(II-10)}$$

where $T_{op} = T_a + T_e$

and T_a = equivalent noise of the antenna referred to the receiver input in Kelvins

T_e = equivalent noise of the electronics

B = prediction bandwidth in Hz

τ = postdetection time constant in seconds

To reduce the effect of gain fluctuation and thus improve the stability of the microwave radiometer, the Y-measurement technique was designed. The Y-measurement

technique is a gain modulation technique that automatically changes the gain of the radiometer in synchronism with the switching between the antenna and reference noise generator. The Y-factor is defined as

$$Y = \frac{G_A}{G_R} = \frac{T_e + T_R}{T_e + T_A} \qquad \text{(II-12)}$$

where G_A = system gain when the radiometer is connected to the antenna

G_R = system gain when the radiometer is connected to the reference noise generator

T_e = the equivalent electronics noise temperature of the radiometer system

T_A = the antenna temperature

T_R = the reference temperature with which the T_A is compared

Solving for T_A from (II-12):

$$T_A = \frac{T_R + T_e(1-Y)}{Y} \qquad \text{(II-13)}$$

therefore T_A can be determined by determining Y and is independent of the gain. A linear radiometer with a squarelaw detector will have detector output voltages V_A due to $(T_e + T_A)$ and V_R due to $(T_e + T_R)$. Thus, the Y-factor measurement is a measure of the ratio V_R/V_A. For the microwave radiometer system used in this study,

this is done by attenuating V_R by a factor A until $|V_R A - V_A| \leq E$, where E is determined by the required measurement resolution. Setting the error voltage E to zero, the following is obtained

$$A = \frac{V_A}{V_R} = \frac{T_e + T_A}{T_e + T_R} \qquad \text{(II-14)}$$

The incremental changes in A relative to incremental changes of T_A can be determined by taking the derivative of A with respect to A in (II-14). Therefore

$$\frac{dA}{dT_A} = \frac{1}{T_e + T_R} \qquad \text{(II-15)}$$

$$\text{OR} \qquad \frac{dA}{A} = \frac{1}{T_e + T_A}$$

Features of the Passive Microwave Radiometer of the Experiment

The passive microwave radiometer system used for the field experiment of this study is a dual frequency radiometer built by Airborne Instrument Laboratory (a division of Cutler-Hammer, Deer Park, Long Island, New York) for NASA. The two frequencies of the radiometer system are 1.41356 GHz (21.13 cm, L-band) and 10.69 GHz (2.81 cm, X-band) respectively. This dual frequency microwave radiometer system is one of the most advanced systems now in operation.

The L-band RF and receiver sybsystem are essentially the same as the S-194 radiometer used in the Skylab/EREP

program. There are a number of unique features about this dual frequency microwave radiometer system. These are: (1) it is a mobile system, the radiometer system is mounted on a flat bed truck with a 75-foot articulated arm serving as the sensor platform, Figure (II-2), (II-3), and (II-4); (2) it is a self-sustained system with a 25 kw electrical power generator; (3) this radiometer system employs the Y-measurement techniques which makes it possible for the radiometer output to be essentially independent of the receiver gain fluctuations; (4) it processes a computerized data processing subsystem. The hardware consists of a ruggedized minicomputer, a teletype with paper punch and reader, a magnetic tape unit, a control panel, analog strip chart recorder, and interface units.

The Y-measurement technique employed and the data processing subsystem of this system are the two most significant improvements over other microwave radiometer systems. The radiometric data, in the form of a serial digital data train, is formatted in the receiver and output to the computer. Simultaneously, the data are processed by the computer, then the reduced and formatted data are stored in the seven-track magnetic tapes. This computerized data system allows large amounts of data to be collected in short periods of field work. The data are readily evaluated in the field as to data quality, so that

Figure II-2. The Dual Frequency Passive Microwave Radiometer System in the Field.

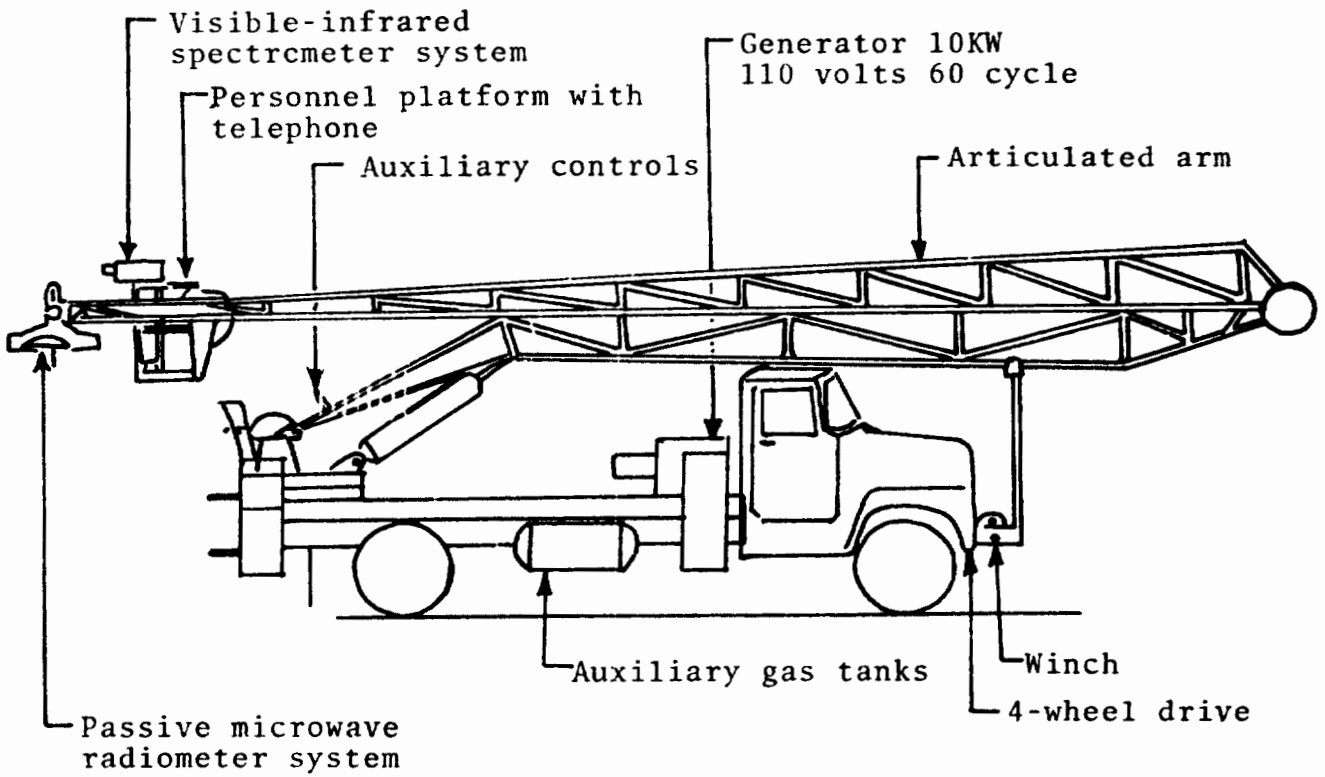

Figure II-3. Truck Mounted Articulated Arm and Sensor Platform [31].

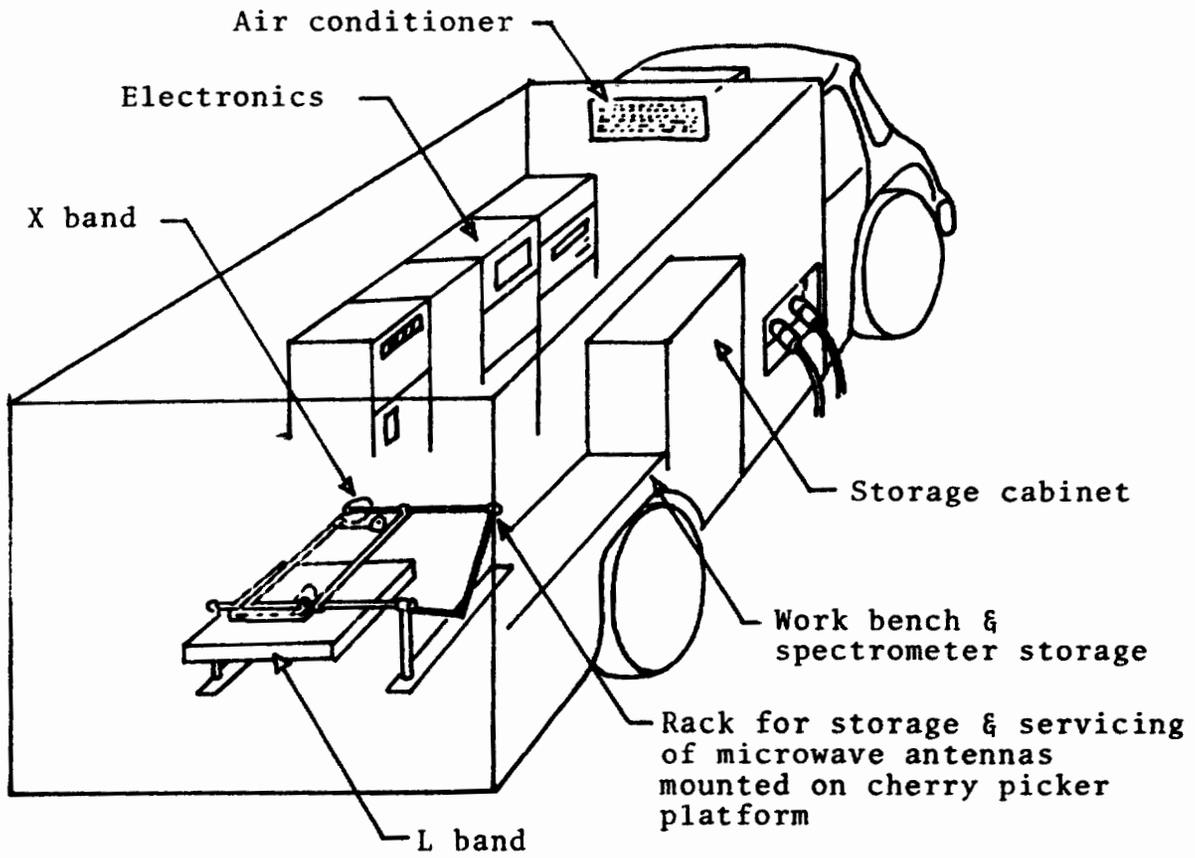

Figure II-4. The Data Van of the Microwave Radiometer System [31].

the acquisition of poor data can be avoided.

A block diagram of this dual frequency radiometer system is illustrated in Figure (II-5). A list of some system parameters are shown on Table (II-1). A parabolic dish shaped antenna is used for the X-band system, and a 64-element dipole phased array is used for the L-band system. These two antennas are shown in Figure (II-6) (a) and (b). Figure (II-6) (a) shows the frontal view of the X and L-band antenna (the L-band antenna is the square shaped one), and the television camera (the box below the X-band antenna) for pinpointing the observing target. Figure (II-6) (b) shows the hind-view of the antennas with their receiver and RF subsystems.

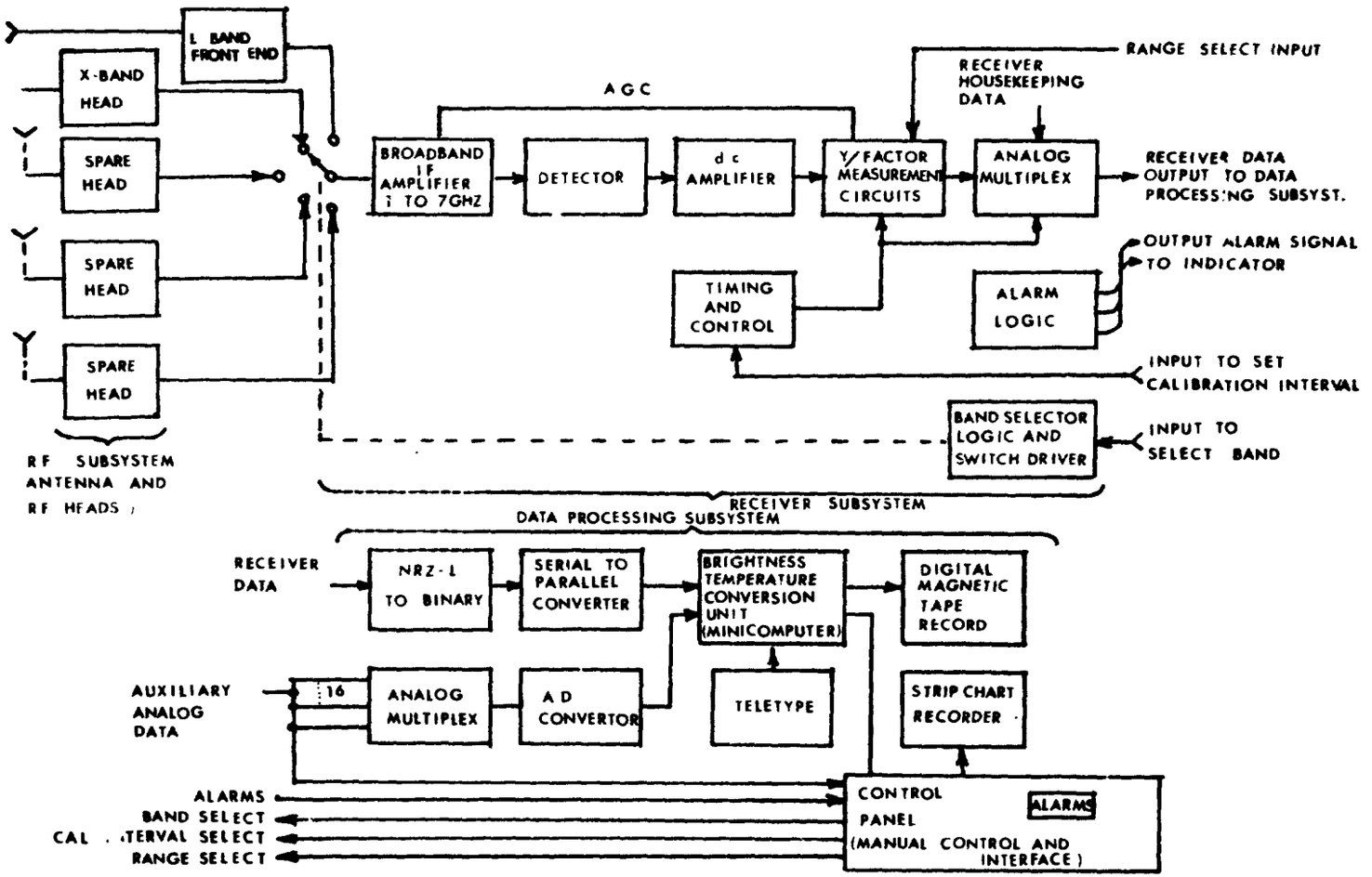

Figure II-5. The Block Diagram of the Dual Frequency Passive Microwave Radiometer Used for This Study, [31].

Table II-1. System Parameters.

Center Frequency (GHz)	Bandwidth (MHz)	Sensitivity* ΔT_{rms} (°K)	Antenna Type	Beamwidth To First Null
1.4135	27	.33	64 element dipole phased array	∿20°
10.69	200	.71	parabolic dish	∿8°

*Calculated using system parameters.

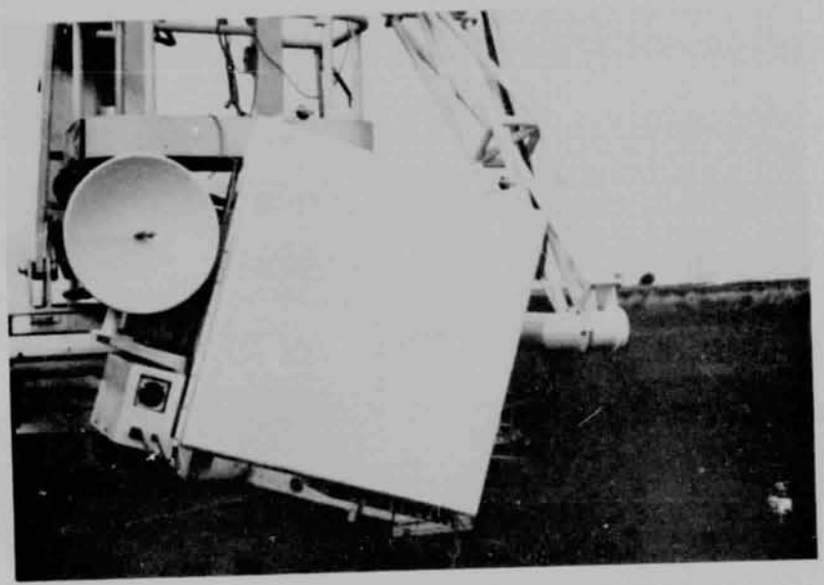

Figure II-a. Frontal-View of the X-band and L-band Antenna, and the Television Camera.

Figure II-b. Hind-view of the Antennas and the RF and Receiver Subsystems.

CHAPTER III

APPARENT TEMPERATURE MODELS

Background

As discussed in Chapter II, it is known that all natural objects above absolute-zero temperature radiate electromagnetic energy. In this real world where all radiating objects are considered non-ideal radiators, this radiated electromagnetic energy can be measured in terms of the apparent temperature of the body. The radiant power and the apparent temperature is approximated by Planck's blackbody radiation law [28]. In the research of remote detection of soil moisture by passive microwave radiometer, the soil moisture conditions are inferred from the apparent temperature measured. To obtain a meaningful interpretation from the apparent temperature information, the emission process of electromagnetic energy originated from within the natural terrain must be carefully studied.

For the purpose of generalization in the examination of electromagnetic radiation from the terrain to the receiving sensor, the natural terrain is assumed to be vegetated in some manner. Basically there are six processes that determine the apparent temperature of the vegetated natural terrain [6], [27]. First a portion of

electromagnetic energy originates from the sub-terrain surface and is transmitted across the boundary toward the sensor. This transmitted field experiences attenuation as it propagates through the vegetation canopy. There is the electromagnetic radiation from the canopy which augments the radiation from the ground. The other processes that contribute to the apparent temperature are the scattered diffused radiation of the atmosphere between the antenna and the terrain surface, the scattered radiation from quasipoint sources such as the sun, and the reflected sky temperature.

The scattering and emission of electromagnetic waves in the course of journeying from the terrain to the sensor are very complicated processes. Completely satisfactory descriptions and explanations on these processes have not yet been achieved. However, progress has been made in identifying and describing some of the factors which affect the scattering and emission process from the natural terrain. Experimental results [6], [14], [12] and theoretical studies [6], [27], [10], have revealed that permittivity values (soil and vegetation), terrain surface roughness, and vegetation coverage are playing important roles in affecting the electromagnetic emission and scattering process. Sibley [27] has made extensive theoretical studies on the effect of vegetation. He has developed

apparent temperature models incooperating with the vegetation and surface roughness effects for the natural terrains. He has shown that vegetation has a masking effect on the soil moisture dependency. Figure III-1, Figure III-2, and Figure III-3 show some of the key theoretical predictions about vegetation effects according to Sibley. Figure III-1 and Figure III-2 indicate that the sensitivity of apparent temperature to variations in moisture content depend on the vegetation volumetric density, vegetation height, frequency, and incidence angle. Figure III-3 is a plot of the height-density product against measured soil moisture content. As the height-density product increases, the apparent soil moisture that could be measured decreases. As shown from these three figures, Sibley shows that as the density or the height of vegetation increases, the apparent temperature increases and becomes less sensitive to variations of soil moisture. The significance of the contribution of the canopy to the apparent temperature also depends on the frequency of radiation considered, the dependence on soil moisture gradually disappears with the higher frequencies (Figure III-1).

In the remote monitoring of soil moisture of natural terrains, there have not been adequate controlled experimental data to test the validity of the theoretical models

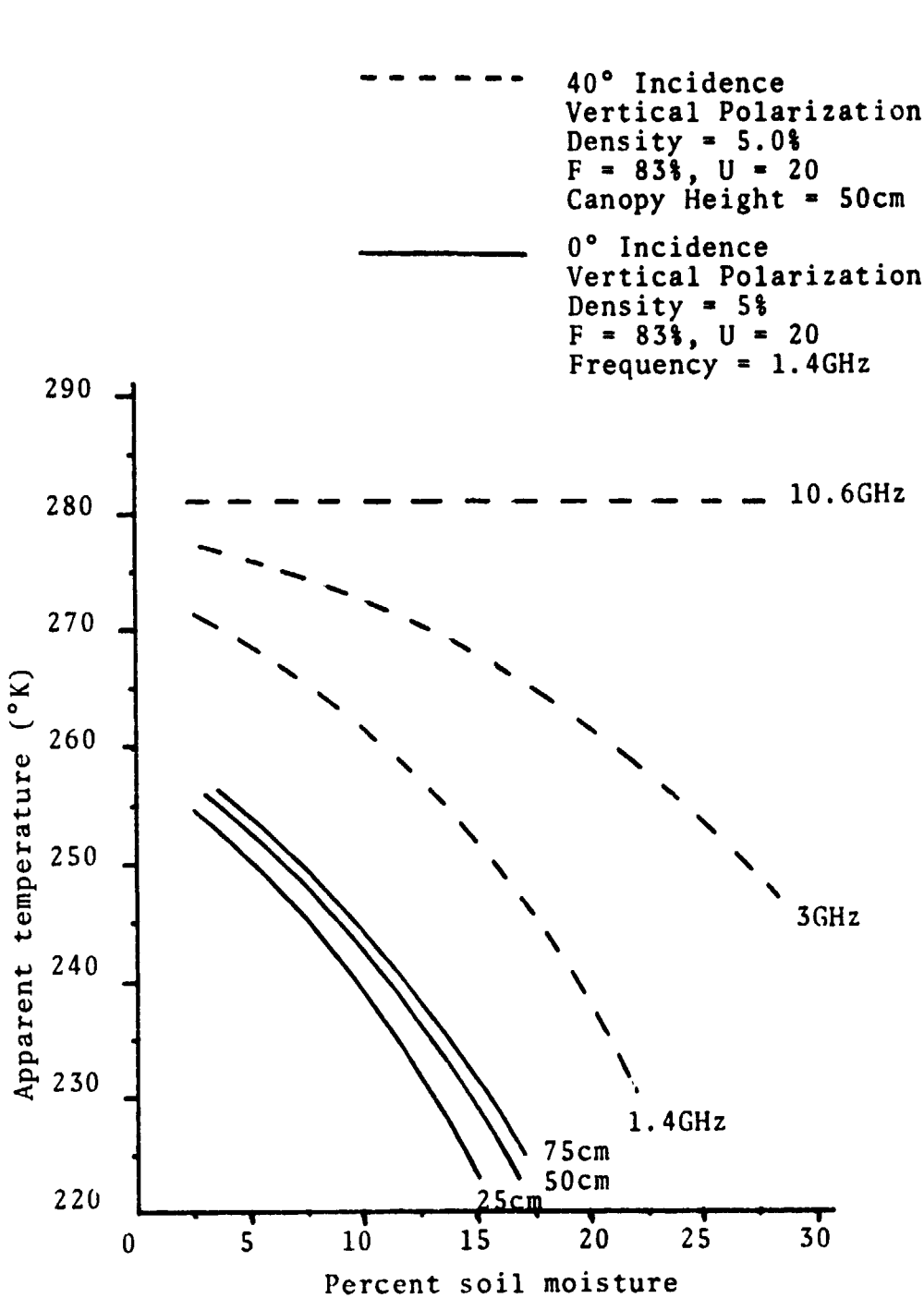

Figure III-1. Calculated Apparent Temperature at Two Incidence Angles of a Uniformly Vegetated Smooth Surface for Various Frequencies and Canopy Heights [27].

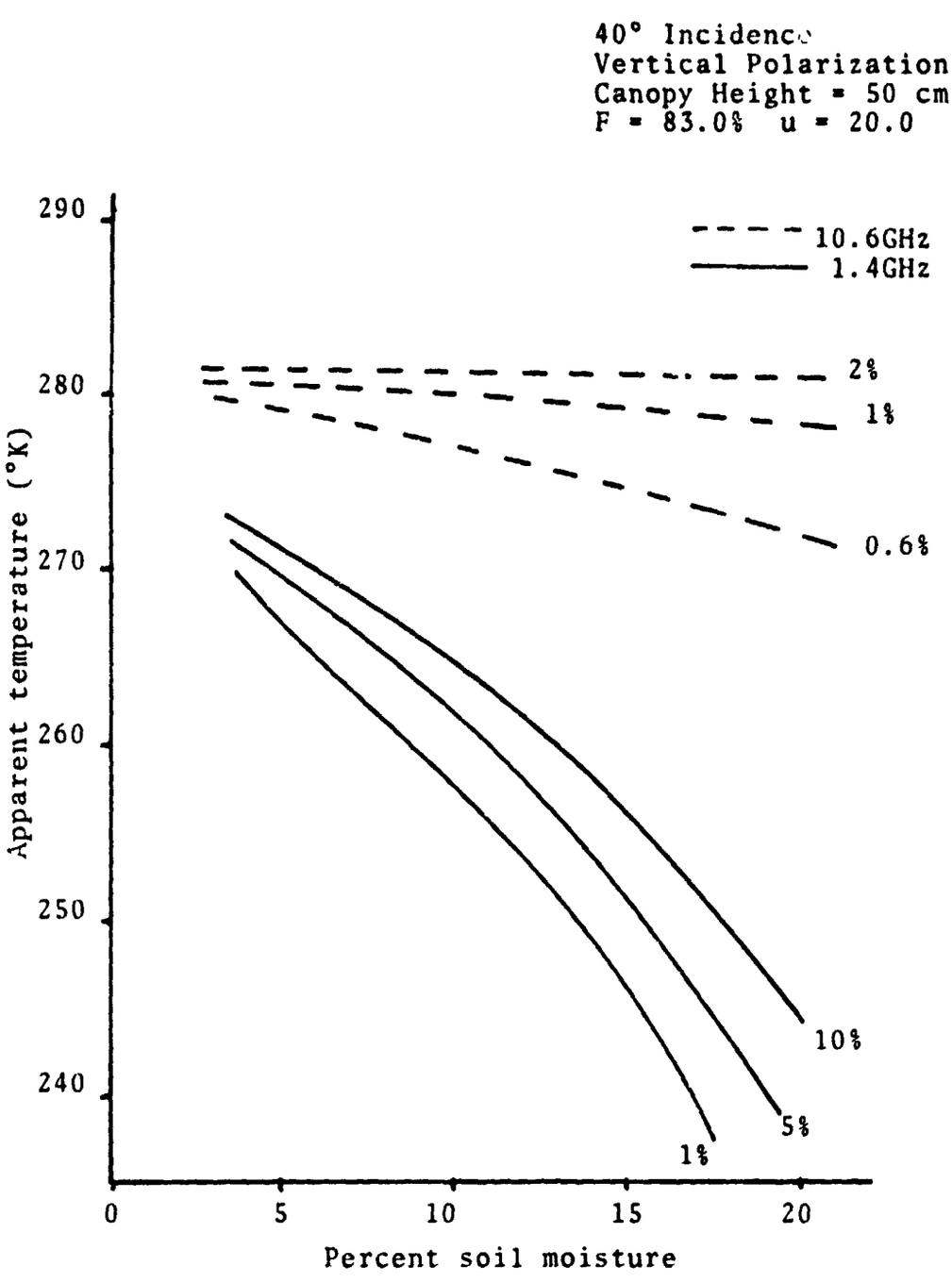

Figure III-2. Apparent Temperatures of Uniformly Vegetated Smooth Surface as a Function of Soil Moisture for Various Densities of Vegetation [27].

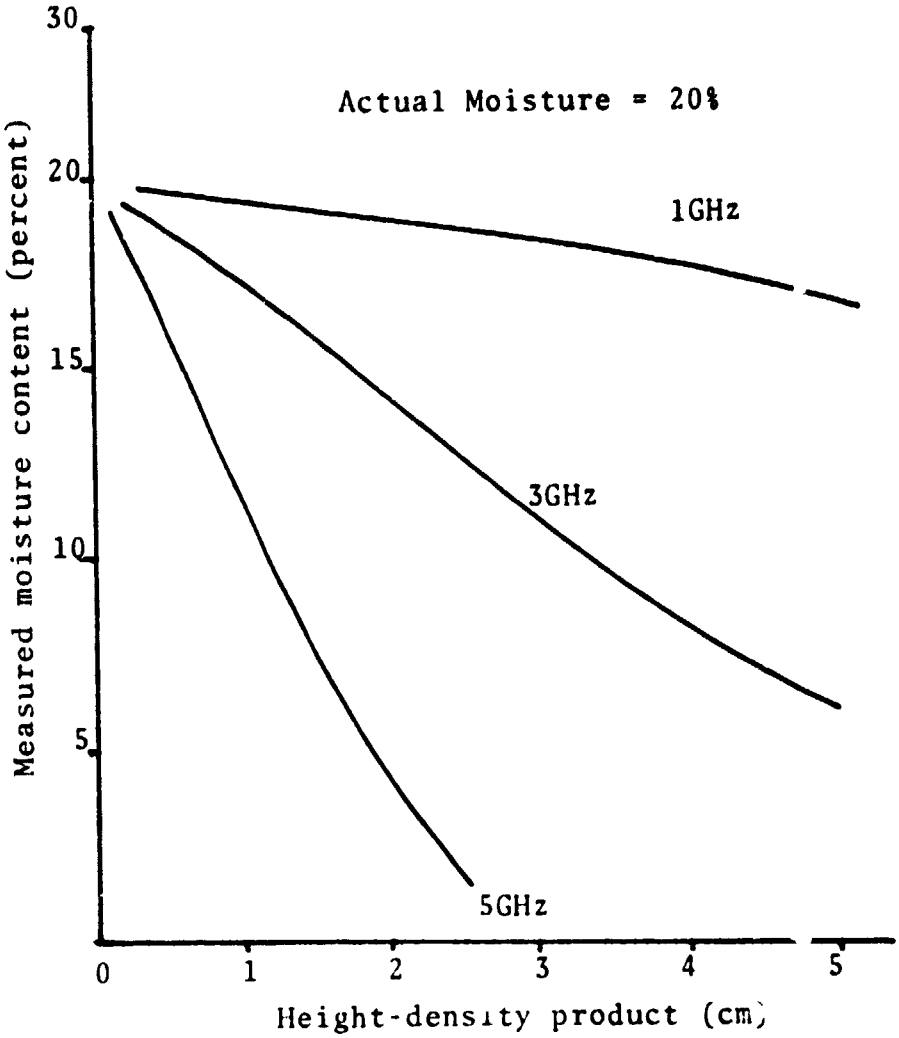

Figure III-3. Moisture Content Determined From Apparent Temperature of Vegetated Soil [27].

developed and to determine the exact natures of the surface roughness and vegetation effects. It is the goal of this study to attempt to determine, with the support of some controlled experimental results, the vegetation effect and surface roughness effect on the feasibility of the passive microwave radiometer to monitor soil moisture content of natural terrains.

The state-of-art of remote monitoring of soil moisture content of natural terrain is still at its infancy, so is the modeling of the emission of natural terrain to determine soil moisture. The most significant theoretical modeling effort has been that by Peake [6], and later by Peake and Chen [7], Stogryn [8], and Johnson [10]. These models are generally too simplistic and too much of an artificial derivation to account for the many parameters that affect the emissive properties of the very complicated terrains. At the same time, these models have made no distinction between bare and vegetated surfaces. Nevertheless, these theoretical studies have made important contributions to the understanding of the problem and the development of better models. Based on Johnson's theoretical developments, Sibley developed an apparent temperature model which would account for the effects of vegetation and surface roughness [27]. Before going into Sibley's model it is appropriate to review the model for

the thermal emission from a rough surface developed by Johnson [10].

Johnson's Model for the Thermal Emission From a Rough Surface

In developing his model for the thermal emission from a rough surface, Johnson [10] attempted to provide a direct visualization of the physical situation. His approach to the thermal radiation problem is that of the Planckian Method [10]. In the approach, it is assumed that the radiation source is an isotropic material in thermal equilibrium and that the internal spectral goniometric irradiance upon the surface is independent of direction and is randomly polarized (Lambertian). However, the emitted radiance for the upper side of the surface is not necessarily Lambertian, although this often is the case. Johnson actually computed the energy generated and subsequently transferred across the rough surface interface. The term known as directional transmittance is used to characterize the surface boundary and to relate the emitted energy to the internal thermal irradiance.

Johnson's model expresses the radiation refracted into direction (θ_s, ϕ_s) in terms of the radiation incident from (θ_i, ϕ_i), and the surface characteristics. The intensities of the refracted radiations are given by the

transmissive scattering coefficients. The surface characteristics are specified by the "surface roughness factor", δ, and the "coefficient of effective area", β. The surface roughness factor is defined as the actual surface area per unit projected area,

$$\delta = \frac{dS}{dA} \qquad \delta \geq 1 \qquad \text{(III-1)}$$

The coefficient of effective area is defined as

$$dA_{eff} = \beta\, dS \quad ; \quad 0 \leq \beta \leq 1 \qquad \text{(III-2)}$$

relating the effective area to the actual surface area. The effective area is that area which is oriented in such a way as to cause specular refraction.

Johnson defined such parameters as local surface normals, local incidence angles, and local polarization to describe the statistical properties of the rough surface. The spatial distribution of local normals, which are defined to completely describe the surface characteristics, is represented by the joint density of its zenith and azimuth angles, $f_{\theta\phi}(\theta_n, \phi_n)$. The surface characteristics are expressed in terms of these localized parameters and the marginal density of the zenith angle of the local normal. The surface roughness factor is expressed as

$$\delta = \frac{1}{\int_0^{\frac{\pi}{2}} f_\theta(\theta_n) \cos\theta_n \, d\theta_n} \qquad \text{(III-3)}$$

and the coefficient of the effective area is

$$\beta = \frac{f_n(\theta_n)}{2\pi \sin\theta_n} \qquad \text{(III-4)}$$

The spectral radiance of a rough surface can then be determined in terms of the internal radiation, the transmissive scattering coefficients, and the surface characteristics [10].

Sibley's Model for Apparent Temperature of Bare Natural Terrain

Apparent Temperature for Bare Smooth Surface

In Sibley's modeling of apparent temperature of terrain as a function of soil moisture content, he only considered the thermal emission of soil and vegetation. The contributions from the atmosphere, quasi-point source, and reflected sky temperature are not included in his model because they are not of the main concern in his modeling and their effects are often negligible.

As the apparent temperature of any object is a measure of the thermal radiation emanating from the body in a particular direction with a particular polarization,

the apparent temperature of the object can be measured in term of the transmission coefficient, T_i, of the two media. Transmission coefficient is a function of the permittivities of the two media, which in this case are the soil and the air above it. The transmission coefficient is defined by

$$T_i = \frac{\text{Power transmitted with polarization i}}{\text{Power incident with polarization i}} \qquad \text{(III-5)}$$

The transmission coefficients for the vertical and horizontal polarizations are determined from Poynting's theorem

$$\bar{P}_{avg} = \frac{1}{2} Re[\bar{E} \times \bar{H}^*] \qquad \text{(III-6)}$$

They are determined respectively as [27]

$$T_v = \frac{|\tau_v|^2}{\eta_0} \left[Re\left(\frac{1}{\eta_1}\right)\right]^{-1} \frac{\cos\theta}{\cos\psi} \qquad \text{(III-7)}$$

$$T_H = \frac{|\tau_H|^2}{\eta_0} \left[Re\left(\frac{1}{\eta_1}\right)\right]^{-1} \frac{\cos\theta}{\cos\psi} \qquad \text{(III-8)}$$

Where τ_H = transmission coefficient for the horizontally polarized wave [34, pp. 492-496]

τ_V = transmission coefficient for the vertically polarized wave [34, pp. 492-496]

η_o = the intrinsic impedance of the air =377 ohms [35]

η_1 = the intrinsic impedance of the soil

ψ = angle of incidence of the incident field in the soil

θ = angle of transmission of the transmitted field in the air

Thus assuming negligible effects from the atmosphere, quasi-point source, and reflected sky temperature, as it is the case in this ground-based experiment, the apparent temperature for a bare smooth surface is equal to the product of the ground temperature, the emissivity of the soil, and the transmission coefficient [27]

$$(T_{ai})_{\text{SMOOTH SOIL}} = T_g \varepsilon_s T_i \qquad \text{(III-9)}$$

Where T_g = ground temperature

ε_s = emissivity of soil

T_i = transmission of coefficient for polarization i.

Apparent Temperature for Bare Rough Surface

The rough surface model adopted for this study is the one developed by Johnson [10]. Sibley modified Johnson's rough surface model and applied it to the measurement of apparent temperature. Applying the definition of transmission coefficient, (III-5), and the results of Johnson's development, Sibley derived a

"transmission coefficient" expression for the rough surface case. The expression is expressed in terms of the surface characteristics (β and δ), local angle of incidence from the surface to the receiving antenna (θ_{in}) and the angle below the surface from which energy is refracted into the local angle of incidence (θ_i), and the transmissive scattering coefficients [10]. The transmission coefficient for the rough surface that Sibley used is

$$\iint \frac{\beta\delta\cos\theta_{in}}{\cos\theta_i}\left(\tau_{EIV}\tau_{HIV}+\tau_{EIV}\tau_{HIV}\right)d\Omega_i \qquad \text{(III-10)}$$

The first subscript of the transmissive scattering coefficients indicates electric (E) or magnetic (H) scattering coefficient; the second indicates the polarization of the scattered field; the third indicates the polarization of the incident field. Assuming the refracted radiation can be confined into a direction (θ_s, ϕ_s) through the various orientations of the surface elements and assuming that the vertical and horizontal components of the incident radiations are equivalent, Sibley's apparent temperature model for a bare rough surface is [27]

$$T_{aI} = T_g \varepsilon_{SOIL} \iint \frac{\beta\delta\cos\theta}{\cos\theta}\left(\tau_{EIV}\tau_{HIV}+\tau_{EIH}\tau_{HIH}\right)d\Omega_i \qquad \text{(III-11)}$$

Where the subscript I denotes either vertical or horizontal polarization.

Sibley's Model for Apparent Temperature of Uniformly Vegetated Natural Terrain

The approach that Sibley used to model the apparent temperature of uniformly vegetated natural terrain is straightforward. He characterizes the vegetated natural terrain, composing of the soil and the vegetation-air medium, by their respective permittivities. According to Sibley, there are three basic processes that make up the total apparent temperature. These are: 1) thermal emission from the soil, 2) attenuation on the soil emission by the canopy, and 3) thermal radiation from the canopy. Sibley developed apparent temperature models for a uniformly vegetated surface and a surface with row crops. In this study, only the case of uniformly vegetated surface is investigated. For the uniformly vegetated terrain, the vegetation is described by its height, volumetric density, water content in the plant, and a mixing term called Formzahl [27].

In determining the total apparent temperature of the vegetated terrain, a knowledge of the permittivities of the soil and the vegetation canopy is very important. The permittivity of soil determines the transmission

coefficient of the soil surface which affects the emission process. It is a measurable parameter, a detailed discussion on one of the measurement methods will be given in Chapter IV. The vegetation canopy is a mixture of plant material and air. The permittivity of this canopy is needed in the calculation of the attenuation constant of the canopy; thus it determines indirectly the amount of attenuation imposed on the thermal emission from the ground by the canopy. The attenuation constant of the canopy is given as

$$\alpha = \omega \sqrt{\frac{\mu_o \varepsilon'_{canopy}}{2} \left(\sqrt{1 + \left(\frac{\varepsilon''_{canopy}}{\varepsilon'_{canopy}} \right)^2} - 1 \right)} \qquad \text{(III-12)}$$

where μ_o = permeability of free space = 4×10^{-7} henry/meter

ε''_{canopy} = imaginary part of the permittivity of the vegetation canopy

ε'_{canopy} = real part of the permittivity of the vegetation canopy

The permittivity of the vegetation canopy is approximated by Weiner model for a dielectric mixture as presented by Evans [36] as

$$\varepsilon_{CANOPY} = \frac{\varepsilon_v (1 + PU) + U(1 - P)}{\varepsilon_v (1 - P) + P + U} \qquad \text{(III-13)}$$

where ε_v = permittivity of the vegetation

P = volumetric density of the vegetation

U = Formzhal, which describes the dispersion of one medium within the other. Generally it is assumed to have a value between 10 and 25.

The permittivity of the vegetation is approximated by Peake and Oliver [37]. The approximation is

$$\varepsilon_v = \frac{F}{2} Re(\varepsilon_w) + j \frac{F}{3} Im(\varepsilon_w) \qquad \text{(III-14)}$$

where F = fraction of water by weight in the plant

ε_w = permittivity of water

The permittivity of water was found experimentally making use of its Debye type relaxation [38]. Debye relaxation is defined by the exponential behavior of the displacement current in a dielectric to which an electric field is suddenly applied [39]. The permittivity of water is given by

$$\varepsilon_w = \varepsilon_\infty + \frac{\varepsilon_s - \varepsilon_\infty}{1 + jf/f_o} \qquad \text{(III-15)}$$

where ε_∞ = instantaneous dielectric constant ≈ 5.5 [36]

ε_s = static dielectric constant

f = frequency of observation

f_o = relaxation frequency

= 9.0 + 0.405 (T-273) GHz

Therefore the net contribution of the soil to the total apparent temperature is [27]

$$(T_{ai})_{SOIL} = T_g \varepsilon_s T_i e^{-2\alpha H \sec\theta} \qquad \text{(III-16)}$$

where T_g = ground temperature

ε_s = emissivity of soil

T_i = transmission coefficient for polarization i

α = attenuation constant of canopy

H = canopy height

θ = angle of observation

The contribution from the canopy thermal emission is given by [27]

$$(T_a)_{CANOPY} = T_c f (1 - e^{-2\alpha H \sec\theta}) \qquad \text{(III-17)}$$

where T_c = canopy thermometric temperature

f = energy transfer factor

This expression is developed from the apparent temperature of a dielectric layer model by Fung et al. [9]. The energy transfer factor, f, has a value of less than one if there is a gain of energy by the plant, and it is greater than one if there is a loss of energy by the plant. The first case is generally true for the daytime; the second case represents water stress condition and the phenomenon at nighttime.

The total apparent temperature representing a smooth, uniformly vegetated natural terrain is therefore

$$T_{ai} = T_g \xi_s T_i e^{-2\alpha H \sec\theta} + T_c f (1 - e^{-2\alpha H \sec\theta}) \qquad \text{(III-18)}$$

Since (III-18) is a special case of the formulation of a rough surface, the total apparent temperature of a rough, vegetated terrain is formulated in the same manner except T_i is replaced by (III-10)

$$\iint \frac{\beta \delta \cos\theta_{in}}{\cos\theta_i} (\tau_{EIV} \tau_{HIV} + \tau_{EIH} \tau_{HIH}) d\Omega_i$$

The rough vegetated surface apparent temperature is

$$T_{ai} = T_g \xi_s e^{-2\alpha H \sec\theta} \left[\iint \frac{\beta \delta \cos\theta_{in}}{\cos\theta_i} (\tau_{EIV} \tau_{HIV} + \tau_{EIH} \tau_{HIH}) d\Omega_i \right] + T_c f (1 - e^{-2\alpha H \sec\theta}) \qquad \text{(III-19)}$$

CHAPTER IV

CONTROLLED EXPERIMENTAL PROGRAM

Introduction

In the past few years attempts to measure soil moisture remotely had been made with aircraft equipped with passive microwave radiometers [24], [14]. Most analysis of the collected data suggested that ground based studies of the problem should also be conducted to examine the characteristics of various parameters in the problem and to gather the basic, rigidly controlled data for the improvement of remote sensing techniques and the proper interpretation of the remote collected data [12], [14].

Of the many parameters that affect microwave emission of soils and thus the remote sensing of soil moisture, three parameters appear to be more important than the others and special investigation on these are desired. As remote sensing of soil moisture is to use the electrical parameters of the soil as a diagnostic signature, it is therefore necessary to establish the definite relationship between the complex dielectric constant of the soil observed and its water content. The second and third parameters concern the effects of the terrestrial surface roughnesses and vegetation on the ability to measure soil

moisture content by passive microwave radiometers.

This chapter describes the ground based experimental program that was conducted for this study. In the following, a description of the field preparations and a discussion of the ground truth measurement techniques employed during the experiments are presented. In addition, an investigation into the permittivity of the soil of the experiment is included.

Controlled Field Experiment

The primary investigations in the ground based experiment were devoted to the study of the effects of surface roughness and vegetation. A bare field experiment was first conducted, followed by a vegetated field experiment. The field activities involved the preparations of the field, collection of information on various parameters, and the radiometric measurements. The ground based passive microwave radiometric measurement was conducted in cooperation with the Johnson Space Center, and Lockheed Electronics Co. The experiment site was located at the E29 plot of the Texas A&M University Farm in Burleson County, Texas. The plot has an area of 50 meters by 50 meters.

Bare Field Experiment

The bare field experiment began in June 1973. This experiment mainly concerns the effect of terrain roughness on the detection of soil moisture by passive microwave radiometers. The observed field was totally barren. The field was partitioned into three equal areas of 50 meters by 17 meters each. Three types of surface roughness were created for the study. The first area was made very smooth, the second area was disced to give a medium rough condition, and the third area was plowed to give a very rough surface texture. These three types of surfaces are shown in Figure IV-1a, 1-b, and Figure IV-2. The relative locations of these three surfaces and the field labellings are as shown in Figure IV-3.

The roughnesses of the surface were described by a parameter Γ, which is defined as

$$\Gamma = \frac{\text{soil surface area above a level area of one foot squared}}{\text{reference level area of one foot squared (i.e. 1 ft.}^2\text{)}}$$

The soil surface area above the standard level area was approximated from the conformed area obtained by overlaying a very thin plastic sheet on top of the soil surface. With Γ as the roughness characterization, the following

Figure IV-1a. The Bare Smooth Surface.

Figure IV-1b. The Medium Rough Surface.

Figure IV-2. The Rough Surface.

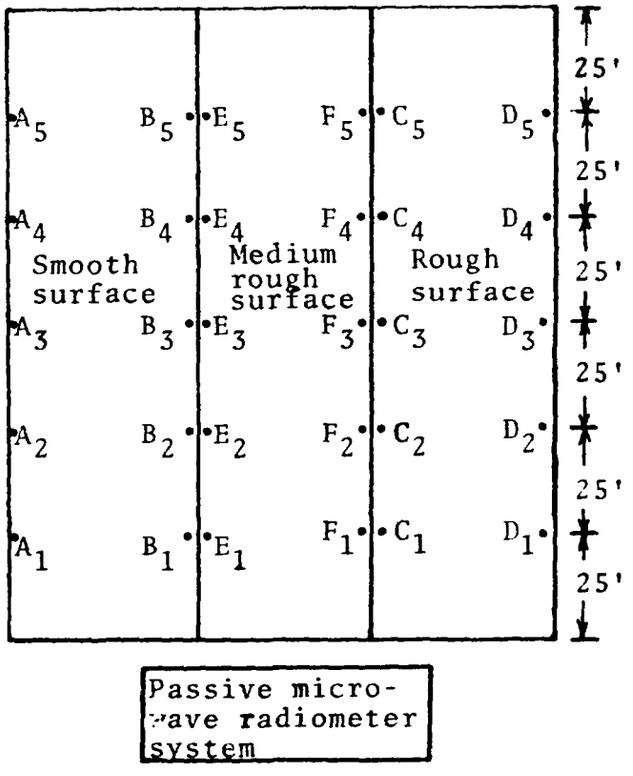

Figure IV-3. Field Labelling and Relative Locations of the Three Type of Surface Roughnesses.

average values were obtained for the three surfaces:

Smooth surface, Γ_S = 1.1527

Medium Rough Surface, Γ_M = 1.617

Rough Surface, Γ_R = 2.49

Other soil roughness parameters for the three bare fields were noted and their statistics are shown in Table IV-1. To determine the ability of the passive microwave radiometer to detect soil moisture and the variation of soil moisture content, the field was irrigated and several radiometric measurements were made at various time periods after the irrigations. The irrigation technique used was the sprinkling method of irrigation. The field was irrigated to the extent that the soil was saturated with water to a depth of about 0.4-0.6 meter.

Extensive soil sample collection for determination of soil moistures and soil temperature thermometric measurements was conducted simultaneous with the radiometric measurements. Soil samples and soil temperature measurements were taken at the locations shown in Figure IV-3. Soil samples were taken at the depths of 0 cm (the surface), 4 cm, 5 cm and 18 cm. The top surface soil samples were obtained by scrapping the top soil with a flat scraper. To collect the subsurface soil samples, two techniques were possible. The first technique was to dig

Table IV-1. Roughness Parameters of Bare and Oats Vegetated Fields.

Field Description	Average Γ	Average Clod Size	Average Distance Between Ridges	Average Depth of Ridges
Smooth Field	1.15	2.0cm X 1.0 cm	---	---
Medium Rough Field	1.62	4.6cm X 2.8 cm	16.5cm	5.0cm
Rough Field	2.49	23.0cm X 10.5cm	70.0cm	24.0cm

into the soil to the deepest depth of interest (18 cm) then soil samples at various desired depths were extracted on the wall of the hole. The second method was to dig out a large vertical profile of soil, then this soil block was leveled to various desired depths and the soil at these depths was extracted. The first method worked for both wet and dry soil. The latter method worked best for relatively wet soil.

The soil samples collected were taken to the laboratory and the determination of the percentage of soil moisture was processed the same day. Soil moisture profiles were then plotted after the percentage of soil moisture were determined.

The moisture content of the soil was determined by the gravimetric methods with oven drying to remove the water in the soil. The gravimetric methods involve weighing the wet sample, removing the water, and reweighing the sample to determine the amount of water removed. The percentage of soil moisture is determined from the formula below:

$$\%\text{soil moisture by weight} = \frac{W_w - W_d}{W_d} \times 100 \qquad \text{(IV-1)}$$

where W_w = wet soil weight

W_d = dry soil weight

The soil samples were dried in a ventilated oven at a constant temperature of 105°C and a drying time of approximately twenty-four hours [12], [40], and [41]. Soil is made up of coloidial and noncolloidial mineral particles, organic materials, volatile liquid, water and chemical substances dissolved in water. A drying temperature of 105°C and a drying period of approximately twenty-four hours is the standard laboratory procedure to determine soil moisture content. These specifications are adopted to avoid excessive oxidation and decomposition of soil organic matters in the drying process. Many soils contain only small amounts of organic material, much of which is fairly stable. Inaccuracies introduced by uncertainties in the drying of organic materials can often be neglected [41].

At the same time the soil samples were taken, soil temperatures were taken. Soil temperatures at the surface, 2 cm, 4 cm, 8 cm, and 16 cm below the surface were recorded. Thermister probes and platinum-resistance sensors were used for soil temperature measurements.

Vegetated-Field Experiment

This experiment was devoted to the investigation of vegetation effects. The experiment began in early September, 1973. Oats were planted on September 3, 1973. Oats grass was chosen primarily because it can survive through the winter and it can grow to the desired height of about two feet above ground. One hundred pounds of oats seed was sown evenly on each of the three 50 meters by 17 meters partitions. The amount used gave a uniform, thick vegetation coverage on the soil when the plant was full grown. Pictures of eight-week oats on the three types of surfaces are shown in Figures IV-4a, 4b, 5a, and 5b. The oats as shown on these pictures were about twenty-five centimeters tall. A close up view of eight-week old oats on the rough surface is shown in Figure IV-5b.

During the radiometric measurements, the same soil sample collection and soil temperature measurement routines were performed, with the additional task of oats sample collection. The oats samples were taken for the determination of the percentage of water that was in the plant. To further characterize the oats vegetation, photographs were taken, the height of the oats was measured and the volumetric density of the oats vegetation was estimated. The volumetric density of the oats

Figure IV-4a. Eight-Week Oat on Smooth Soil Surface.

Figure IV-4b. Eight-Week Oat on Medium Rough Soil Surface.

Figure IV-5a. Eight-Week Oat on Rough Soil Surface.

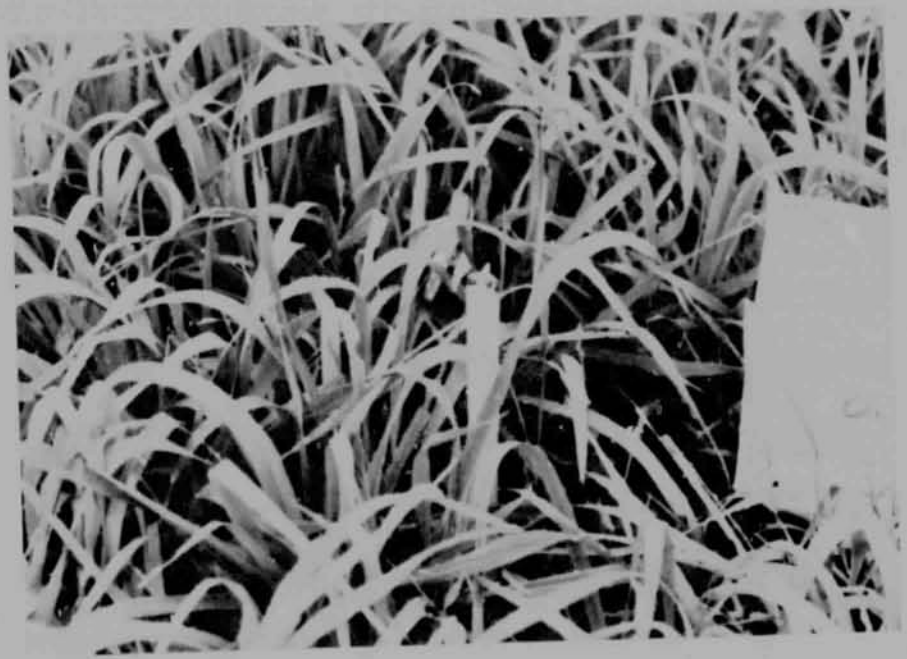

Figure IV-5b. Closeup View of the Eight-Week Oat on the Rough Soil Surface.

vegetation is taken tc be the volume of oats vegetation in a cubic foot. The method used to determine this volumetric density required the use of the density (mass/volume) of the oats vegetation. After the density was determined, the volumetric density (volume of vegetation within a cubic foot) was obtained simply by dividing the mass of oats clipped from a one cubic foot volume by the density of the oats vegetation.

A listing of the entire soil moisture and thermometric temperature data is given in Appendix A. Soil moisture profiles for all the radiometric measurements are also presented. The vegetation characterizations are given in Chapter V.

Laboratory Measurement of Dielectric Constant of Soil

The first phase of the ground based experiment program was the measurement of complex dielectric constant of the soil from the experimental fields, observed as a function of soil moisture content. This information is important because it is known that the emitted energy measured by the microwave radiometer is dependent on the dielectric constant of surface being scanned [42]. The soil moisture and dielectric constant relationship is a key parameter used in the theoretical models for the

prediction of the soil apparent temperatures from which soil moisture conditions can be inferred.

To provide true characteristics of the electrical property of the soil observed for the experiment, soil samples used for the determination of relative dielectric constant of soil were taken from different locations distributed representatively over the entire experimental field. Soil samples were collected to a depth of about 0.4 meter. The soil samples were analyzed by the Soil and Crop Science department at Texas A&M University. The result indicated that the soil for this experiment observation is very homogeneously Miller Clay type, which is composed of 49% clay, 35% silt, and 16% sand. The result of this soil chemical analysis is indicated in Table IV-2.

Clay tends to be very difficult to work with when it is moistened. A special technique for handling clay or similar soils for dielectric constant measurements is presented in the Appendix B. In the hope of preserving the soil's genuineness, distilled water was used to moisten the soil. After the distilled water was added to the soil, the soils were allowed to set for at least 24 hours before any dielectric constant measurements were made, this insured resemblance with the irrigated soil conditions in the actual field observations.

Table IV-2. Chemical Analysis of the Soil of the Experiment.

Field	Smooth Field	Medium Rough Field	Rough Field
pH (Negative logarithm of hydrogen ion activity in soil water solution)	7.65	7.0	7.35
Soluable Salt (Parts per two million)	563	256	486
% $CaCO_3$	15	14	14
% Clay (Less than 0.002mm)	49	44	—
% Silt (0.002mm - 0.05mm)	35	41	—
% Sand (0.5mm - 2 mm)	16	15	—

Different methods of measuring the dielectric constant of soils or other materials have been investigated by many investigators. Some of these include the "phase shift method" proposed by Rouse and Giarola [43], the radar power reflectance technique employed by Davis, Lundien, and Williamson [19], the "impedance method" proposed by Rouse and Giarola [43], the time-domain reflectometry introduced by Hewlett-Packard Co. [44], the "free space method" investigated by Hertal et al. [45] and Wiebe [46], and the "waveguide method" investigated by Wiebe [46].

In this study, the measurements of the complex dielectric constant of soil were performed at the Remote Sensing Center, Texas A&M University with the waveguide system introduced by Wiebe. As a check of the results obtained, the complex dielectric constant measurements of the same soil type were performed with the modified Wiebe waveguide system proposed by Giarola [47] at Texas A&M University.

Measurements with Wiebe Waveguide System

A block diagram of Wiebe's waveguide system is shown in Figure IV-6 and a photograph of the experimental apparatus is shown in Figure IV-7. To facilitate rapid dielectric constant measurements on a large scale, a

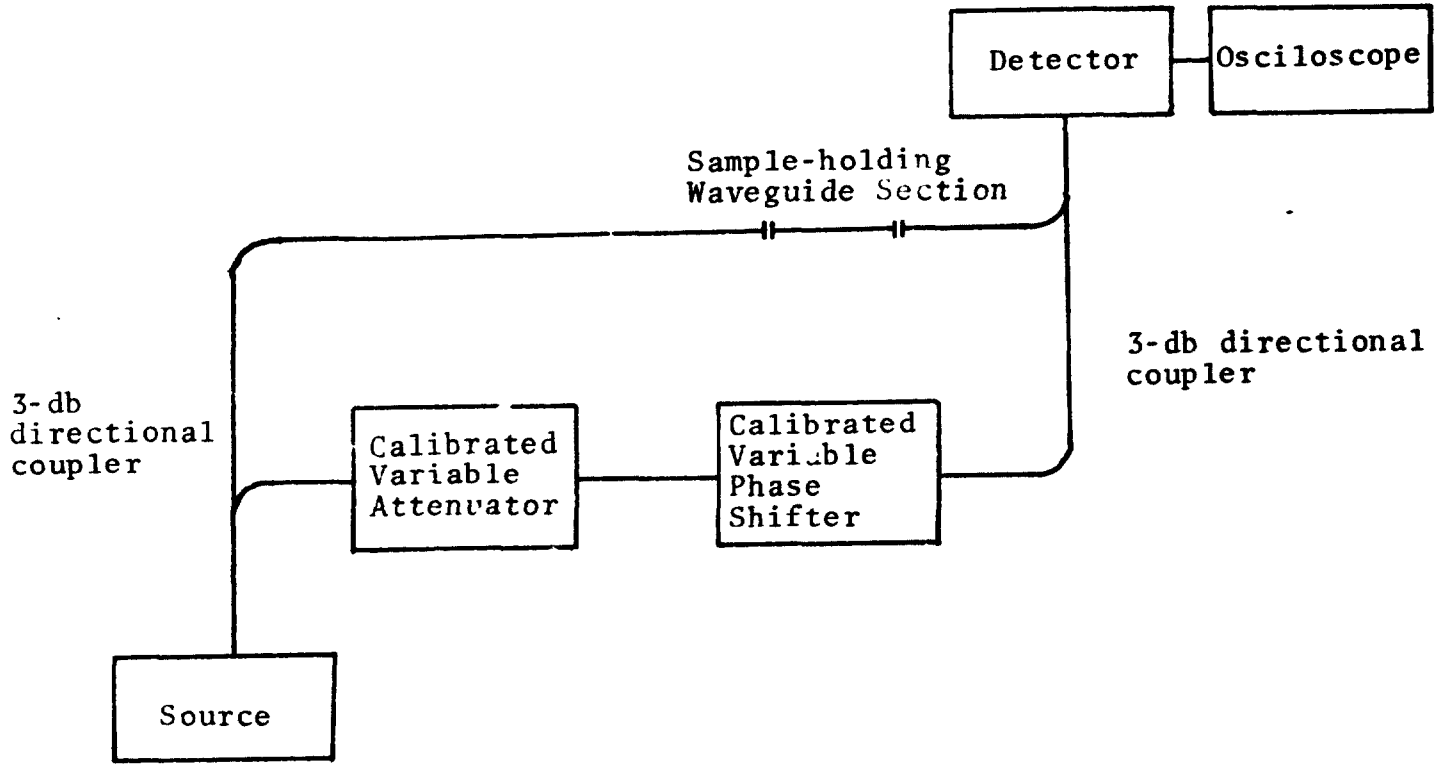

Figure IV-6. A Block Diagram of Wiebe's "Waveguide Method" Dielectric Constant Measurement System.

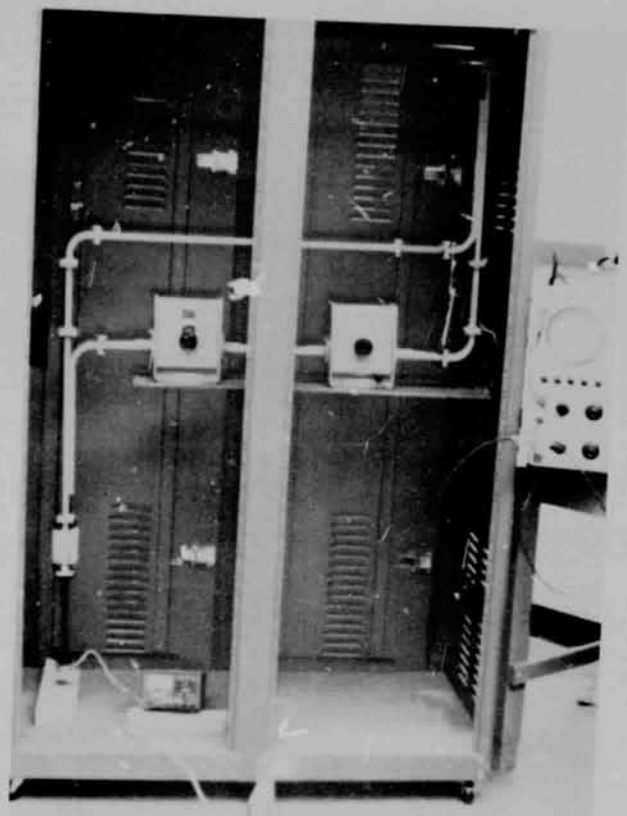

Figure IV-7. Wiebe's "Waveguide Method" Dielectric Constant Measurement System.

special sample holder (Figure IV-8) was used for accomodating the section of the waveguide which holds the sample of soil. The frequency used for the dielectric constant measurements for this study was 10.5 GHz which closely approximates one of the two frequencies used in this study. This frequency was provided by a waveguide cavity Gunn Oscillator (MA86131).

The complex relative dielectric constant of the soil was determined from the curves of attenuation and phase shift versus the soil sample length. Each of these curves is the end product of an iterative process for each value of soil moisture content. For each soil moisture value, the measurements of attenuation and phase shift are made for at least five different sample lengths. The length of the soil sample used for attenuation and phase shift measurements varies with the amount of moisture that is in the soil. For very dry soil, soil sample length can begin from 3 cm and be incremented at increments of 1 cm up to beyond 7 cm. But for very wet soil, sample length might begin from 0.35 cm (shortest length that could be handled) and be incremented at increments of about 0.15 cm up to about 1.15 cm. At the operating power level (100 mw), the attenuation can be measured accurately to about 28dB. This attenuation value can serve as a guideline for the longest sample length that could be used to still

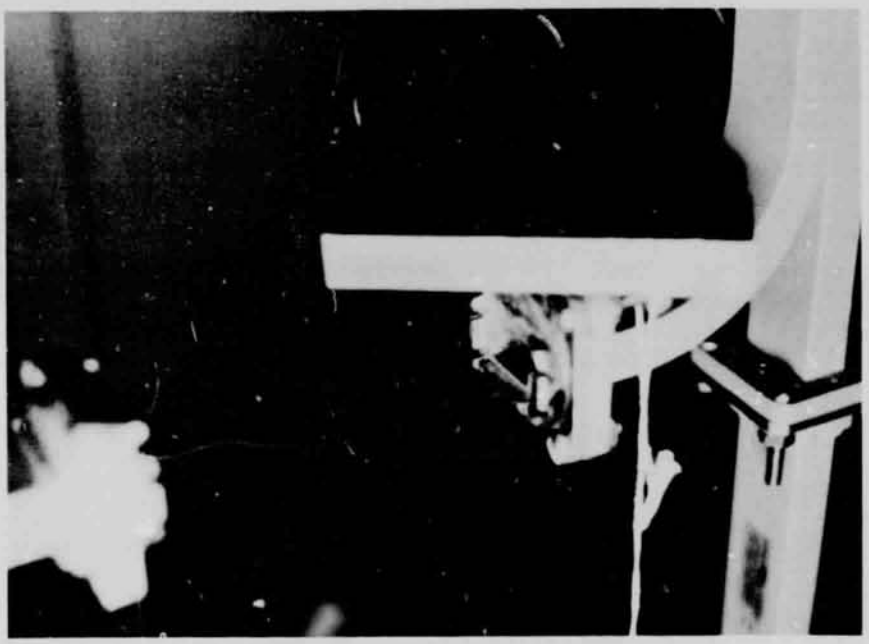

Figure IV-8. The Piece of Sample-Holding Waveguide and the Special Waveguide Connector (the Sample Holder).

obtain a meaningful measurement.

Working with a specific soil moisture content, the iterative process of measuring phase shifts and attenuation begins with placing small amounts of soil into the sample-holding waveguide section. The detector output is connected to channel 1 and channel 2 of a dual beam oscilloscope, the input polarity of channels 1 and 2 are to be of opposite polarities. The attenuator and the phase shifter are adjusted to give a null on the oscilloscope. The null occurs when the waveforms of channels 1 and 2 barely touch, any non-null values of phase shift and attenuation would cause the two waveforms to diverge. After the attenuation and phase shift values at the null are recorded for this sample length, the same process is repeated for another incremented sample length. These measurements of attenuation and phase shifts at different sample lengths constitute the attenuation and phase shift versus soil sample length curves for a particular soil moisture content value. Several of these curves over the 0% soil moisture to the saturated soil moisture range are necessary to compute the complex dielectric constant of the soil.

The relative complex dielectric constant, k'-jk", for the waveguide method are computed by the following formulas [48]:

$$k' = \frac{\varepsilon'}{\varepsilon_o} = \frac{\beta^2 - \alpha^2 + K_c^2}{\beta_o} \qquad \text{(IV-2)}$$

$$k'' = \frac{\varepsilon''}{\varepsilon_o} = \frac{2\alpha\beta}{\beta_o} \qquad \text{(IV-3)}$$

where $\beta_o = \frac{2\pi}{\lambda_o} = \frac{2\pi}{\text{Wavelength in the free space}}$

α = attenuation constant in neper = $\frac{A}{8.686}$, A is the slope of the attenuation curve plotted in db per meter and 8.686 is the conversion factor for nepers and decibels.

$\beta = B+\beta_o$, B is the slope of the phase shift curve in radian per meter.

$K_c = \frac{2\pi}{\text{cutoff wavelength of the waveguide [35]}}$

To facilitate the computation for the relative dielectric constants of the soil, a computer program was written [49] for such a calculation using the attenuation and phase shift measurements taken in the laboratory. The slopes of the attenuation and phase shift curves, A and B respectively, are determined with a least mean squared error technique subroutine.

Relative dielectric constant measurements as a function of soil moisture were made on the soils taken from five different locations within this test field: L_1, L_3, M_1, and R_2 respectively (Figure IV-9). The results of the relative complex dielectric constant measurements as a function of soil moisture of these five soil samples are shown compositely (five sets of curves were generated) in Figure IV-10. As can be seen, the results of the five disjoint measurements results were nearly identical. This checks the point that the soils are of the same type as reported from soil analysis, and indicates that the relative dielectric constant of the soil of this project is accurately represented by the two composite curves the real part k', and the imaginary part k". An estimate of the relative dielectric constant from the composite curves was made with a Statistical Analysis System (SAS) computer program which employed nonlinear regression techniques to generate best fitting curves for data supplied. This SAS best fitting result representing the relative dielectric constants of the soil of this project is shown in Figure IV-11.

Several parameters that might affect the accuracy of dielectric constant measurements were investigated [12]. These parameters include the accuracy in sample thickness measurements, accuracy in attenuation and phase shift

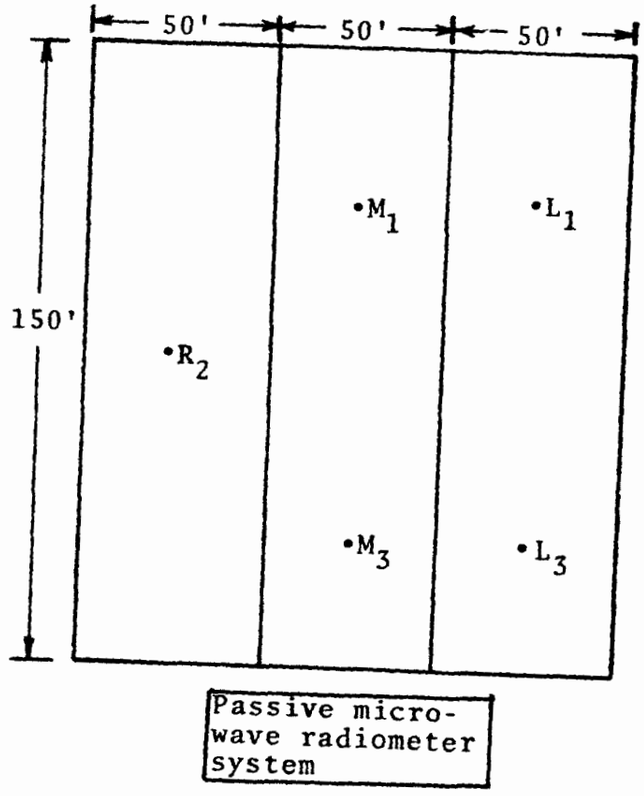

Figure IV-9. Locations of L_1, L_3, M_1, M_3 and R_2 in the Experiment Field Plot.

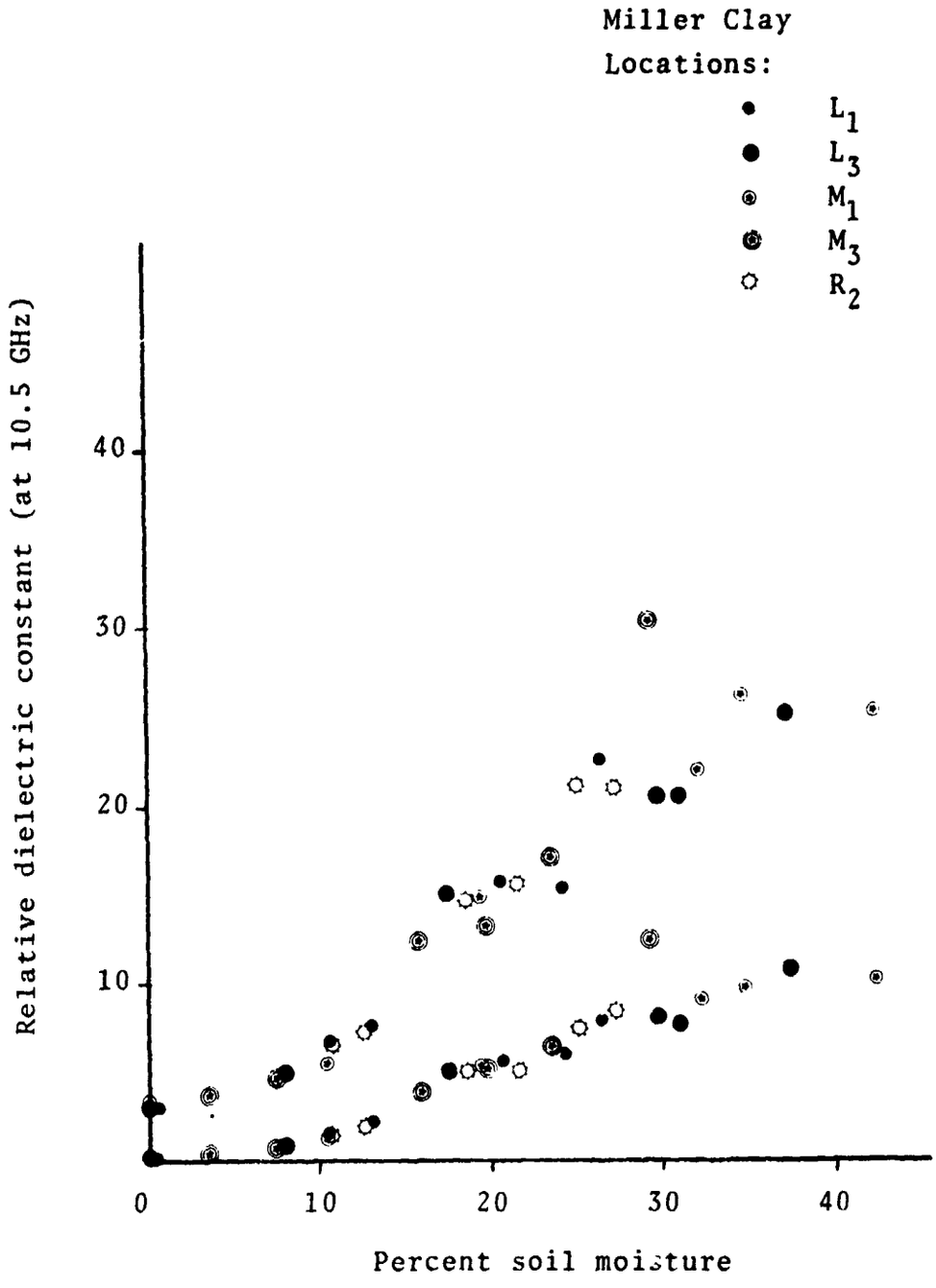

Figure IV-10. A Composite Representation of the Relative Dielectric Constants of Soils from Five Different Locations in the Field. Results of RSC's Wiebe-System.

Miller Clay

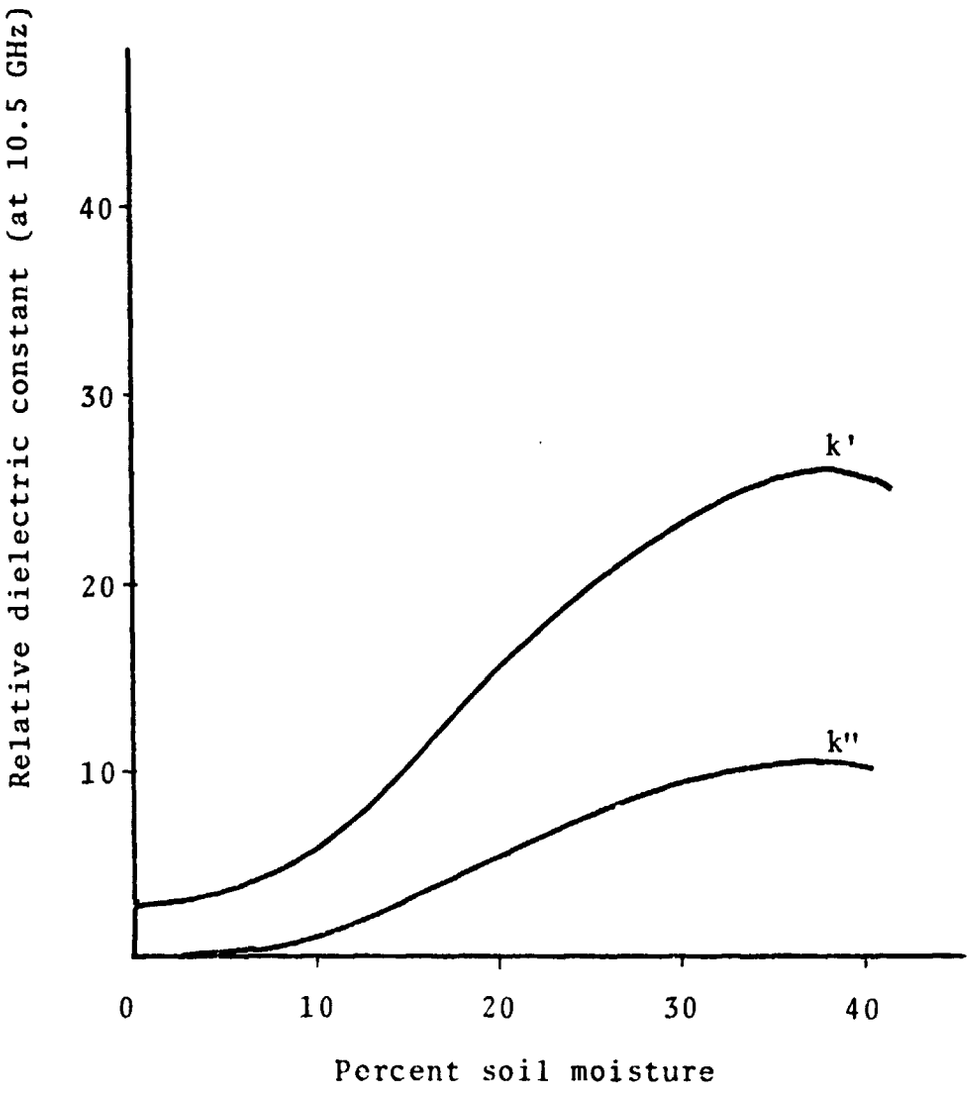

Figure IV-11. The SAS Best-Fitting Result of the RSC's Wiebe-System.

measurements, and the effect of compaction on the soil samples. Assuming the thickness of soil sample measurements could be measured to within 0.05 cm, and the accuracy of the phase shifter and attenuator are within ± 1.5° and ± 1.5 dB respectively, the following values were determined for the accuracy of the real and imaginary part of the relative dielectric constant.

$$\text{Real Part Accuracy} = \pm 1\% \qquad \text{(IV-4)}$$

$$\text{Imaginary Part Accuracy} = \pm 1\% \qquad \text{(IV-5)}$$

To eliminate the effect of compaction, a device which provide constant and uniform compaction was used [49]. The compaction force generated by this device gave the soil a compaction simular to most natural soil compaction. This device was applicable to relatively dry soil samples. For wet clay samples, the clay was packed to a degree that resembles the natural wet clay.

Measurements with Giarola's Modified Waveguide Method

As a check of the dielectric constant measurements obtained with Wiebe's waveguide system at the Remote Sensing Center, the same soils measured at the same

frequency (10.5 GHz) were tested with Giarola's modified waveguide method at the Electrical Engineering Department, Texas A&M University. A block diagram of the system used is as illustrated in Figure IV-12 [47]. The modification made to Wiebe's system was the addition of the loop 1 which helped to reduce reflections occurring at the first interface of air and dielectric, and also additional attenuators in the upper arm of loop 2 allowed for calibration purposes.

The results of measurements of dielectric constant on soils at different locations are shown in Figure IV-13. A comparison between this measurement result with the SAS fitted RSC-system result indicated two things. First, it shows that there is good agreement between the results made with two slightly different systems. Secondly, the comparison suggests that for the present system setups, the effect of reflection is not significant. (A technique for handling clay and for reducing the possible reflection effect of clay is discussed in Appendix B).

After many extensive measurements on both Giarola's system and Wiebe's system, it was concluded that both systems were essentially the same. The additional attenuators for the calibration of the empty sample-holding waveguide section is not necessary because the dielectric constants are obtained in terms only of the slopes of the

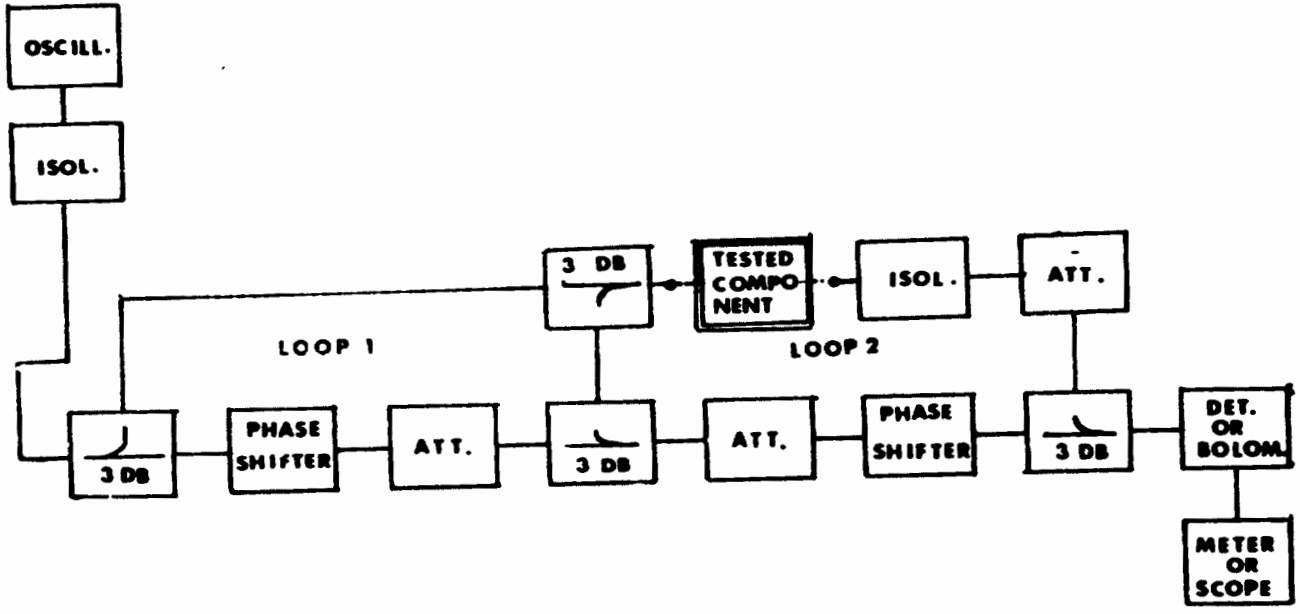

Figure IV-12. Giarola's Modified Wiebe's System For Measuring Dielectric Constants of Dielectrics [47].

Miller Clay

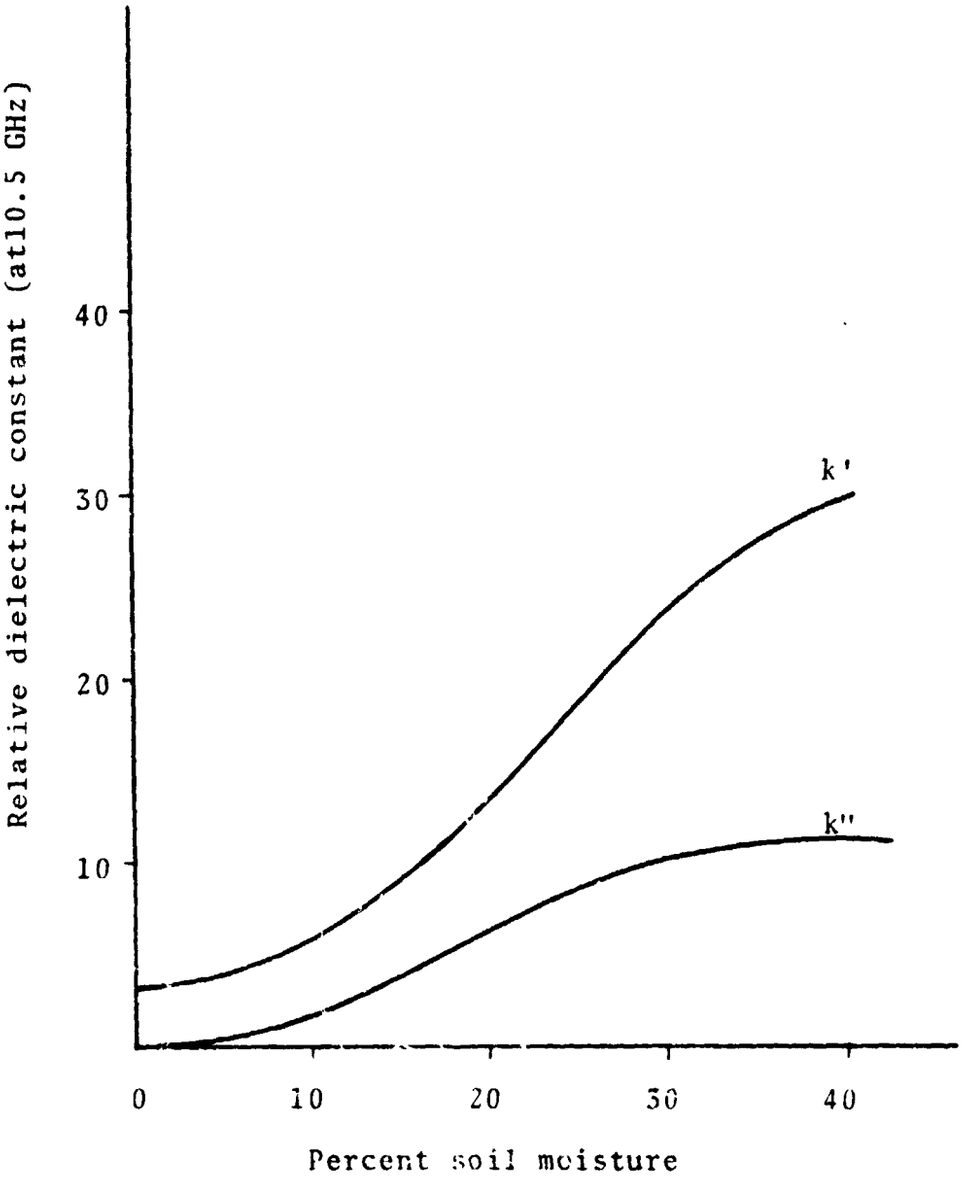

Figure IV-13. Results Obtained from Ciarola's System.

attenuation and phase shift values. The calibration process only enables the measurements to start out on a zero reference level (Figure IV-14), the slopes of the attenuation and phase shift curves do not change.

(a)

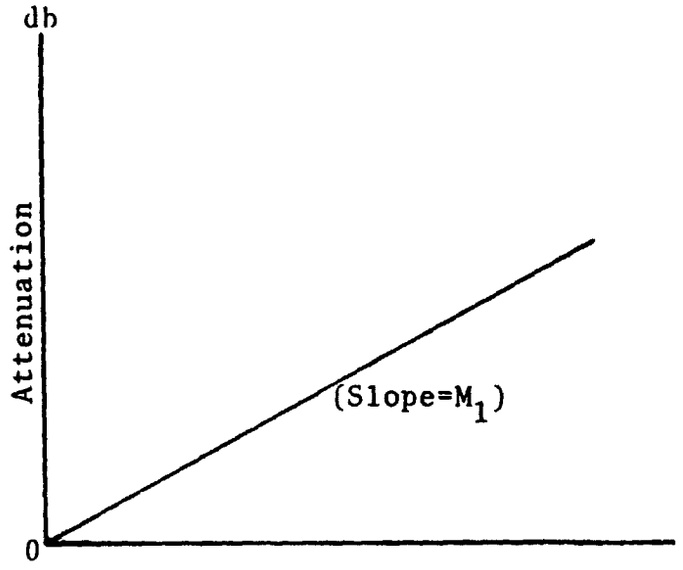

(b)

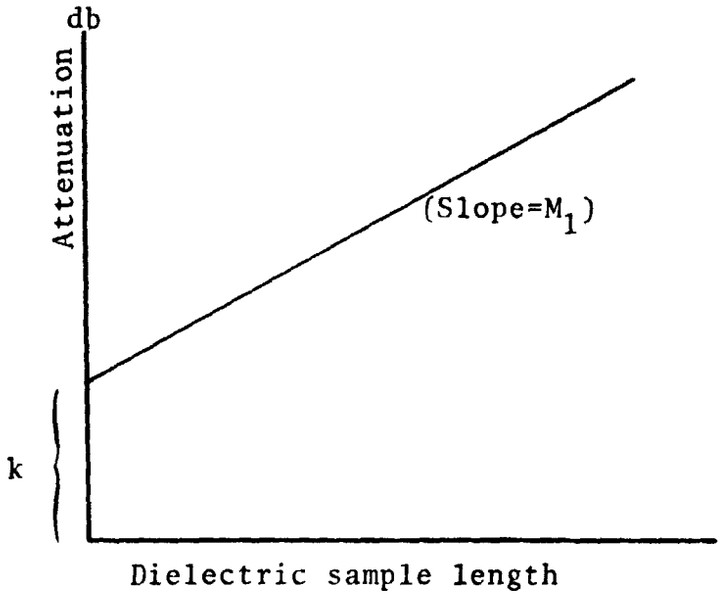

Figure IV-14. (a) With Calibration
(b) With No Calibration

CHAPTER V

RESULTS AND ANALYSIS

Introduction

Remote sensing of soil moisture by passive microwave radiometry cannot be perfected until the effects of a few important parameters which possibly affect the emission process are determined. Two of these parameters appear to be particularly influential, yet their effects have not been well documented or clearly understood; they are the surface roughness and vegetation coverage of the natural terrain. This chapter presents the results and analysis of the effects of these two parameters on the data obtained in the ground based experiment program discussed in Chapter IV. The objective of the analysis is to determine the potential of passive microwave radiometer as a remote sensor for soil moisture detection. Results calculated from Sibley's theoretical models for the bare smooth surface case and uniformly vegetated smooth surface case are compared with the empirical results. Recent soil moisture detection experimental results by other investigators are also presented for comparison.

Experimental Results and Analysis

Before presenting the experimental results, a few comments are helpful in following the analysis of the experimental data. The first concerns the soil moisture information obtained in the experiment program. This is very important information because the ultimate objective is to correlate the field soil moisture with the apparent temperature measured. A tabulation of the soil moisture information is given in Appendix A, Table A-1. From the study of these data it was found that the range of surface moisture contents observed was quite variable from almost 0.0% to 40.0%. The subsurface moisture content was more uniform, ranging from 5.0% to 35%. Histograms showing the distribution of the 0-2 centimeters average soil moisture and 0-18 centimeter average soil moisture (of all three fields for the entire experiment) are shown in Figure V-1.

As it is customary in other investigations to choose a "most representative" soil thickness to relate the microwave signal to water content, the 0-2 cm. average soil moisture and 0-18 cm. average soil moisture are used for the following data analysis. However, it was felt that such a "representative" thickness is too arbitrary and most likely inaccurate, the approach of

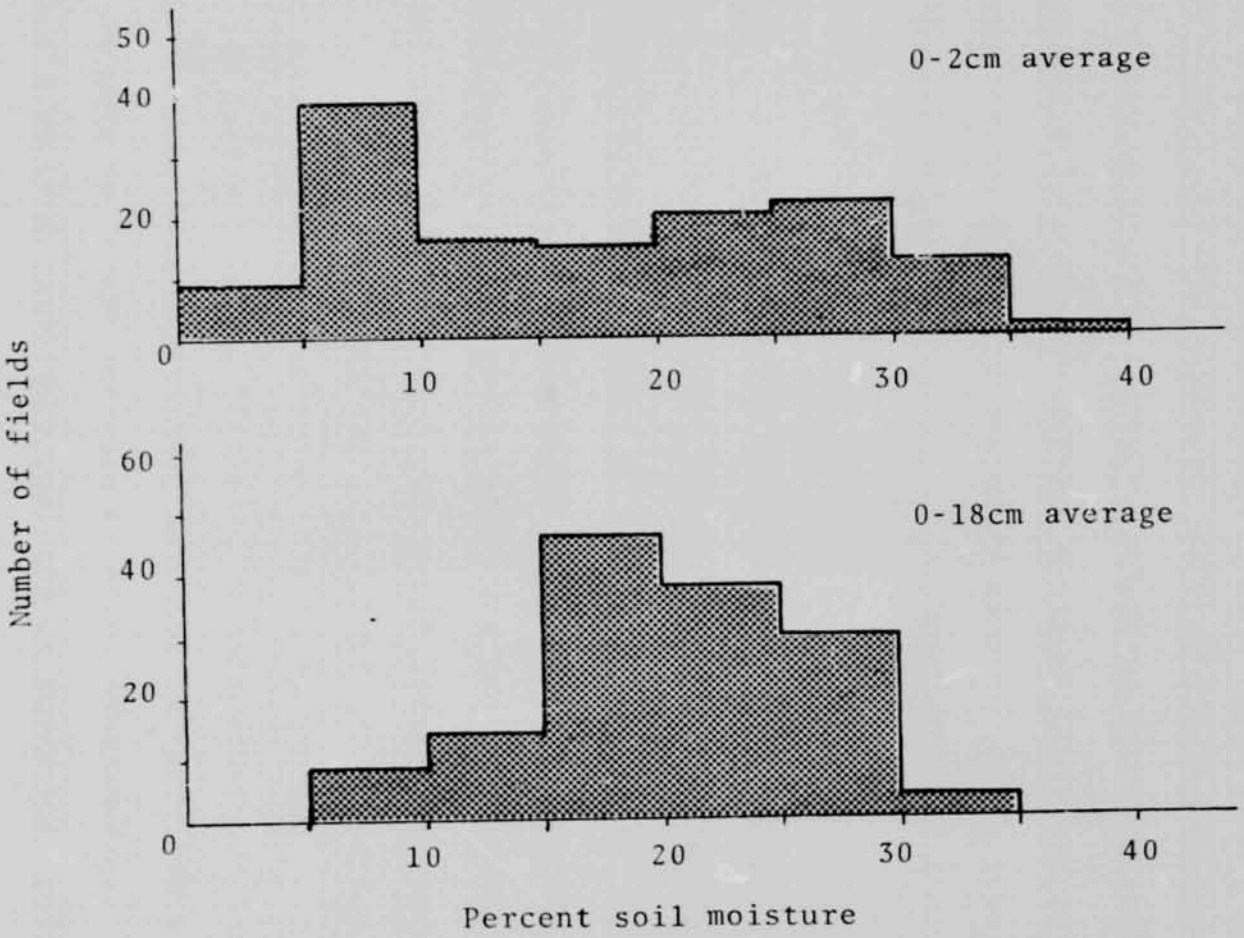

Figure V-1. Histogram of the Entire Experimental Program (Three Fields Combined).

using a "skin depth" thickness of soil and the concept of "equivalent soil moisture" at skin depth [50] was also used.

The skin depth is conventionally defined as that depth at which the electric field is attenuated by a factor of 1/e. The "equivalent soil moisture" is defined as that soil moisture content that would, if constant with soil depth, produce the same skin depth as the actual soil moisture profile of the soil. The "equivalent soil moisture" at the skin depth is also used as a soil moisture parameter in the correlation of the apparent temperature with soil moisture in the following data analysis.

A discussion on the determination of skin depth and the corresponding "equivalent soil moisture content" is given in Appendix C. The skin depths and "equivalent soil moistures" for X- and L-band for the three surfaces are shown in Figures A-1 through A-6.

The second comment concerns the precise knowledge of the radiometer null-to-null ground coverage for the acquisition of apparent temperature at different angles. This knowledge helps to pinpoint the exact area at which the radiometer is sensing, therefore provides a better correlation between the apparent temperature and soil

moisture content at that particular observation angle. X- and L-band radiometric measurements were obtained at both vertical and horizontal polarization for observation angles from 0° to 50°, generally in 10° increments. An illustration of the scaled beam footprints at these observation angles with respect to the scaled field size is shown in Figure V-2. A listing of all the soil moisture data at various angles within the antenna beam footprints for the three surfaces on all measurement dates are given in Appendix A, Table A-2. These soil moisture data are inferred from the soil moisture contour maps which are constructed from the soil moisture data of Table A-1. The corresponding radiometric apparent temperature data are given in Appendix A, Table A-3.

Finally, to facilitate the interpretation and analysis of the data the following legend is adopted throughout the data analysis (pages 87 and 88):

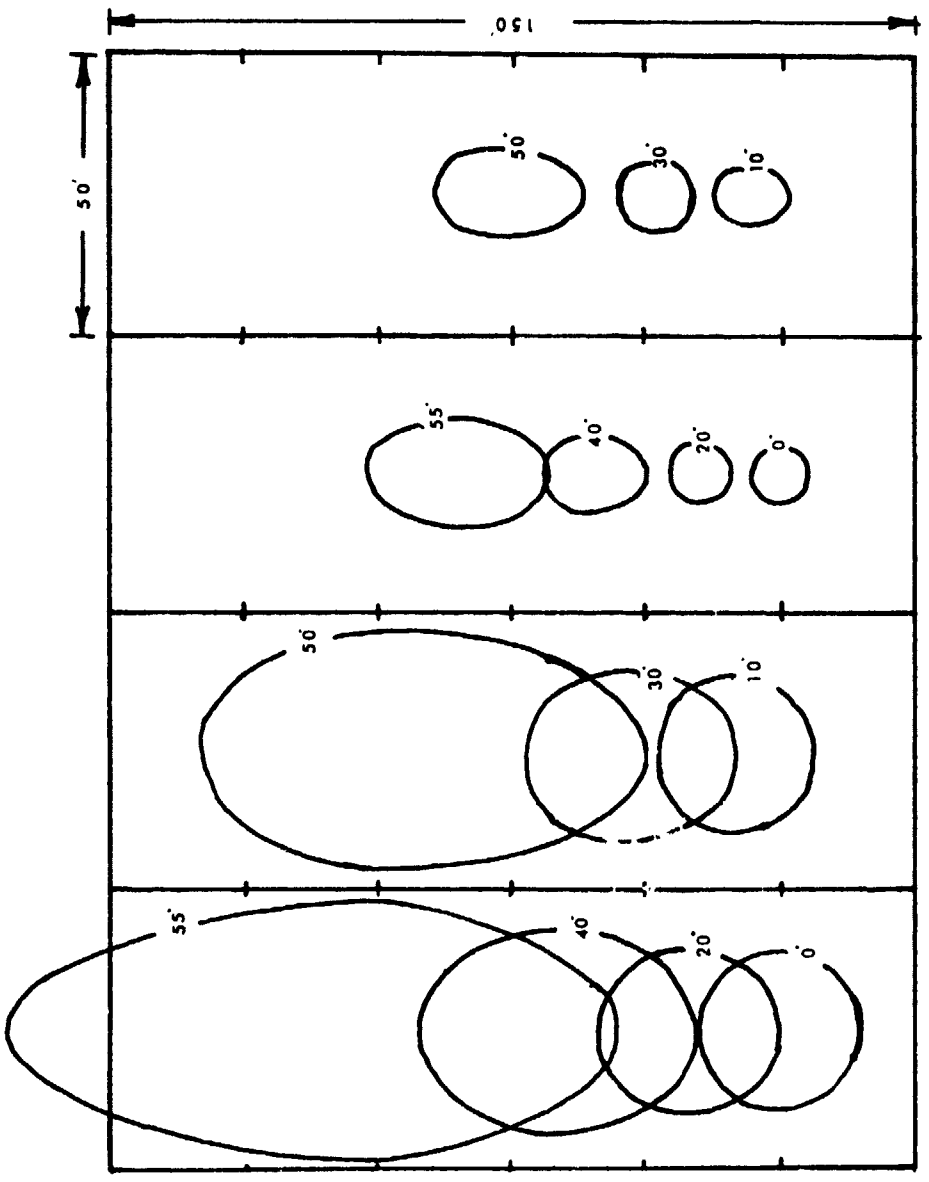

Figure V-2. Scaled Antenna Footprints at Various Observation Angles.

Inscription	Representation
.	Bare, July 23, 1973. Rough surface.
.	Bare, July 24, 1973. Smooth and medium rough surfaces.
•	Bare, July 26, 1973. Three surfaces.
●	Bare, July 30, 1973. Five days after irrigation. Three surfaces.
o	5"* oats, September 25, 1973. Three surfaces.
O	10" oats, October 30, 1973. Smooth and medium rough surfaces.
O	11" oats, October 30, 1973 Rough surface.
▫	11" oats, November 9, 1973. Smooth surface nine days after irrigation.
◘	13" oats, November 8, 1973. Medium rough surface eight days after irrigation.
◘	14" oats, November 8, 1973. Rough surface eight days after irrigation.

* This length is not the actual length of the plant but the mean height of the plant from the ground.

Inscription	Representation
□	12" oats, February 12, 1974. Smooth surface.
□	14" oats, February 13, 1974. Medium rough surface.
□	14" oats, February 13, 1974. Rough surface.
S ———————	Smooth surface.
M —— - —— - —	Medium rough surface.
R - - - - - - - - -	Rough surface.
L	L-band (1.41356GHz, wavelength=21.1339cm).
X	X-band (10.69GHz, wavelength=2.81cm).
V	Vertical polarization.
H	Horizontal polarization.
( )	Slope of the line (degree Kelvin/percent soil moisture).

Effects of Surface Roughness

The effects of surface roughness on the capability of the passive microwave radiometer to detect soil moisture was studied. Bare field condition exists for the July 23, July 24, July 26, and July 30, 1973 measurements. The three fields (smooth surface, medium rough

surface, and rough surface) were irrigated in the same manner on July 25, 1973. Generally the three surfaces had very similar soil moisture conditions and thus a comparison of the apparent temperatures for the three different surface roughnesses is possible.

Figures V-3 through V-11 are plots of the bare field apparent temperature measurements on the four dates. Apparent temperature is plotted for the various observation angles for X- and L-band and for the vertical and horizontal polarizations. The 0-2 centimeter average soil moisture contour maps are shown below the apparent temperature plots. The crosses on the soil moisture contour maps indicate the locations at which temperature data were taken. The dependence on polarization is clearly illustrated. The vertical polarization temperatures are higher than those of the horizontal polarization. On the whole, it appears that temperatures measured are fairly independent of the observation angles, but are dependent on soil moisture variations.

From these measurement data, the data obtained at the 30° observation angle are chosen to investigate the surface roughness effects. This choice is quite arbitrary as it is seen that apparent temperature measurements are fairly independent of the observation angles.

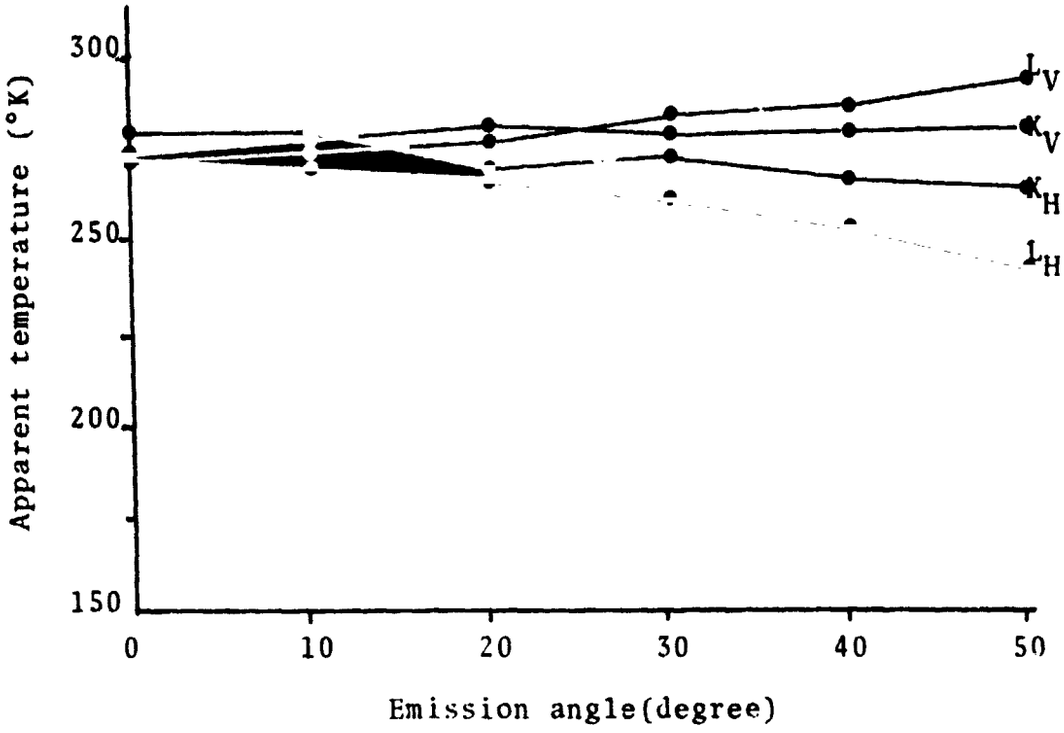

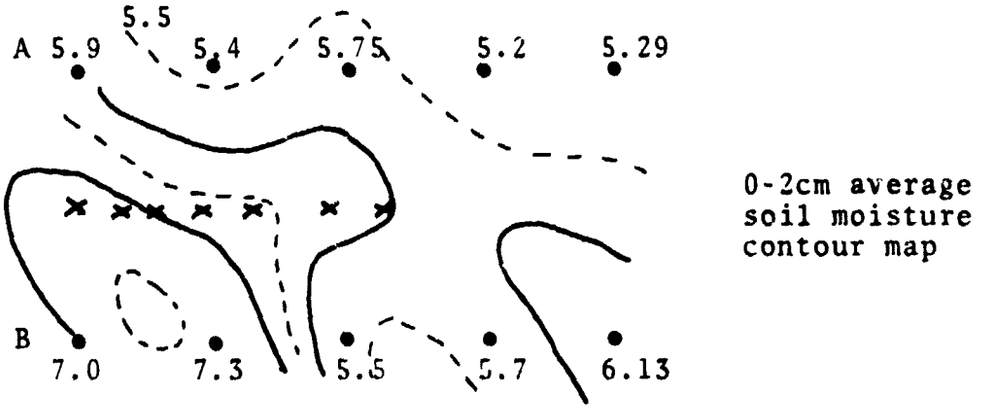

Figure V-3. Apparent Temperature for Smooth Field on July 24, 1973.

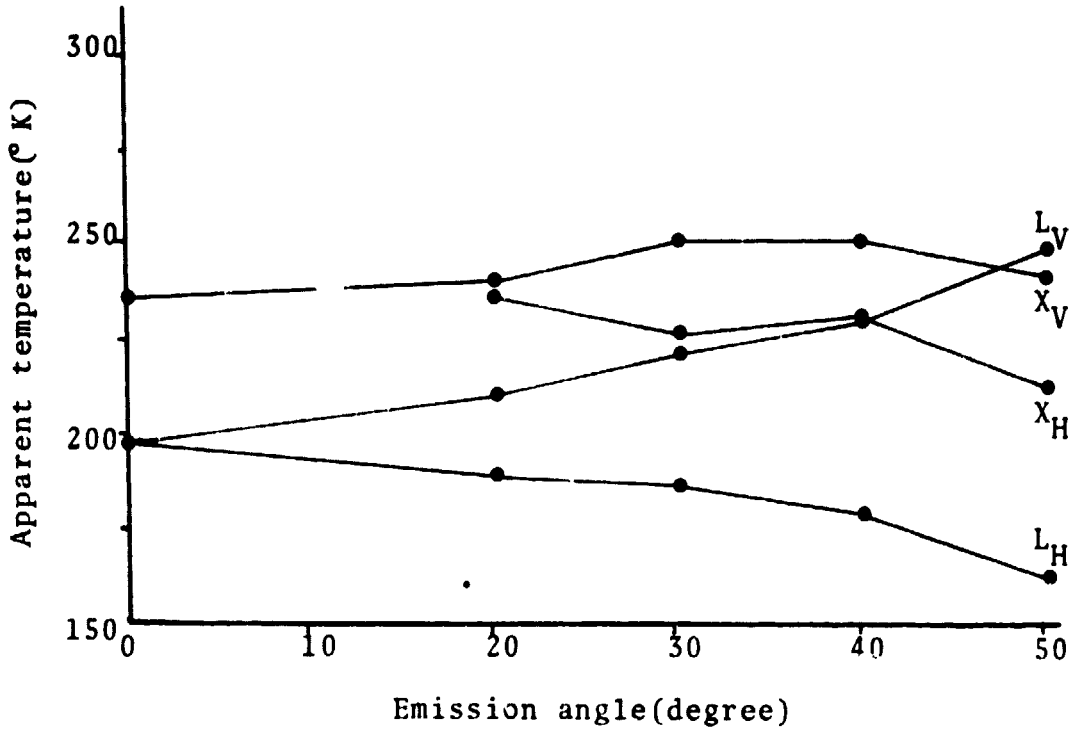

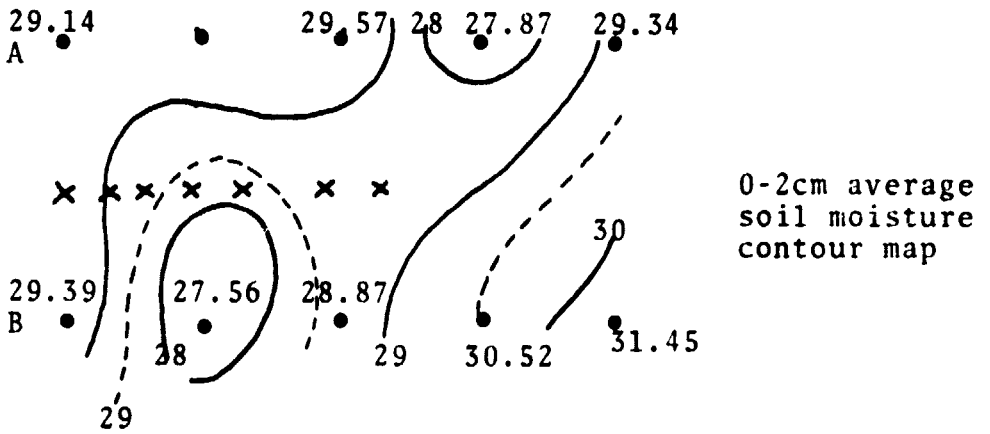

Figure V-4. Apparent Temperature for the Smooth Field on July 26,1973.

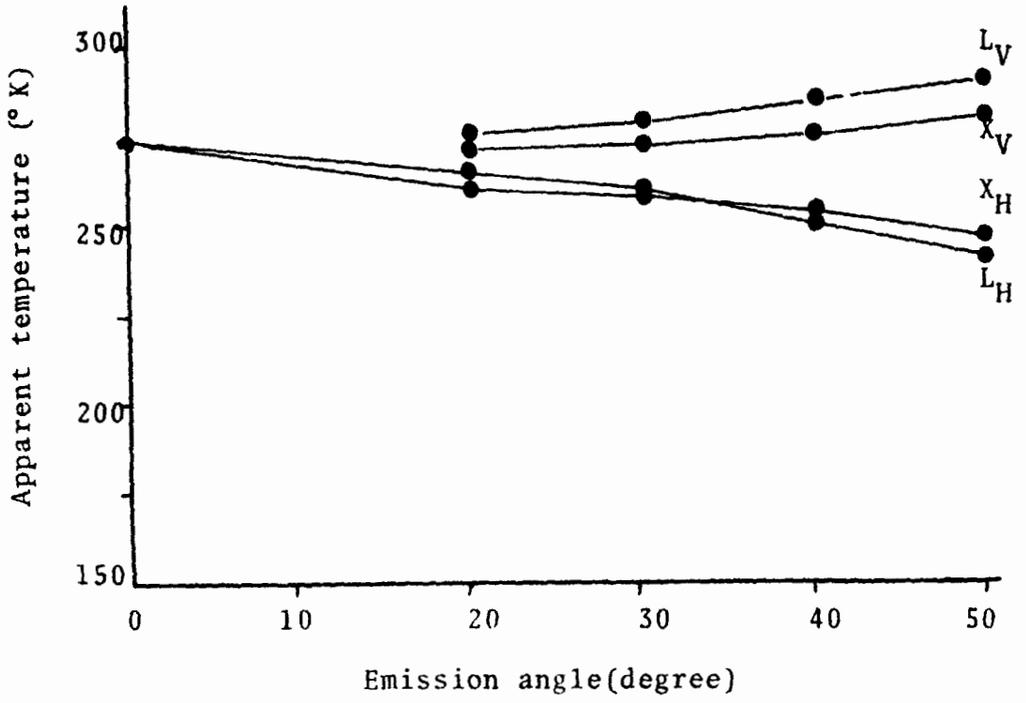

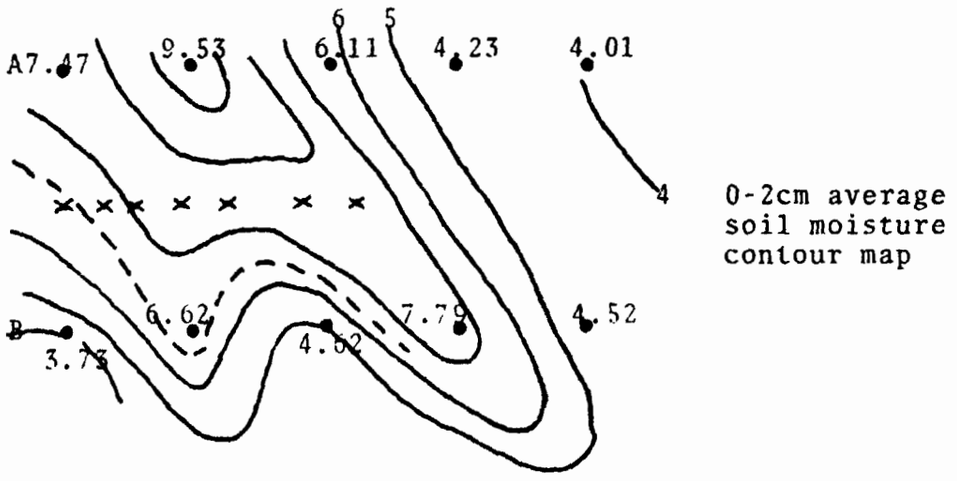

Figure V-5. Apparent Temperature for the Smooth Field on July 30, 1973.

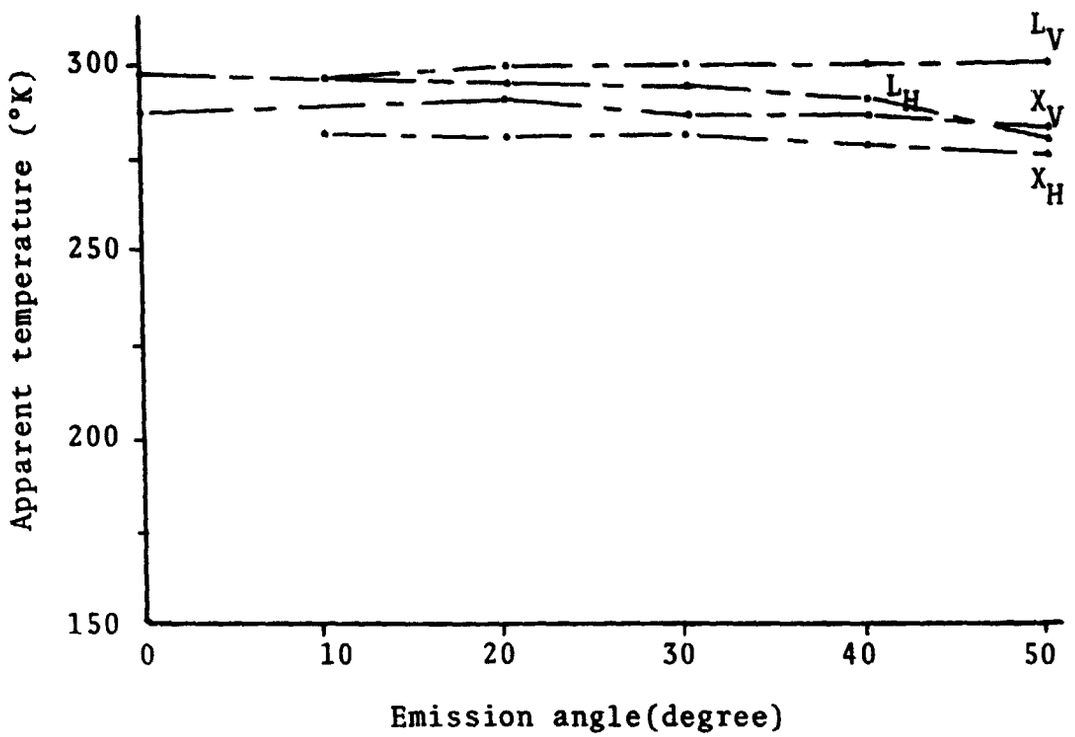

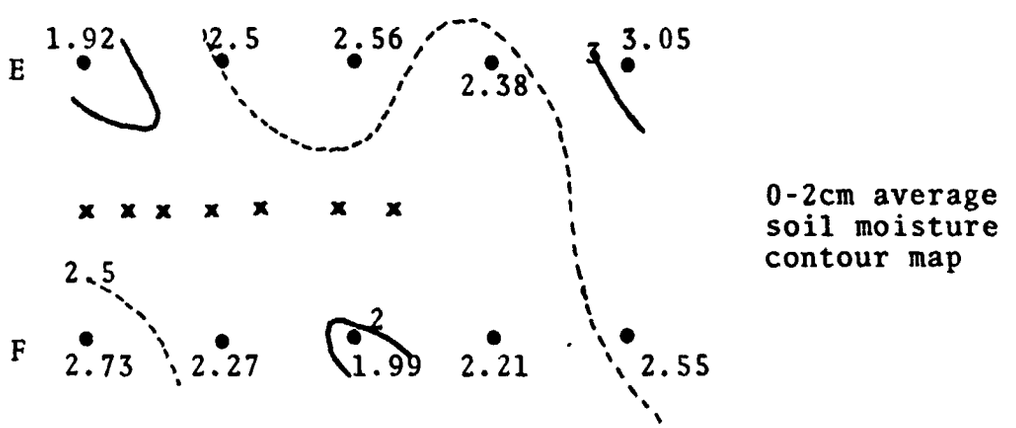

Figure V-6. Apparent Temperature for the Medium Rough Field on July 24, 1973.

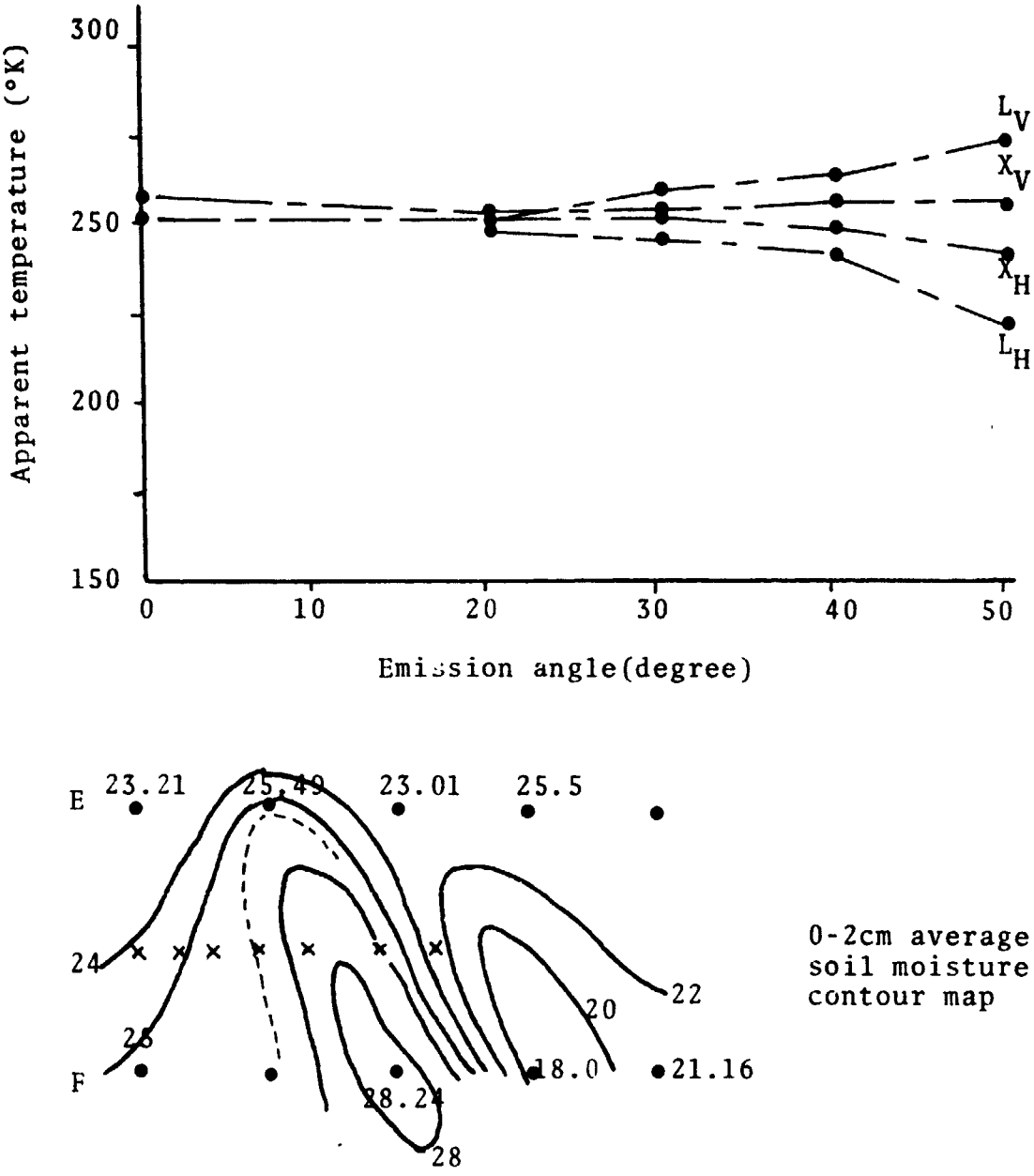

Figure V-7. Apparent Temperature for the Medium Rough Field on July 26, 1973.

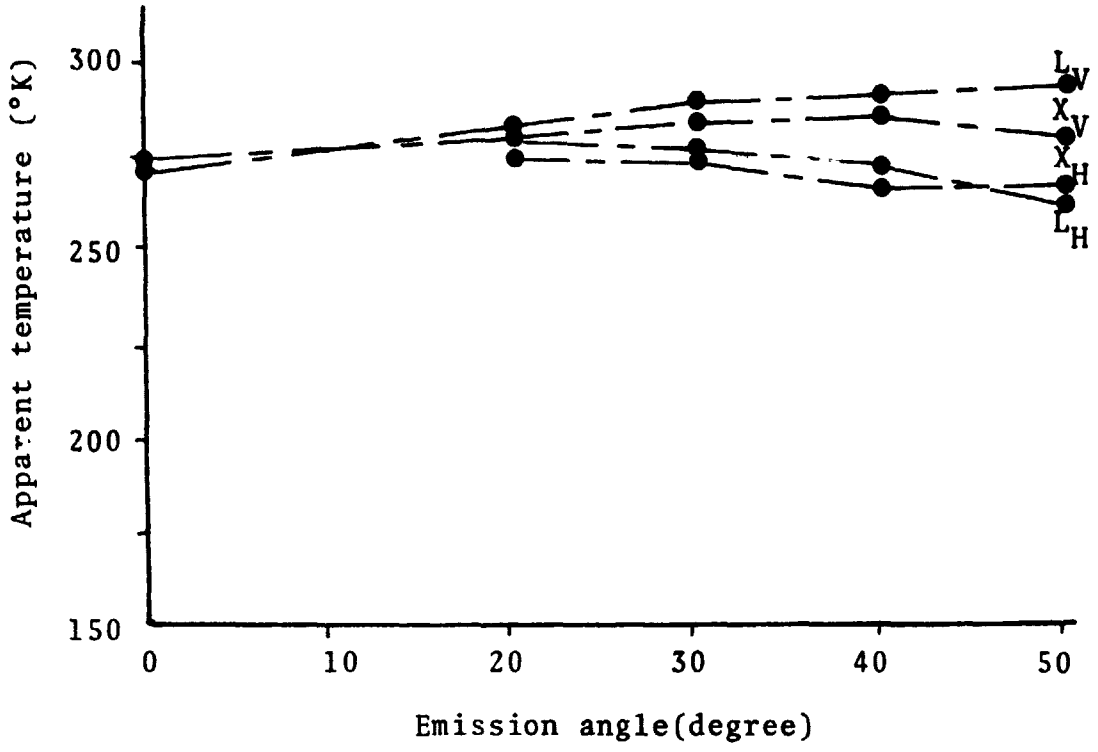

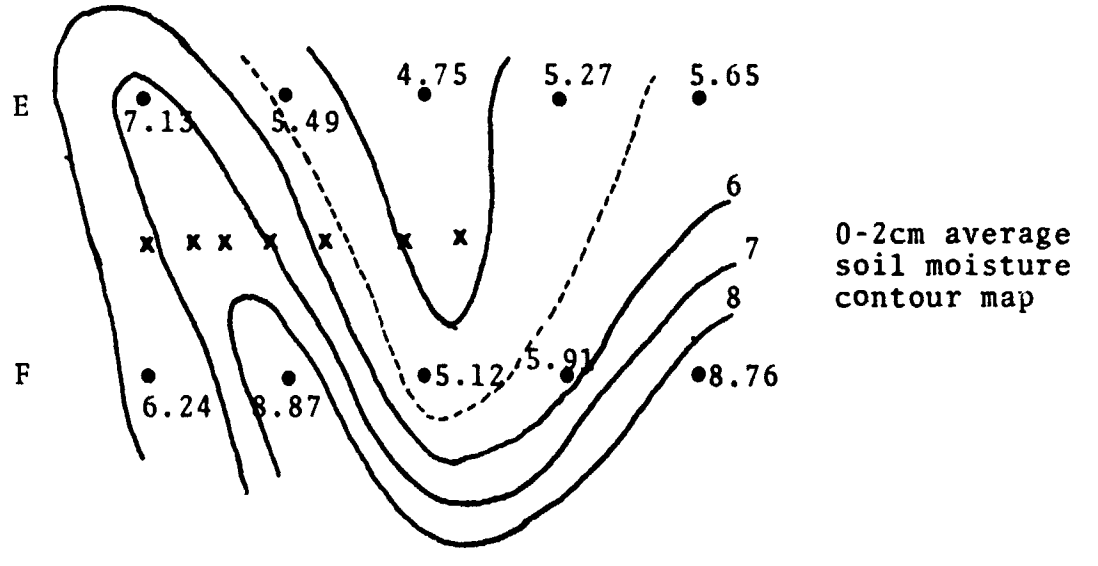

Figure V-8. Apparent Temperature for the Medium Rough Field on July 30, 1973.

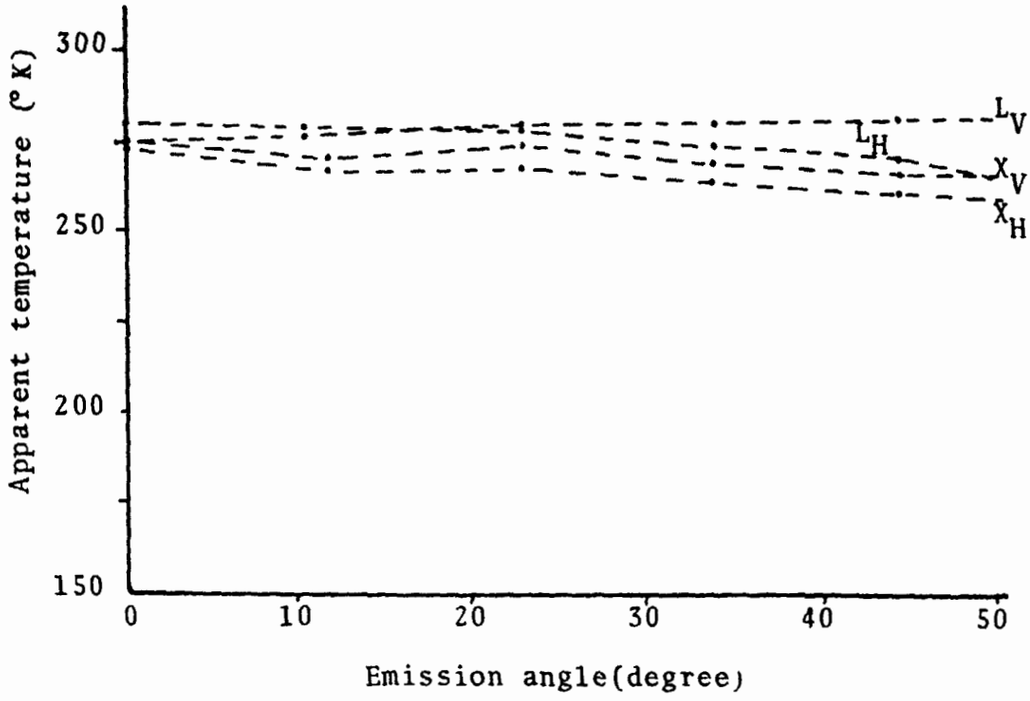

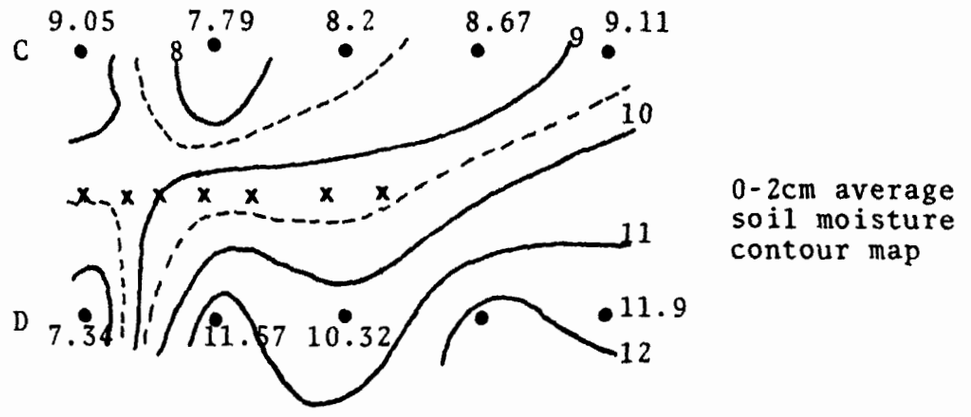

Figure V-9. Apparent Temperature for the Rough Field on July 23, 1973.

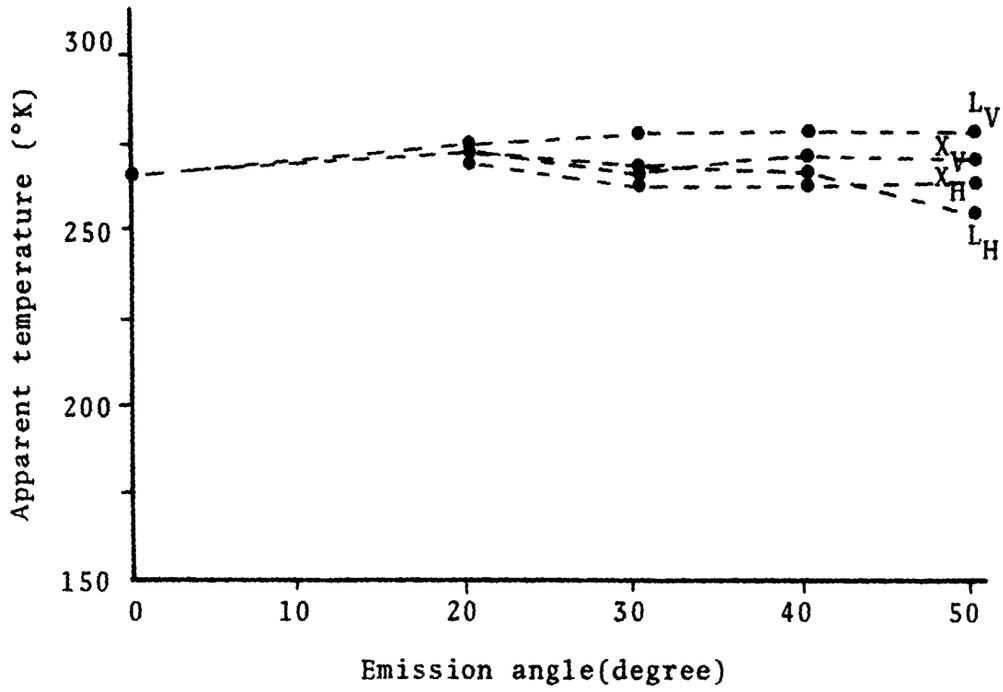

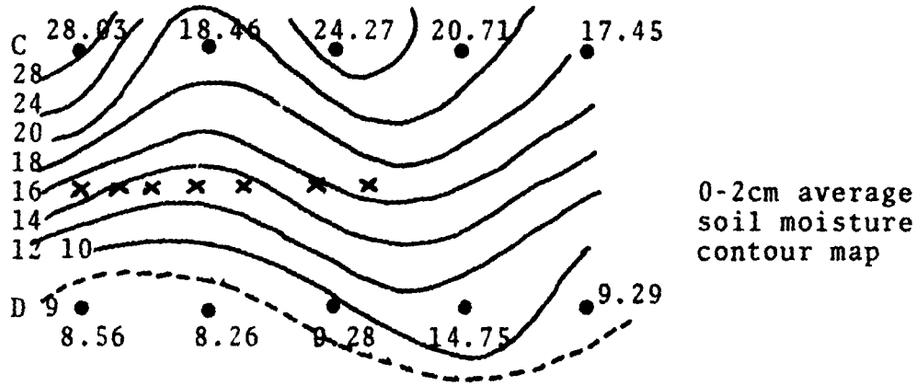

Figure V-10. Apparent Temperature for the Rough Field on July 26, 1973.

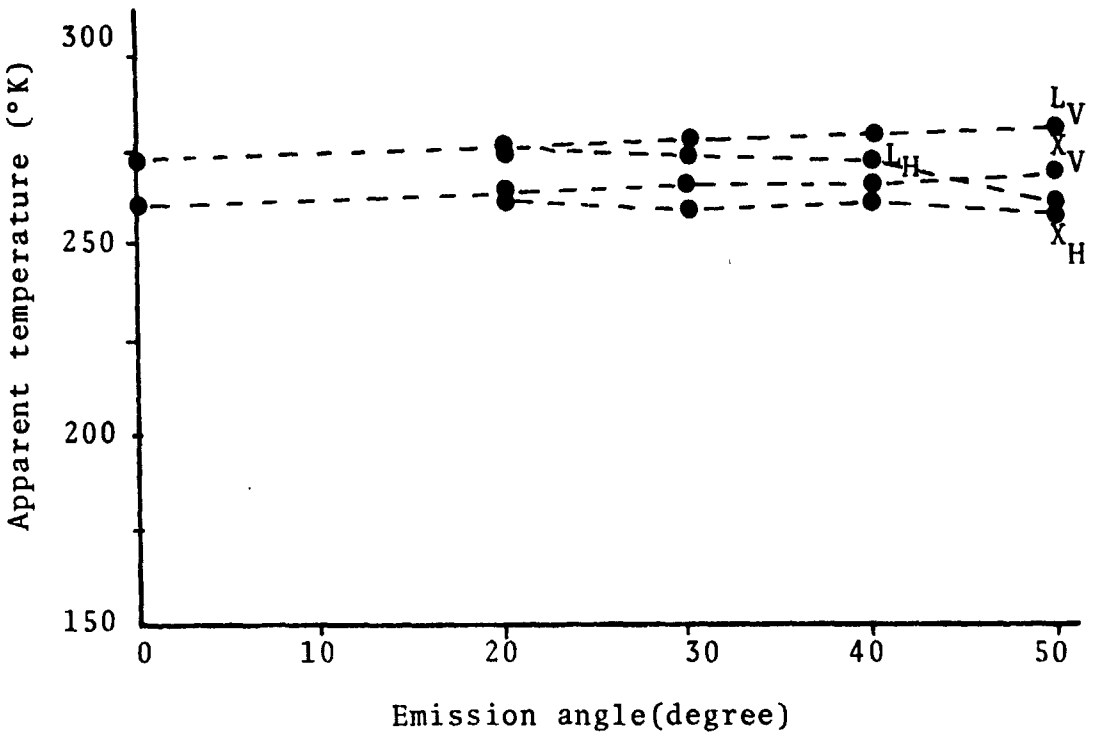

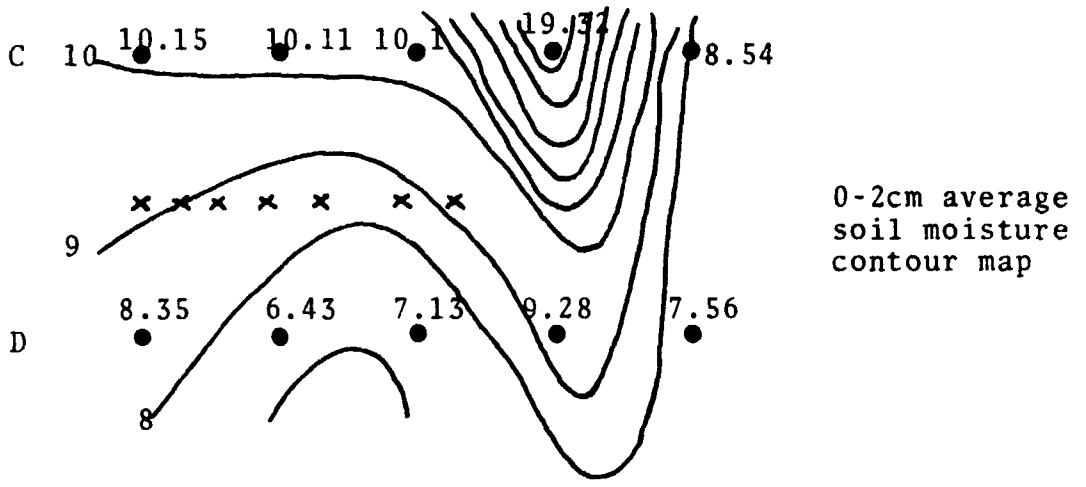

Figure V-11. Apparent Temperature for the Rough Field on July 30, 1973.

Figures V-12 through V-23 are plots of apparent temperatures of the three surfaces versus soil moisture content. These plots are shown for both X- and L-band frequencies at vertical and horizontal polarizations. The 0-2 cm average soil moistures and 0-18 cm average soil moistures are used to correlate with the apparent temperatures. The parameter of equivalent soil moisture at the conventionally defined skin depth is also used to correlate with the apparent temperature, but the apparent temperature used is that of the average of the apparent temperatures of the various observation angles. The equivalent soil moisture represents the effective soil moisture condition of the field on the particular day. Its accuracy was computed to be within minus seven-percent and plus five-percent for any particular day and field. Studying the correlations of these three soil moisture parameters with apparent temperature, an attempt was made to determine an optimal soil moisture parameter.

Examining the L-band results (Figures V-12 through V-16) and X-band results (Figures V-17 through V-19), several observations can be made of the effects of surface roughness, regardless of the measurement frequencies. The data seem to indicate that for wet soil there is a monotonic increase in apparent temperature as

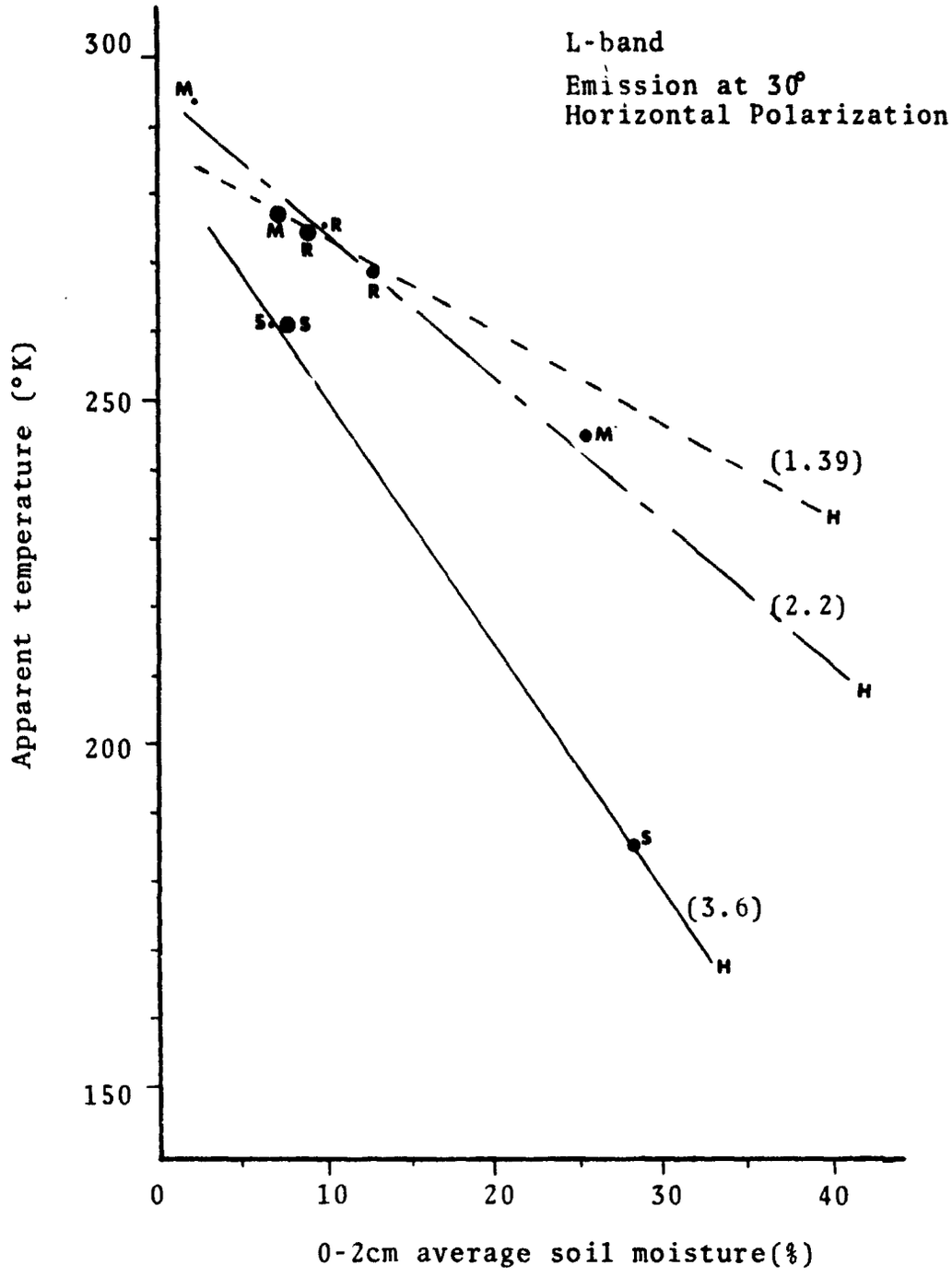

Figure V-12. Apparent Temperature versus Soil Moisture Content, Bare Condition.

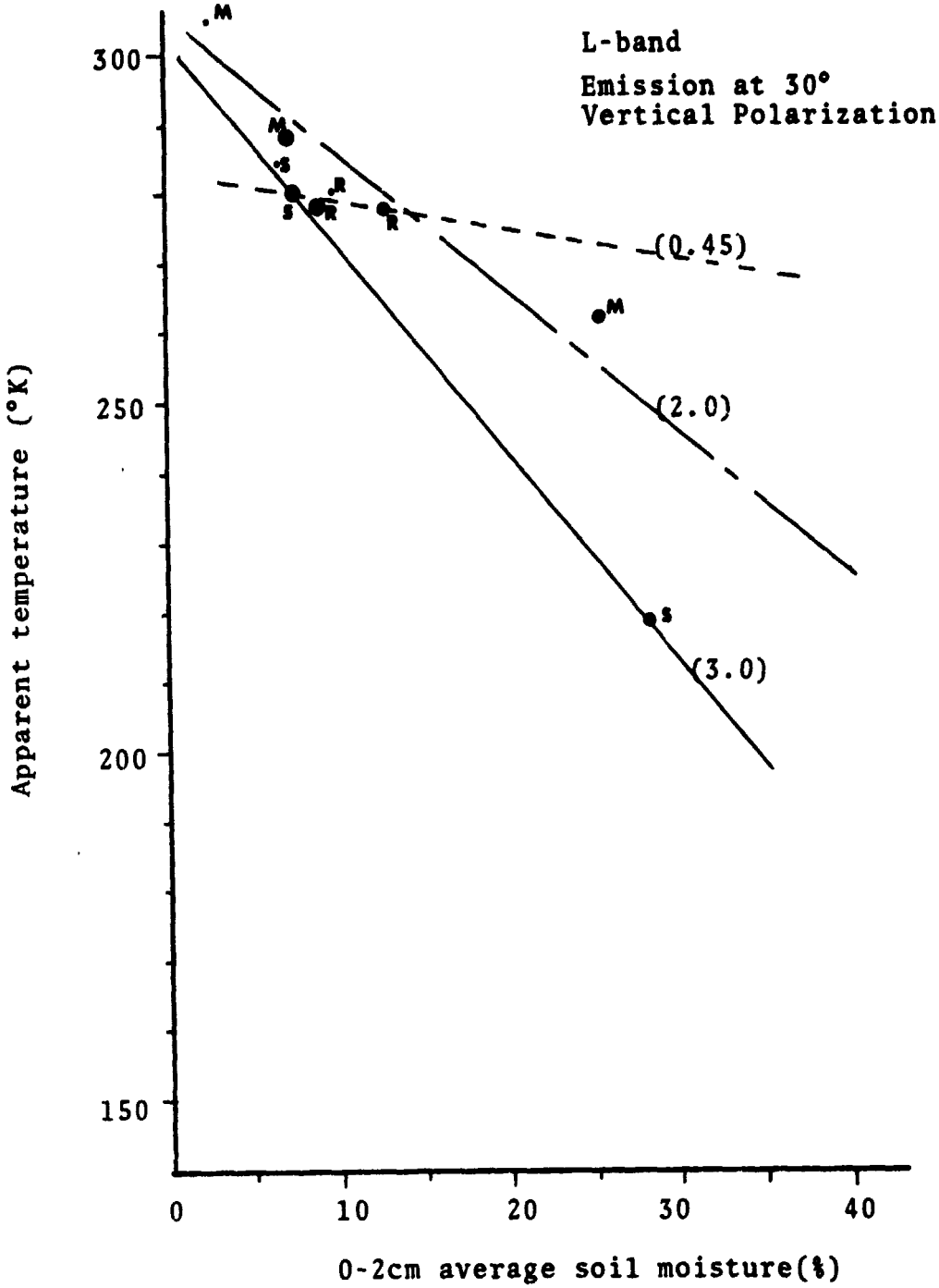

Figure V-13. Apparent Temperature versus Soil Moisture Content, Bare Condition.

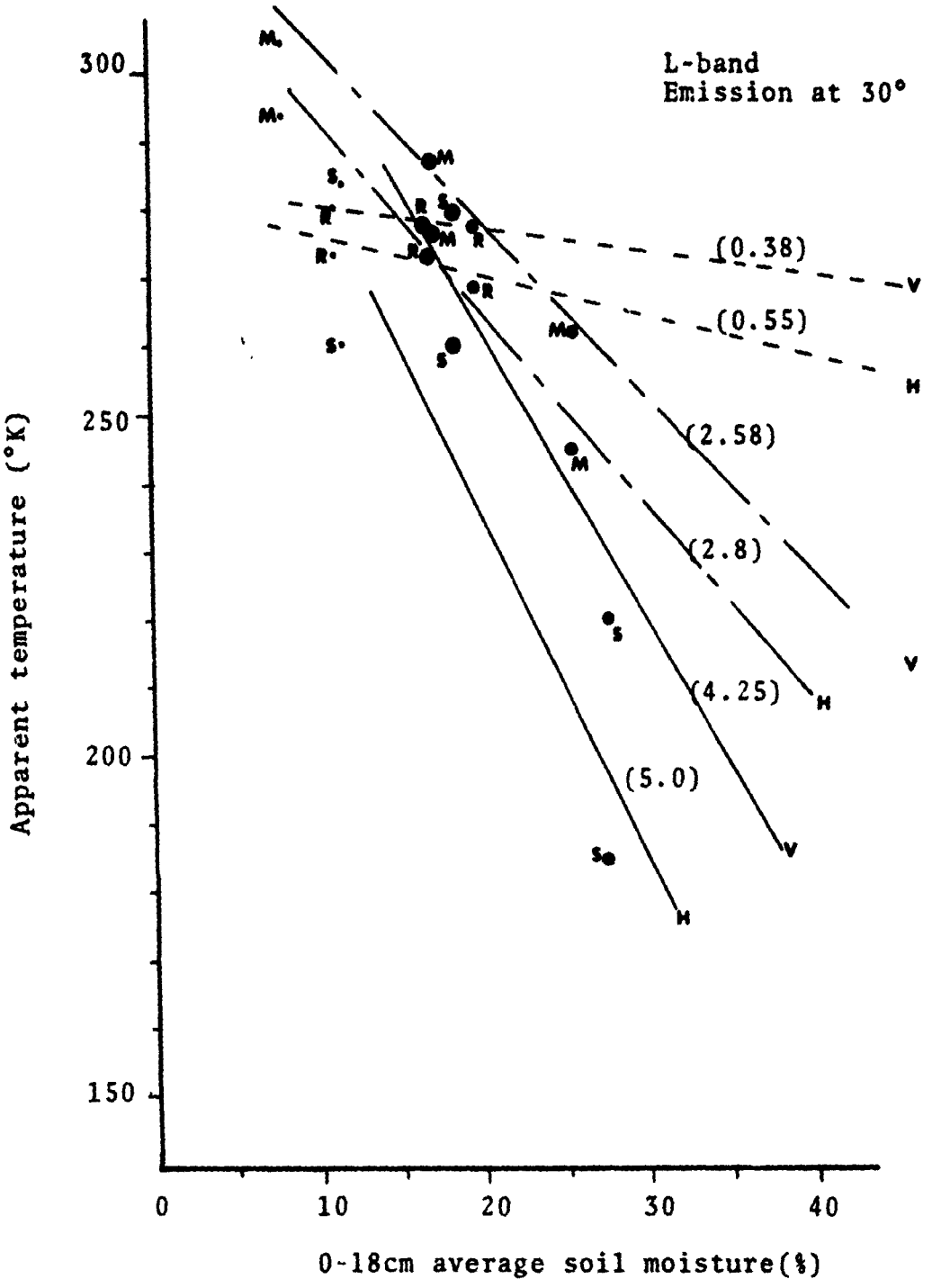

Figure V-14. Apparent Temperature versus Soil Moisture Content, Bare Condition.

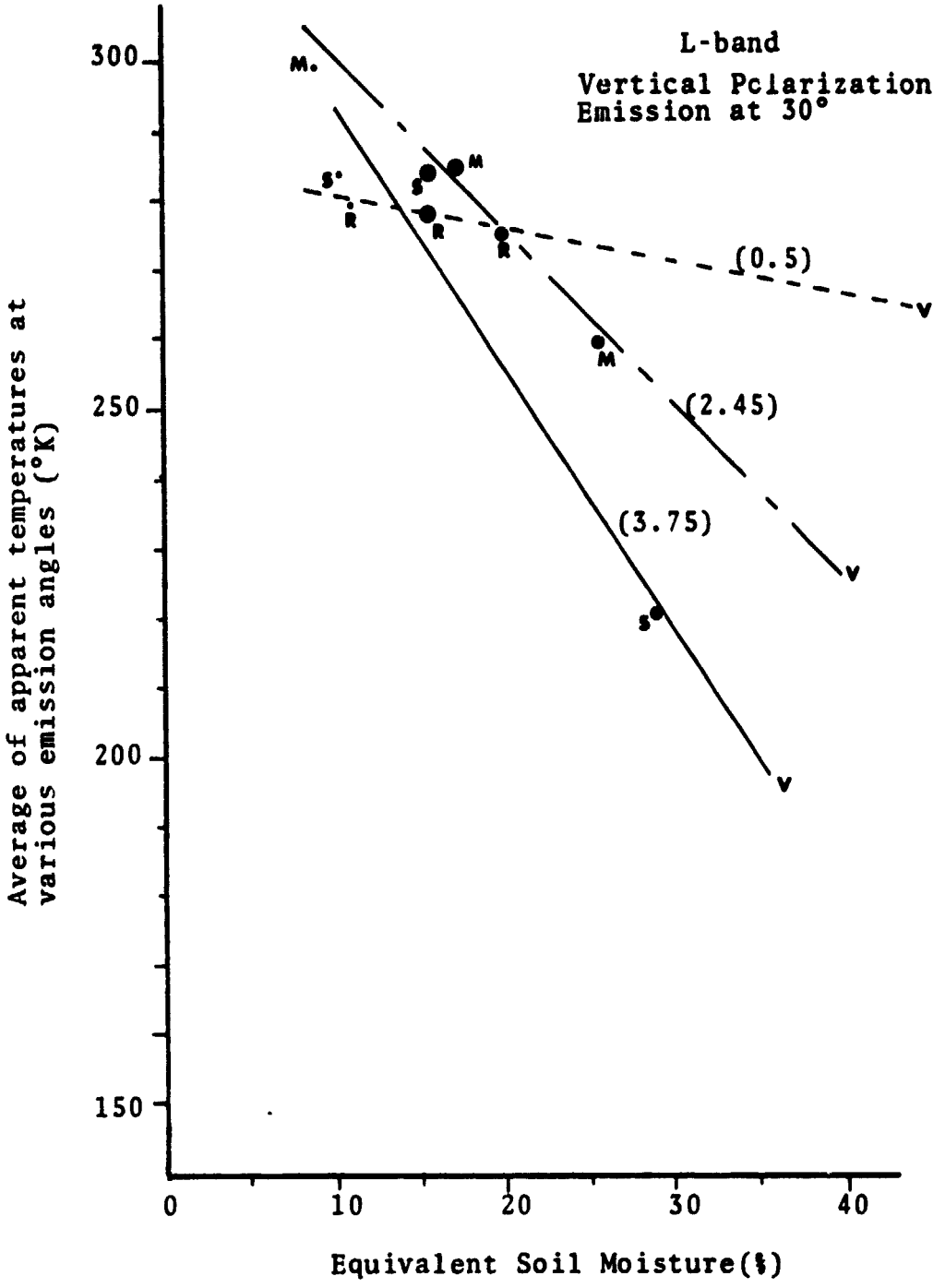

Figure V-15. Apparent Temperature versus Soil Moisture Content, Bare Condition.

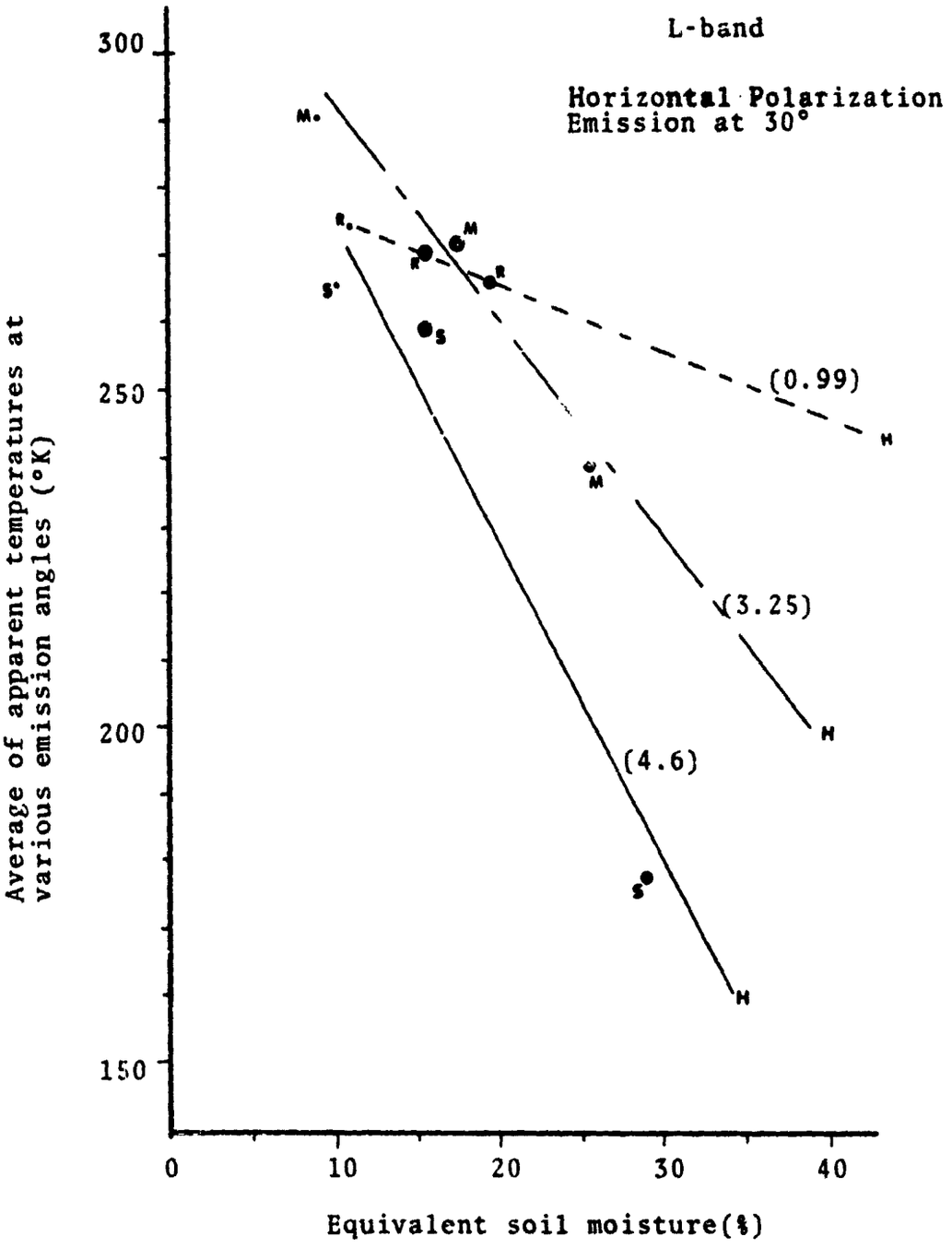

Figure V-16. Apparent Temperature versus Soil Moisture Content, Bare Condition.

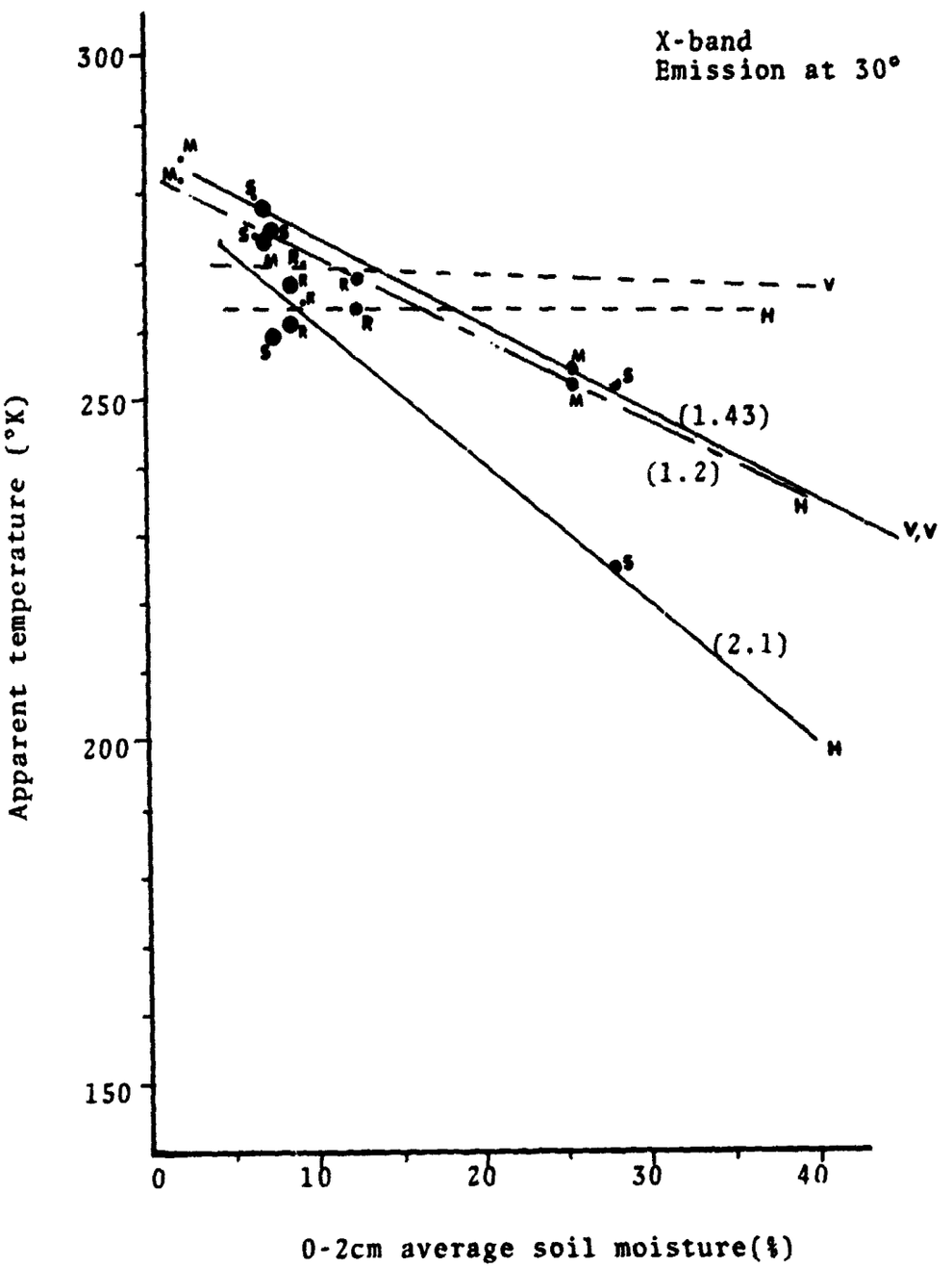

Figure V-17. Apparent Temperature versus Soil Moisture Content, Bare Condition.

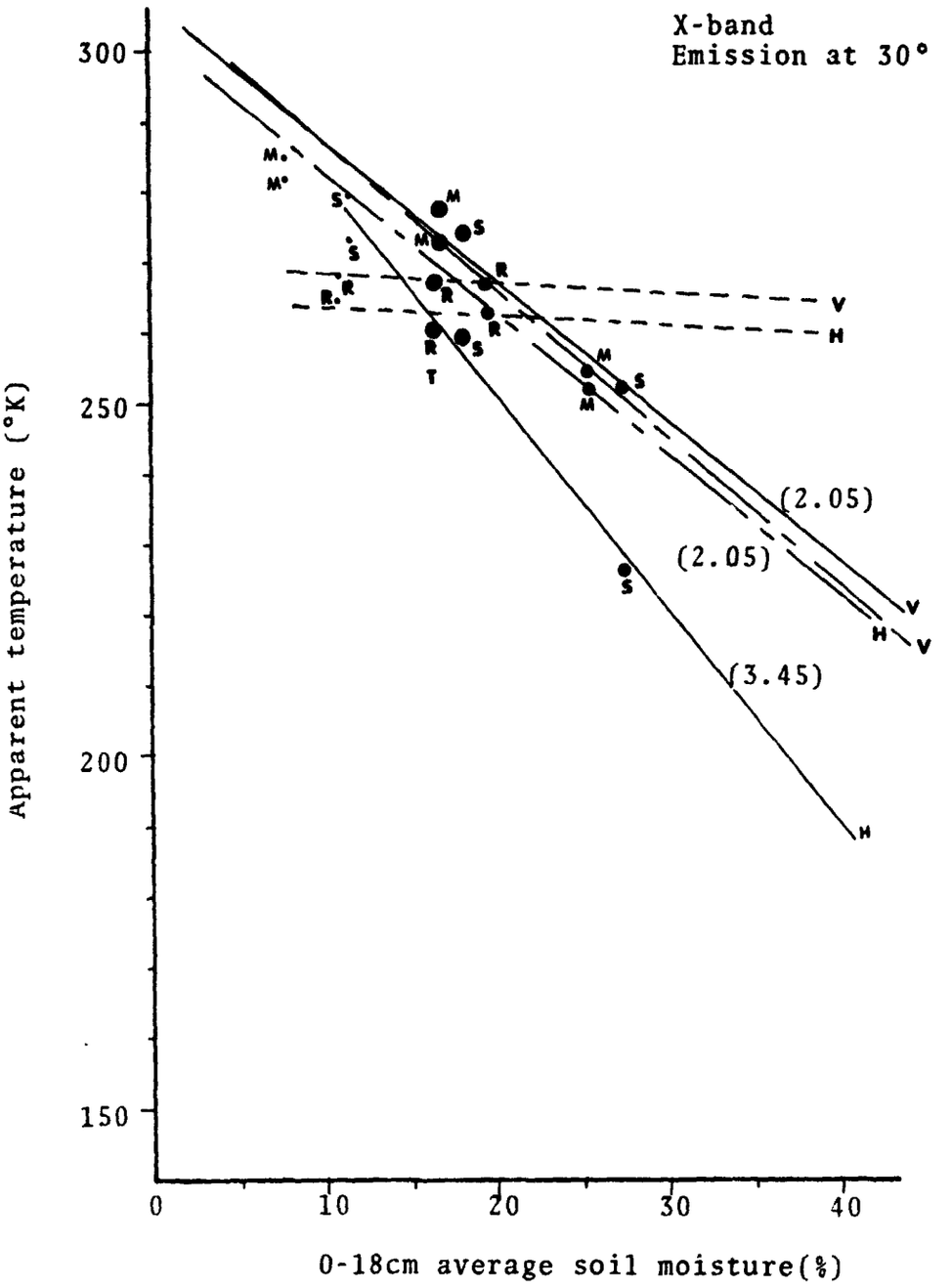

Figure V-18. Apparent temperature versus Soil Moisture Content, Bare Condition.

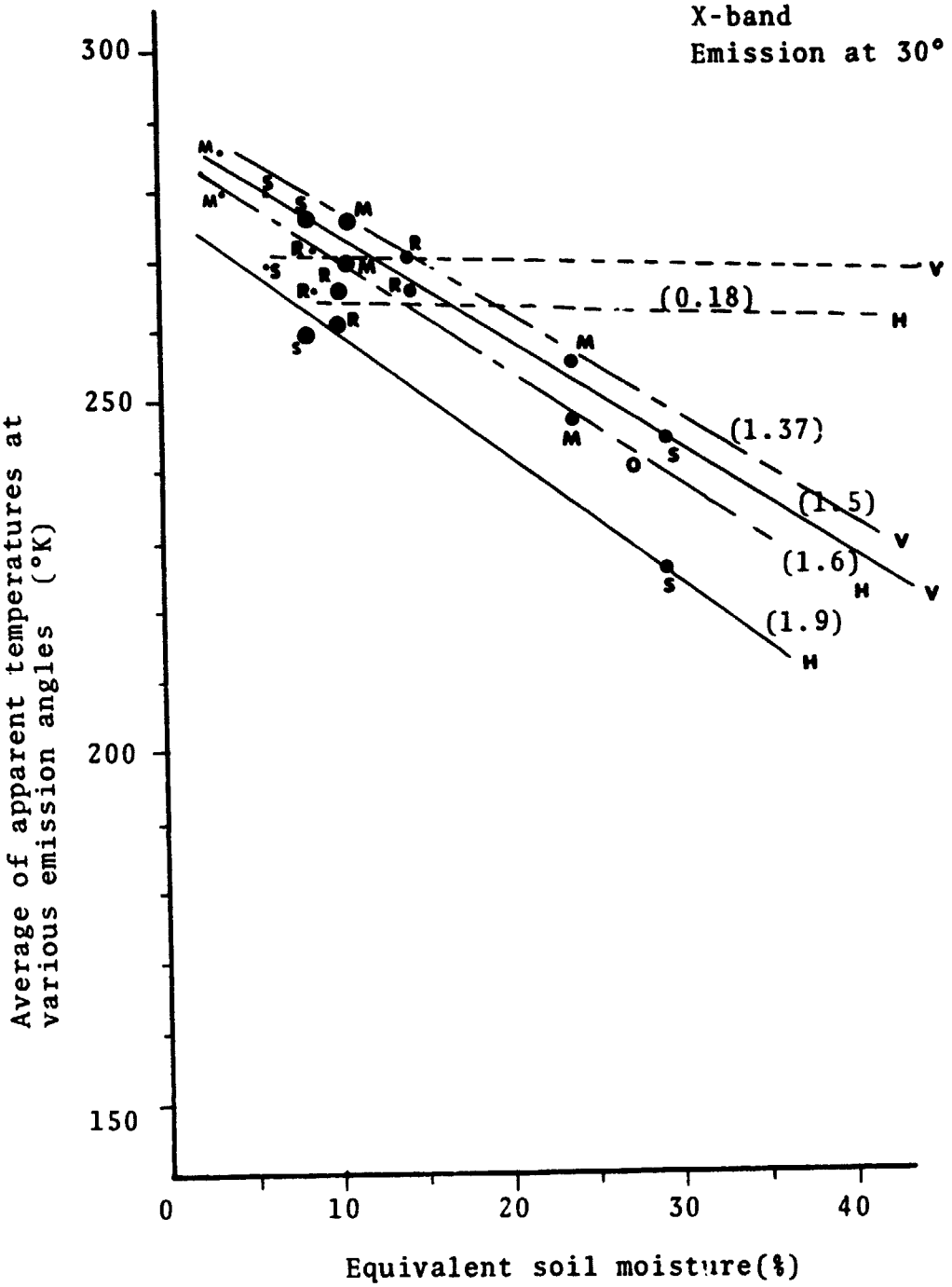

Figure V.19. Apparent Temperature versus Soil Moisture Content, Bare Condition.

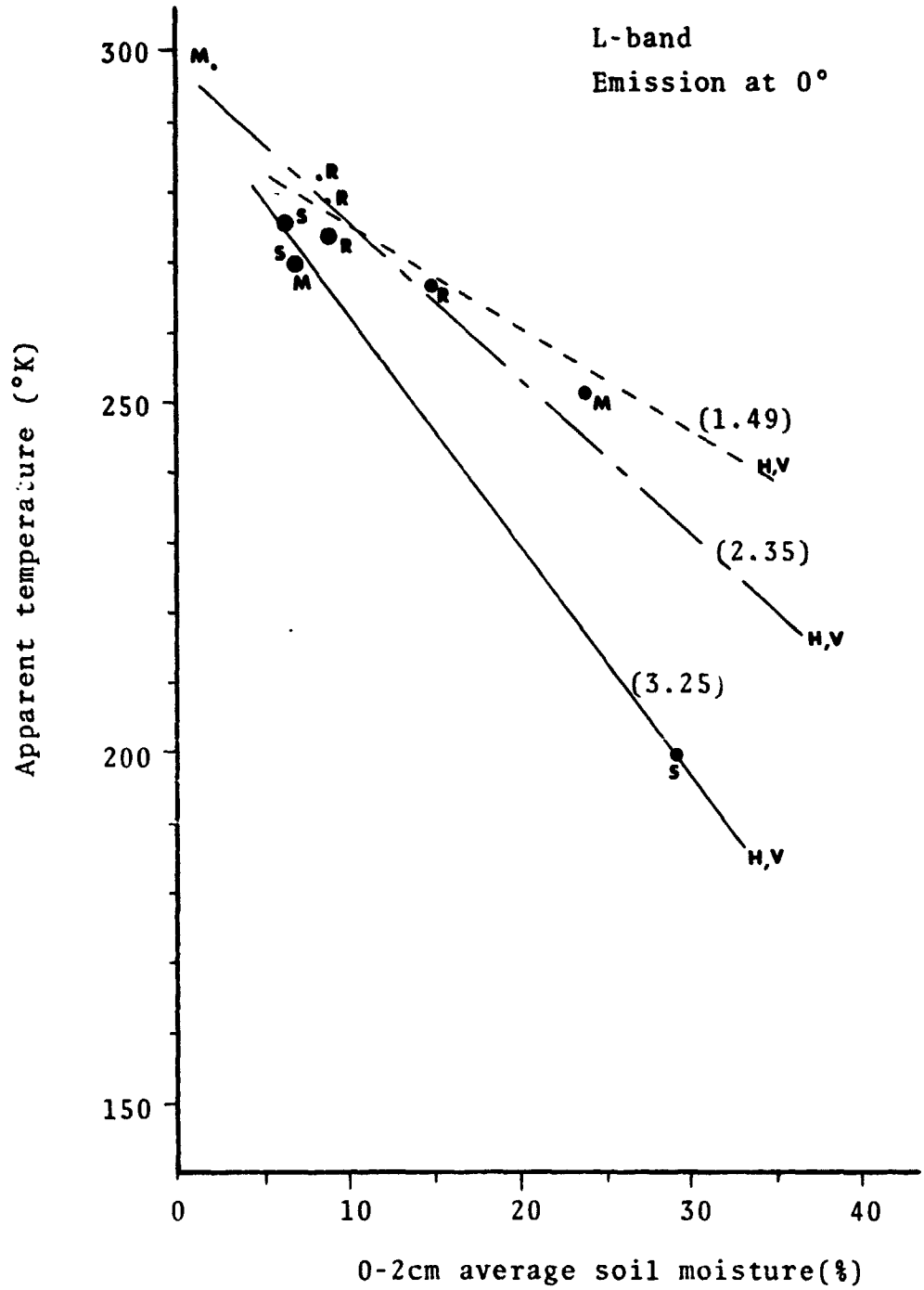

Figure V-20. Apparent Temperature versus Soil Moisture Content, Bare Condition.

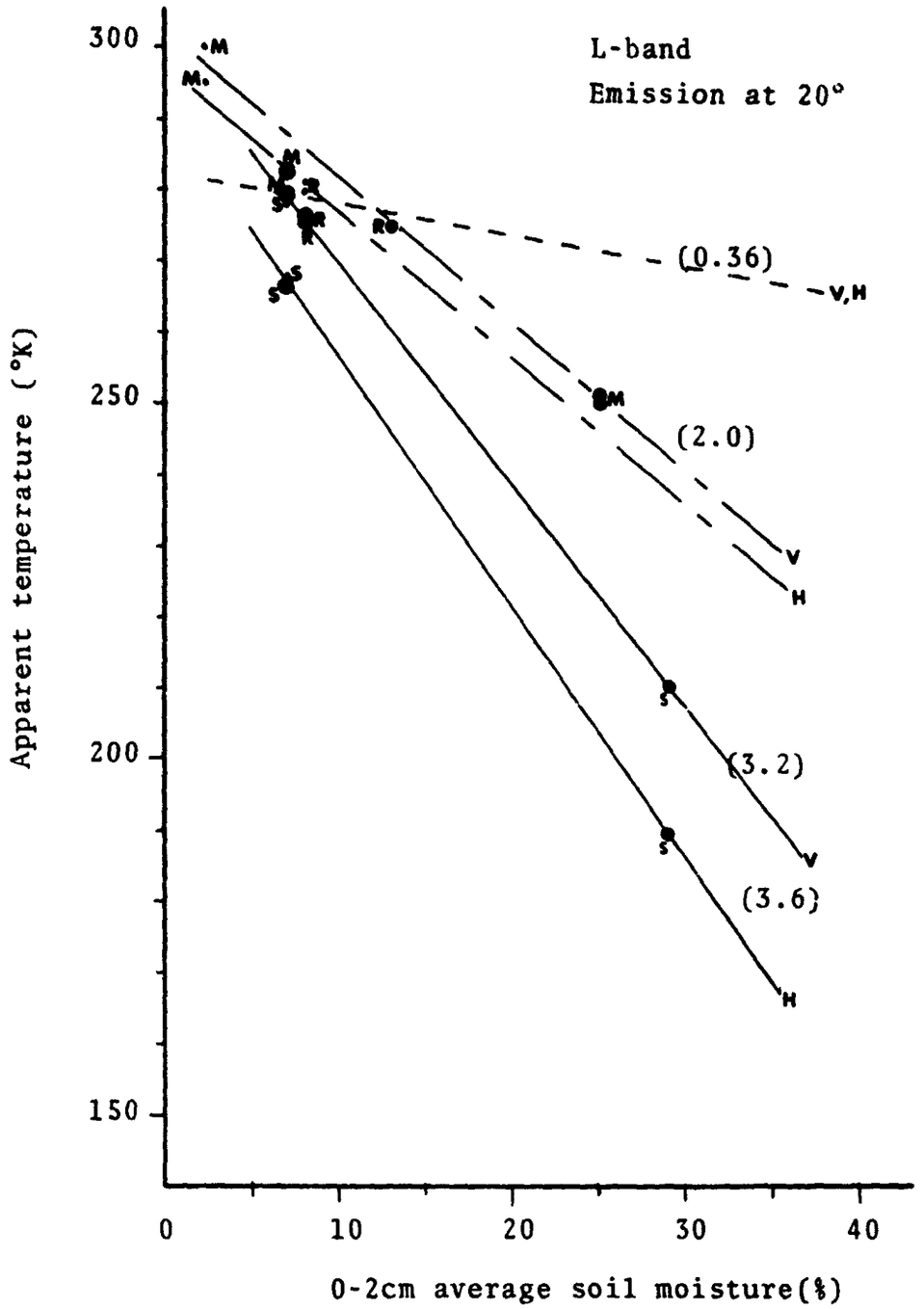

Figure V-21. Apparent Temperature versus Soil Moisture Content, Bare Condition.

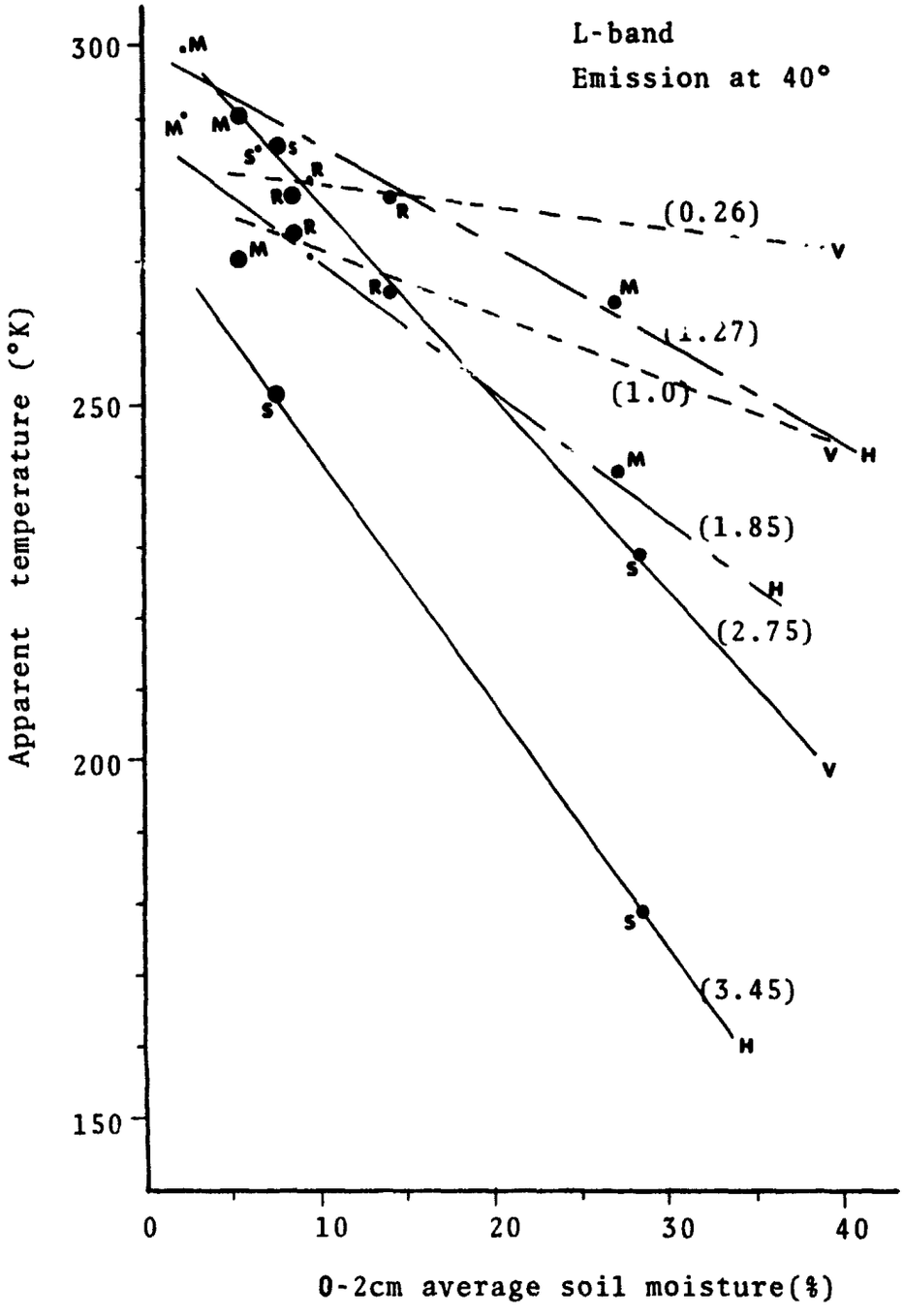

Figure V-22. Apparent Temperature versus Soil Moisture Content, Bare Condition.

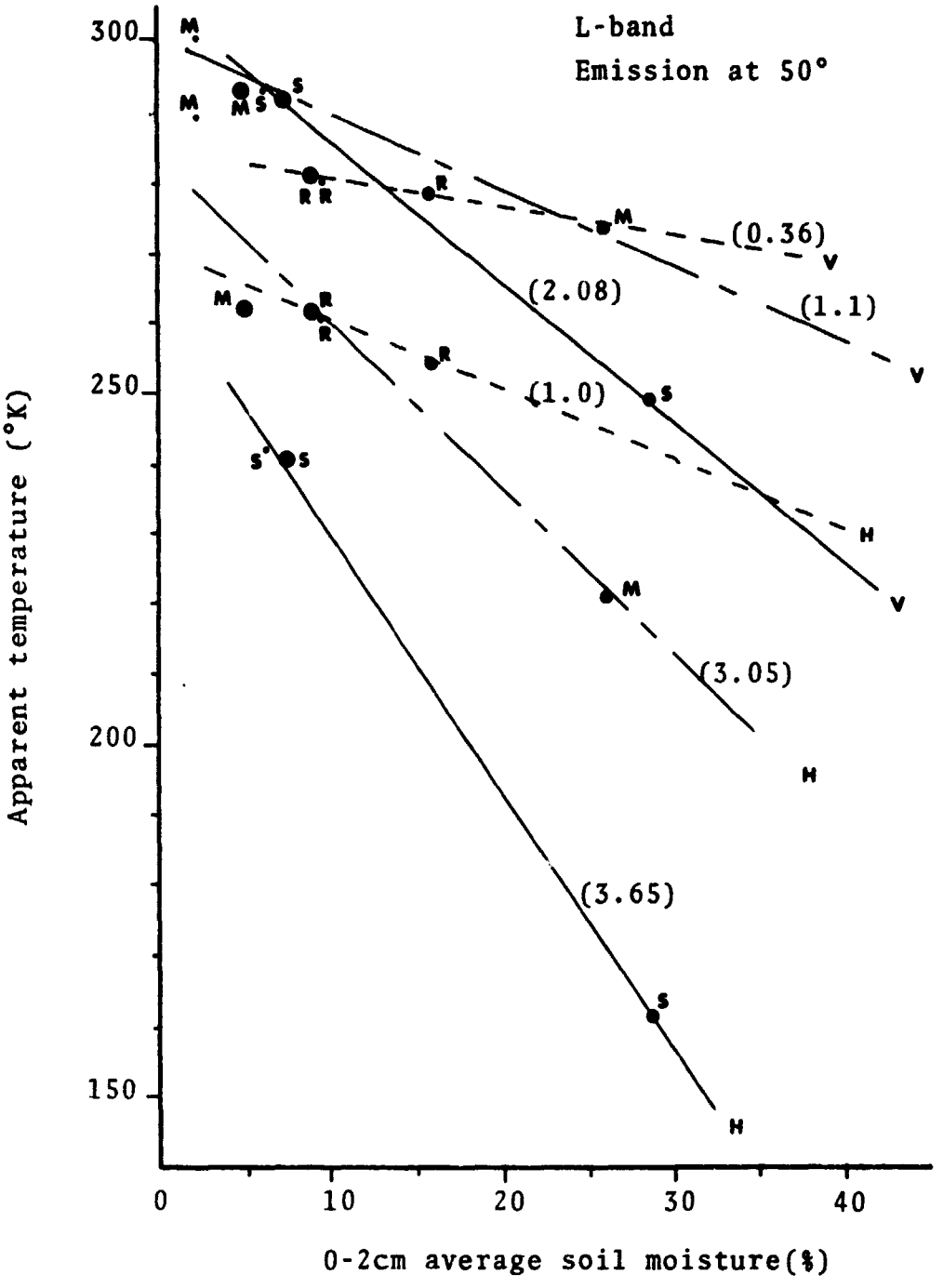

Figure V-23. Apparent Temperature versus Soil Moisture Content, Bare Condition.

surface roughness increases. This phenomenon is due to the fact that as the surface roughness increases, the surface area available for emission also increases. However, it is interesting to note that for the lower moisture range, the apparent temperatures for the very rough surface fall below those of the medium rough field for the L-band measurements and fall below those of the smooth surface for the X-band measurements. But the behavior of the available rough surface data suggest that as the moisture content increases, the apparent temperatures would exceed those of the medium rough field.

Another observation that can be made about the roughness effects is its effect on polarizations, this effect can be readily seen from Figures V-12, V-13, V-15, V-16, and V-17. It is shown that roughness has little effect on vertical polarization measurements; whereas at horizontal polarization the effects of roughness are readily apparent. This effect is particularly pronounced for the X-band measurements of the smooth surface on July 24th and July 30th, Figures V-17. For these two dates, the 2 cm. soil moisture average is essentially the same despite the fact that the field was irrigated on July 25. Assuming that the irrigation process (a sprinkling process) caused the field to appear smoother than it was on July 23, the data indicate that horizontal polar-

ization is affected by surface roughness to a much greater extent than vertical polarization.

The sensitivities (degree Kelvin/percent soil moisture) of all the measurement results are calculated and are indicated within the parenthesis on the figures. Examining these data, it is noted that the response to soil moisture decreases as the surface gets rougher. This pattern of behavior is apparently independent of the observation angles, as indicated on Figures V-20, V-21, V-12, V-13, V-22, and V-23. It should be noted that sensitivities stay essentially the same at all observation angles. While the horizontal polarization is more sensitive to surface roughness than the vertical polarization, it is also more sensitive to soil moisture variations than the vertical polarization for both L-band and X-band and for all three surface roughnesses. There are good sensitivities for the smooth surface and medium rough surface measurements at both L-band and X-band. However, the available data suggest that the sensitivity almost disappears for the very rough surface of this experiment (the roughness characteristics are given in Table IV-1).

Comparing the L-band and X-band measurements, a choice for the more optimal frequency for soil moisture detection is obvious. It can be seen that the L-band is more sensitive to soil moisture variations than the X-band for

all surface types. This is another effect of surface roughness, as roughness is not an absolute measure, but a relative measure expressed in wavelength units. For surface roughness much less than a wavelength, the surface appears smooth, while for surface roughness on the order of a wavelength or more, the surface appears rough [17]. For the field surfaces of this experiment (roughness characteristics shown on Table IV-1), the surfaces appear rougher to the X-band (wavelength λ = 2.82 cm) than they are to the L-band (wavelength λ = 21.2cm). It therefore is not a surprising observation that the X-band measurements are less sensitive in detecting soil moisture than L-band, since it was observed that sensitivity decreases as roughness increases.

After studying the correlation of apparent temperature with the three soil moisture parameters (0-2 cm average soil moisture, 0-18 cm average soil moisture, and equivalent soil moisture at conventionally defined skin depth) several observations can be made. For the X-band the 0-2 cm average soil moisture and the equivalent soil moisture parameters give better correlation than the 0-18 cm average soil moisture parameter. The correlation is reasonably good for the 0-2 cm average soil moisture parameter and particularly good for the

equivalent soil moisture parameter. It therefore appears that for X-band, the equivalent soil moisture at skin depth would be a valid and perhaps the optimal soil moisture parameter.

For L-band, the case is a little different. For the medium rough and rough surfaces, the equivalent soil moisture parameter gives better correlation with apparent temperature than the 0-2 cm average and 0-18 cm average soil moisture parameters. It appears that the equivalent soil moisture parameter is again the optimal soil moisture parameter to use for the medium rough and rough surfaces. However, its validity for the smooth surface case is questionable. Examining the data, the apparent temperature of the smooth field for July 24 and July 30 plotted as a function of average soil moisture in the 0-2 cm depth fall very close together. However, plotted as a function of equivalent soil moisture, they spread apart. It is difficult to draw conclusions as to the validity of the equivalent soil moisture parameter for the smooth surface case from this observation, since there are only two data points in this soil moisture range available for comparison.

From these measurement results it is clearly indicated that surface roughness has a definite effect

on the radiometric apparent temperature measurements for soil moisture on various rough surfaces. It has also demonstrated that there is a definite correlation between the apparent temperature of the soil and the soil moisture content. Based on the correlations with equivalent soil moisture as the optimal soil moisture parameter, the following sensitivity values are observed: for the L-band, sensitivities of vertical polarization measurements are 3.75, 2.45, and 0.5 degree Kelvin/percent soil moisture for the smooth, medium rough, and rough surface respectively; likewise, sensitivities of horizontal measurements are 4.6, 3.25, and 0.99 degree Kelvin/percent soil moisture. For the X-band, the vertical polarization measurement sensitivities are 1.5, 1.37, and 0.15 degree Kelvin/percent soil moisture for the smooth, medium rough, and rough surface respectively; the horizontal polarization measurements are 1.9, 1.66, and 0.18 respectively.

Effects of Vegetation

Effects of vegetation are observed from the results of the entire experiment program, from the period when the fields are bare and throughout the period when the fields are vegetated. Since the field roughness remained essentially the same throughout the entire experiment, any new effect observed after the fields were vegetated

would come primarily from the vegetation.

Oats were sowed on the three fields on September 3, 1973. The vegetation characteristics necessary for the evaluation of Sibley's model [27] were noted on each radiometric measurement. This information is provided on Table V-1. From this table it can be seen that the oats of this experiment exhibited roughly three stages of growth. It was a very young vegetation in September, 1973; it became full grown and healthy throughout October and November, then it exhibited retrogradation in growth by February, 1974.

An unusual behavior in the polarization dependency of apparent temperature was noted when studying the measurement data. The phenomena observed are the change in dependence on polarization and the lack of dependence on polarization. These observations are noted on October 30, 1973 for the smooth surface and medium rough surface, on October 30 and November 8, 1973 for the rough surface. They are as shown on Figures V-24 through V-27. Notice that this change in dependence on polarization seems to occur only for the X-band measurements. The horizontal polarization data are consistently higher than the vertical polarization data. There is also a lack of dependence on polarization for these X-band measurements, this behavior is particularly apparent on November 8, 1973 for

Table V-. . The Oats Vegetation Characterizations

Date	Surface Type	Fraction of Water By Weight in the Oats, F	Volumetric Density of Oats, D	Height of Oats, H
Sept. 25, 1973	Smooth	84%	0.3%	5"
	Medium rough	85%	0.3%	5"
	Rough	85%	0.3%	5"
October 30, 1973	Smooth	87%	1.7%	10"
	Medium rough	87%	1.8%	10"
	Rough	88%	1.85%	11"
November 8, 1973	Smooth	81.5%	1.3%	11"
	Medium rough	83.5%	1.4%	13"
	Rough	84.9%	1.4%	14"
February 13, 1973	Smooth	72.6%	0.8%	12"
	Medium rough	75%	0.9%	14"
	Rough	76%	0.9%	14"

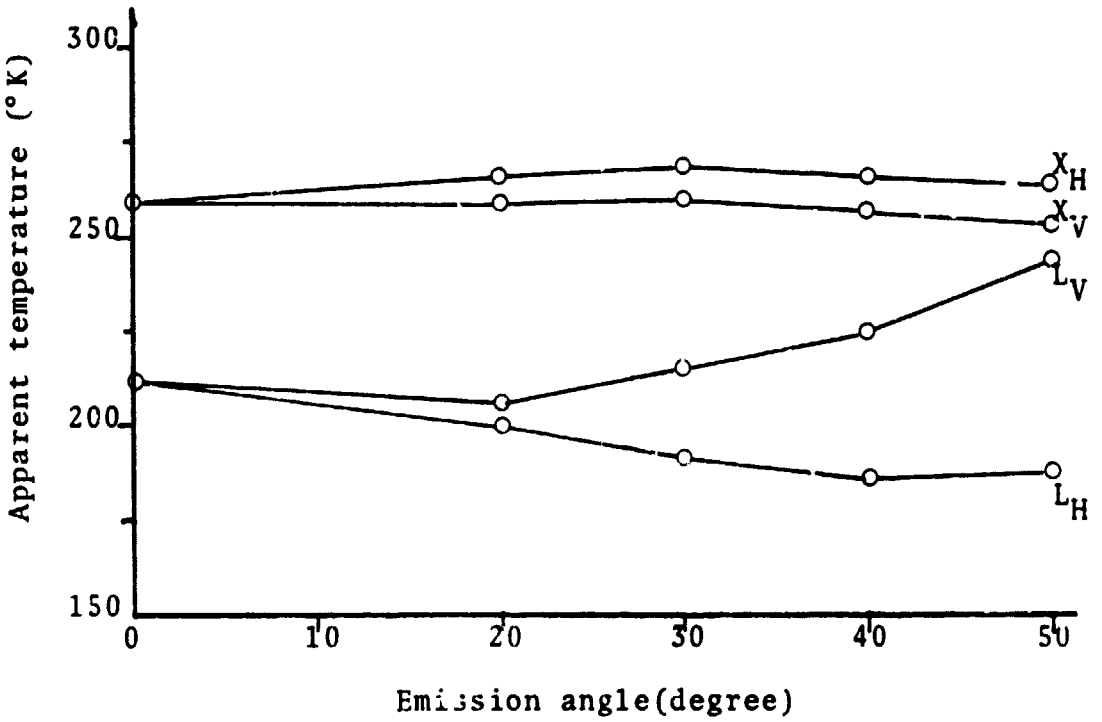

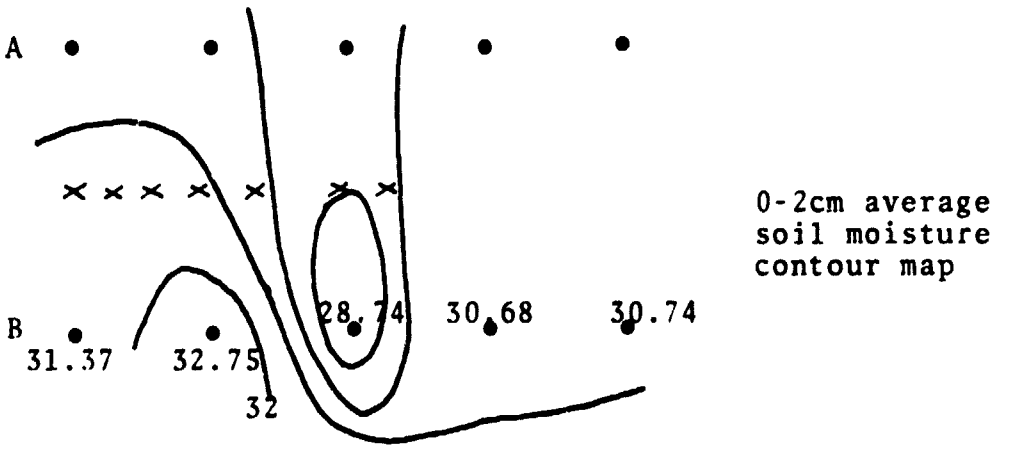

Figure V-24. Apparent Temperature for the Smooth Field on October 30, 1973.

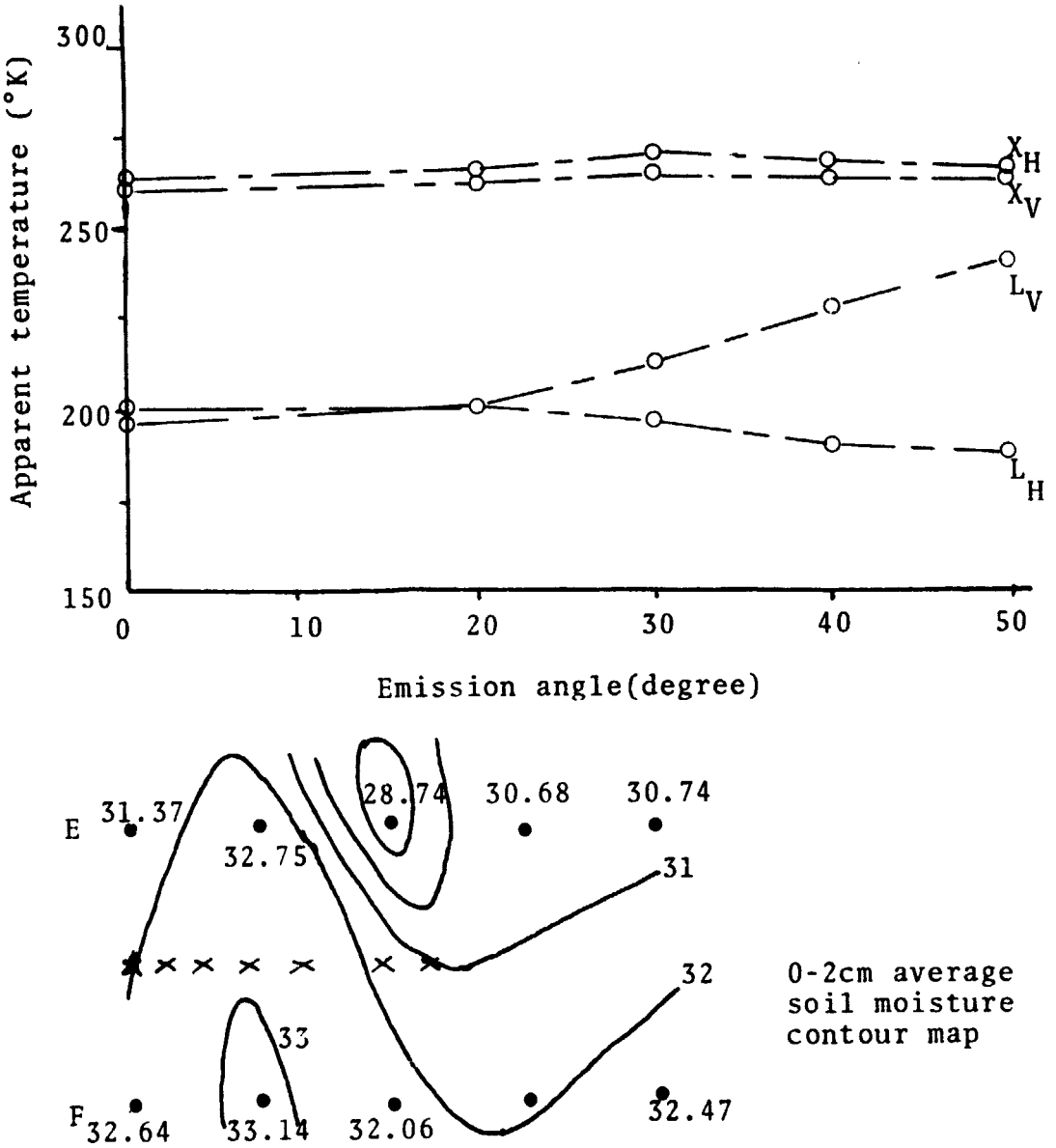

Figure V-25. Apparent Temperature for the Medium Rough Field on October 30, 1973.

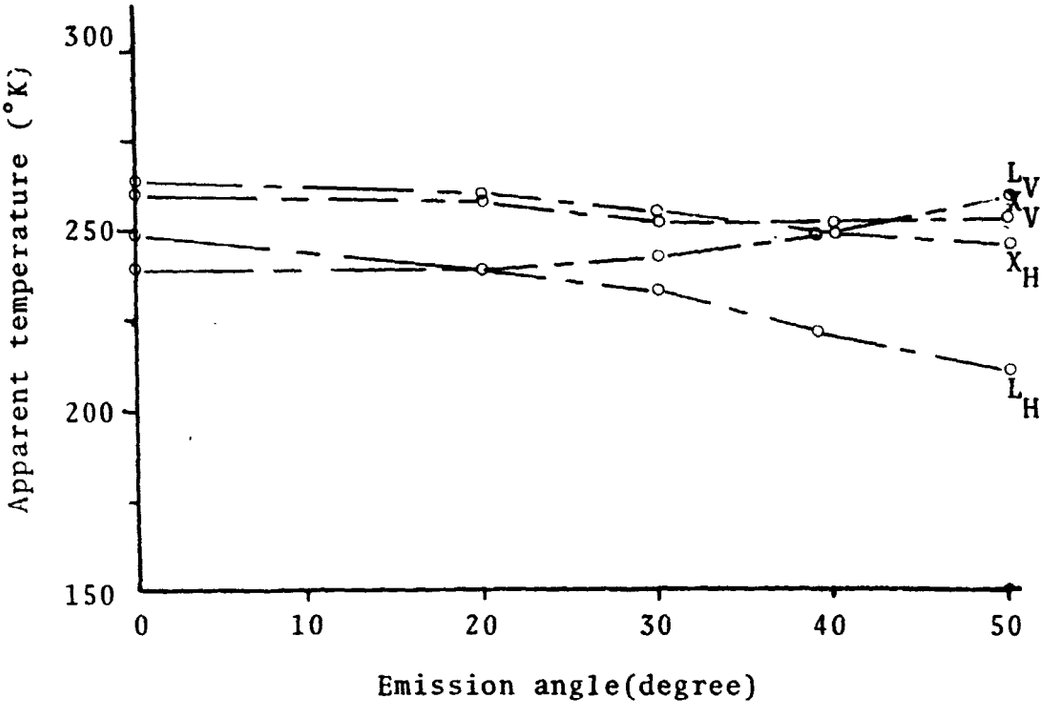

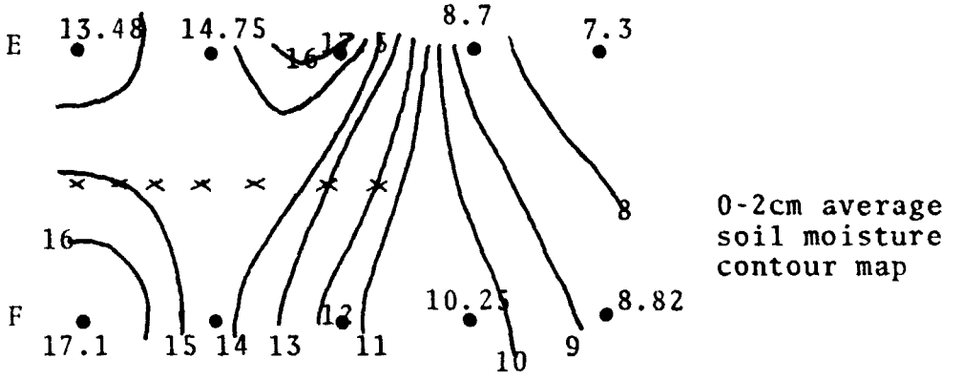

Figure V-26. Apparent Temperature for the Medium Rough Field on September 25, 1973.

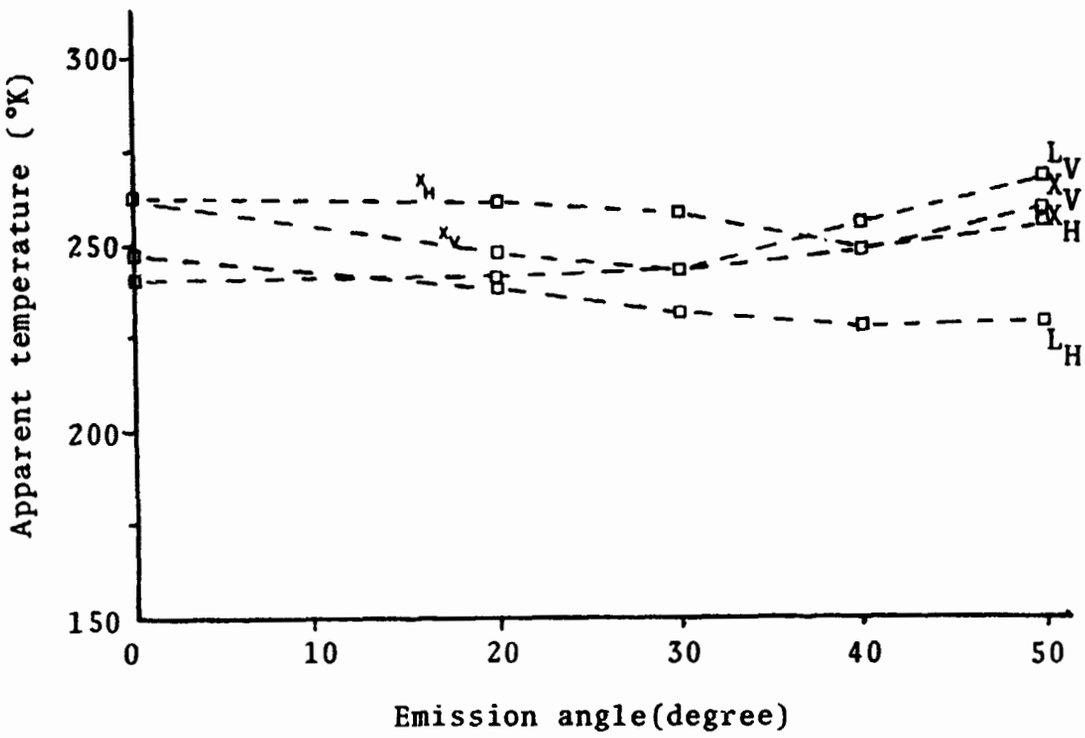

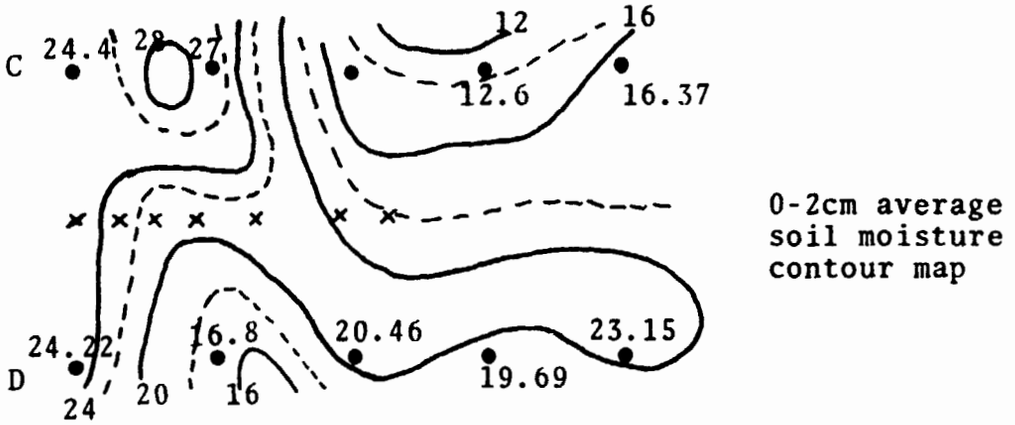

Figure V-27. Apparent Temperature for the Rough Field on November 8, 1973.

the rough field (Figure V-27). These are some observations made for the vegetated fields, at the present the available theoretical models are still inadequate to explain such phenomena.

Effects of vegetations are investigated from Figures V-28 through Figure V-41. Although the 0-2 cm average and 0-18 cm average soil moisture parameters are used in the analysis study, the observations presented below will primarily be pertaining to those shown for the equivalent soil moisture parameter. This is because the equivalent soil moisture parameter appears to be the optimal soil moisture parameter to be used from the bare field roughness effects analysis.

The vegetation measurement data and the comparisons between the vegetated measurements and bare field measurements are very encouraging. They tend to support Sibley's model [27] which predicts that the vegetation is essentially an attenuator at low vegetation density and a predominant emitter at high vegetation density. As an attenuator, the vegetation lowers the apparent temperature measurement; as a predominant emitter, it contributes and raises the apparent temperature.

Figures V-30, V-32, and V-34 illustrate the effects of vegetation at L-band for the three surfaces. It is

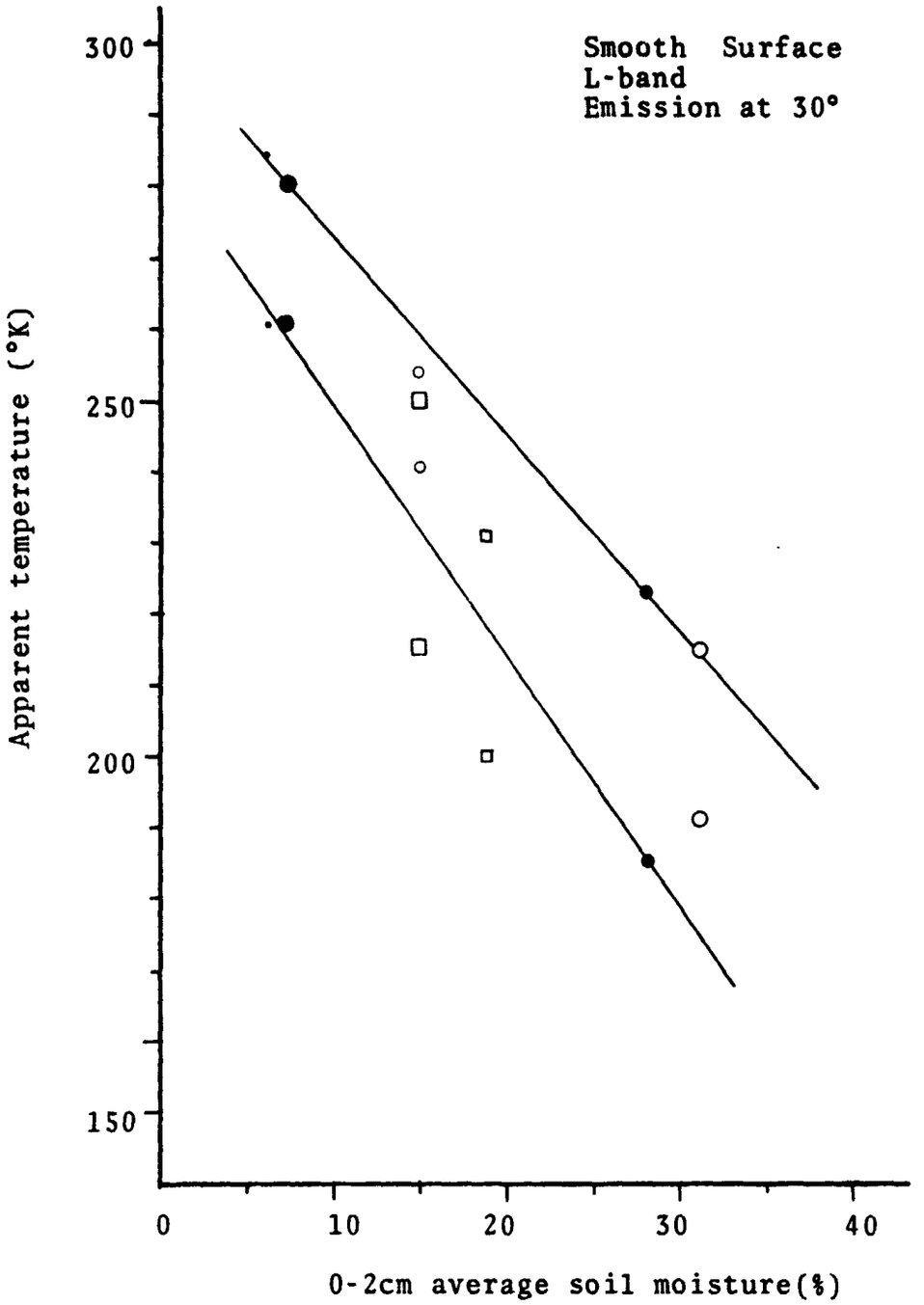

Figure V-28. Apparent Temperature versus Soil Moisture Content, Bare and Vegetated Measurements.

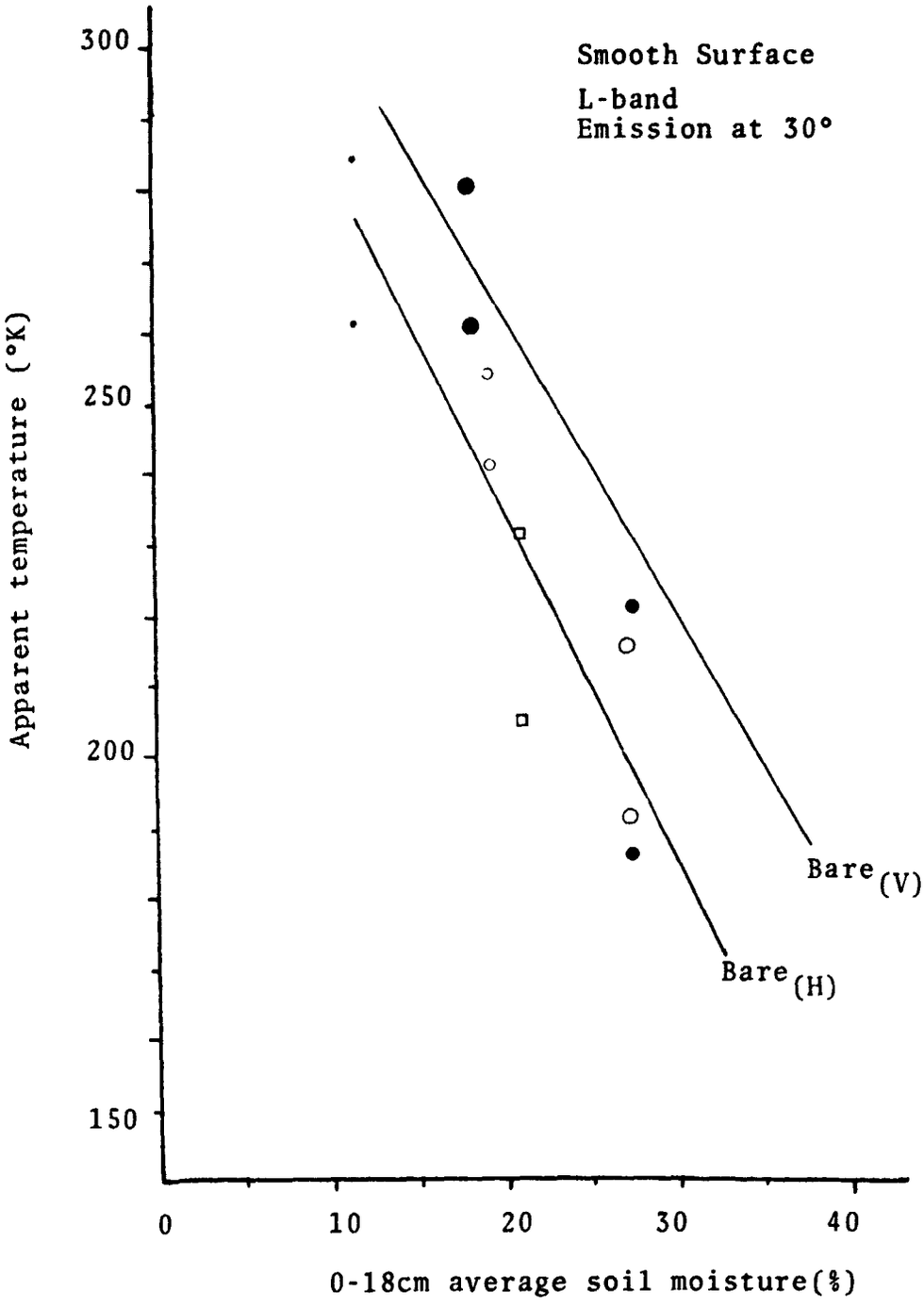

Figure V-29. Apparent Temperature versus Soil Moisture Content, Bare and Vegetated Measurements

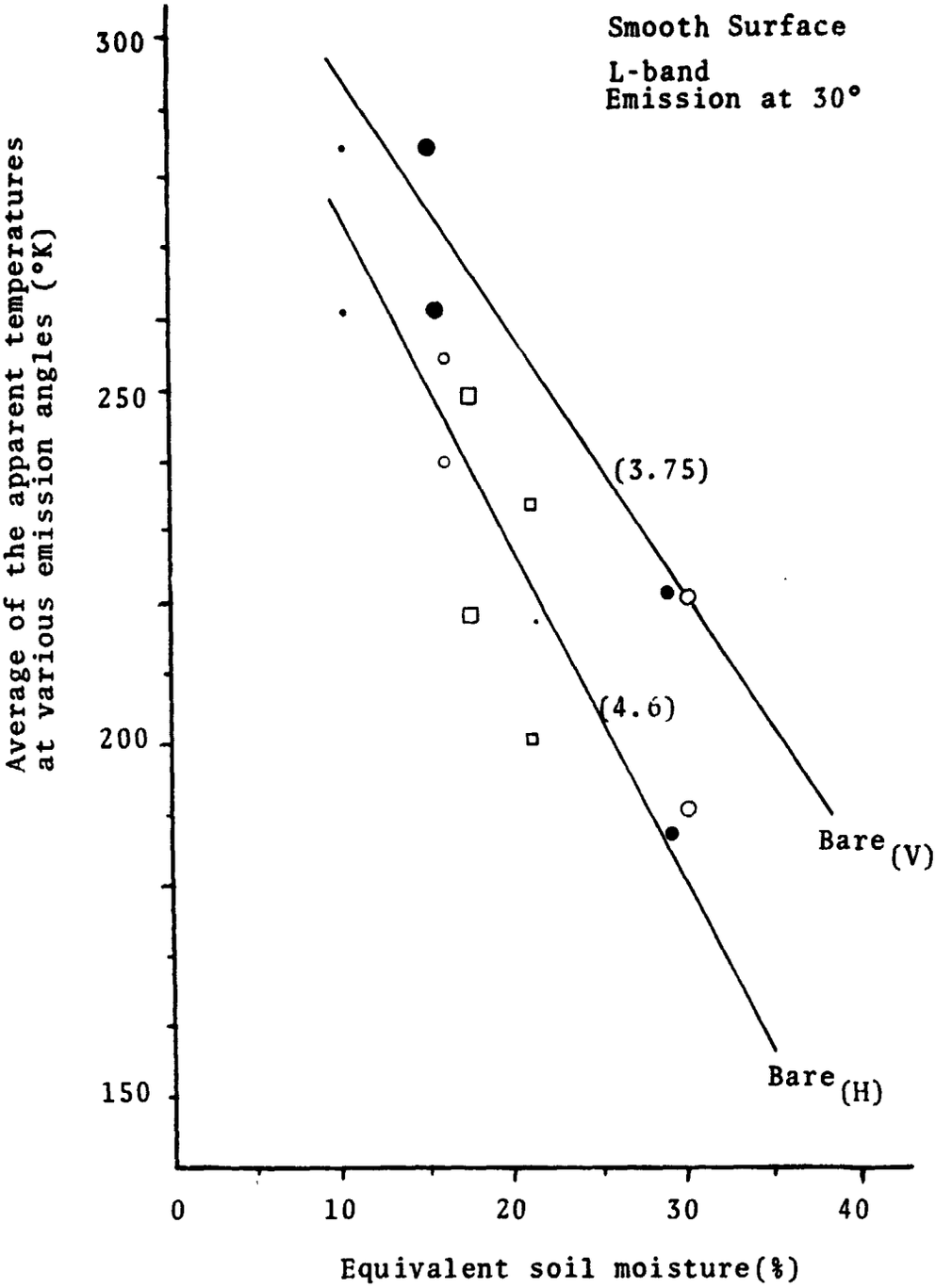

Figure V-30. Apparent Temperature versus Soil Moisture Content, Bare and Vegetated Measurements.

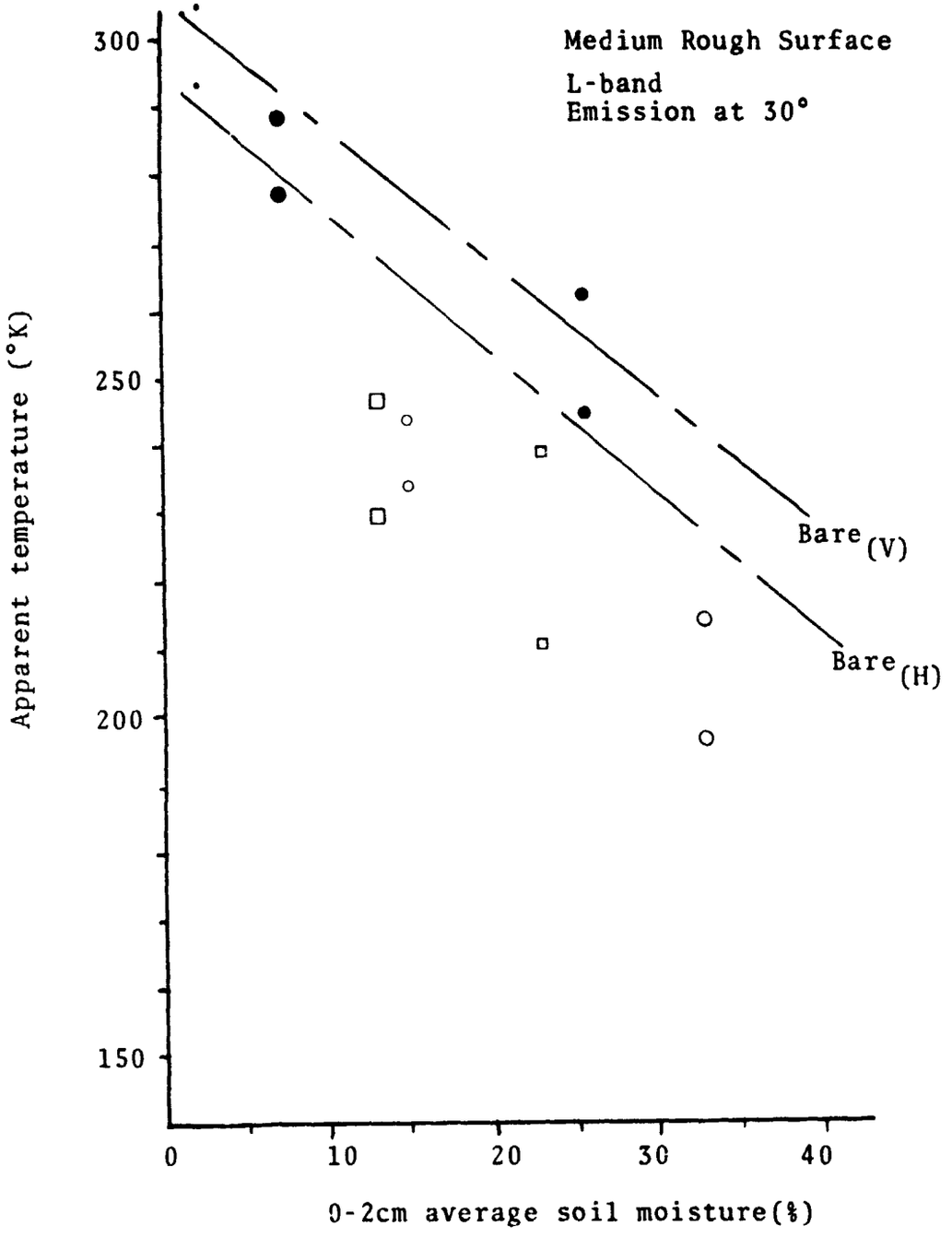

Figure V-31. Apparent Temperature versus Soil Moisture Content, Bar and Vegetated Measurements.

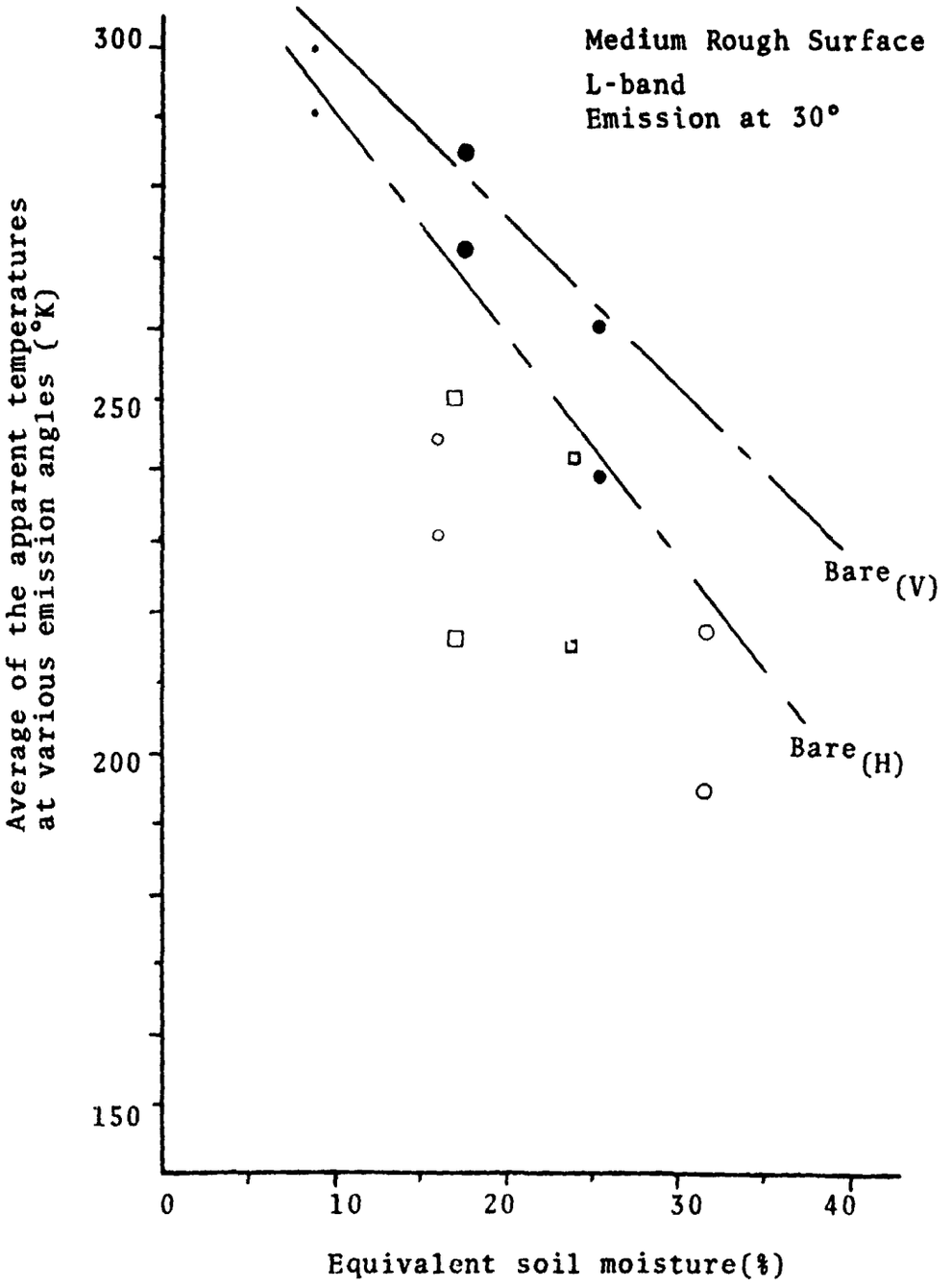

Figure V-32. Apparent Temperature versus Soil Moisture Content, Bare and Vegetated Measurements.

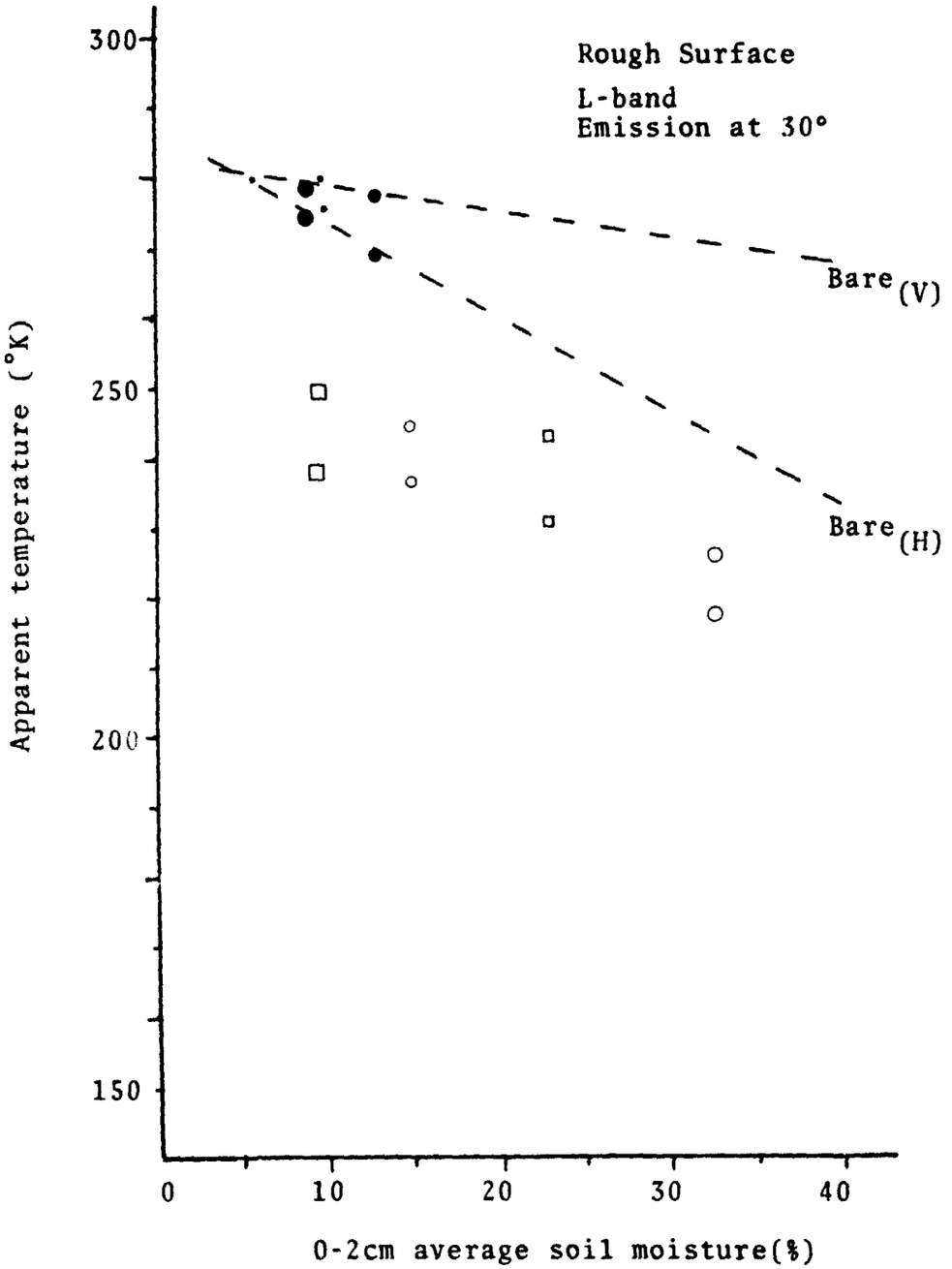

Figure V-33. Apparent Temperature versus Soil Moisture Content, Bare and Vegetated Measurements.

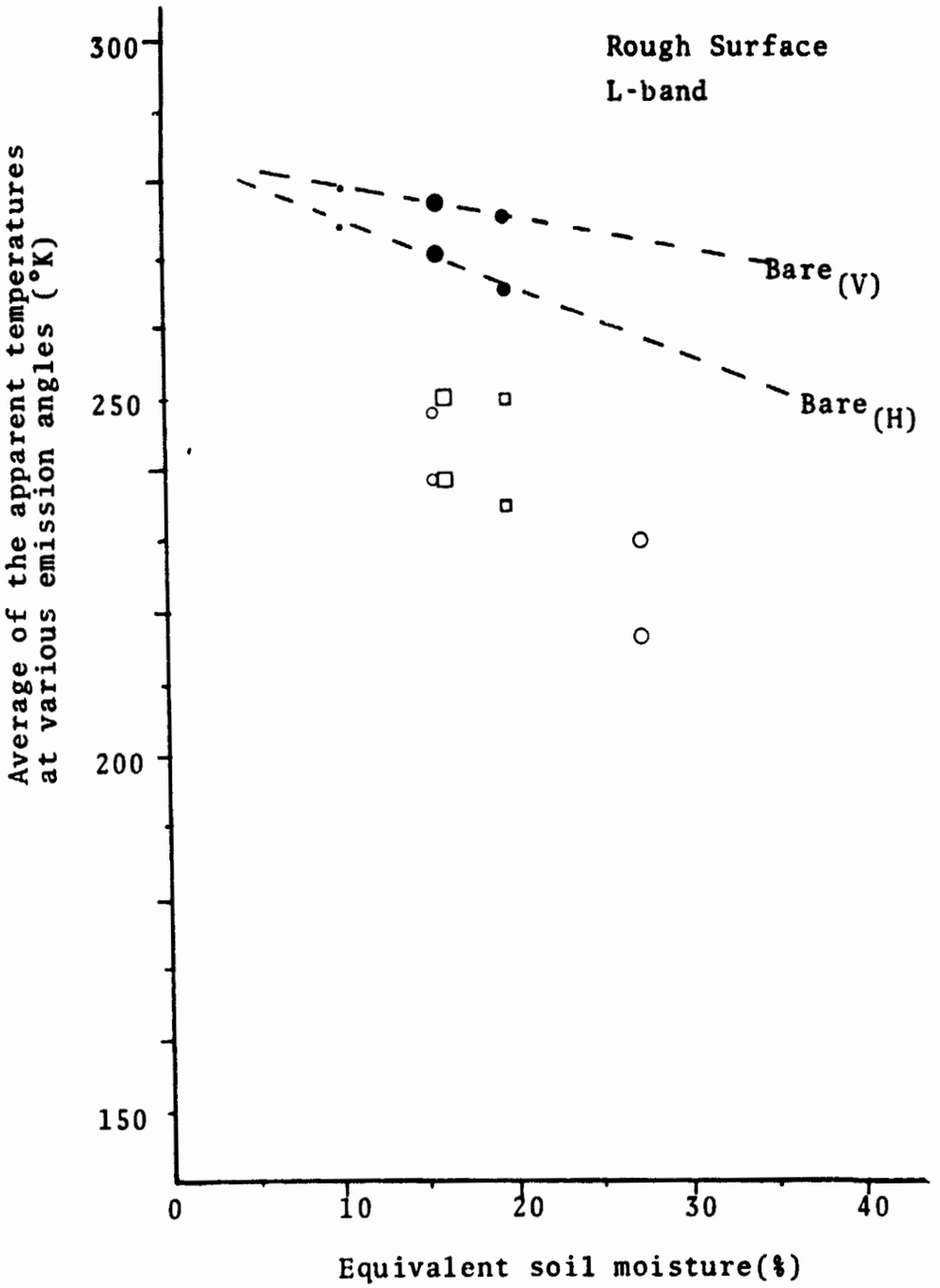

Figure V-34. Apparent Temperature versus Soil Moisture Content, Bare and Vegetated Measurements.

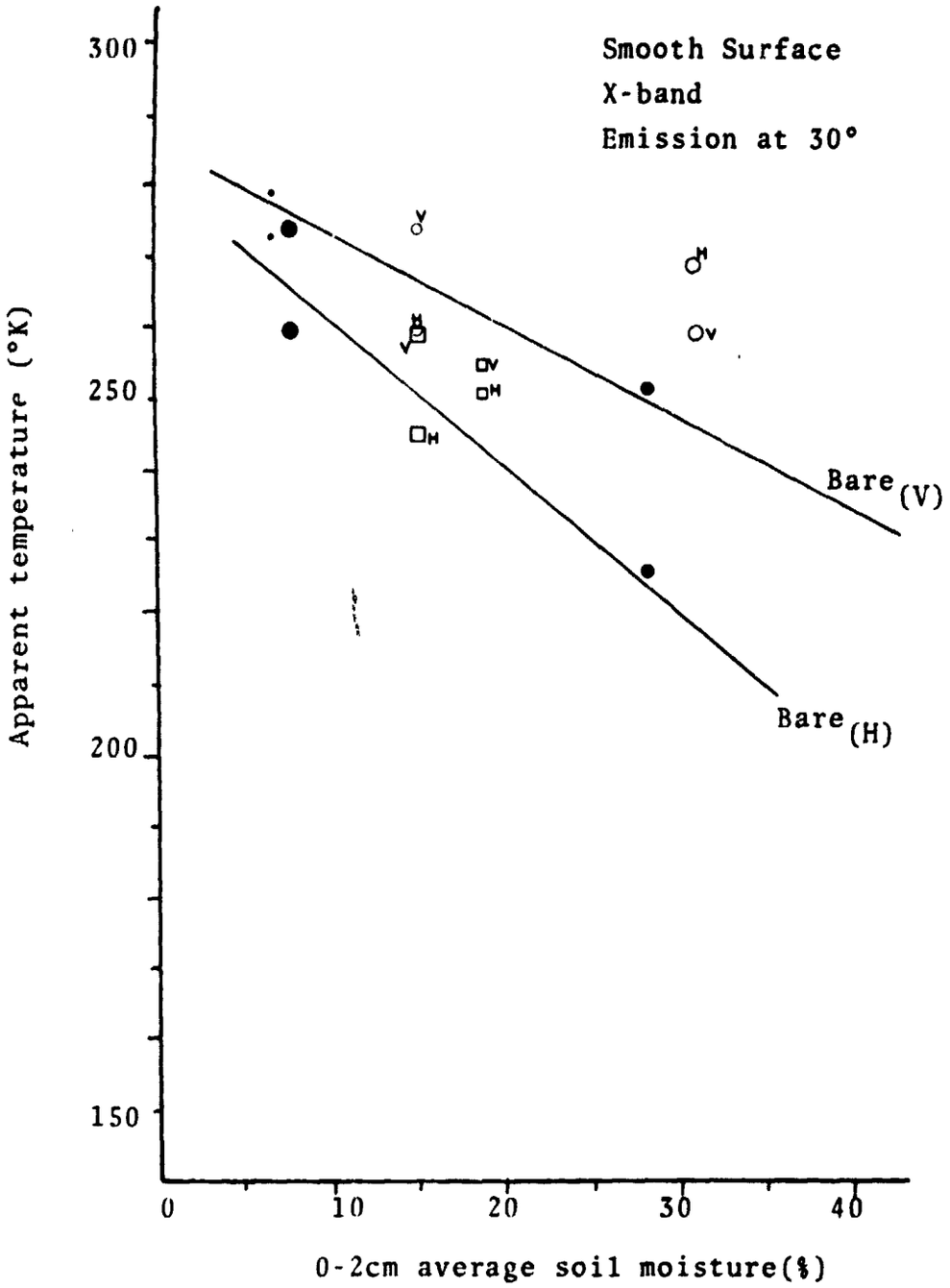

Figure V-35. Apparent Temperature versus Soil Moisture Content, Bare and Vegetated Measurements.

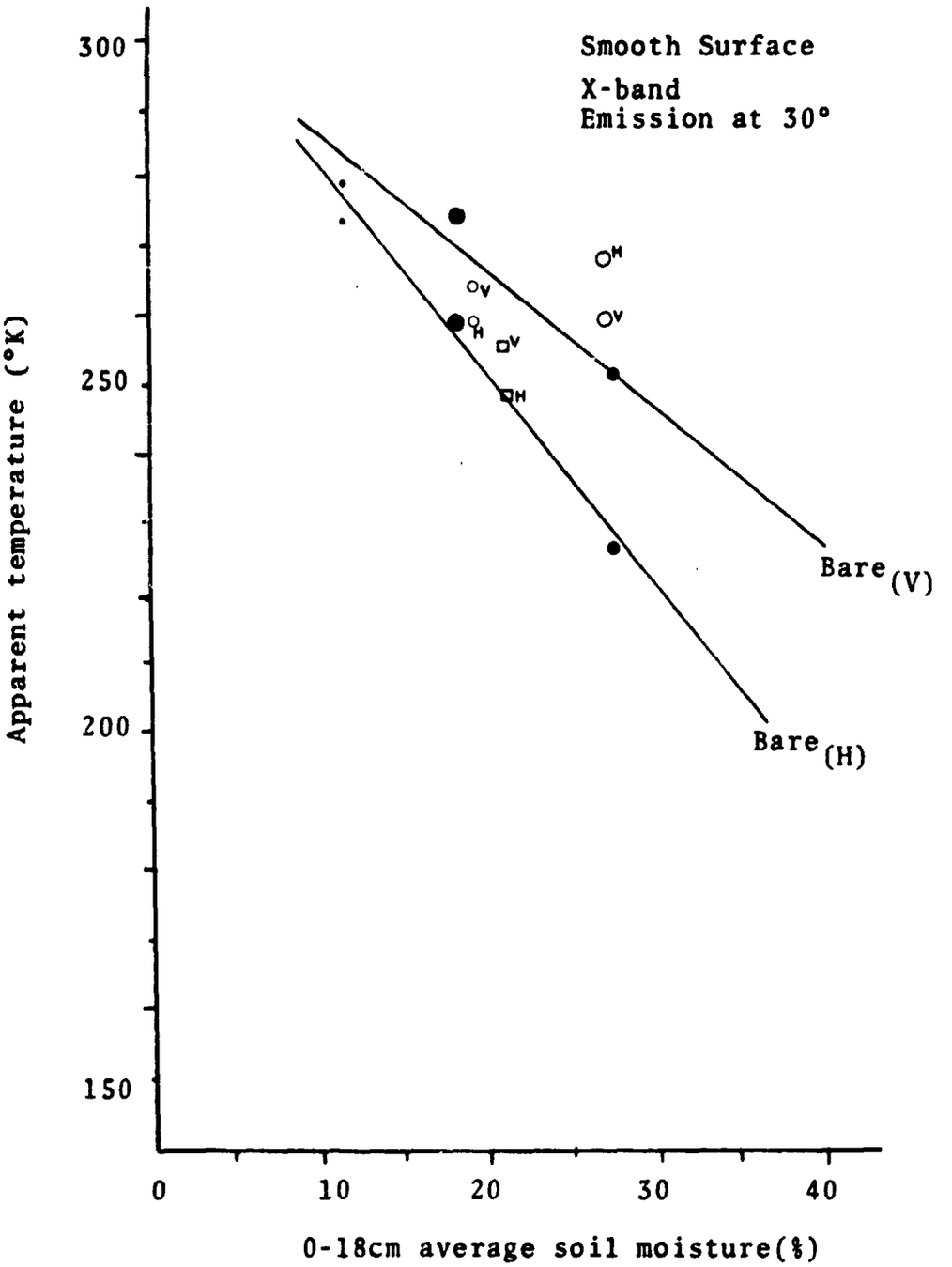

Figure V-36. Apparent Temperature versus Soil Moisture Content, Bare and Vegetated Measurements.

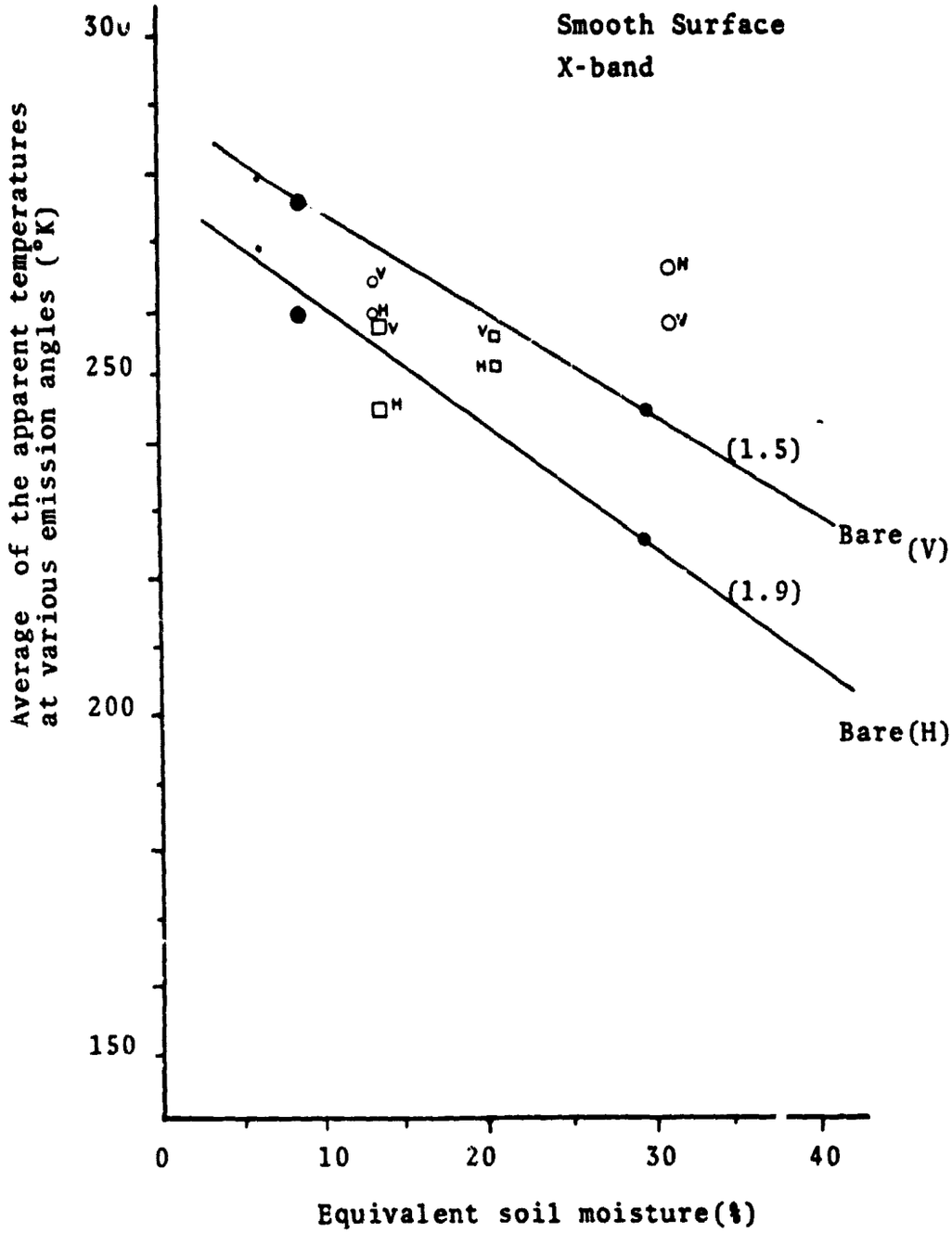

Figure V-37. Apparent Temperature versus Soil Moisture Content, Bare Vegetated Measurements.

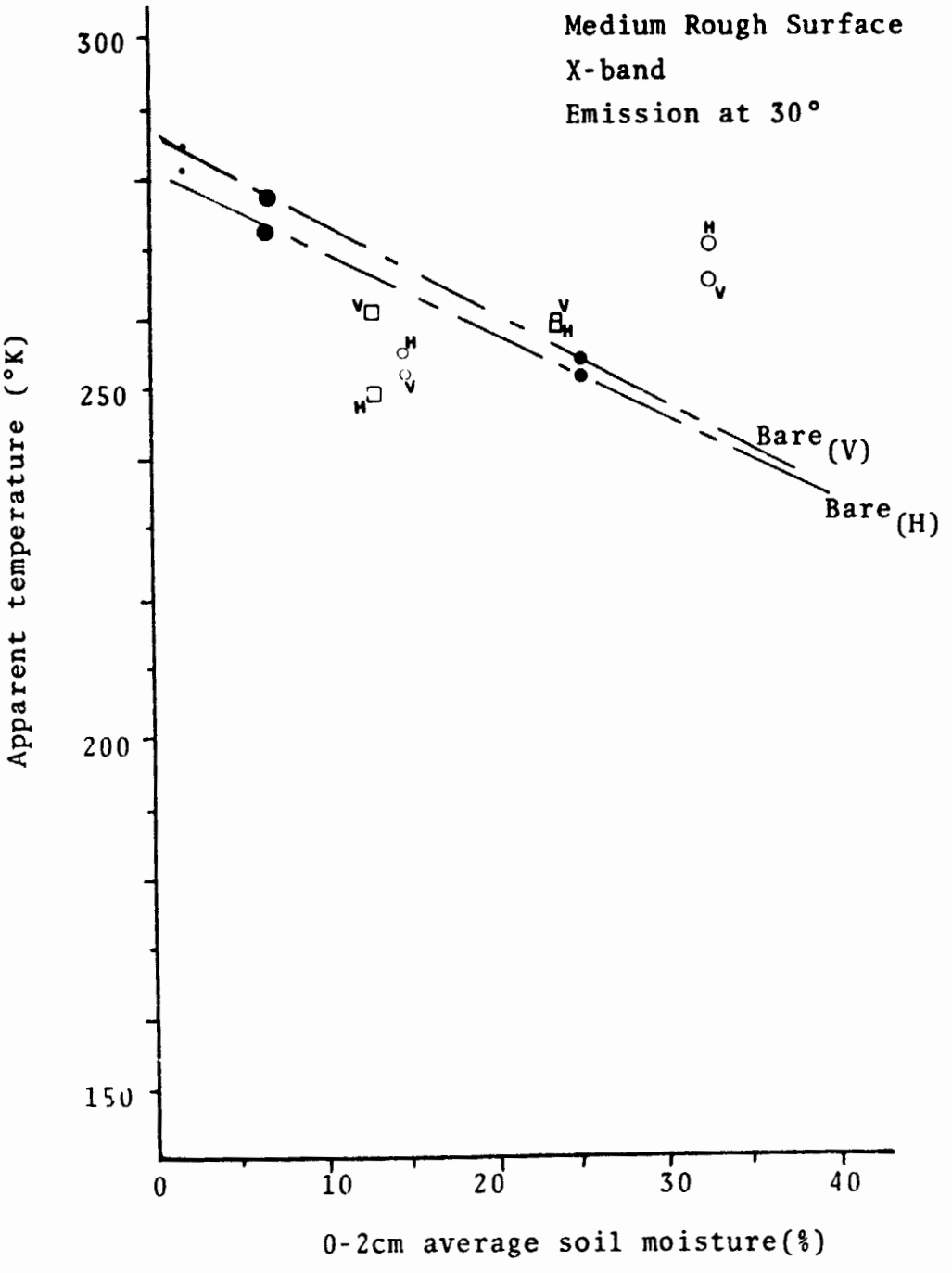

Figure V-38. Apparent Temperature versus Soil Moisture Content, Bare and Vegetated Measurements.

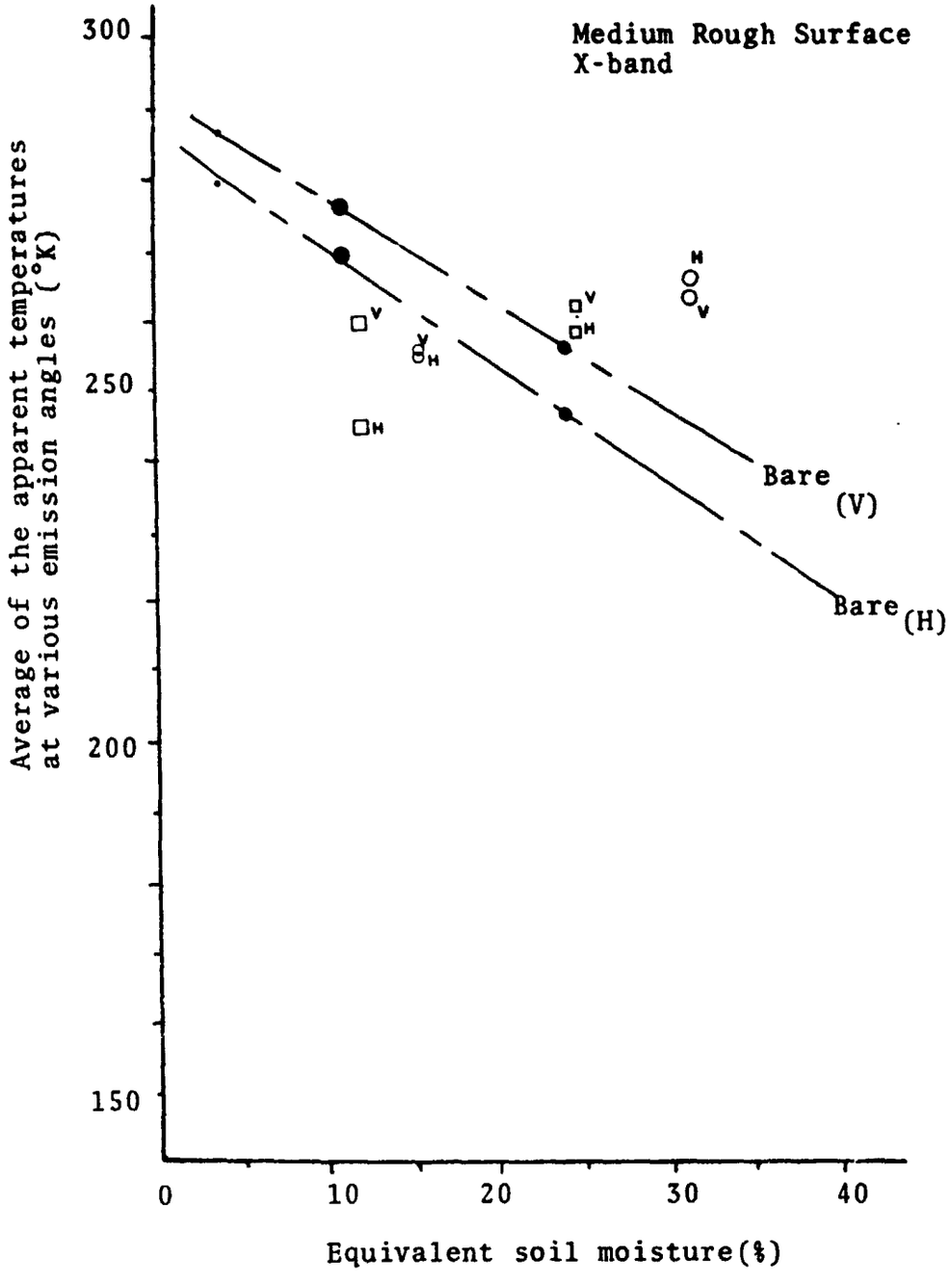

Figure V-39. Apparent Temperature versus Soil Moisture Content, Bare and Vegetated Measurements.

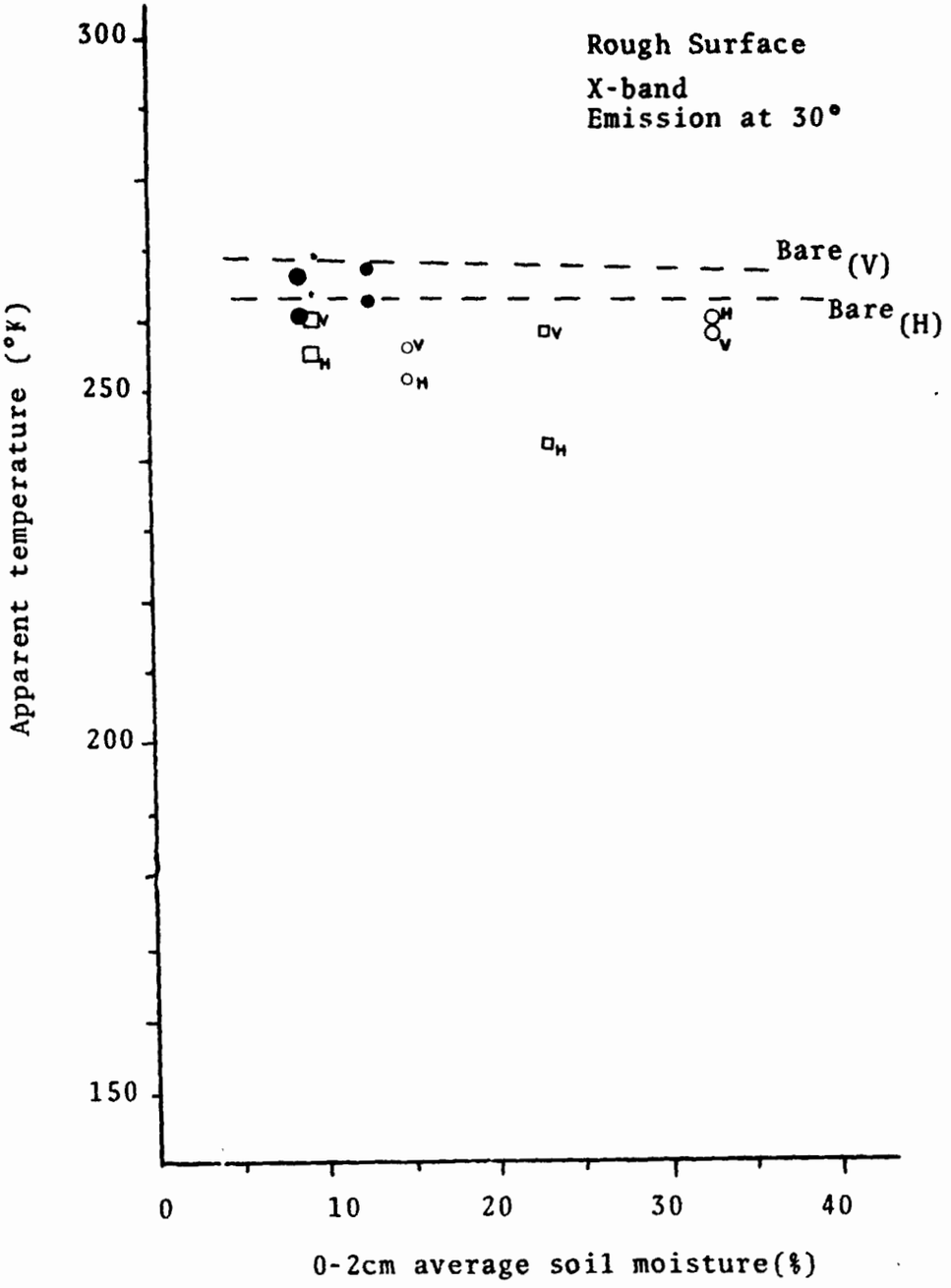

Figure V-40. Apparent Temperature versus Soil Moisture Content, Bare and Vegetated Measurements.

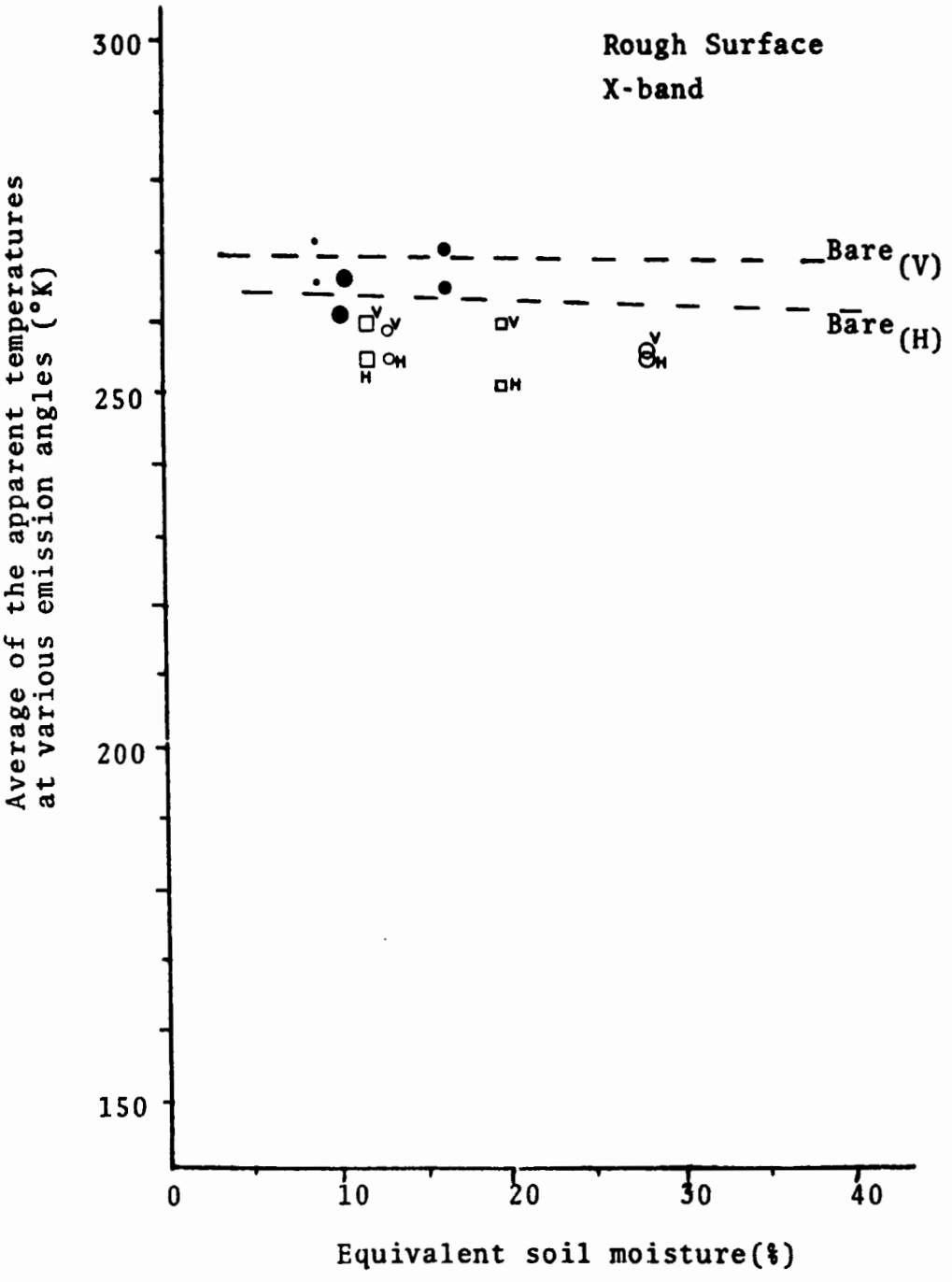

Figure V-41. Apparent Temperature versus Soil Moisture Content, Bare and Vegetated Measurements.

obvious that for the vegetation conditions of this experiment, the vegetation generally exhibits an attenuating effect such that the apparent temperature of the vegetated fields is significantly lower than the bare fields at the same moisture content. The degree of vegetation effects on the detection of soil moisture varies with the surface roughness. The smooth surface is least affected by vegetation while the medium rough surface and the rough surface are affected to a greater degree. As the vegetation density increases, Sibley's model predicts that emission from the vegetation becomes more predominant, though the vegetation still attenuates. This prediction appears to be verified from the October 30, 1973 data indicated on Figures V-30. On October 30, the oats were at its maximum growth and healthiest condition. Therefore the effect of the emission from oats vegetation is the greatest on this date and this is indicated as such on Figure V-30. For the smooth surface on October 30, the vegetation apparent temperature measurement is shown to be about the same as the bare field measurement for that particular soil moisture. This seems to suggest that on that day, the contributing emission from the oats "equalizes" its attenuation effect. For the medium rough surface, the effect of

vegetation is mainly that of attenuation; however, the effect of contributing emission from the vegetation is observable. Based on this line of reasoning, the data point of October 30, 1973 on the rough field is an uncertainty. It is shown that the opposite is true for the rough field on October 30, the data suggest that the attenuation effect of the oats is the predominant effect on that date. Again, a conclusion cannot be drawn for the rough surface from such a limited amount of data.

The underlying effect of surface roughness is also indicated on the vegetation measurements. The data show a trend toward a monotonic increase of apparent temperature with increasing surface roughness. Also, the response to soil moisture variations decreases with increasing surface roughness. The vegetation effect on sensitivities at both polarizations of the three surfaces are only slightly affected relative to their sensitivities at bare conditions. These data indicate that the L-band is a promising frequency to use for soil moisture detection.

For the X-band, the analysis was made primarily from Figures V-37, V-39, and V-41. Overlaying these three figures, an interesting result is revealed. It can be seen that the sensitivities at both vertical and

horizontal polarizations of the three vegetated surfaces are essentially the same; practically no response to soil moisture variations. It is also noted that the data of the three different roughnesses are falling in the same general vicinity. These two observations suggest that for X-band, the oats vegetation had completely masked the soil contribution, regardless of surface roughness. The apparent temperatures measured are merely those of the oats.

Although the amount of data available is limited, the effects of vegetation are apparent. It appears that the L-band passive microwave radiometer has high potential for remote sensing of soil moisture of natural bare or vegetated terrains. However, the data suggest that the X-band passive microwave radiometer is only capable of detecting soil moisture for some bare terrains.

Theoretical Predictions

Theoretical predictions were computed from Sibley's model, Equation (III-18)

$$T_{ai} = T_g \epsilon T_i e^{-2\alpha H \sec\theta} + T_c f (1 - e^{-2\alpha H \sec\theta})$$

and were made only on the smooth surface case for the

bare and vegetated conditions. An evaluation on the validity of Sibley's smooth surface model for bare or uniformly vegetated terrain is attempted through the comparison of the theoretical predictions with the experimental results. Theoretical predictions will not be made for the medium rough and rough surface cases based on Sibley's rough surface model. It is felt that Sibley's rough surface model (Equation III-19) which is derived from Johnson's model [10] is still inadequate to actually be applied to the very complicated real world rough surfaces. For example the joint probability density $f_{\theta\phi}(\theta_n, \phi_n)$ or the distribution of normals in (III-19), a necessary quantity to evaluate the rough surface model (III-19), is an extremely difficult quantity to obtain in the real world.

Comparisons of the theoretical predictions and experimental results are presented on Figures V-42 through V-47. The analysis employs to the equivalent soil moisture data (Figures V-42, V-43, and V-44).

Analyzing first the bare field condition, it is noted that the theoretical predictions for botn L- and X-bands are significantly lower than the experimental results. Studying the model, it appears that the discrepancies could have resulted from three factors. They are namely the emissivity of the soil, the

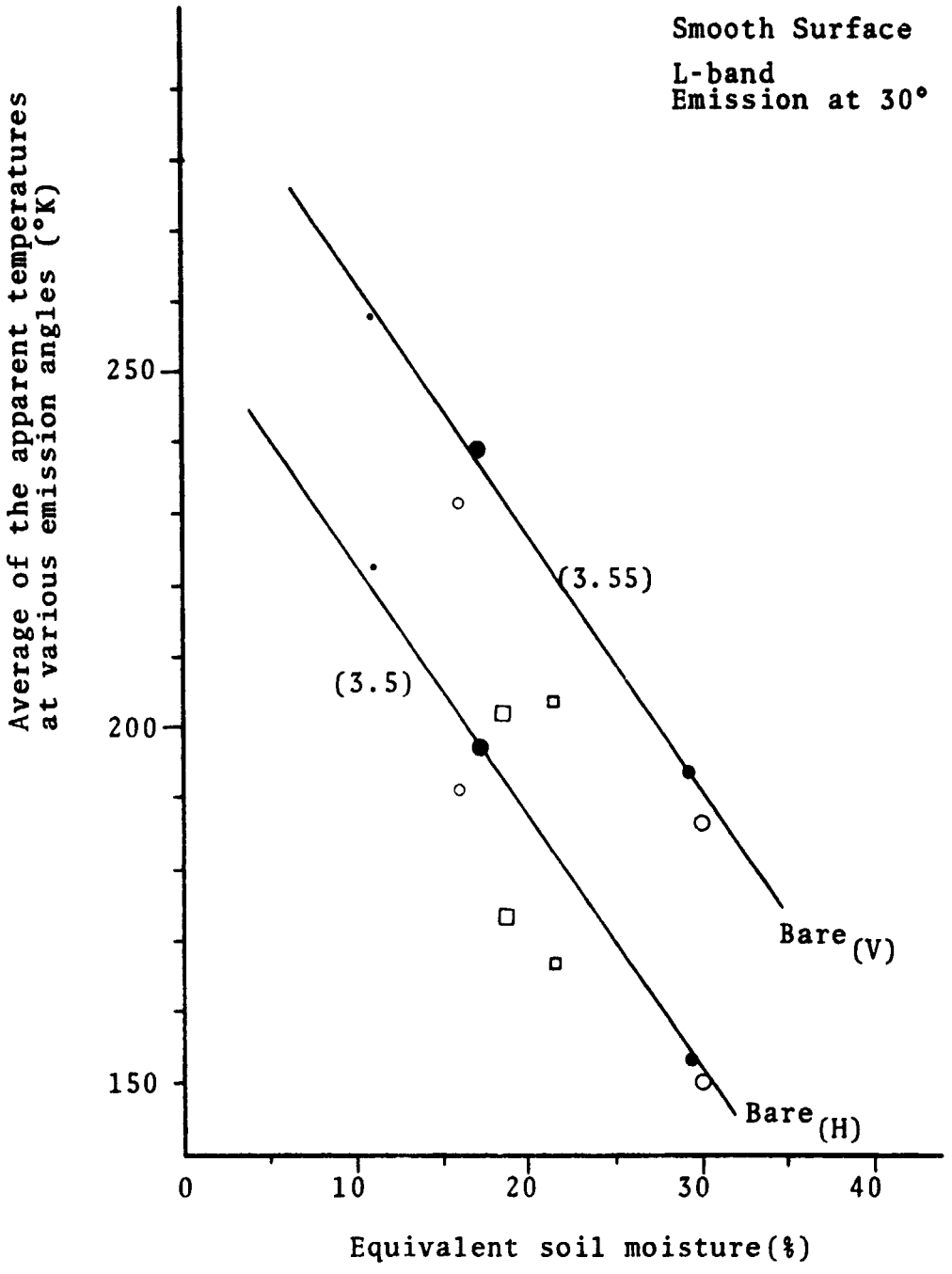

Figure V-42. Apparent Temperature versus Soil Moisture Content for Bare and Vegetated Conditions: Theoretical Predictions.

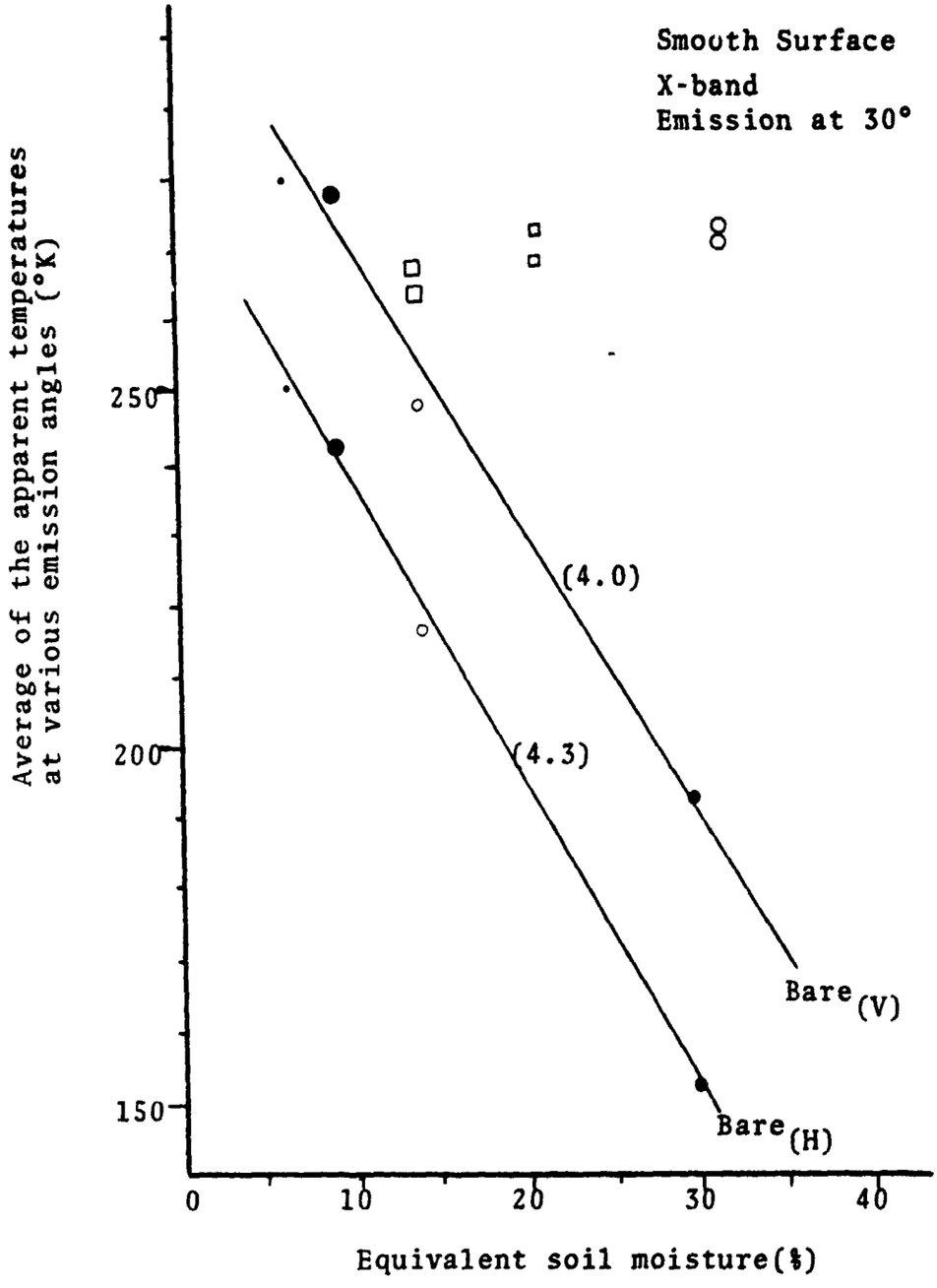

Figure V-43. Apparent Temperature versus Soil Moisture Content for Bare and Vegetated Conditions: Theoretical Predictions.

permittivity of the soil, and the antenna pattern, which is not accounted for in the theoretical model used. Note that in the model for bare smooth surface

$$T_{ai} = T_g \epsilon_s T_i$$

T_g and ϵ_s are assumed to be constant, the only variable is the transmission coefficient, T_i, which is a function of the permittivity of soil. It can be seen that the accuracy in predicting the apparent temperature of the soil depends heavily on the absolute correctness of the soil permittivity (dielectric constant). Documented dielectric constant measurements of soil are scarce, the only Miller Clay measurement data were that of Wiebe [46]. The comparison of these measurements is shown on Figure V-44. Differences are shown, however, it is not known if this discrepancy has been caused by the differences of chemical and physical properties between the two soils compared. While the Miller Clay dielectric constants measured for this study differ from Wiebe's measurements, they match reasonably well with the dielectric constant measurements by Hoekstra, et. al. [51] on certain clays.

Apparent temperature predictions computed for the X-band using Wiebe's Miller Clay dielectric constant values are shown in Figure V-45. It was observed that

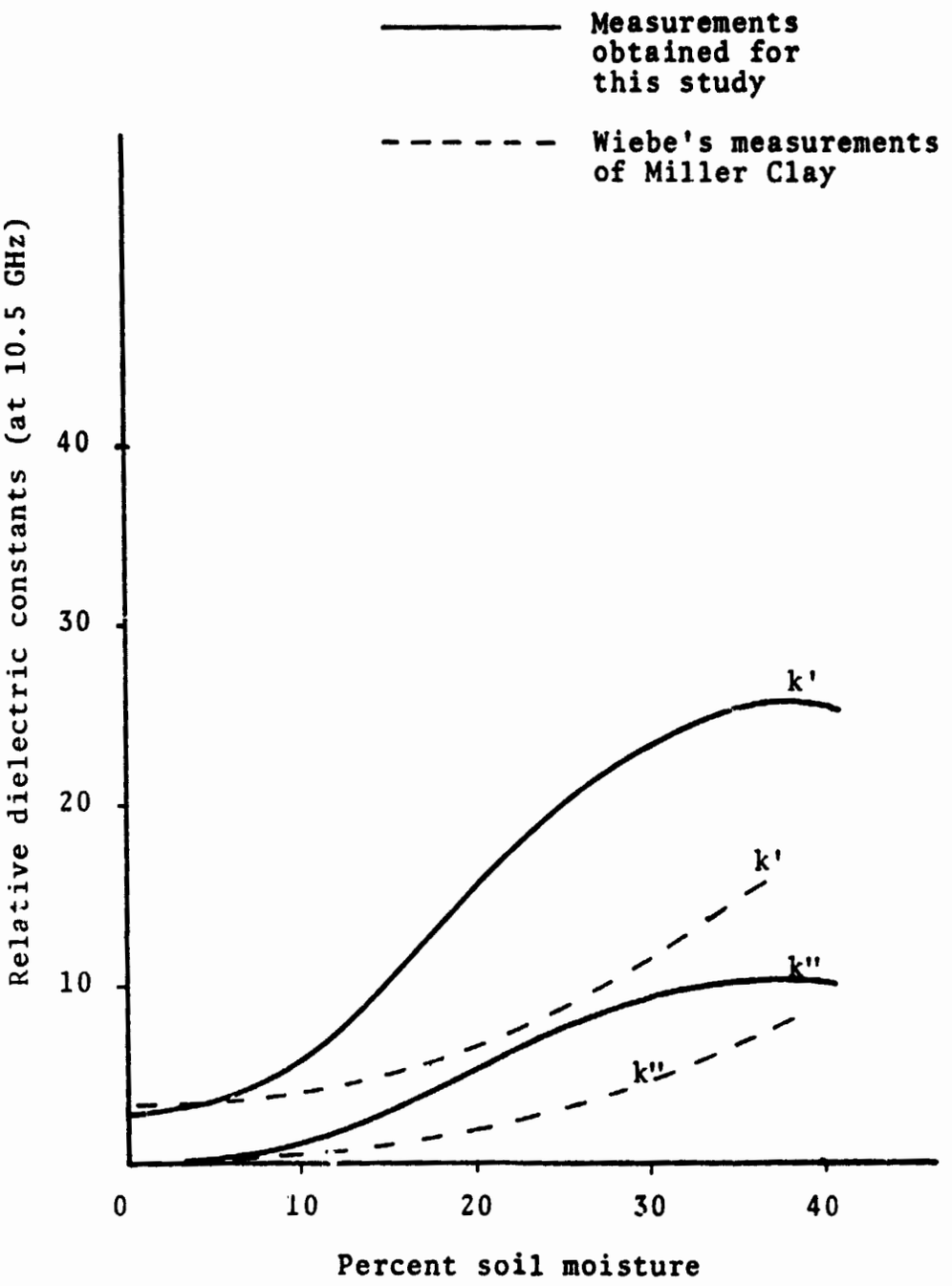

Figure V-44. A Comparison of Miller Clay Relative Dielectric Constant Measurement Results.

the predictions computed from Wiebe's dielectric constant data compare to the experimental results better than the predictions based on the dielectric constant values obtained in this experiment. Further investigations on soil dielectric constant measurements are still necessary.

For the bare field comparison, it is also noted that the L-band theoretical results and X-band theoretical results are almost identical, which is definitely not the case for all the experimental data shown. This could possibly be explained by two key parameters of the bare smooth surface model used. The first possible explanation concerns the value of emissivity that should be used. As emissivity is a function of surface configuration, polarization, and angle, it might not be valid to assume the customarily used and reasonable value for emissivity (between 0.5 to 1.0 [11], [13]) in the computation for the apparent temperature (a value of 0.98 was used for the emissivity in the theoretical predictions). The other possible explanation concerns the behavior of dielectric constant of soil with regard to variation in frequency. The dielectric constant measurements made at 10 GHz are also used for L-band theoretical predictions. As the transmission coefficient which is a function of dielectric

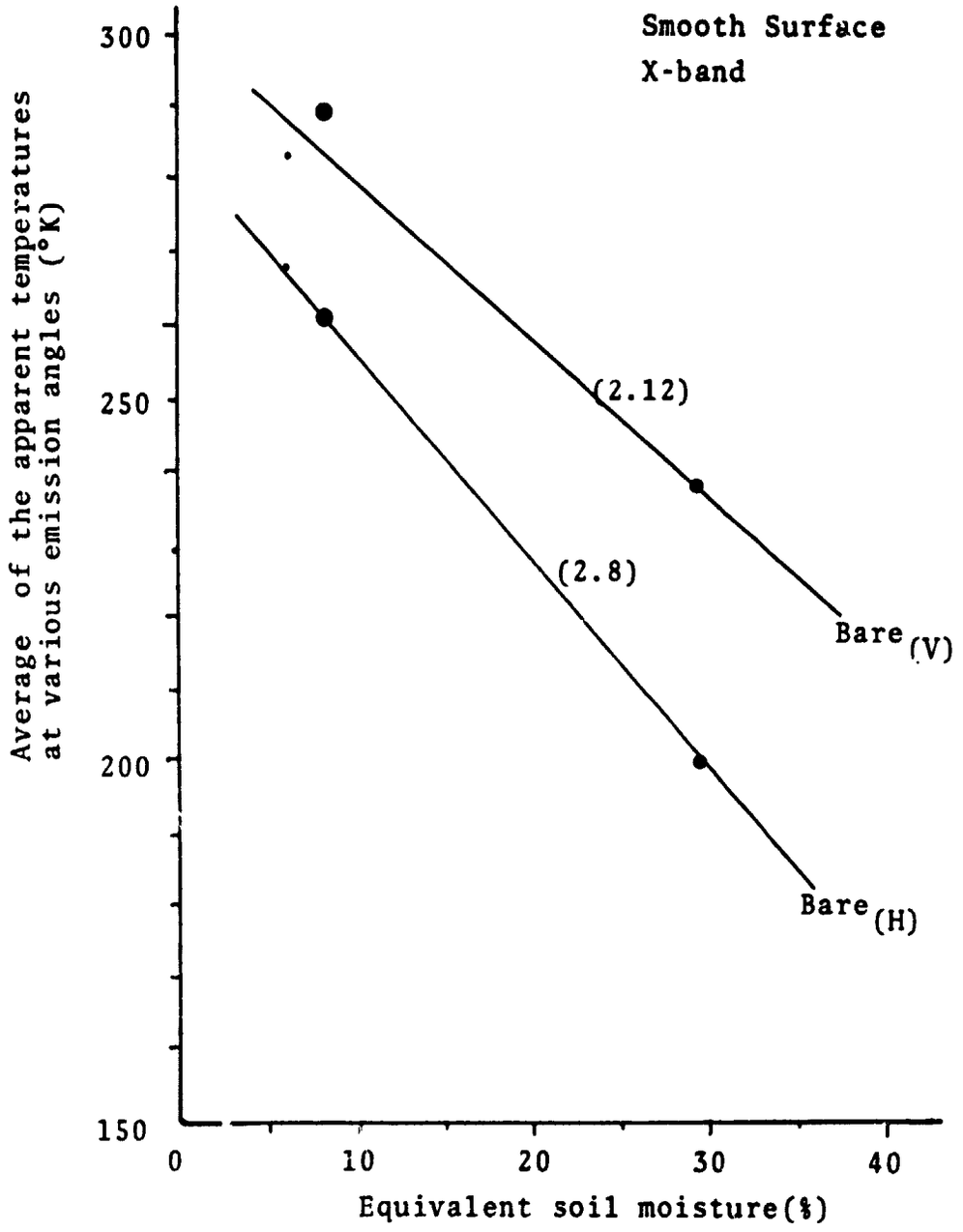

Figure V-45. Apparent Temperature versus Soil Moisture Content: Theoretical Predictions using Wiebe's Relative Dielectric Constant Measurement Data for Miller Clay.

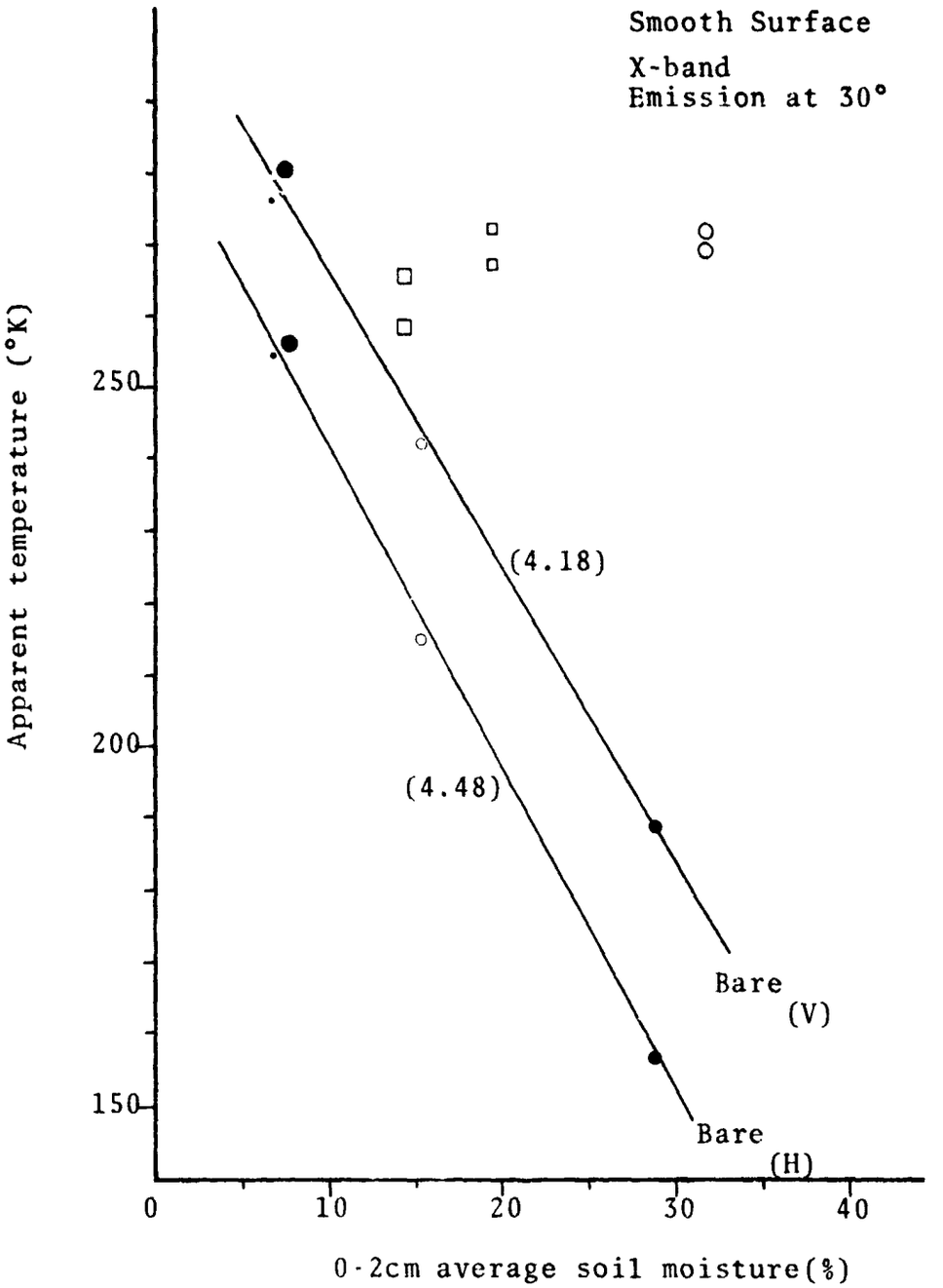

Figure V-46. Apparent Temperature versus Soil Moisture Content for Bare and Vegetated Conditions: Theoretical Predictions.

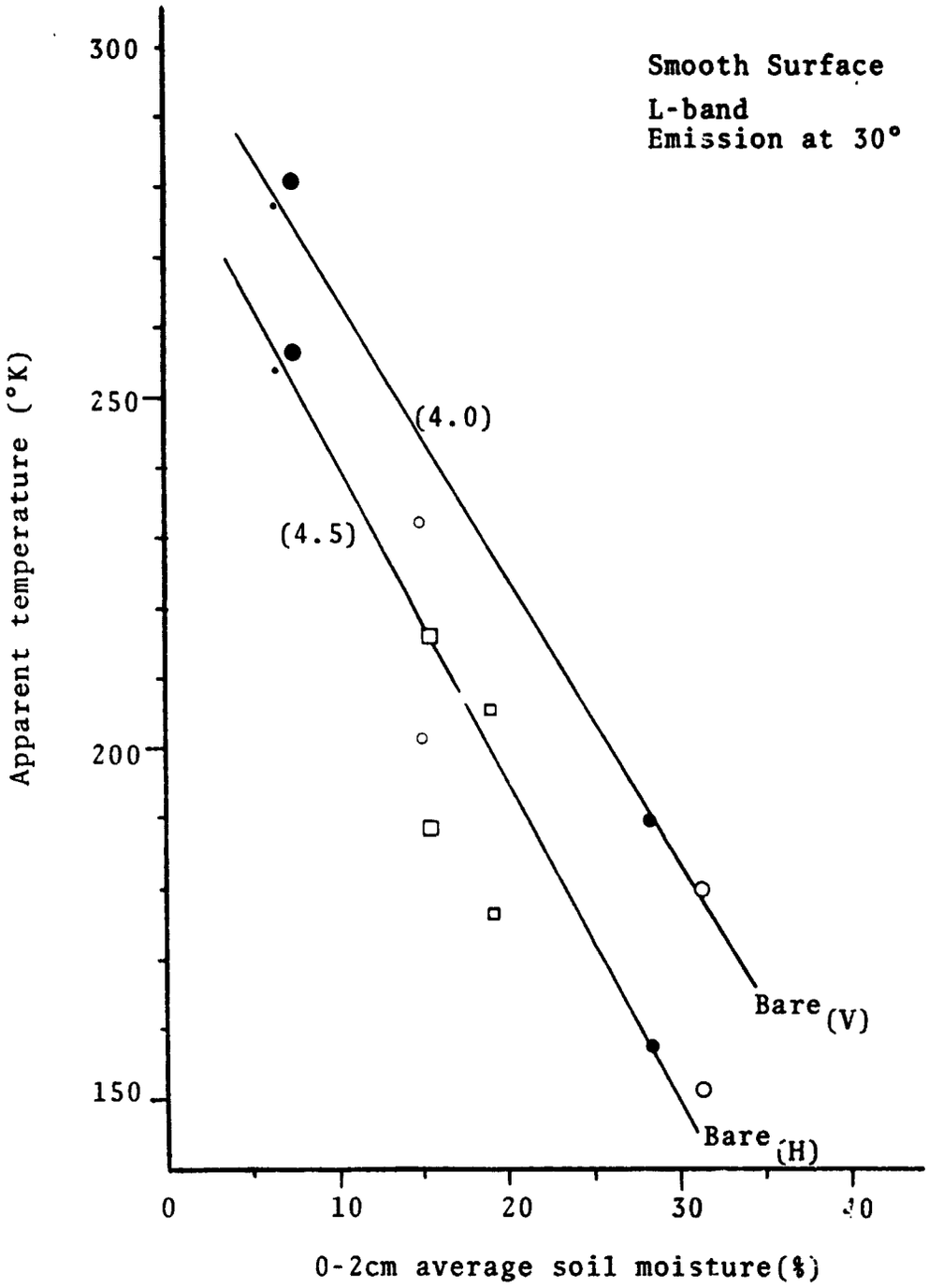

Figure V-47. Apparent Temperature versus Soil Moisture Content for Bare and Vegetated Conditions: Theoretical Predictions.

constant, is the only variable in the model, naturally the L-band and X-band apparent temperature computed would be the same.

Despite the discrepancy in magnitude, the sensitivities of the theoretical predictions for both L- and X-band compare quite favorably with the experimental results.

To conclude for the bare smooth surface case, the uncertainty of the actual value of the soil dielectric constants has affected the comparison between the theoretical prediction and the experimental results.

Comparisons of theoretical prediction and experimental measurements in the vegetated case show some encouraging observations in regard to Sibley's uniform vegetation model for smooth surface. Despite the discrepancy in magnitude, which is inherent from results of the bare smooth surface model, the predictions for the vegetated case of both frequencies agree reasonably well with the behavior experimental measurements. The attenuating and contributing effects of the vegetation apparent temperature measurements are clearly indicated. A significant observation is the prediction for October 30 for the L-band measurement, the model predicts exactly the same vegetation effect as that which happened in the experiment. The very close comparisons of the theoretical predictions

of the other dates with the respective experimental results support the validity of this prediction.

For the X-band, though the theoretical predictions also compare well with the experimental results, the model shows a stronger contributing effect of the vegetation than indicated by the experimental results. Again, as shown by the experimental results for X-band, a complete masking of the soil by vegetation is predicted by the model. From these comparisons, it appears that the uniform vegetation model for smooth surface has given a reasonable prediction of the effects of vegetation on masking soil moisture dependency.

Comparison with Recent Research Effort

Many past investigations on remote sensing of soil moisture have shown that there is a definite relationship between the measured soil apparent temperature and soil moisture content. The results obtained from this ground-based control experiment have again affirmed and supported such a relationship. A summary of the results of this experiment are shown pictorially on Figures V-48, V-49, V-51, and V-52. They are the results based on the equivalent soil moisture as the soil moisture parameter. Recent research effort such as those by Jean [13], Schmugge [11], and Kroll [14] are reviewed and their findings will

be compared with those of this experiment.

Jean has investigated some airborne microwave radiometer measurements (taken at a 915 meter altitude) over selected flight lines near Weslaco, Texas. The fields over which the measurements were made were mostly barren and plowed. The surface roughness of these fields are estimated to be in between the roughness of the medium rough field and the rough field of this study. It was determined that the 1.42 GHz data were sufficiently correlated to moisture content data. His results are shown on Figure V-48. Each data point corresponds to each field. The agreement between Jean's results and those of this study is strikingly good. If a least squares straight lines was fit to his data, the resulting sensitivity would very closely approximate that of the medium rough field.

Another airborne passive microwave radiometer remote sensing of soil moisture was conducted by Schmugge, et. al. The measurements were made over some barren agricultural areas in the vicinity of Phoenix, Arizona. The radiometers covered the wavelength range 0.8 cm to 21 cm (37.5 GHz to 1.4 GHz). Schmugge's results are compared with this ground based results on Figures V-48, V-49, and V-50. The soil moisture parameter he used was the 0-15 cm average soil moisture. Schmugge's results compare favorably with

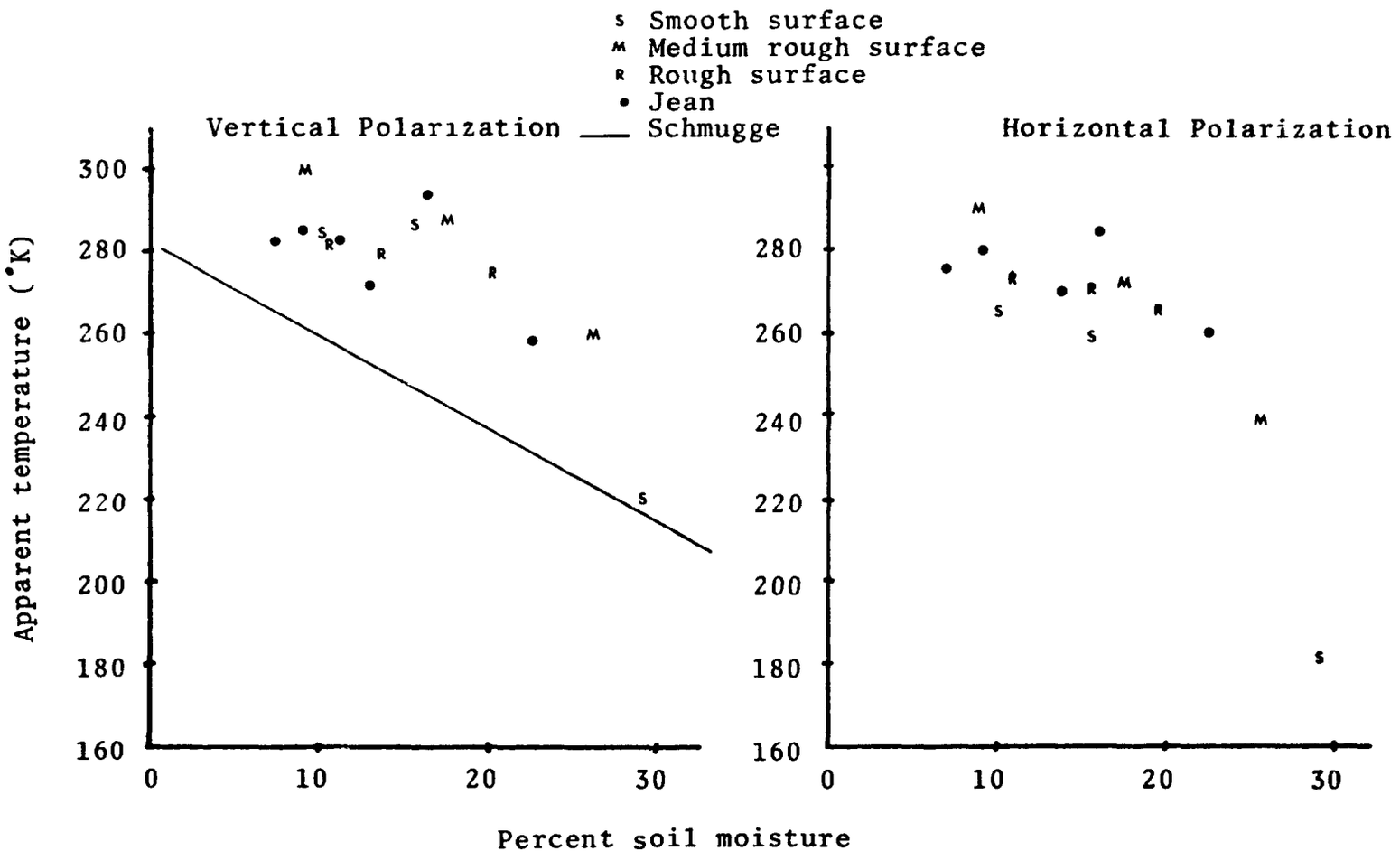

Figure V-48. A Comparison of Results of 1.42GHz Radiometer, Bare Condition.

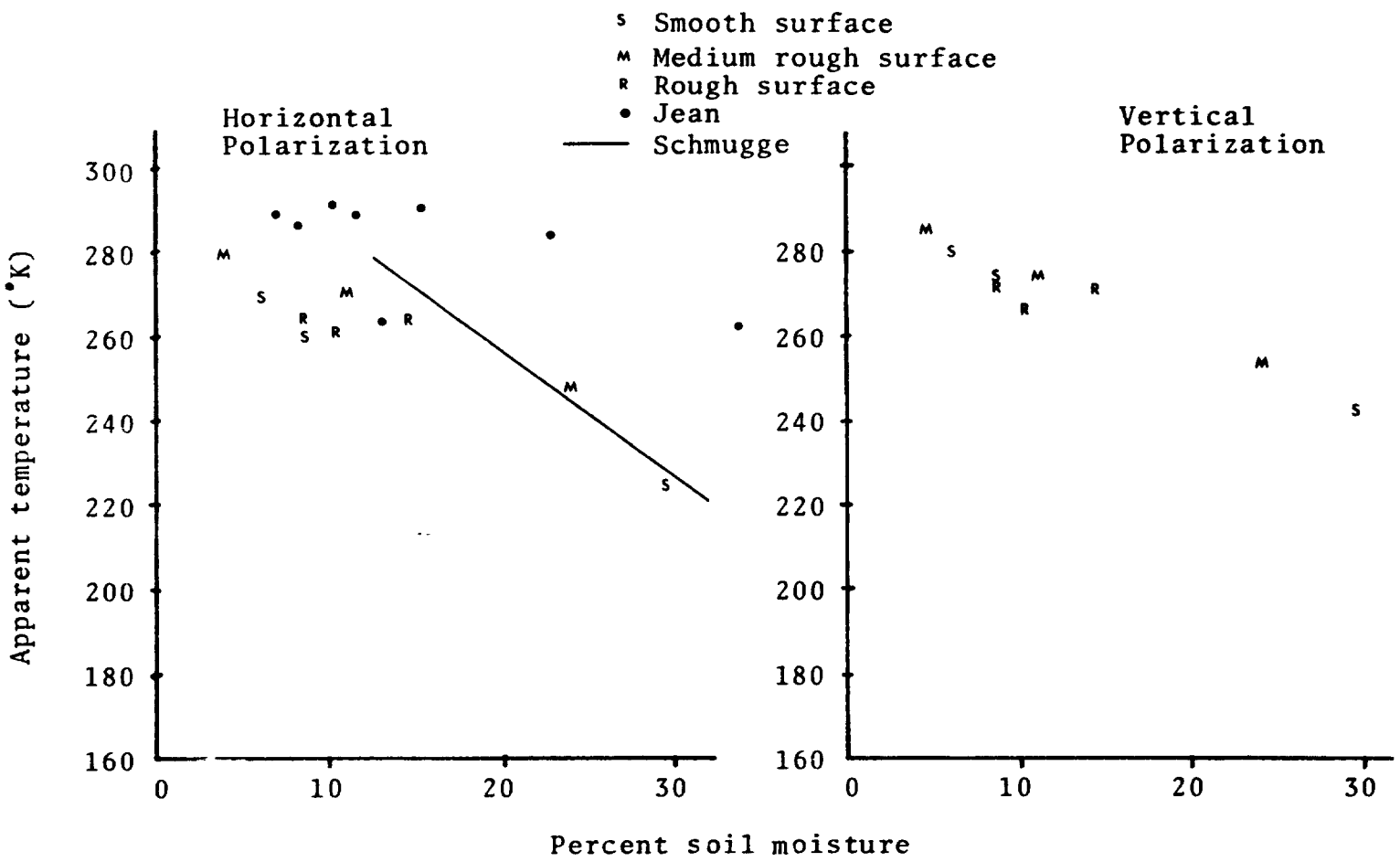

Figure V-49. A Comparison of Results of the 10.6GHz Radiometer, Bare Condition.

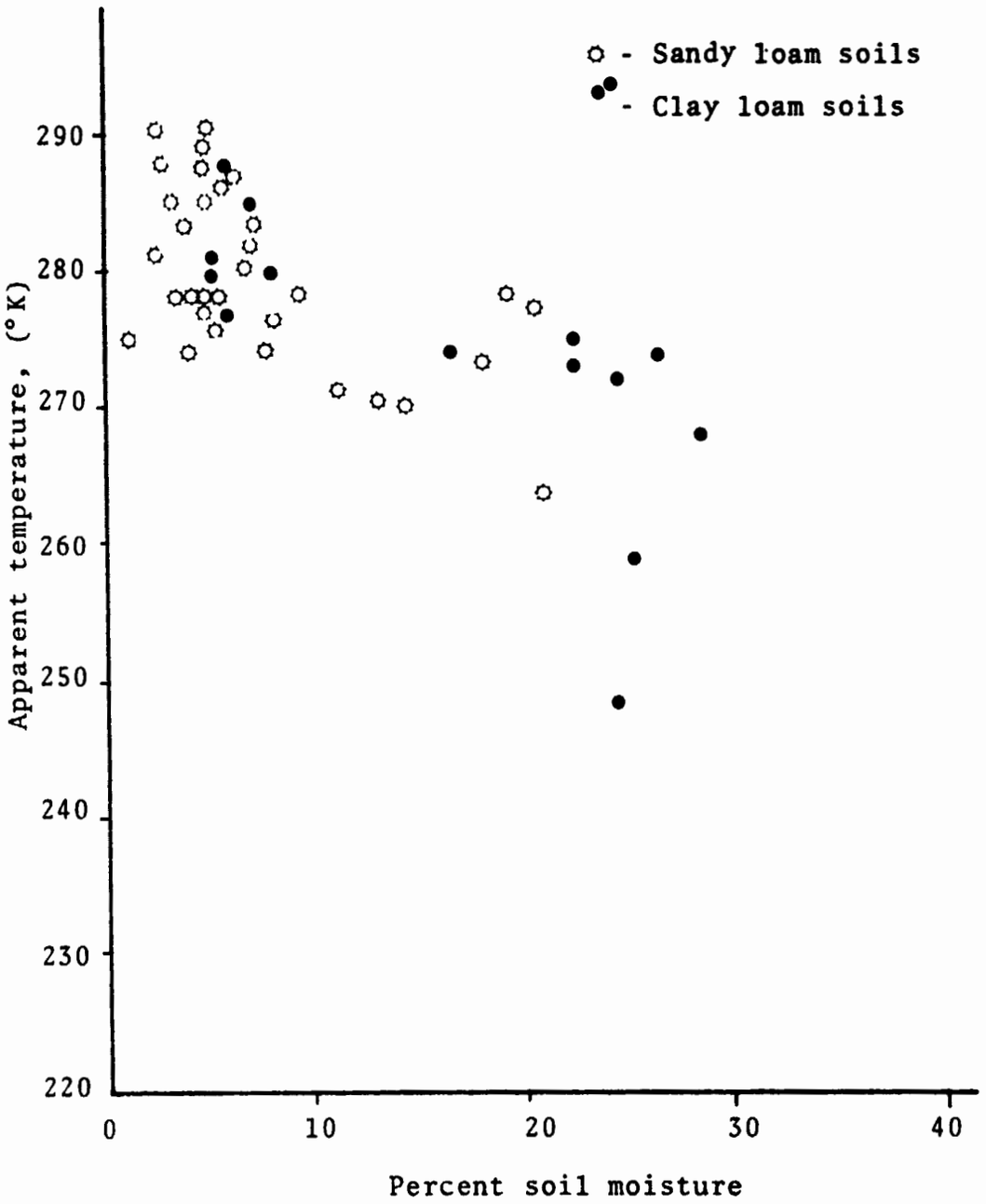

Figure V-50. Apparent Temperature results of the 37.5 GHz Radiometer, Bare Fields, Phoenix, Arizona [11].

the results of this study. The effects of roughness on various frequencies measurements are shown. It was noted [11] that the 10.6 GHz radiometer was especially sensitive to the surface moisture. Those fields which had soil moisture above 16% were irrigated within one week prior to the flight and probably had soil moisture values greater than 10% in the top half cm of the soil. Once the moisture content in this layer drops below 10% the apparent temperature measurements showed poor sensitivity. On the other hand, the emission appears to be a linear function of soil moisture over the range of 0 to 35% for the 1.42 GHz measurements. For the 37.5 GHz measurements, the results indicate that measurements at this frequency is sensitive to surface moisture only, because the coldest measurements belong to the fields that had been irrigated three days before the flight and were flat.

Kroll also has investigated some airborne passive microwave measurements on soil moisture. His data from Chickasha were chosen for comparison. The measurements were made at 1.4 GHz. The fields were mostly medium rough surface with vegetation coverage and were fairly dry (<20° moisture content). His results are shown and compared with the vegetated measurement results of this study on Figures V-51. The effects of vegetation and roughness are shown very pronouncely on his results.

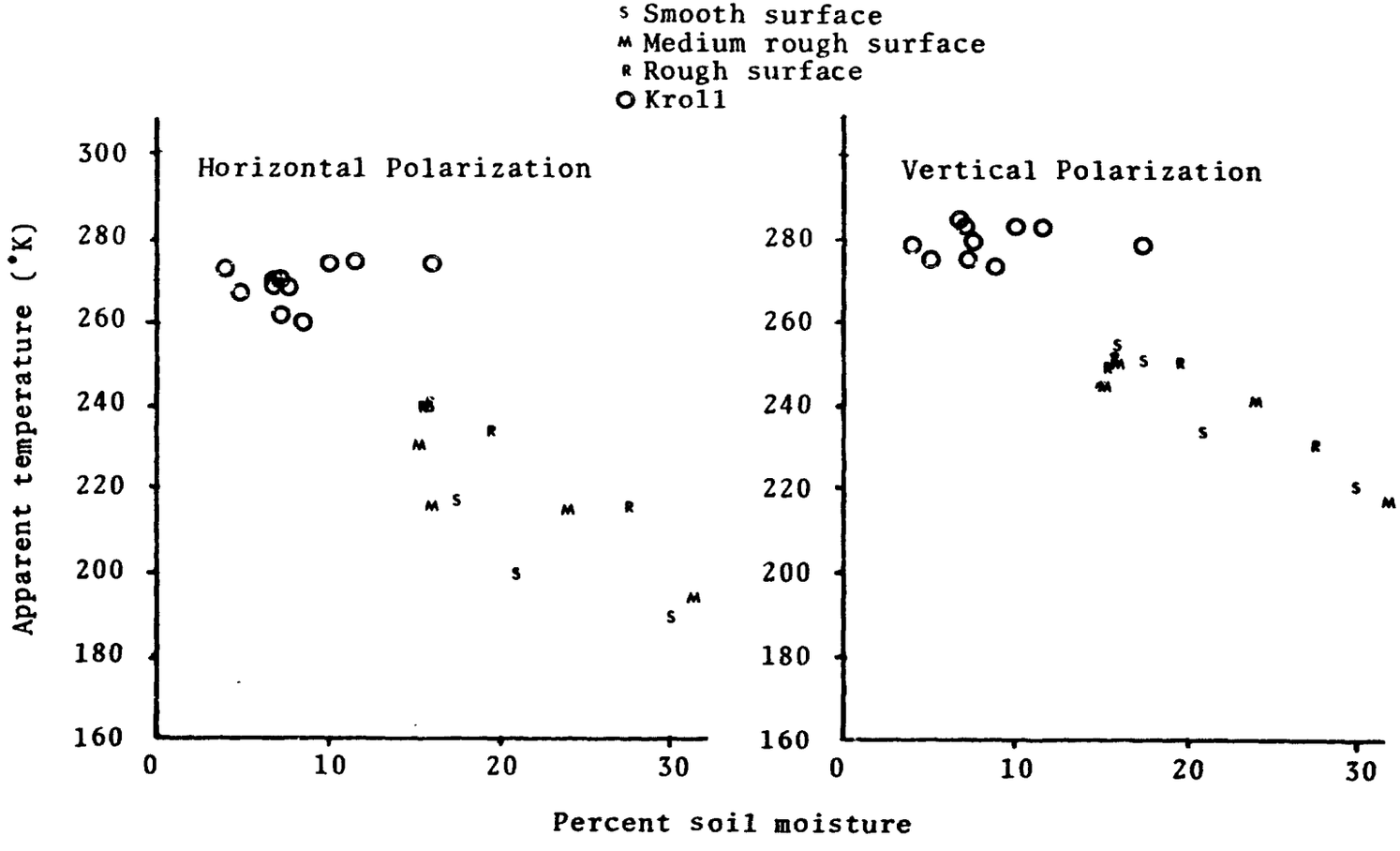

Figure V-51. A Comparison of Results of the 1.42GHz Radiometer, Vegetated Condition.

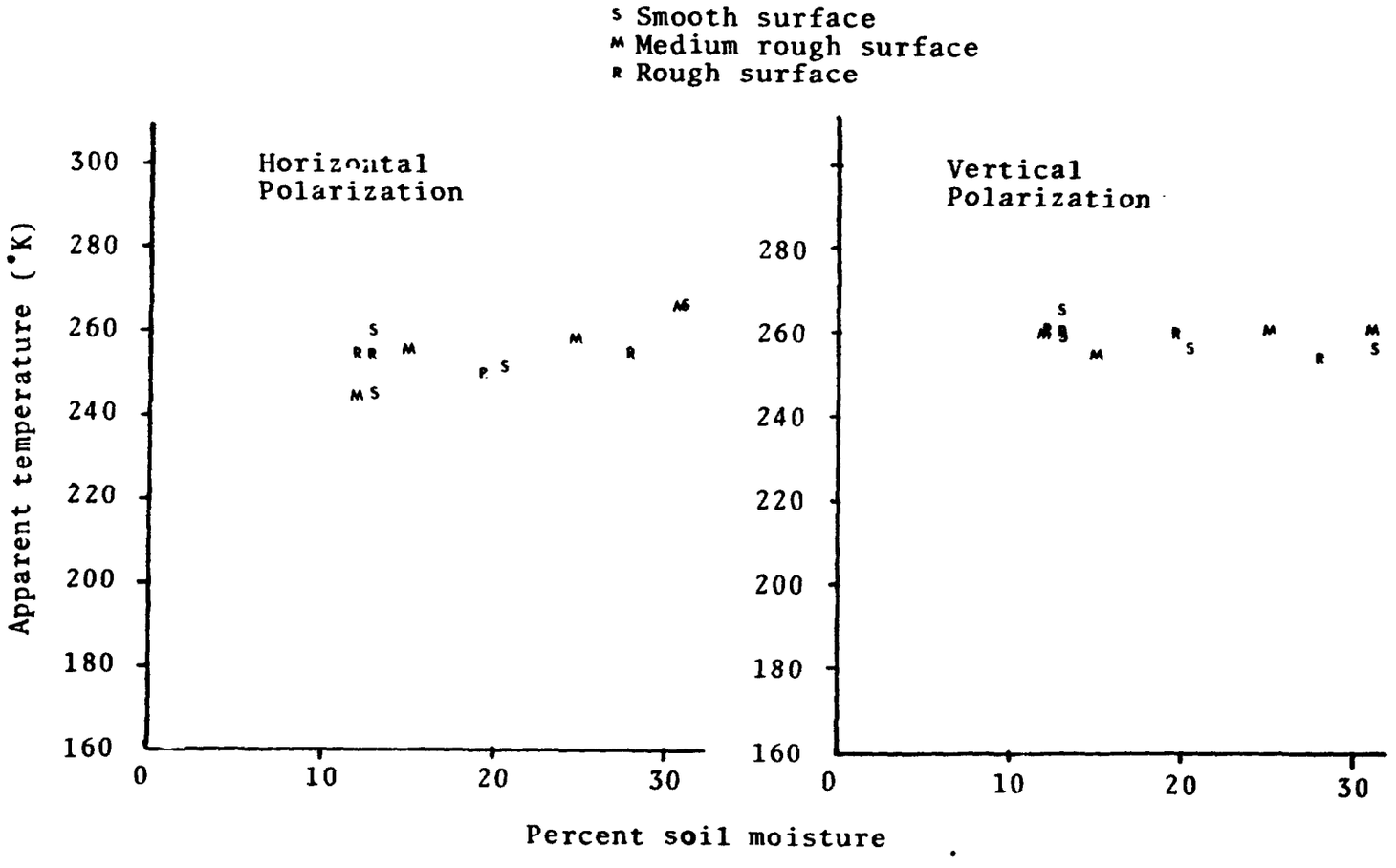

Figure V-52. Results of the 10.6GHz Radiometer, Vegetated Condition.

However, a conclusion concerning the comparison cannot be drawn because Kroll's data were made at soil moisture ranges that this study unfortunately did not cover.

The measurement results of this study have identified and shown the effects of surface roughness and vegetation. The comparisons of this ground based experimental results with some recent airborne measurement results have demonstrated that airborne passive microwave radiometers have the potential to monitor soil moisture variations.

CHAPTER VI

CONCLUSIONS AND RECOMMENDATIONS

Conclusions

This research study has presented the results of a series of controlled ground based passive microwave radiometric measurements on soil moisture. From the ground based experiment, certain effects of surface roughness and vegetation, which partly determine the capability of passive microwave radiometer to detect soil moisture, were identified and studied.

Radiometric measurements were made at 1.42 GHz and 10.6 GHz from an altitude of about 50 feet and for angles from 0° to 50°, generally in 10° increments. Measurement results have demonstrated that surface roughness and vegetation have definite effects on the microwave emission process. Their effects are in some cases very influential and they play decisive roles in regard to the capability of the passive microwave radiometers to detect soil moisture.

Comparing the measurement results from the smooth, medium rough and rough bare surfaces, several effects of roughness were readily identified. The data show that for the wetter soils, there was a monotonic increase in

apparent temperature as surface roughness increases, regardless of the measuring frequency. It was also noted that sensitivity (degree Kelvin/percent soil moisture) changed with regard to surface roughness; the response to soil moisture variations decreases as the surface gets rougher. This phenomenon is apparently independent of the observation angles. For the rough field of this study, the X-band measurements showed no apparent sensitivity, while the L-band measurements still indicated a low sensitivity. It was clearly indicated from these data that the L-band radiometer is more applicable to detection soil moisture than the X-band radiometer. It was observed that the horizontal polarization is more sensitive to surface roughness than the vertical polarization and it is also more sensitive to soil moisture variation than the vertical polarization for both frequencies, and all three surfaces.

In correlating the apparent temperature with soil moisture content, three soil moisture parameters were investigated. They were the 0-2 cm average and 0-18 cm average soil moisture, and the equivalent soil moisture at conventionally defined skin depth. It was found that the equivalent soil moisture parameter was the optimal soil parameter on the whole, in the sense that it provided the best correlation between apparent temperature

and soil moisture.

Vegetation effects for the three surface roughnesses were observed from the entire measurement program data by comparing the results of the different vegetated conditions to the results of the bare condition. An undetermined abnormal behavior in the polarization dependency of apparent temperature for some X-band measurements among the data was observed.

For the vegetation of this study (having a height of only about 0.4 meter at full growth), the vegetation behaves primarily as an attenuator for the L-band measurement, and it exhibited a masking effect over the soil for the X-band measurements, regardless of surface roughness. In another words, the X-band radiometer is incapable of soil moisture detection under the vegetated condition of this study. The L-band radiometer on the other hand, appears to be highly applicable. While the attenuating effect of vegetation lowered the apparent temperature magnitude, the sensitivities were hardly affected. The data also show that the vegetation was an attenuator as well as a contributor to the soil emission, as predicted by Sibley.

Theoretical predictions were made only for the smooth surface case and were computed from Sibley's apparent temperature model for bare and vegetated smooth

surface. The magnitude of the predictions were all significantly lower than the experimental results, though the sensitivities compare reasonably well. It was suspected that the values of the soil dielectric constant measured, an important parameter in the theoretical model, were too high.

The vegetation model has demonstrated to be a valid model, it predicted essentially the same vegetation effects as shown by the experimental results. Good agreements were seen for the comparisons between the results of this study and the results of some recent research effort (all airborne).

The results of this conjunctive study effort have indicated that despite the existance of the vegetation and surface roughness effects, the application of the passive microwave radiometer for remote sensing of soil moisture of natural terrains has bright promises and high potential. Passive microwave radiometers in the lower frequency band are the more useful and capable radiometers for this purpose.

Recommendations

Based on the findings of this study it is recommended that:

Soil dielectric constant measurement. Although careful attention was given to the dielectric constant measurement procedure, the repetitiveness of measurements, the sample handling, the homogeneity of soil, and the effect of compression on soil, the absolute correctness of the results obtained was still not established. This conclusion is based upon the comparisons between the theoretical predictions with the experimental results. Future study on dielectric constant measurements should examine the effect of power reflection by the soil sample during the measurements. To insure that the correct dielectric constant values would be generated by the measurement system, the system should be initially calibrated by measuring a material of known dielectric constant which has been measured by other investigators in the country working this field. In addition to improvements on the measuring network, the relation of soil moisture to its dielectric constant with regard to the effect of frequency must also be investigated.

Continuation of the groundbased experiment and improvement of the data acquisition scheme. The importance of a groundbased experiment, while considering the effects of various parameters that determine the capability of the passive microwave radiometer to monitor soil moisture, is clearly recognized through the various

observations of this study. Future research involving the remote sensing of soil moisture by passive microwave radiometers should be continued with ground based study efforts which adopt a revised data acquisition scheme as proposed in the following. The study of soil moisture profiles indicates that the drying stage of the soil, particularly that in the top 6 cm, is very dynamic. It was observed, for example, that it took only 30 hours for the soil in top 2 cm to completely dry. Since the passive microwave radiometric response to soil moisture comes primarily from the top soil layers, it is necessary to take frequent measurements throughout the drying process after irrigation. It is recommended that measurements be made initially at six hour intervals until the most dynamic stage of soil drying has been completed, then increased to longer intervals until the desired soil dryness is reached.

Optimal soil moisture parameter. In correlating the radiometric apparent temperature with the soil moisture content, there is a need for a soil moisture parameter to which the radiometric temperature correlates optimally. It was determined from this study that the equivalent soil moisture at the conventionally defined skin depth was a reasonably satisfactory soil moisture parameter. However, future research should investigate the possibility of a

more optimal soil moisture parameter at the soil depth where the electric field is attenuated by a factor other than e^{-1}. One approach to such a determination is by the trial and error method. This is done by plotting the apparent temperature data set against the various soil moisture data sets for different values of e^{-x}, where x is any real number including 1.0. The e^{-x} value that gives the best correlation between apparent temperature and soil moisture would then be the most optimal soil moisture parameter.

Improvement of theoretical models. There is a common deficiency shared by the existing apparent temperature models. This deficiency is that the models are considering only a single ray path of thermal emission. Future research in theoretical modeling should work toward a model which would account for integration of emission over the entire antenna illumination area and the range of angles actually viewed. This would require the incorporation of the antenna pattern in the model. In describing the emission problem, the intrinsic properties of the radiating medium, the dielectric constant and the thermometric temperature which vary with depth, have to be considered. The work by Stogryn [52] and England [53] are two recommended modeling efforts that are working in this direction.

In treating the emission problem of natural terrains,

it is also suggested that the thermal emission should be dependent only on the intrinsic properties of the radiating medium and be independent of the surface roughness characteristics. Roughness models should be developed independently and be treated only as an imposing factor on the thermal emission to cause its magnitude to vary with respect to the particular surface characteristics. Improvements regarding to the vegetation models, uniform vegetation case and row crops case, cannot be suggested at the present. These models still await further experimental observations and verifications.

REFERENCES

[1] D. R. Leuder, "Gray Tones," Aerial Photographic Interpretation, McGraw-Hill, New York, 1959, pp. 76-101.

[2] F. F. Sabins, "Infrared Imagery and Geological Aspects," Photogramm. Eng. 33(7), 1967, pp. 743-750.

[3] D. C. Parker, "Remote Sensing for Engineering Investigations of Terrain Infrared Systems," Proceedings of the Fifth Symposium on Remote Sensing of Environment, University of Michigan, Ann Arbor, Michigan, April 1968, pp. 701-710.

[4] J. M. Kennedy, "Electromagnetic Sensor Correlation Study," Final Report 29167-5, prepared for ESSA, Office of Hydrology, by Ryan Aeronautical Company, Electronic and Space Systems, San Diego, California, January, 1968.

[5] A. T. Edgerton, "Engineering Application of Microwave Radiometry," Proceedings of the Fifth Symposium on Remote Sensing of Environment, University of Michigan, Ann Arbor, Michigan, April 1969, pp. 711-724.

[6] W. Peake, "Interaction of Electromagnetic Waves with Some Natural Surfaces," IRE Transactions on Antennas and Propagation (special supplement), vol. AP-7, December 1959.

[7] S. Chen and W. Peake, "Apparent Temperatures of Smooth and Rough Terrain," IRE Transaction on Antennas and Propagation, vol. AP-9, November 1961, pp. 567-572.

[8] A. Stogryn, "Electromagnetic Scattering from Rough Finitely Conducting Surfaces," Radio Science, Vol. 2, April 1967, pp. 415-428.

[9] A. Fung, F. Ulaby, and S. Wu, "Apparent Temperature and Emissivity of Natural Surfaces at Microwave Frequencies," Technical Report 133-12, Center for Research, Inc., The University of Kansas, Lawrence, Kansas, March 1970.

[10] L. F. Johnson, "On the Performance of Infrared Sensors in Earth Observations," Technical Report RSC-37, Remote Sensing Center, Texas A&M University, College Station, Texas, August 1972.

[11] T. Schmuggee, P. Gloersen, T. Wilheit, and F. Geiger, "Remote Sensing of Soil Moisture with Microwave Radiometers," Journal of Geophysical Research, Volume 79, January 1974.

[12] J. A. Richerson, "An Experimental Evaluation of a Theoretical Model of the Microwave Emission of a Natural Surface," Technical Report RSC-10, Remote Sensing Center, Texas A&M University, College Station, Texas, August 1971.

[13] B. R. Jean, "Selected Applications of Microwave Radiometric Techniques," Technical Report RSC-30, Remote Sensing Center, Texas A&M University, College Station, Texas, August 1971.

[14] C. L. Kroll, "Remote Monitoring of Soil Moisture Using Airborne Microwave Radiometers," Technical Report RSC-43, Remote Sensing Center, Texas A&M University, College Station, Texas, June 1973.

[15] J. W. Rouse, Jr., "On the Effect of Moisture Variations on Radar Backscatter from Rough Soil Surfaces," Technical Memorandum RSC-52, Remote Sensing Center, Texas A&M University, College Station, Texas, July 1972.

[16] R. K. Moore, F. Dickey, C. King, and J. Hotzman, "Moisture Dependency of Radar Backscatter from Irrigated and Non-Irrigated Fields at 400 MHz and 13.3 GHz," Technical Report, University of Kansas, Lawrence, Kansas, 1972.

[17] W. P. Waite and H. C. MacDonald,""Vegetation Penetration" with K-band Imaging Radars," IEEE Transactions on Geoscience Electronics, Volume GE-9, No. 3, July 1971.

[18] W. P. Waite and H. C. MacDonald, "Soil Moisture Detection with Imaging Radars," Water Resources Research, Vol. 7, No. 1, February 1971, pp. 100-110.

[19] B. R. Davis, J. R. Lundien, and A. N. Williamson, Jr., "Feasibility Study of the Use of Radar to Detect Surface and Ground Water," U. S. Army Engineering Waterways Experimental Station, Technical Report 3-727, Vicksburg, Mississippi, April 1966, pp. 1-50.

[20] J. Kennedy, A. Edgerton, R. Sakamoto, and R. Mandl, "Passive Microwave Measurements of Snow and Soil," Technical Report No. 2, Space-General Cooperation SGD 829R-4, El Monte, California, November 5, 1966.

[21] A Edgerton et al., "Passive Microwave Measurements of Snow, Soils, and Snow-Ice-Water Systems," Technical Report No. 4, Space-General Corporation SGD 829-6, El Monte, California, February 1968.

[22] J. Kennedy, "A Microwave Radiometric Study of Buried Karst Topology," Geological Society of America Bulletin, Vol. 79, June 1968, pp. 735-742.

[23] A. Edgerton and M. Meier, "Microwave Emission from Snow-A Progress Report," Proceedings of the Seventh Symposium on Remote Sensing of Environment, University of Michigan, Ann Arbor, May 1971.

[24] C. Mason,"Detecting Soil Moisture Content with Remote and Contact Temperature Sensors," NASA Manned Spacecraft Center, Houston, Texas, October 1969.

[25] A. E. Basharinov and A. M. Shutko, "The Microwave Radiometric Measurements of Soil Moisture," Institute of Radio Engineering and Electronics of the Academy of Science of the USSR, 1970.

[26] C. Poe, A. Stogryn, and A. T. Edgerton, "Determination of Soil Moisture Content Using Microwave Radiometry," Summary Report 1684R-2, Aerojet-General Corporation, El Monte, California, February 1971.

[27] T. G. Sibley, "Microwave Emission and Scattering from Vegetated Terrain," Technical Report RSC-44, Remote Sensing Center, Texas A&M University, College Station, Texas 77843.

[28] M. Planck, The Theory of Heat Radiation, New York: Dover Publications, 1959.

[29] H. P. Taylor, "The Radiometer Equation," The Microwave Journal, May 1967, p. 39.

[30] W. Peake, "The Microwave Radiometer as a Remote Sensing Instrument with Application to Geology," Note Prepared for a Short Course on Geologic Remote Sensing, Standford University, December 4-8, 1967.

[31] J. C. Harlan, C. A. Morgan, and R. W. Newton, "Data Acquisition for a Remote Sensing Field Measurement Program," Proceeding of the National Telecommunications Conference, Vol. 1, Atlanta, Georgia, November 26-28, 1973, pp. 9B1-9B8.

[32] AIL, a division of Cutler-Hammer, "Passive Microwave Radiometer System," Prepared for NASA/MSC, In Response to RFP BB321-54-1-321P, Exhibit A to Proposal J-5617, May 1971, Deer Park, Long Island, New York.

[33] R. H. Dicke, "The Measurement of Thermal Radiation at Microwave Frequencies," The Review of Scientific Instruments, Vol. 17, No. 7, July 1946.

[34] Stratton, J. A., Electromagnetic Theory, First Edition, McGraw-Hill Book Company, Inc., New York, 1941.

[35] E. C. Jordan and K. G. Balmain, Electromagnetic Waves and Radiating Systems, 2nd ed., Englewood Cliffs, New Jersey: Prentice-Hill, Inc., 1968.

[36] Evans, S., "Dielectric Properties of Ice and Snow," Journal of Glaciology, Vol. 5, No. 42, pp. 773-792, October 1962.

[37] Peake, W. H. and T. L. Oliver, "The Response of Terrestrial Surfaces at Microwave Frequencies," Technical Report AFAL-TR-70-301, Electroscience Laboratory, Ohio State University, Columbus, Ohio, May 1971.

[38] Hasted, J. B., "The Dielectric Properties of Water", Progress in Dielectrics, Vol. 3, pp. 101-149, New York, John Wiley and Sons, Inc., 1961.

[39] Cole, R. H., "Theoreis of Dielectric Polarization and Relaxation," Progress in Dielectrics, Vol. 3, pp. 47-99, New York: John Wiley and Sons, Inc., 1961.

[40] R. L. Lytton, Private Communication, Civil Engineering Department, Texas A&M University, College Station, Texas, March 1974.

[41] C. A. Black, D. D. Evans, J. L. White, L. E. Ensniger and F. E. Clark, Methods of Soil Analysis, Part 1, Number 9 in the Series Agronomy, American Society of Agronomy, Inc., Publisher, Madison, Wisconsin, 1965.

[42] B. R. Jear, "Comments on Microwave Radiometry as a Remote Sensor for the Geosciences," Remote Sensing Center Technical Memorandum RSC-06, Texas A&M University, College Station, Texas, 1970.

[43] J. W. Rouse, Jr., and A. J. Giarola, "Proposal for Use of Lunar Soil for Experimental Analyses Using Microwave Engineering and Neutron Activation Methods," Texas Engineering Experiment Station, Texas A&M University, College Station, Texas, June 1, 1970.

[44] Hewlett Packard, "Dielectric Measurements with Time Domain Reflectometry," Hewlett Packard Application Note 118, Houston, Texas, March 1970.

[45] P. Hertel, A. W. Straiton and C. W. Tolbert, "Dielectric Constant Measurements at 8.6 Millimeter Wavelength," Electrical Engineering Research Laboratory Report No. 65, The University of Texas, Austin, Texas, March 1953.

[46] M. L. Wiebe, "Laboratory Measurement of the Complex Dielectric Constant of Soils," Technical Report RSC-23, Remote Sensing Center, Texas A&M University, College Station, Texas, October 1971.

[47] A. J. Giarola, "Experiment on Microwave Measurements, E. E. 403 Lab," Electrical Engineering Department, Texas A&M University, College Station, Texas, Spring, 1973.

[48] C. L. Kroll and T. G. Sibley, "Complex Dielectric Constant Measurements for Selected Soil Types," Technical Memorandum RSC-45, Remote Sensing Center, Texas A&M University, College Station, Texas, May 1972.

[49] T. G. Sibley, "Discussion of a Simplified Procedure for Measuring Dielectric Constant of Soil as a Function of Moisture Content," Technical Memorandum RSC-51, Remote Sensing Center, Texas A&M University, College Station, Texas, July 1972.

[50] S. L. Lee, "The Determination of Soil Skin Depth and the "Equivalent Soil Moisture Content";" Technical Memorandum RSC-84, Remote Sensing Center, Texas A&M University, College Station, Texas, December 1973.

[51] P. Hoekstra and A. Delaney, "Dielectric Properties of Soils at UHF and Microwave Frequencies," Journal of Geophysical Research, Vol. 79, No. 11, April 10, 1974, pp. 1699-1708.

[52] A. Stogryn, "The Brightness Temperature of a Vertically structured Medium," Radio Science, Vol. 5, No.12, December 1970, pp. 1397-1406.

[53] A. W. England, "Thermal Microwave Emission from a Halfspace Containing Scatterers," Radio Science, Vol. 9, No. 4, April 1974, pp. 447-454.

APPENDIX A

REDUCED SOIL MOISTURE AND RADIOMETRIC TEMPERATURE DATA

This appendix contains tabulations of reduced soil moisture and apparent temperature data for the entire experiment, they are presented in Table A-1, Table A-2, abd Table A-3 respectively. Soil moisture profiles were constructed from the data of Table A-1 and are shown in figures A-1 through A-6. Skin depth and "equivalent soil moisture content" for both L- and X-band were calculated and are indicated on these soil moisture profiles.

Table A-1. A Listing of the Entire Soil Moisture and Ground Thermometric Temperature Data of the Experiment.

SMOOTH SURFACE

		LOCATION DEPTH	SOIL MOIST.%	AVE θ DEPTH	AVE. AT LOCATION	SOIL TEMP	
L-BAND	X-BAND						
73JULY24SK IN DEPTH=10.32	, 7.55CM	R1 0 CM	7.00	5.92		94.0000 AT	2CM
SOSM=10.31	, 6.23 %	4	8.49	8.29		89.0000	4
		6	11.06	11.13		0.5660	8
		18	19.25	20.73	11.45	0.5465	16
		R2 0	7.37	5.92		99.0000	2
		4	8.16	8.29		96.0000	4
		6	12.28	11.13		0.5699	8
		18	19.82	20.73	11.99	0.5478	16
		R3 0	5.59	5.92		99.0000	2
		4	7.97	8.29		92.5000	4
		6	9.73	11.13		0.5691	8
		18	18.91	20.73	10.53	0.5479	16
		R4 0	5.69	5.92		96.0000	2
		4	8.78	8.29		92.0000	4
		6	11.03	11.13		0.5714	8
		18	19.40	20.73	11.23	0.5471	16
		R5 0	6.13	5.92		99.0000	2
		4	8.17	8.29		93.0000	4
		6	9.89	11.13		0.5691	8
		18	21.31	20.73	11.36	0.5477	16
		A1 0	5.91	5.92		101.0000	2
		4	7.74	8.29		93.0000	4
		6	15.04	11.13		0.5738	8
		18	20.44	20.73	12.28	0.5482	16
		A2 0	5.40	5.92		105.0000	2
		4	8.70	8.29		97.0000	4
		6	11.49	11.13		0.5757	8
		18	21.27	20.73	11.70	0.5484	16
		A3 0	5.75	5.92		101.0000	2
		4	8.52	8.29		96.0000	4
		6	9.44	11.13		0.5767	8
		18	19.74	20.73	10.86	0.5495	16
		A4 0	5.20	5.92		100.0000	2
		4	7.93	8.29		95.0000	4
		6	10.41	11.13		0.5763	8
		18	22.08	20.73	11.41	0.5493	16
		A5 0	5.29	5.92		98.0000	2
		4	8.52	8.29		94.0000	4

Continuation of Table A-1.

A Listing of the Entire Soil Moisture and Ground Thermometric Temperature Data of the Experiment.

		6	10.92	11.13		0.5738	8	
		18	25.03	20.73	12.46	0.5505	16	
73JULY26SKIN DEPTH= 3.47 , 0.44CM	B1	0 CM	29.39	29.30		91.5000 AT	2CM	
EQSM=29.00 ,29.35 %		4	28.62	28.67		89.0000	4	
		6	28.01	28.65		85.9000	8	
		18	29.41	25.17	28.61	0.5484	16	
	B2	0	27.56	29.30		92.5000	2	
		4	28.61	28.67		89.5000	4	
		6	28.67	28.65		82.0000	8	
		18	25.96	25.17	27.70	0.5473	16	
	B3	0	28.87	29.30		92.0000	2	
		4	26.87	28.67		5.0000	4	
		6	27.27	28.65		90.5000	8	
		18	22.97	25.17	26.46	86.7000	16	
	B4	0	30.52	29.30		0.5484	2	
		4	28.32	28.67		94.5000	4	
		6	28.36	28.65		90 9000	8	
		18	23.26	25.17	27.62	86.9000	16	
	B5	0	31.45	29.30		0.5493	2	
		4	29.38	28.67		92.4000	4	
		6	28.78	28.65		89.4000	8	
		18	24.71	25.17	28.58	0.5486	16	
	A1	0	29.14	29.30		86.5000	2	
		4	29.50	28.67		85.0000	4	
		6	28.80	28.65		83.1000	8	
		18	23.96	25.17	27.85	0.5440	16	
	A2	0	*****	29.30		85.0000	2	
		4	28.36	28.67		84.5000	4	
		6	28.99	28.65		82.5000	8	
		18	25.40	25.17	27.58	0.5483	16	
	A3	0	29.57	29.30		86.7000	2	
		4	28.86	28.67		84.5000	4	
		6	28.27	28.65		83.5000	8	
		18	23.85	25.17	27.64	0.5469	16	
	A4	0	27.87	29.30		86.0000	2	
		4	28.81	28.67		86.0000	4	
		6	30.28	28.65		87.4000	8	
		18	25.00	25.17	27.99	0.5459	16	
	A5	0	29.34	29.30		82.8000	2	
		4	29.45	28.67		87.1000	4	
		6	29.14	28.65		84.5000	8	
		18	29.27	25.17	29.02	0.5468	16	
73JULY30SKIN DEPTH= 6.24 , 1.7[illegible]CM	B1	0 CM	3.73	5.86		103.6000 AT	2CM	
EQSM=15.40 , 8.42 %		4	22.20	21.63		100.5000	4	
		6	22.98	22.88		94.9000	8	
		18	22.65	23.36	17.89	0.5517	16	
	B2	0	6.62	5.86		105.6000	2	
		4	21.06	21.63		97.5000	4	
		6	21.25	22.88		94.5000	8	
		18	20.38	23.36	17.33	0.5541	16	
	B3	0	4.62	5.86		110.0000	2	
		4	20.73	21.63		104.5000	4	
		6	21.54	22.88		94.0000	8	
		18	22.22	23.36	17.28	0.5554	16	
	B4	0	7.79	5.86		108.2000	2	
		4	21.67	21.63		103.5000	4	
		6	22.21	22.88		98.3000	8	
		18	22.86	23.36	18.63	0.5554	16	
	B5	0	4.52	5.86		110.0000	2	
		4	22.11	21.63		102.0000	4	

Continuation of Table A-1.

A Listing of the Entire Soil Moisture and Ground Thermometric Temperature Data of the Experiment.

		6	23.35	22.88		95.0000		8
		18	24.51	23.36	18.62	0.5570		16
	A1	0	7.47	5.86		108.5000		2
		4	18.56	21.63		98.0000		4
		6	20.72	22.88		97.5000		8
		18	22.61	23.36	17.39	0.5541		16
	A2	0	9.53	5.86		106.5000		2
		4	20.49	21.63		103.5000		4
		6	23.23	22.88		97.0000		8
		18	23.17	23.36	19.10	0.5536		16
	A3	0	6.11	5.86		110.0000		2
		4	22.52	21.63		107.5000		4
		6	23.75	22.88		99.0000		8
		18	21.28	23.36	18.42	0.5559		16
	A4	0	4.23	5.86		109.5000		2
		4	23.87	21.63		104.5000		4
		6	25.39	22.88		96.0000		8
		18	26.89	23.36	20.10	0.5581		16
	A5	0	4.01	5.86		110.0000		2
		4	23.08	21.63		106.5000		4
		6	24.21	22.88		96.5000		8
		18	26.99	23.36	19.57	0.5571		16
73SEPT25SKIN DEPTH= 5.96 , 1.01CM	R1	0 CM	13.04	13.00		95.8000	AT	0CM
FOS%=16.01 ,13.05 %		4	22.54	17.68		92.3000		2
		6	22.25	17.74		89.1000		4
		18	22.93	19.74	20.19	83.0000		8
	R2	0	17.03	13.00		86.7000		0
		4	22.49	17.68		87.6000		2
		6	22.21	17.74		84.7000		4
		18	20.31	19.74	20.51	82.0000		8
	R3	0	17.07	13.00		90.0000		0
		4	22.73	17.68		89.9000		2
		6	23.48	17.74		87.4000		4
		18	21.67	19.74	21.24	82.5000		8
	R4	0	12.27	13.00		93.7000		0
		4	16.48	17.68		93.6000		2
		6	15.36	17.74		88.9000		4
		18	19.49	19.74	15.90	84.8000		8
	R5	0	9.09	13.00		94.9000		0
		4	10.96	17.68		98.3000		2
		6	12.75	17.74		91.9000		4
		18	17.22	19.74	12.50	84.8000		8
	A1	0	14.16	13.00		92.8000		0
		4	16.45	17.68		88.6000		2
		6	16.27	17.74		88.3000		4
		18	20.24	19.74	16.78	84.6000		8
	A2	0	12.04	13.00		100.5000		0
		4	19.67	17.68		93.0000		2
		6	17.78	17.74		91.7000		4
		18	21.01	19.74	17.62	86.1000		8
	A3	0	16.05	13.00		92.0000		0
		4	20.37	17.68		89.6000		2
		6	18.94	17.74		88.5000		4
		18	18.30	19.74	18.41	83.4000		8
	A4	0	10.17	13.00		94.5000		0
		4	13.58	17.68		95.3000		2
		6	14.78	17.74		87.8000		4
		18	19.40	19.74	14.46	84.3000		8
	A5	0	9.07	13.00		100.0000		0
		4	11.54	17.68		99.0000		2

Continuation of Table A-1.

A Listing of the Entire Soil Moisture and Ground Thermometric Temperature Data of the Experiment.

		6	13.60	17.74		89.7000		4
		18	16.81	19.74	12.75	85.9000		8
[illegible] SKIN DEPTH= 3.43 , 0.44CM	B1	0 CM	31.37	30.85		68.7000	AT	0CM
FOSH=29.67 ,30.92 %		4	27.87	28.02		67.6000		2
		6	27.88	27.84		66.8000		4
		18	24.71	22.94	27.96	66.6000		8
	B2	0	32.75	30.85		69.8000		0
		4	29.80	28.02		68.2000		2
		6	29.68	27.84		67.5000		4
		18	22.96	22.94	28.79	67.1000		8
	B3	0	28.74	30.85		68.3000		0
		4	25.57	28.02		67.5000		2
		6	24.41	27.84		66.8000		4
		18	19.68	22.94	24.60	66.6000		8
	B4	0	30.69	30.85		69.2000		0
		4	27.03	28.02		68.5000		2
		6	27.30	27.84		67.5000		4
		18	23.34	22.94	27.09	67.2000		8
	B5	0	30.74	30.85		69.5000		0
		4	29.83	28.02		67.8000		2
		6	29.93	27.84		67.0000		4
		18	23.99	22.94	28.62	66.7000		8
[illegible]. SKIN DEPTH= 4.45 , 0.60CM	B1	0 CM	22.14	20.48		67.8000	AT	0CM
FOSH=20.99 ,20.43 %		4	22.49	21.61		65.3000		2
		6	21.42	21.79		65.8000		4
		18	23.30	24.09	22.34	66.5000		8
	B2	0	19.87	20.48		65.7000		0
		4	21.04	21.61		65.7000		2
		6	23.30	21.79		66.3000		4
		18	24.34	24.09	22.14	66.8000		8
	B3	0	19.85	20.48		64.2000		0
		4	20.57	21.61		64.8000		2
		6	21.97	21.79		65.3000		4
		18	21.49	24.09	20.97	66.5000		8
	B4	0	23.88	20.48		65.1000		0
		4	23.96	21.61		65.8000		2
		6	27.58	21.79		66.2000		4
		18	23.61	24.09	23.50	66.8000		8
	B5	0	24.43	20.48		65.3000		0
		4	23.70	21.61		65.8000		2
		6	21.68	21.79		66.4000		4
		18	23.19	24.09	23.25	67.0000		8
	A1	0	20.52	20.48		64.2000		0
		4	21.24	21.61		66.0000		2
		6	21.41	21.79		66.4000		4
		18	24.04	24.09	21.80	67.3000		8
	A2	0	17.57	20.48		65.0000		0
		4	19.11	21.61		65.6000		2
		6	20.48	21.79		66.4000		4
		18	23.51	24.09	20.17	67.3000		8
	A3	0	21.45	20.48		65.2000		0
		4	22.28	21.61		65.9000		2
		6	19.75	21.79		66.5000		4
		18	23.56	24.09	21.76	67.2000		8
	A4	0	15.92	20.48		65.5000		0
		4	20.24	21.61		66.5000		2
		6	24.03	21.79		67.0000		4
		18	25.46	24.09	21.41	68.1000		8
	A5	0	19.15	20.48		64.5000		0
		4	21.47	21.61		65.9000		2

Continuation of Table A-1.

A Listing of the Entire Soil Moisture and Ground Thermometric Temperature Data of the Experiment.

		6	21.25	21.79		66.5000	4
		18	28.35	24.09	22.56	67.5000	8
74FEB.13SP IN DEPTH=13.30 , 0.98CM	R1	0 CM	11.59	13.09		107.1000 AT	4CM
EOSM=17.50 , 5.40 %		4	17.17	20.93		105.7000	8
		6	17.14	20.36		102.6000	16
		18	21.30	22.58	16.80	101.4000	32
	R2	0	9.56	13.09		107.9000	4
		4	22.91	20.93		106.6000	8
		6	23.79	20.36		103.5000	16
		18	22.81	22.58	19.76	101.9000	32
	R3	0	17.51	13.09		108.0000	4
		4	22.28	20.93		106.7000	8
		6	23.55	20.36		103.5000	16
		18	23.01	22.58	20.34	102.0000	32
	B4	0	12.70	13.09		107.7000	4
		4	24.09	20.93		106.7000	8
		6	24.07	20.36		103.3000	16
		18	23.92	22.58	21.19	101.9000	32
	B5	0	11.90	13.09		108.2000	4
		4	24.48	20.93		102.4000	8
		6	24.34	20.36		103.8000	16
		18	25.90	22.58	22.15	102.0000	32
	A1	0	11.08	13.09		107.3000	4
		4	20.50	20.93		107.1000	8
		6	21.26	20.36		104.0000	16
		18	22.52	22.58	18.84	102.2000	32
	A2	0	21.12	13.09		106.5000	4
		4	19.22	20.93		105.6000	8
		6	7.40	20.36		102.7000	16
		18	23.73	22.58	17.87	101.3000	32
	A3	0	11.05	13.09		107.5000	4
		4	20.67	20.93		106.3000	8
		6	20.80	20.36		102.9000	16
		18	21.73	22.58	18.56	101.5000	32
	A4	0	15.38	13.09		107.7000	4
		4	20.21	20.93		106.7000	8
		6	20.72	20.36		103.2000	16
		18	21.31	22.58	19.41	101.7000	32
	A5	0	14.06	13.09		107.7000	4
		4	17.76	20.93		106.7000	8
		6	18.57	20.36		103.5000	16
		18	19.53	22.58	17.48	101.7000	32

Continuation of Table A-1.

A Listing of the Entire Soil Moisture and Ground Thermometric Temperature Data of the Experiment.

MEDIUM ROUGH SURFACE

	LOCATION	DEPTH	SOIL MOIST.%	AVE @ DEPTH	AVE. AT LOCATION	SOIL TEMP	
73JULY24SKIN DEPTH=12.50 , 4.46CM	E1	0 CM	1.92	2.42		105.0000 AT	4CM
EOSM= 8.88 , 3.86 %		4	5.47	5.40		0.5903	8
		6	7.97	8.31		0.5545	16
		18	18.13	19.42	8.37	0.5465	32
	E2	0	2.50	2.42		106.9000	4
		4	5.29	5.40		0.5879	8
		6	8.95	8.31		0.5536	16
		18	18.36	19.42	8.77	0.5486	32
	E3	0	2.56	2.42		101.5000	4
		4	5.99	5.40		96.3000	8
		6	7.94	8.31		0.5547	16
		18	19.54	19.42	9.01	0.5480	32
	E4	0	2.38	2.42		102.5000	4
		4	6.82	5.40		93.7000	8
		6	7.99	8.31		0.5541	16
		18	19.22	19.42	9.10	0.5472	32
	E5	0	3.05	2.42		105.2000	4
		4	6.70	5.40		91.5000	8
		6	11.59	8.31		0.5527	16
		18	19.10	19.42	10.11	0.5475	32
	E1	0	2.73	2.42		106.0000	4
		4	5.30	5.40		98.0000	8
		6	9.61	8.31		0.5521	16
		18	16.83	19.42	8.62	0.5467	32
	E2	0	2.27	2.42		105.0000	4
		4	4.08	5.40		97.5000	8
		6	7.54	8.31		0.5572	16
		18	18.52	19.42	8.10	0.5475	32
	E3	0	1.99	2.42		104.5000	4
		4	4.02	5.40		93.5000	8
		6	5.88	8.31		0.5504	16
		18	18.80	19.42	7.67	0.5466	32
	E4	0	2.21	2.42		104.0000	4
		4	4.73	5.40		95.0000	8
		6	7.88	8.31		0.5512	16
		18	21.93	19.42	9.19	0.5463	32
	E5	0	2.55	2.42		102.5000	4
		4	5.56	5.40		92.7000	8

Continuation of Table A-1.

A Listing of the Entire Soil Moisture and Ground Thermometric Temperature Data of the Experiment.

		4	7.78	8.31		0.5503	16	
		18	23.74	19.42	9.91	0.5464	32	
73JULY26SKIN DEPTH= 3.76 , 0.52CM	E1	0 CM	23.21	23.91		98.5000 AT	2CM	
EOSM=25.60 ,24.15 %		4	20.04	27.50		95.5000	4	
		6	26.62	27.42		91.6000	8	
		18	24.22	23.46	25.02	0.5538	16	
	E2	0	25.49	23.91		100.0000	2	
		4	25.69	27.50		94.5000	4	
		6	25.79	27.42		90.6000	8	
		18	23.65	23.46	25.15	0.5528	16	
	E3	0	23.01	23.91		97.5000	2	
		4	27.83	27.50		93.4000	4	
		6	27.70	27.42		90.0000	8	
		18	20.99	23.46	24.88	0.5502	16	
	E4	0	25.50	23.91		99.5000	2	
		4	26.74	27.50		96.0000	4	
		6	27.73	27.42		89.5500	8	
		18	24.19	23.46	26.04	0.5432	16	
	E5	0	*****	23.91		99.5000	2	
		4	30.19	27.50		96.5500	4	
		6	29.13	27.42		90.5000	8	
		18	23.51	23.46	27.60	0.5480	16	
	F1	0	25.22	23.91		101.0000	2	
		4	25.36	27.50		97.5000	4	
		6	26.28	27.42		92.5000	8	
		18	22.06	23.46	24.73	0.5502	16	
	F2	0	25.37	23.91		101.5500	2	
		4	26.65	27.50		98.5500	4	
		6	26.05	27.42		91.5000	8	
		18	23.27	23.46	25.34	0.5489	16	
	F3	0	28.24	23.91		98.5000	2	
		4	27.93	27.50		95.5000	4	
		6	29.32	27.42		89.5000	8	
		18	25.17	23.46	27.67	0.5476	16	
	F4	0	18.01	23.91		99.2000	2	
		4	26.38	27.50		97.0000	4	
		6	24.75	27.42		92.0000	8	
		18	24.14	23.46	23.32	0.5472	16	
	F5	0	21.16	23.91		99.0000	2	
		4	32.18	27.50		95.2000	4	
		6	30.82	27.42		91.0000	8	
		18	*****	23.46	28.05	0.5476	16	
73JULY30SKIN DEPTH= 5.44 , 1.26CM	E1	0 CM	7.13	6.32		107.6000 AT	2CM	
EOSM=17.35 ,10.99 %		4	22.35	20.83		105.0000	4	
		6	21.04	21.12		93.8000	8	
		18	22.80	22.25	18.33	0.5465	16	
	E2	0	5.49	6.32		107.1000	2	
		4	20.02	20.83		102.5000	4	
		6	21.35	21.12		93.5000	8	
		18	20.54	22.25	16.85	0.5521	16	
	E3	0	4.75	6.32		110.0000	2	
		4	20.25	20.83		101.5000	4	
		6	21.25	21.12		94.0000	8	
		18	22.42	22.25	17.17	0.5545	16	
	E4	0	5.27	6.32		105.1000	2	
		4	19.27	20.83		99.7000	4	
		6	22.26	21.12		93.2000	8	
		18	23.44	22.25	17.56	0.5505	16	
	E5	0	5.65	6.32		100.3000	2	
		4	22.13	20.83		97.3000	4	

Continuation of Table A-1.

A Listing of the Entire Soil Moisture and Ground Thermometric Temperature Data of the Experiment.

		6	22.79	21.12		91.0000	8	
		18	22.86	22.25	18.61	0.5538	16	
	F1	0	6.24	6.32		95.6000	2	
		4	19.98	20.83		92.5000	4	
		6	20.61	21.12		87.0000	8	
		18	20.97	22.25	16.95	0.5482	16	
	F2	0	8.87	6.32		97.5000	2	
		4	19.58	20.83		93.5000	4	
		6	19.81	21.12		86.5000	8	
		18	20.23	22.25	17.12	0.5480	16	
	F3	0	5.12	6.32		103.0000	2	
		4	19.33	20.83		98.4000	4	
		6	20.26	21.12		95.0000	8	
		18	20.24	22.25	16.24	0.5494	16	
	F4	0	5.91	6.32		104.2000	2	
		4	20.90	20.83		102.5000	4	
		6	18.75	21.12		92.5000	8	
		18	22.98	22.25	17.14	0.5509	16	
	F5	0	8.76	6.32		104.1000	2	
		4	23.48	20.83		99.2000	4	
		6	23.08	21.12		90.5000	8	
		18	26.05	22.25	20.34	0.5508	16	
73SEPT25SKIN DEPTH= 6.22 , 1.08CM	F1	0 CM	13.48	12.35		87.1000 AT	0CM	
EQSM=15.44 ,12.35 %		4	19.84	17.39		92.2000	2	
		6	19.91	17.85		85.8000	4	
		18	20.29	19.75	18.38	81.5000	8	
	E2	0	14.75	12.35		85.6000	0	
		4	21.40	17.39		85.3000	2	
		6	20.96	17.85		82.9000	4	
		18	19.01	19.75	19.03	80.7000	8	
	F3	0	17.51	12.35		.6000	0	
		4	21.71	17.39		86.0000	2	
		6	22.67	17.85		83.5000	4	
		18	21.06	19.75	20.74	80.9000	8	
	F4	0	8.71	12.35		88.5000	0	
		4	14.35	17.39		85.6000	2	
		6	15.46	17.85		84.2000	4	
		18	19.98	19.75	14.63	81.1000	8	
	F5	0	7.73	12.35		90.6000	0	
		4	10.27	17.39		91.0000	2	
		6	11.84	17.85		87.4000	4	
		18	17.42	19.75	11.92	84.9000	8	
	F1	0	17.10	12.35		92.2000	0	
		4	21.29	17.39		86.7000	2	
		6	20.12	17.85		83.9000	4	
		18	22.03	19.75	20.14	80.6000	8	
	F2	0	14.18	12.35		89.4000	0	
		4	20.24	17.39		88.6000	2	
		6	20.49	17.85		82.9000	4	
		18	19.86	19.75	18.69	80.0000	8	
	F3	0	11.01	12.35		89.5000	0	
		4	17.94	17.39		87.2000	2	
		6	18.08	17.85		84.0000	4	
		18	*****	19.75	16.39	80.5000	8	
	F4	0	10.25	12.35		88.3000	0	
		4	14.23	17.39		88.9000	2	
		6	14.14	17.85		83.7000	4	
		18	20.29	19.75	14.73	81.9000	8	
	F5	0	8.82	12.35		89.4000	0	
		4	12.61	17.39		87.7000	2	

Continuation of Table A-1.

A Listing of the Entire Soil Moisture and Ground Thermometric Temperature Data of the Experiment.

		6		14.80	17.85		86.9000	4
		18		18.99	19.75	13.81	83.0000	8
73OCT.30SKIN DEPTH= 3.33 , 0.43CM	F1	0	CM	32.64	32.58		68.0000 AT	0CM
EQSM=31.54 ,33.46 %		4		31.30	29.56		67.2000	2
		6		31.30	29.98		66.6000	4
		18		26.49	24.22	30.43	66.0000	8
	E2	0		33.14	32.58		67.6000	0
		4		29.10	29.56		66.8000	2
		6		28.69	29.98		66.6000	4
		18		24.05	24.22	28.74	66.3000	8
	E3	0		32.06	32.58		68.0000	0
		4		26.29	29.56		67.7000	2
		6		26.00	29.98		67.2000	4
		18		21.57	24.22	26.48	66.9000	8
	E4	0		32.47	32.58		69.2000	0
		4		31.53	29.56		67.6000	2
		6		33.93	29.98		66.8000	4
		18		24.75	24.22	30.67	66.5000	8
73NOV. 8SKIN DEPTH= 3.99 , 0.52CM	E1	0	CM	24.40	24.11		75.3000 AT	0CM
EQSM=23.67 ,24.24 %		4		23.50	22.91		75.1000	2
		6		23.03	23.24		74.8000	4
		18		26.24	23.15	24.29	73.7000	8
	E2	0		27.03	24.11		75.3000	0
		4		25.61	22.91		75.1000	2
		6		24.46	23.24		74.6000	4
		18		22.81	23.15	24.98	74.4000	8
	E3	0		22.33	24.11		75.3000	0
		4		21.06	22.91		75.2000	2
		6		22.06	23.24		75.0000	4
		18		19.60	23.15	21.26	74.2000	8
	E4	0		23.87	24.11		75.9000	0
		4		20.96	22.91		75.7000	2
		6		20.95	23.24		75.5000	4
		18		21.45	23.15	21.77	74.5000	8
	F5	0		22.99	24.11		74.5000	0
		4		23.42	22.91		74.5000	2
		6		25.78	23.24		74.3000	4
		18		25.65	23.15	24.46	73.8000	8
74FEB.13SKIN DEPTH=13.30 , 0.98CM	F1	0	CM	11.57	11.72		106.6000 AT	4CM
EQSM=17.50 , 5.40 %		4		20.60	20.35		106.2000	8
		6		20.99	20.64		103.6000	16
		18		22.83	21.98	19.00	102.2000	32
	F2	0		15.50	11.72		106.4000	4
		4		22.98	20.35		106.0000	8
		6		23.41	20.64		103.5000	16
		18		22.55	21.98	21.11	102.1000	32
	E3	0		10.26	11.72		106.6000	4
		4		20.45	20.35		106.2000	8
		6		21.07	20.64		103.5000	16
		18		21.38	21.98	18.37	102.1000	32
	E4	0		10.44	11.72		106.5000	4
		4		20.02	20.35		106.2000	8
		6		21.25	20.64		103.5000	16
		18		22.56	21.98	18.57	102.1000	32
	F5	0		12.97	11.72		106.9000	4
		4		21.93	20.35		106.4000	8
		6		22.93	20.64		103.5000	16
		18		23.58	21.98	20.35	102.1000	32
	F1	0		12.53	11.72		107.3000	4
		4		20.77	20.35		106.6000	8

Continuation of Table A-1.

A Listing of the Entire Soil Moisture and Ground Thermometric Temperature Data of the Experiment.

	6	21.75	20.64		103.6000	16
	18	23.77	21.98	19.70	102.1000	32
F2	0	10.82	11.72		107.4000	4
	4	22.32	20.35		106.8000	8
	6	17.67	20.64		103.9000	16
	18	20.30	21.98	17.78	102.2010	32
F3	0	9.35	11.72		107.2000	4
	4	18.15	20.35		106.7000	8
	6	19.37	20.64		103.7000	16
	18	19.96	21.98	16.71	102.3000	32
F4	0	8.21	11.72		107.1000	4
	4	17.48	20.35		106.6000	8
	6	18.69	20.64		103.6000	16
	18	20.32	21.98	16.18	102.2000	32
F5	0	15.29	11.72		107.0000	4
	4	18.85	20.35		106.5000	8
	6	19.28	20.64		103.8000	16
	18	22.59	21.98	19.00	102.2000	32

ROUGH SURFACE

	LOCATION	DEPTH	SOIL MOIST.%	AVE @ DEPTH	AVE. AT LOCATION	SOIL TEMP	
73JULY23SKIN DEPTH=10.47 , 1.68CM	D1	0 CM	7.34	9.64		95.4000 AT	2CM
FOSM=10.21 , 8.78 %		4	7.97	8.19		94.9000	4
		6	12.83	11.42		0.5450	8
		18	11.86	13.54	10.00	0.5490	16
	D2	0	11.57	9.64		94.3000	2
		4	8.04	8.19		93.1000	4
		6	10.68	11.42		0.5450	8
		18	11.76	13.54	10.51	0.5500	16
	D3	0	10.32	9.64		95.6000	2
		4	10.15	8.19		93.5000	4
		6	10.16	11.42		0.5470	8
		18	14.63	13.54	11.32	0.5510	16
	D4	0	12.41	9.64		93.5000	2
		4	4.31	8.19		93.2000	4
		6	10.01	11.42		0.5470	8
		18	16.03	13.54	10.69	0.5530	16
	D5	0	11.91	9.64		93.1000	2
		4	8.57	8.19		93.7000	4
		6	9.88	11.42		0.5490	8
		18	14.43	13.54	11.20	0.5530	16
	C1	0	9.05	9.64		91.1000	2
		4	8.14	8.19		93.9000	4
		6	12.10	11.42		0.5480	8
		18	14.25	13.54	10.88	0.5520	16
	C2	0	7.70	9.64		91.8000	2
		4	8.20	8.19		93.9000	4
		6	12.53	11.42		0.5480	8
		18	14.81	13.54	10.83	0.5520	16
	C3	0	8.20	9.64		90.6000	2
		4	8.81	8.19		91.2000	4
		6	13.09	11.42		0.5480	8
		18	12.91	13.54	10.75	0.5500	16
	C4	0	8.67	9.64		90.5000	2
		4	8.61	8.19		92.9000	4
		6	11.75	11.42		0.5500	8
		18	17.30	13.54	10.34	0.5510	16
	C5	0	9.11	9.64		91.7000	2
		4	9.13	8.19		93.0000	4

Continuation of Table A-1.

A Listing of the Entire Soil Moisture and Ground Thermometric Temperaure Data of the Experiment.

		6	11.14	11.42		0.5470	8	
		16	12.46	13.54	10.46	0.5520	16	
73JULY26SKIN DEPTH= 4.82 , 0.77CM	D1	0 CM	8.56	15.90		106.5000 AT	2CM	
EOSM=19.40 ,16.38 %		4	18.60	22.66		102.5000	4	
		6	19.46	23.28		99.0000	8	
		18	22.17	23.98	17.20	0.5500	16	
	D2	0	8.26	15.90		105.0000	2	
		4	19.18	22.66		103.0000	4	
		6	19.94	23.28		96.5000	8	
		18	20.65	23.98	17.01	0.5530	16	
	D3	0	9.28	15.90		107.4000	2	
		4	20.11	22.66		100.0000	4	
		6	20.11	23.28		95.5000	8	
		18	21.11	23.98	17.65	0.5500	16	
	D4	0	14.75	15.90		99.5500	2	
		4	22.04	22.66		99.5000	4	
		6	23.33	23.28		95.5000	8	
		18	23.40	23.98	20.88	0.5512	16	
	D5	0	9.29	15.90		107.5000	2	
		4	23.17	22.66		116.0000	4	
		6	25.79	23.28		99.5000	8	
		18	25.88	23.98	21.03	0.5490	16	
	C1	0	28.03	15.90		100.0000	2	
		4	26.29	22.66		98.5000	4	
		6	26.95	23.28		95.0000	8	
		18	28.70	23.98	27.49	0.5520	16	
	C2	0	18.46	15.90		101.5000	2	
		4	22.46	22.66		100.5000	4	
		6	23.13	23.28		96.9000	8	
		18	22.62	23.98	21.72	0.5510	16	
	C3	0	24.27	15.90		99.5000	2	
		4	23.99	22.66		100.0000	4	
		6	23.99	23.28		95.6000	8	
		18	25.06	23.98	24.18	0.5530	16	
	C4	0	20.71	15.90		100.0000	2	
		4	25.35	22.66		99.0000	4	
		6	24.87	23.28		97.0000	8	
		18	23.66	23.98	23.64	0.5520	16	
	C5	0	17.45	15.90		100.0000	2	
		4	25.26	22.66		95.5000	4	
		6	25.79	23.28		94.0000	8	
		18	26.55	23.98	23.76	0.5515	16	
73JULY30SKIN DEPTH= 6.10 , 1.32CM	D1	0 CM	8.35	9.61		83.0000 AT	2CM	
EOSM=15.71 ,10.61 %		4	17.39	18.64		81.5000	4	
		6	20.52	51.00		82.0000	8	
		18	21.70	21.86	16.99	0.5488	16	
	D2	0	6.43	9.61		87.0000	2	
		4	17.55	18.64		82.5000	4	
		6	18.28	51.00		83.0000	8	
		18	19.58	21.86	15.46	0.5485	16	
	D3	0	7.13	9.61		84.5000	2	
		4	18.13	18.64		82.5000	4	
		6	18.14	51.00		82.5000	8	
		18	20.15	21.86	15.89	0.5488	16	
	D4	0	9.28	9.61		82.5000	2	
		4	20.07	18.64		82.5000	4	
		6	20.49	51.00		82.1000	8	
		18	20.86	21.86	17.67	0.5480	16	
	D5	0	7.56	9.61		85.5000	2	
		4	18.91	18.64		82.5000	4	

Continuation of Table A-1.

A Listing of the Entire Soil Moisture and Ground Thermometric Temperature Data of the Experiment.

		6	22.65	51.00		83.2000	A	
		18	23.31	21.86	18.11	0.5470	16	
	C1	0	10.15	9.61		86.5000	2	
		4	20.24	18.64		86.0000	4	
		6	23.75	51.00		87.3000	8	
		18	24.27	21.86	19.60	0.5470	16	
	C2	0	10.19	9.61		87.5000	2	
		4	20.27	18.64		89.0000	4	
		6	20.54	51.00		82.5000	8	
		18	22.26	21.86	18.31	0.5478	16	
	C3	0	10.10	9.61		88.9000	2	
		4	18.75	18.64		85.5000	4	
		6	19.17	51.00		83.5000	8	
		18	20.71	21.86	17.18	0.5478	16	
	C4	0	19.32	9.61		86.7000	2	
		4	17.82	18.64		89.5000	4	
		6	24.05	51.00		83.5000	8	
		18	21.08	21.86	19.32	0.5479	16	
	C5	0	7.54	9.61		87.5000	2	
		4	22.31	18.64		82.5000	4	
		6	22.39	51.00		80.5000	8	
		18	24.68	21.86	19.23	0.5465	16	
73SEPT25SKIN DEPTH= 6.26 , 1.02CM	D1	0 CM	11.52	13.03		79.0000 AT	0CM	
EOSM=15.35 ,12.92 %		4	12.75	16.03		78.3000	2	
		6	18.46	18.59		77.9000	4	
		18	24.48	20.86	16.80	78.8000	8	
	D2	0	12.59	13.03		79.4000	0	
		4	12.39	16.03		78.3000	2	
		6	16.81	18.59		78.0000	4	
		18	21.16	20.86	15.74	78.5000	8	
	D3	0	11.83	13.03		79.9000	0	
		4	13.01	16.03		78.9000	2	
		6	14.90	18.59		78.6000	4	
		18	17.88	20.86	14.42	79.0000	8	
	D4	0	11.94	13.03		80.0000	0	
		4	13.56	16.03		78.6000	2	
		6	14.12	18.59		78.5000	4	
		18	19.48	20.86	14.78	78.8000	8	
	D5	0	13.33	13.03		79.7000	0	
		4	13.09	16.03		78.9000	2	
		6	17.96	18.59		78.7000	4	
		18	19.53	20.86	15.98	78.7000	8	
	C1	0	12.78	13.03		80.7000	0	
		4	21.46	16.03		79.0000	2	
		6	22.59	18.59		78.6000	4	
		18	24.79	20.86	20.28	78.5000	8	
	C2	0	13.29	13.03		80.7000	0	
		4	20.49	16.03		79.9000	2	
		6	20.41	18.59		79.2000	4	
		18	20.31	20.86	18.63	78.9000	8	
	C3	0	18.63	13.03		81.7000	0	
		4	19.75	16.03		79.9000	2	
		6	20.58	18.59		79.2000	4	
		18	19.84	20.86	19.70	78.8000	8	
	C4	0	12.86	13.03		79.9000	0	
		4	18.73	16.03		79.3000	2	
		6	20.47	18.59		78.8000	4	
		18	19.97	20.86	18.01	78.7000	8	
	C5	0	11.51	13.03		82.2000	0	
		4	15.08	16.03		81.5000	2	

Continuation of Table A-1.

A Listing of the Entire Soil Moisture and Ground Thermometric Temperature Data of the Experiment.

		6	19.55	18.59		79.5000		4
		18	21.62	20.86	16.94	79.5000		8
73OCT.30SKIN DEPTH= 3.60 , 0.46CM	D1	0 CM	29.27	27.93		68.4000	AT	0CM
FOSM=27.24 ,28.00 %		4	29.46	26.29		68.1000		2
		6	31.46	26.60		67.5000		4
		18	22.02	22.57	28.05	64.2000		8
	D2	0	29.22	27.93		67.3000		0
		4	27.59	26.29		66.5000		2
		6	28.85	26.60		65.4000		4
		18	24.08	22.57	27.44	64.1000		8
	D3	0	26.93	27.93		67.9000		0
		4	25.43	26.29		66.8000		2
		6	24.14	26.60		66.2000		4
		18	22.03	22.57	24.63	64.7000		8
	D4	0	24.61	27.93		67.8000		0
		4	23.98	26.29		66.8000		2
		6	24.53	26.60		65.7000		4
		18	18.00	22.57	22.94	64.9000		8
	D5	0	64.00	27.93		69.3000		0
		4	30.64	26.29		67.9000		2
		6	30.72	26.60		67.2000		4
		18	30.54	22.57	28.24	65.3000		8
	C1	0	21.08	27.93		68.2000		0
		4	29.75	26.29		66.8000		2
		6	27.66	26.60		66.[illegible]00		4
		18	28.15	22.57	27.36	[illegible]0		8
	C2	0	23.90	27.93		00		0
		4	28.69	26.29		000		2
		6	24.39	26.60		[illegible]000		4
		18	25.38	22.57	25.47	[illegible]000		8
	C3	0	23.61	27.93		67.8000		0
		4	23.45	26.29		66.8000		2
		6	22.69	26.60		66.2000		4
		18	27.19	22.57	21.83	65.5000		8
	C4	0	18.99	27.93		68.5000		0
		4	25.64	26.29		68.1000		2
		6	23.12	26.60		67.4000		4
		18	23.29	22.57	23.99	66.0000		8
	C5	0	23.92	27.93		70.1000		0
		4	31.28	26.29		68.9000		2
		6	27.82	26.60		67.4000		4
		18	27.44	22.57	28.48	66.4000		8
73NOV. 9SKIN DEPTH= 4.78 , 0.67CM	D1	0 CM	24.22	18.21		77.4000	AT	0CM
FOSM=19.54 ,18.38 %		4	24.98	20.70		77.0000		2
		6	26.10	22.21		76.4000		4
		18	24.91	22.35	25.05	75.4000		8
	D2	0	16.81	18.21		80.1000		0
		4	21.08	20.70		79.1000		2
		6	21.32	22.21		76.9000		4
		18	20.50	22.35	19.93	76.4000		8
	D3	0	20.46	18.21		82.9000		0
		4	19.81	20.70		80.5000		2
		6	20.53	22.21		79.1000		4
		18	22.42	22.35	20.81	76.8000		8
	D4	0	19.69	18.21		80.5000		0
		4	20.71	20.70		80.1000		2
		6	21.08	22.21		78.5000		4
		18	23.28	22.35	21.19	77.0000		8
	D5	0	22.15	18.21		79.2000		0
		4	22.17	20.70		77.8000		2

Continuation of Table A-1.

A Listing of the Entire Soil Moisture and Ground Thermometric Temperature Data of the Experiment.

		6	22.89	22.21		76.7000	4	
		18	22.43	22.35	22.71	74.8000	8	
	C1	0	*****	18.21		78.7000	0	
		4	*****	20.70		77.8000	2	
		6	*****	22.21		77.3000	4	
		18	*****	22.35	*****	76.8000	8	
	C2	0	*****	18.21		77.8000	0	
		4	*****	20.70		77.3000	2	
		6	23.53	22.21		76.8000	4	
		18	*****	22.35	*****	75.2000	8	
	C3	0	12.40	18.21		79.9000	0	
		4	16.41	20.70		79.3000	2	
		6	*****	22.21		78.6000	4	
		18	20.49	22.35	16.50	77.0000	8	
	C4	0	12.61	18.21		77.2000	0	
		4	18.63	20.70		76.8000	2	
		6	20.33	22.21		76.2000	4	
		18	20.13	22.35	17.92	75.0000	8	
	C5	0	16.37	18.21		74.9000	0	
		4	21.96	20.70		74.8000	2	
		6	21.92	22.21		74.6000	4	
		18	24.31	22.35	21.11	71.9000	8	
74FEB.13SK IN DEPTH=10.80 , 1.30CM	D1	0 CM	14.97	10.47		106.5000 AT	4C	
FOSM=15.80 , 6.05 F		4	17.99	18.05		106.5000	8	
		6	17.64	22.38		104.6000	16	
		18	20.93	20.67	17.88	102.5000	32	
	D2	0	8.03	10.47		106.6000	4	
		4	16.39	18.05		106.3000	8	
		6	17.47	22.38		103.9000	16	
		18	19.09	20.67	15.17	102.3000	32	
	D3	0	7.55	10.47		106.7000	4	
		4	17.74	18.05		106.7000	8	
		6	18.38	22.38		103.7000	16	
		18	18.83	20.67	15.63	102.2000	32	
	D4	0	8.29	10.47		106.6000	4	
		4	18.13	18.05		106.3000	8	
		6	20.53	22.38		103.6000	16	
		18	20.70	20.67	16.91	102.2000	32	
	D5	0	11.26	10.47		106.6000	4	
		4	19.03	18.05		106.3000	8	
		6	49.77	22.38		103.5000	16	
		18	23.55	20.67	25.90	102.2000	32	
	C1	0	11.23	10.47		106.6000	4	
		4	16.07	18.05		106.3000	8	
		6	19.99	22.38		103.8000	16	
		18	21.11	20.67	17.07	102.2000	32	
	C2	0	10.44	10.47		106.6000	4	
		4	17.77	18.05		106.5000	8	
		6	19.90	22.38		103.7000	16	
		18	18.74	20.67	16.66	102.1000	32	
	C3	0	8.70	10.47		106.2000	4	
		4	18.37	18.05		106.0000	8	
		6	18.94	22.38		103.5000	16	
		18	19.74	20.67	16.43	102.0000	32	
	C4	0	12.77	10.47		106.3000	4	
		4	17.72	18.05		106.1000	8	
		6	18.91	22.38		103.6000	16	
		18	20.25	20.67	17.29	102.3000	32	
	C5	0	11.46	10.47		106.2000	4	
		4	22.05	18.05		105.9000	8	
		6	22.60	22.38		103.3000	16	
		18	23.79	20.67	19.98	101.9000	32	

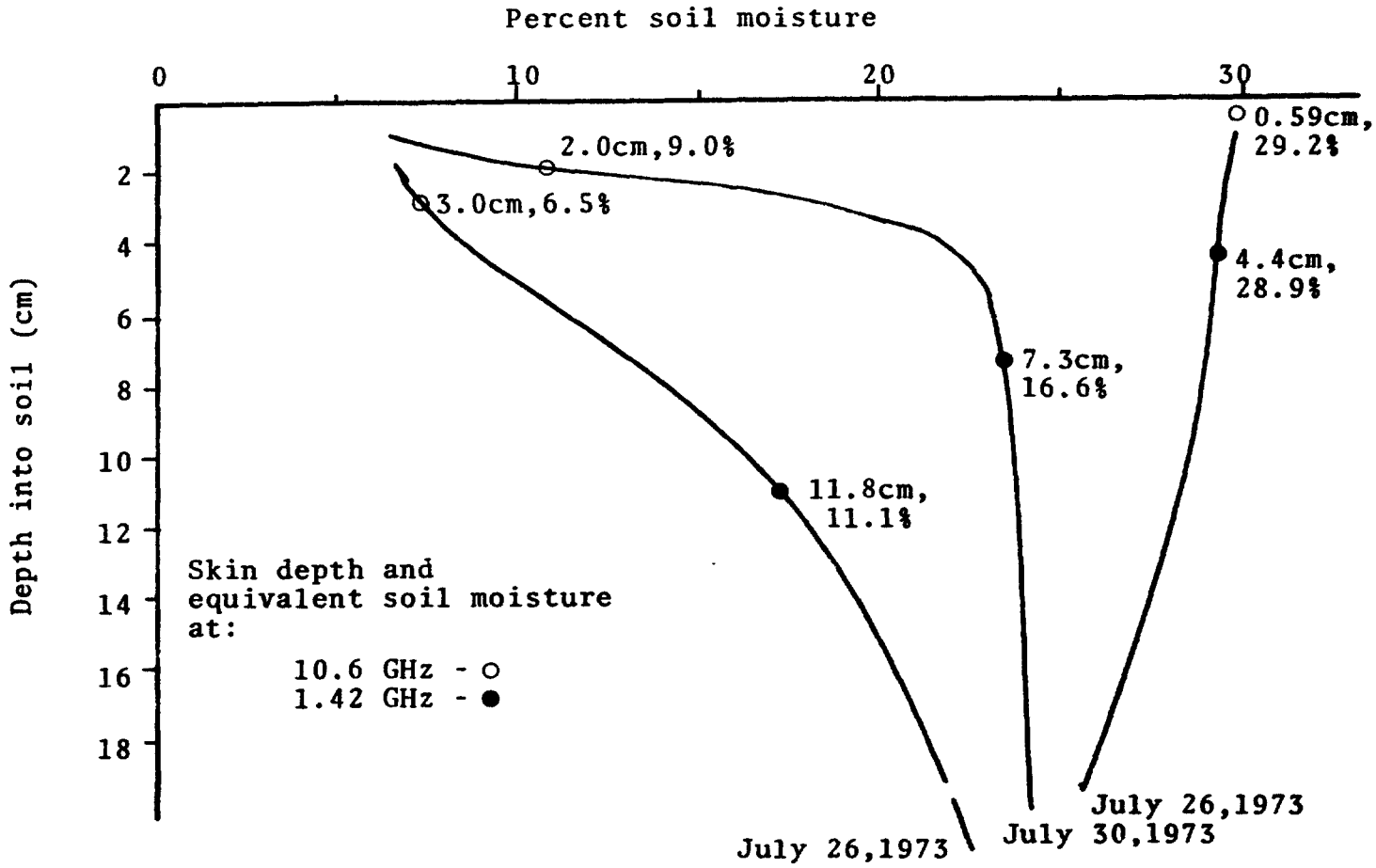

Figure A-1. Soil Moisture Profiles and the Corresponding Skin Depths and "Equivalent Soil Moisture Contents" of the Bare Smooth Surface.

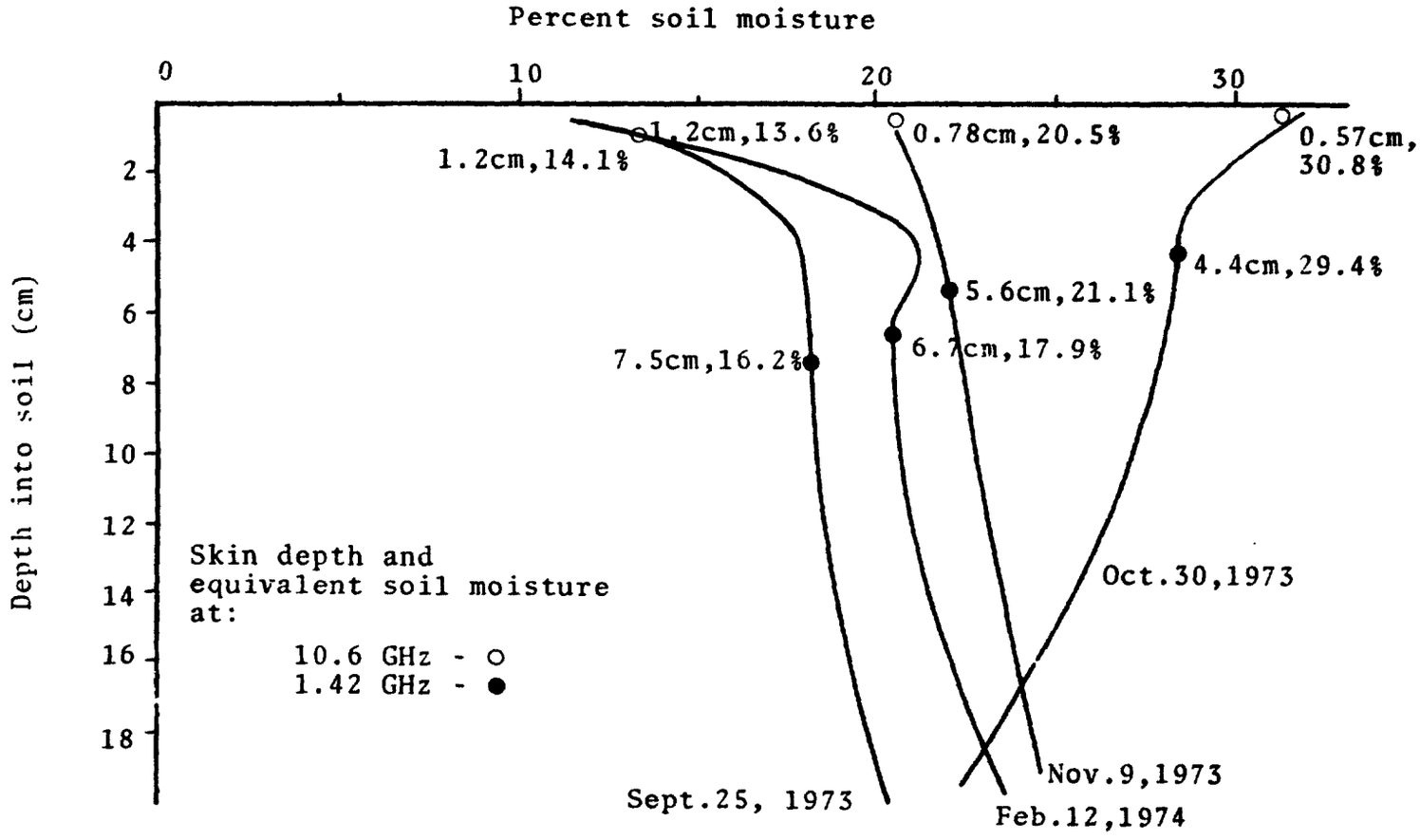

Figure A-2. Soil Moisture Profiles and the Corresponding Skin Depths and "Equivalent Soil Moisture Contents" of the Vegetated Smooth Surface.

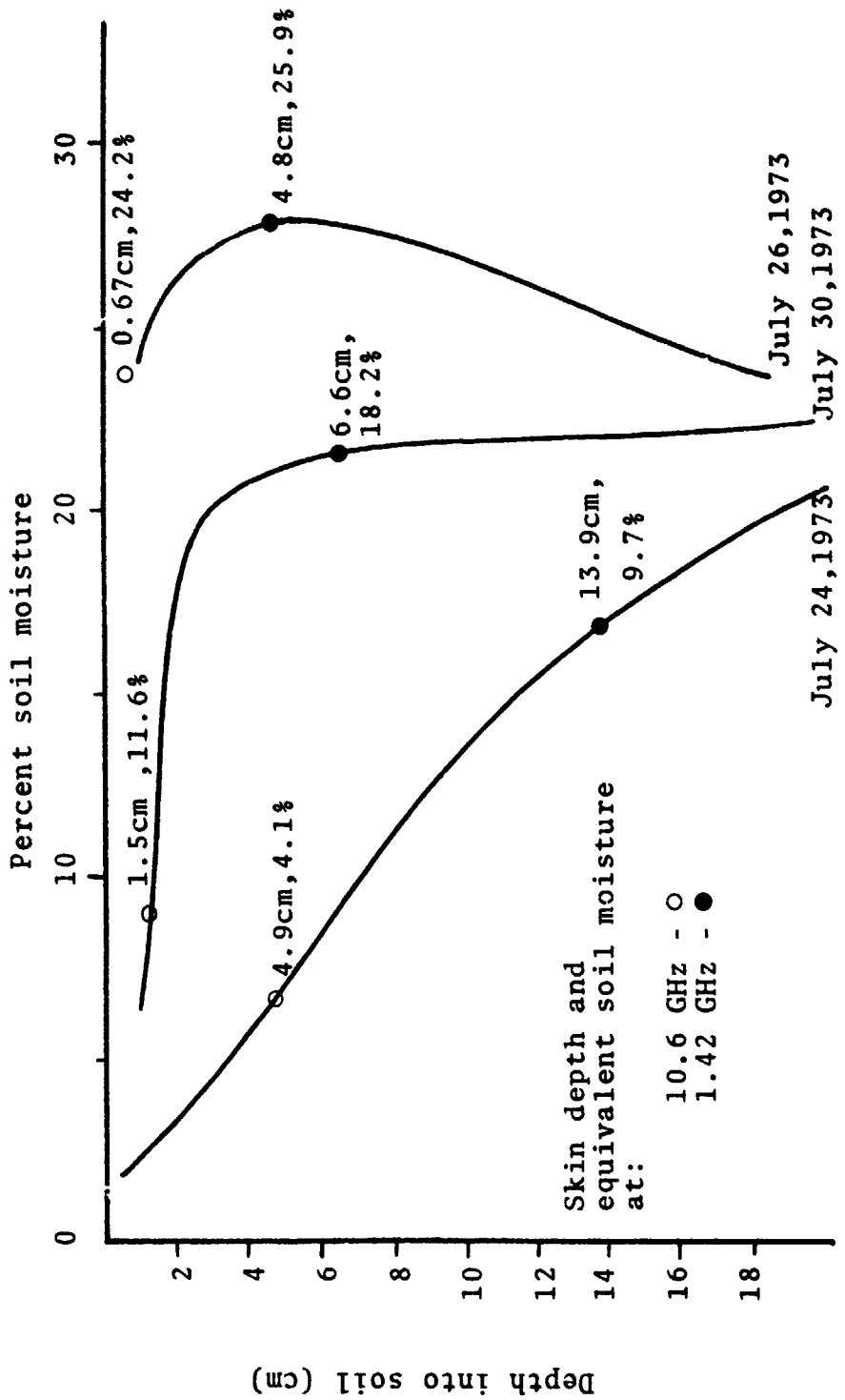

Figure A-3. Soil Moisture Profiles and the Corresponding Skin Depths and "Equivalent Soil Moisture Contents" of the Bare Medium Rough Surface.

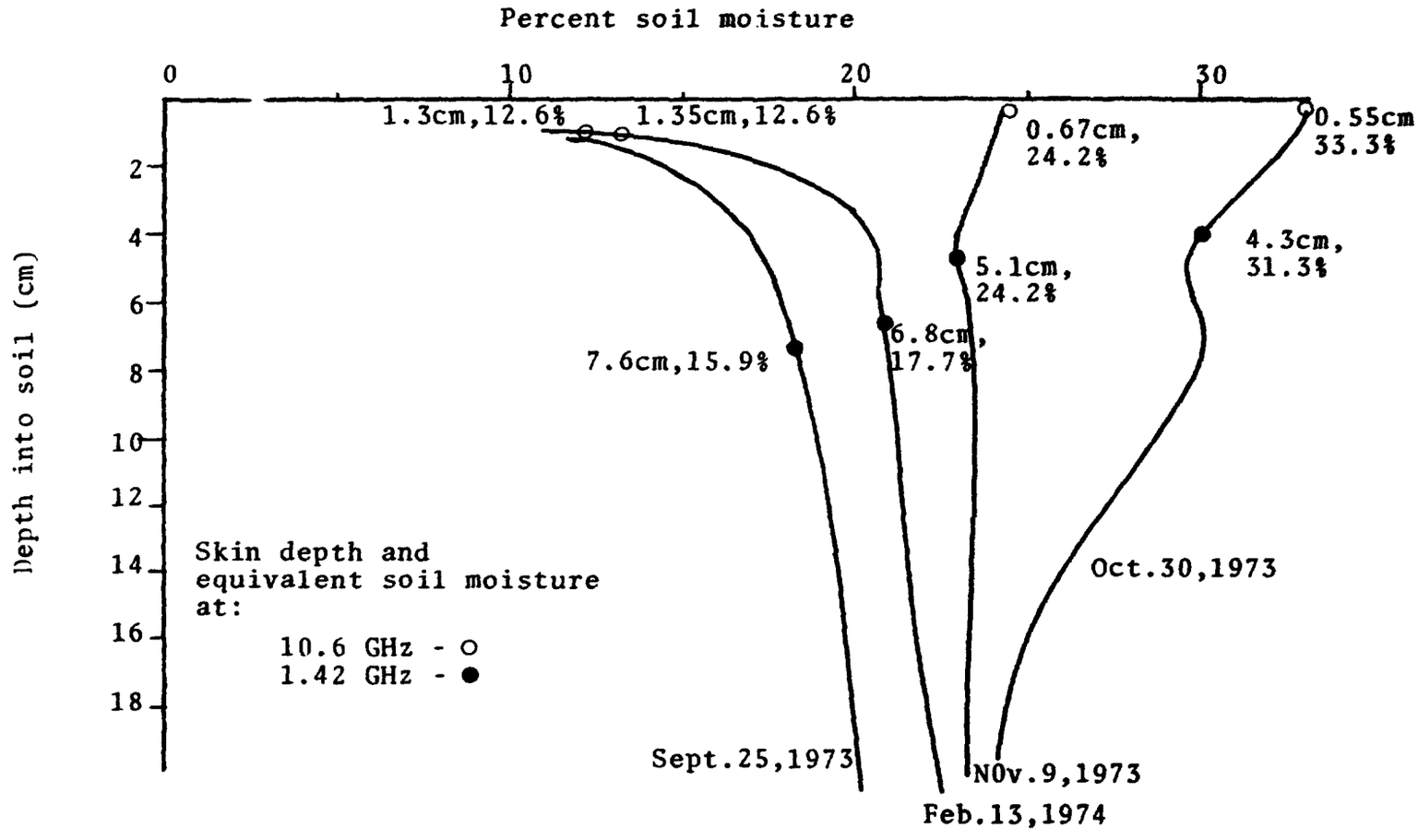

Figure A-4. Soil Moisture Profiles and the Corresponding Skin Depths and "Equivalent Soil Moisture Contents" of the Vegetated Medium Rough Surface.

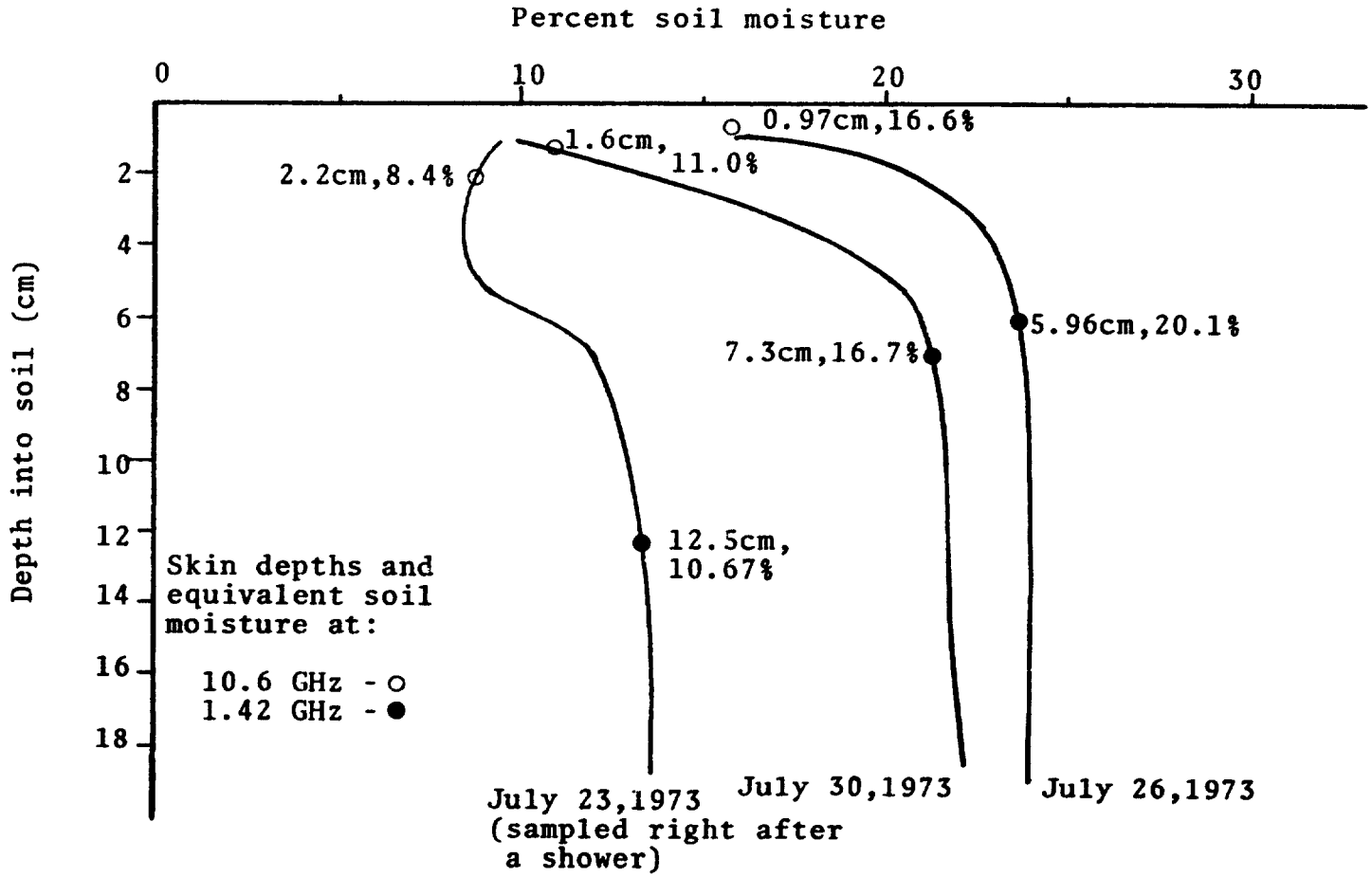

Figure A-5. Soil Moisture Profiles and the Corresponding Skin Depths and "Equivalent Soil Moisture Contents" of the Bare Rough Surface.

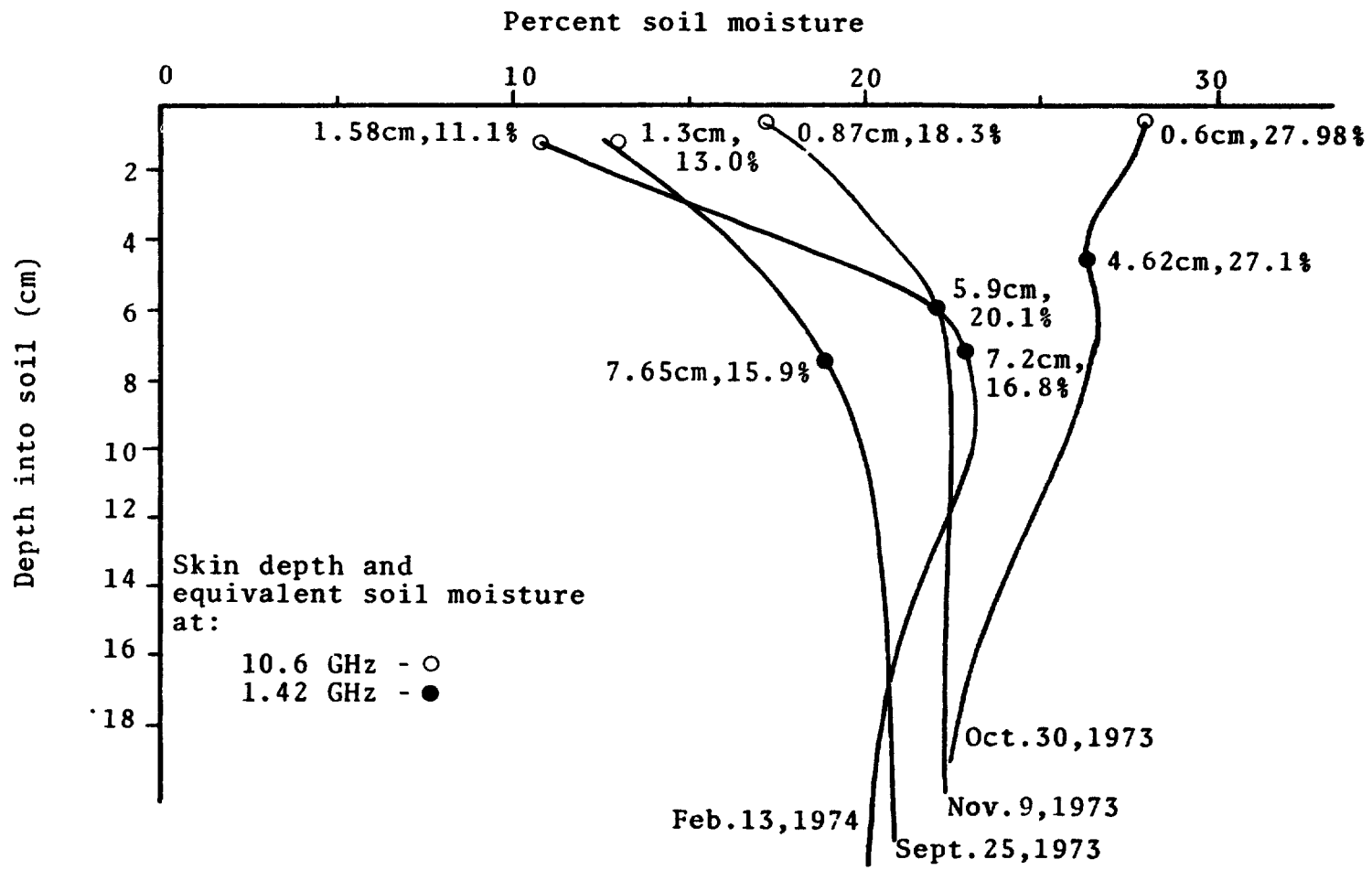

Figure A-6. Soil Moisture Profiles and the Corresponding Skin Depths and "Equivalent Soil Moisture Contents" of the Vegetated Rough Surface.

Table A-2. A Listing of the soil Moisture Data Within the Antenna Footprints at Various Observation Angles.

SMOOTH SURFACE

DATE	OBSERVAING ANGLE	0-18 CM AVERAGE	0-2 CM AVERAGE
7/24/73	0	12.0	7.1
	10	12.1	7.0
	20	12.0	7.0
	30	11.7	6.7
	40	11.3	6.6
	50	11.8	6.2
	55	11.9	5.9
7/26/73	0	28.2	29.3
	10	28.0	29.0
	20	27.8	28.7
	30	27.5	28.2
	40	27.2	28.3
	50	27.0	28.6
	55	27.3	28.8
7/30/73	0	18.0	6.5
	10	18.2	6.8
	20	18.3	7.1
	30	18.3	7.5
	40	18.0	7.5
	50	18.1	7.5
	55	18.6	7.2
9/25/73	0	18.5	14.0
	10	18.7	14.8
	20	19.0	15.1
	30	19.2	15.0
	40	20.0	16.0
	50	19.5	16.3
	55	18.0	15.0
10/30/73	0	27.1	31.2
	10	27.1	31.2
	20	27.2	31.3
	30	27.0	31.0
	40	25.5	30.0
	50	24.8	29.3
	55	25.2	30.0
11/09/73	0	22.0	22.0
	10	21.7	20.6
	20	21.4	19.8
	30	20.8	18.8
	40	20.5	18.2
	50	21.5	20.5
	55	22.0	21.7
2/12/74	0		11.4
	10		12.1
	20		13.7
	30		15.?
	40		13.9
	50		11.9
	55		12.7

Continuation of Table A-2.

A Listing of the Soil Moisture Data Within the Antenna Footprints at Various Observation Angles.

MEDIUN ROUGH SURFACE

DATE	OBSERVAING ANGLE	0-18 CM AVERAGE	0-2 CM AVERAGE
7/24/73	0	8.5	2.3
	10	8.4	2.3
	20	8.3	2.3
	30	8.1	2.3
	40	8.1	2.3
	50	8.5	2.3
	55	8.7	2.3
7/26/73	0	25.0	24.0
	10	25.2	24.9
	20	25.5	25.2
	30	25.5	25.6
	40	26.3	27.0
	50	25.5	26.0
	55	24.5	22.0
7/30/73	0	18.2	7.0
	10	18.0	7.2
	20	17.5	7.6
	30	16.9	7.0
	40	16.5	5.5
	50	16.8	4.9
	55	17.2	5.0
9/25/73	0	19.4	15.2
	10	20.0	15.1
	20	20.5	15.0
	30	20.8	14.8
	40	20.5	14.4
	50	18.5	12.8
	55	16.0	11.5
10/30/73	0	29.0	32.0
	10	29.2	32.2
	20	29.0	32.5
	30	28.5	32.7
	40	27.5	32.4
	50	25.9	31.5
	55	26.2	31.0
11/09/73	0	24.0	23.5
	10	24.2	23.5
	20	24.2	23.4
	30	23.5	23.0
	40	22.1	21.8
	50	21.0	20.2
	55	21.1	20.8
2/13/74	0		12.0
	10		12.3
	20		12.7
	30		13.0
	40		11.9
	50		10.1
	55		9.7

Continuation of Table A-2.

A Listing of the Soil Moisture Data Within the Antenna Footprints at Various Observation Angles.

ROUGH SURFACE

DATE	OBSERVAING ANGLE	0-18 CM AVERAGE	0-2 CM AVERAGE
7/23/73	0	10.7	8.5
	10	10.8	8.6
	20	11.0	9.0
	30	11.0	9.4
	40	10.9	9.4
	50	10.8	9.4
	55	10.7	9.4
7/26/73	0	22.9	15.0
	10	21.5	14.0
	20	20.0	13.0
	30	19.5	12.8
	40	20.0	14.0
	50	21.5	16.0
	55	22.0	17.0
7/30/73	0	18.3	9.1
	10	18.0	9.0
	20	17.5	8.9
	30	16.7	8.7
	40	16.2	8.5
	50	16.6	8.9
	55	17.5	9.3
9/25/73	0	18.5	12.0
	10	18.0	12.5
	20	17.2	13.0
	30	16.8	13.1
	40	16.4	13.5
	50	16.3	13.8
	55	16.3	13.8
10/30/73	0	27.8	24.8
	10	27.5	25.5
	20	27.2	26.0
	30	26.3	26.2
	40	25.0	26.3
	50	22.8	25.2
	55	22.0	24.0
11/09/73	0	22.0	25.0
	10	20.0	23.0
	20	19.0	21.0
	30	18.2	20.0
	40	17.8	21.0
	50	18.0	19.0
	55	19.0	18.0
2/13/74	0		13.1
	10		12.3
	20		10.8
	30		9.3
	40		8.8
	50		8.2
	55		9.1

Table A-3. A Listing of the Entire Radiometric Temperature Data.

SMOOTH SURFACE

DATE	OBSERVATION ANGLE,(°)	1.4153GHZ HORIZONTAL	1.4153GHZ VERTICAL	10.6GHZ HORIZONTAL	10.6GHZ VERTICAL
7/24/73	0	272.6	271.6	279.0	274.2
	10	270.9	274.8	280.5	279.7
	20	267.6	277.7	270.8	280.2
	30	261.4	284.5	273.1	279.0
	40		285.9	266.0	279.8
	50	241.7	293.1	263.7	279.9
	55	223.6	296.9	251.5	280.8
7/26/73	0		198.2		237.6
	20	188.5	210.1	236.0	240.9
	30	186.5	221.2	226.2	251.6
	40	178.4	229.4	230.8	249.9
	50	161.5	248.9	211.2	242.9
7/30/73	0	276.2		276.3	
	20	266.9	278.1	262.8	273.0
	30	261.4	280.6	259.2	274.0
	40	251.3	286.3	254.4	276.8
	50	240.7	291.8	246.4	281.9
9/25/73	0	253.8	249.2	266.3	266.4
	20	245.0	246.4	263.7	264.5
	30	241.0	253.8	259.4	263.8
	40	235.3	259.6	257.0	264.4
	50	224.1	265.8	250.3	261.8
	180	12.4		17.8	
10/30/73	0		211.0		260.1
	20	204.9	205.7	266.9	259.9
	30	191.4	215.5	268.3	259.6
	40	186.3	226.0	265.7	257.2
	50	188.0	244.7	263.0	253.2
11/09/73	0	226.4	226.1	258.0	258.9
	20	215.1	222.9	253.8	253.7
	30	205.7	230.9	251.4	254.6
	40	1913.1	241.0	248.6	255.3
	50	192.1	250.0	249.8	256.4
	180		11.1		18.1
2/12/74	0	231.0	231.0	252.0	253.0
	20	240.0	243.0	251.0	259.0
	30	216.0	250.0	245.0	259.0
	40	207.0	258.0	240.0	258.0
	50	209.0	265.0	238.0	259.0

Continuation of Table A-3.

A Listing of the Entire Radiometric Temperature Data.

MEDIUM ROUGH SURFACE

DATE	OBSERVATION ANGLE,(°)	1.4153GHZ HORIZONTAL	1.4153GHZ VERTICAL	10.6GHZ HORIZONTAL	10.6GHZ VERTICAL
7/24/73	0		297.8		288.7
	10	296.8	296.9	282.3	
	20	295.5	299.6	281.4	290.2
	30	294.4	300.5	281.6	285.0
	40	290.1	299.6	278.1	285.5
	50	279.0	300.3	275.1	281.8
	180		8.5		3.4
7/26/73	0		251.4		258.8
	20	249.5	251.2		254.0
	30	245.8	260.3	251.8	254.7
	40	240.8	264.4	248.9	256.7
	50	221.4	273.0	240.3	255.8
	180		7.4		10.5
7/30/74	0		270.0		273.7
	20	279.1	282.5	273.2	275.0
	30	276.9	288.5	273.4	277.8
	40	271.2	290.2	265.3	279.4
	50	262.0	293.0	266.0	273.6
	180	8.6		13.2	
9/25/73	0	249.7	239.2	263.8	260.2
	20	239.4	239.9	260.1	257.8
	30	233.9	243.6	255.3	251.9
	40	221.3	248.4	248.5	250.7
	50	210.1	258.6	245.6	252.0
	180		12.3		10.3
10/30/73	0	200.0	197.6	263.7	264.3
	20	200.8	208.0	265.5	261.9
	30	196.7	213.9	270.5	264.8
	40	189.0	227.4	267.5	263.4
	50	187.6	239.6	265.4	262.0
11/08/73	0	228.5	225.5	256.3	263.9
	20	219.7	233.0	265.9	267.2
	30	210.8	239.9	258.8	259.4
	40	204.0	249.8	255.4	262.0
	50	194.6	258.4	255.8	260.6
2/13/74	0	237.0	236.0	257.0	255.0
	20	232.0	240.0	250.0	258.0
	30	229.0	247.0	249.0	261.0
	40	212.0	258.0	244.0	264.0
	50	207.0	267.0	245.0	262.0

Continuation of Table A-3.

A Listing of the Entire Radiometric Temperature Data.

ROUGH SURFACE

DATE	OBSERVATION ANGLE,(°)	1.4153GHZ HORIZONTAL	1.4153GHZ VERTICAL	10.6GHZ HORIZONTAL	10.6GHZ VERTICAL
7/23/73	0	281.6	276.9	274.6	276.4
	11.4	280.6	278.8	268.3	271.8
	22.6	279.2	281.1	268.8	276.4
	33.4	274.3	281.0	264.5	269.3
	43.8	270.8	281.1	261.1	266.7
	53.7	260.8	280.4	258.7	267.7
	180		4.9		14.2
7/26/73	0		267.6		268.9
	20	274.7	274.9	269.6	273.5
	30	269.3	278.4	263.2	267.0
	40	267.3	278.9	264.0	272.7
	50	254.3	278.0	263.5	270.3
7/30/73	0		273.6		260.2
	20	276.3	274.9	262.2	264.7
	30	274.1	278.2	260.1	267.0
	40	272.9	279.8	262.2	266.3
	50	261.3	280.9	258.9	269.9
9/25/73	0	251.2	243.6	266.6	265.0
	20	243.2	243.9	256.8	261.3
	30	237.2	244.9	252.1	255.8
	40	233.2	250.7	252.1	257.3
	50	228.7	257.8	249.5	252.5
10/30/73	0	218.7	220.6	255.9	258.4
	20	224.3	221.1	262.8	258.0
	30	217.4	226.0	259.0	257.6
	40	213.0	233.1	253.0	256.2
	50	209.5	244.1	244.5	252.7
	180		11.1		17.3
11/08/73	0	247.8	240.0	263.2	263.6
	20	238.7	241.0	248.0	262.0
	30	231.6	243.5	242.7	258.8
	40	227 7	255.5	248.5	255.3
	50	228.1	267.2	255.6	258.5
	180	10.5		8.7	
2/13/74	0	251.0	248.0	260.0	261.0
	20	243.0	248.0	263.0	253.0
	30	238.0	250.0	255.0	260.0
	40	228.0	251.0	249.0	257.0
	50	227.0	258.0	243.0	257.0

APPENDIX B

A TECHNIQUE TO HANDLE CLAY FOR DIELECTRIC CONSTANT MEASUREMENTS

The soil for this study was clay. Clay is a very cohesive substance, especially when it is wet. Wet clay is quite unmanageable for a task like placing a definite amount into a waveguide for the dielectric constant measurements. After some studies of the problem, a technique was found to handle wet clay very satisfactorily. This technique has three major features. First, it enables the operator to easily handle and place wet clay into the waveguide without contaminating the waveguide walls with clay. Secondly, it provides two flat smooth soil boundary surfaces to reduce the possible effect of reflection. Thirdly, it provides an easy and accurate determination of the soil sample length. A picture of the tools used for this technique is shown in Figure B-1. Five aluminum plates with a space cut in the middle were used. The five aluminum plates were of different thicknesses and were marked as shown. Using various thickness metal plates would be apparent in the following discussion.

There are basically four steps for this technique; they are shown in Figures B2a, B2b, B3a, and B3b. The

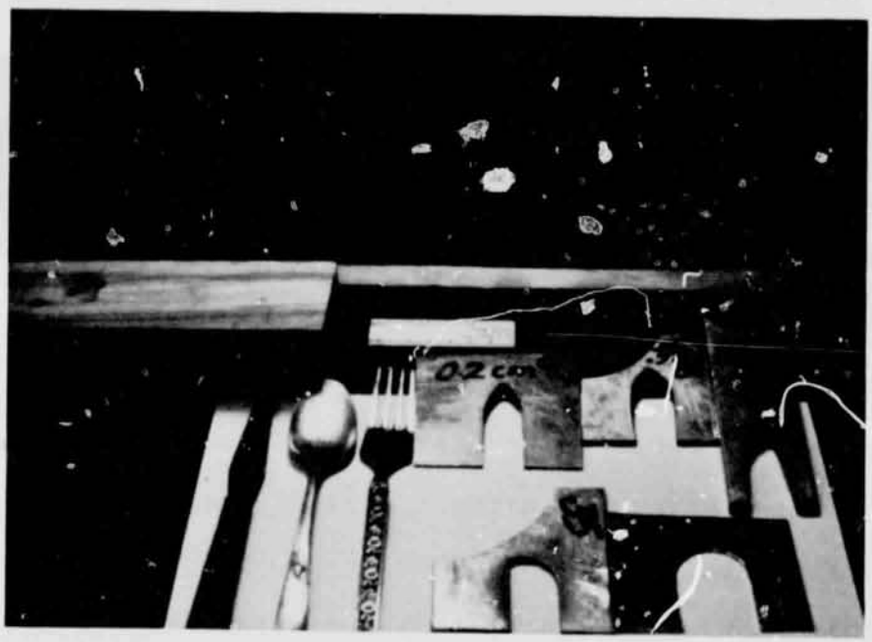

Figure B-1. The Tools of the Special Technique for Handling Clay for Dielectric Constant Measurements.

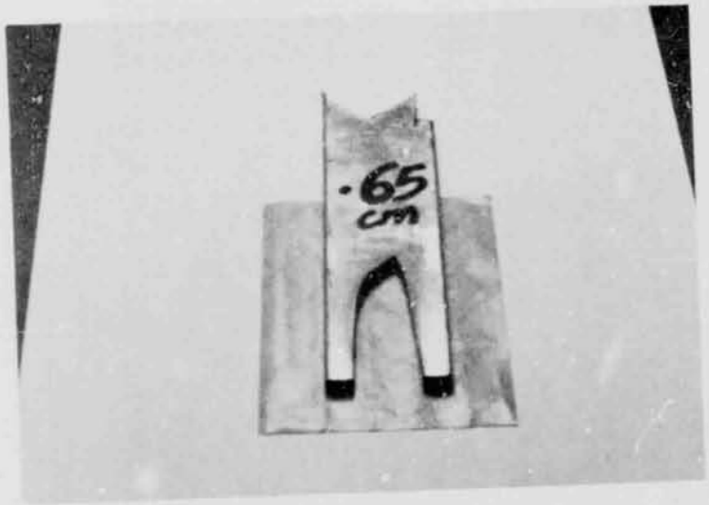

Figure B-2a. Step 1.

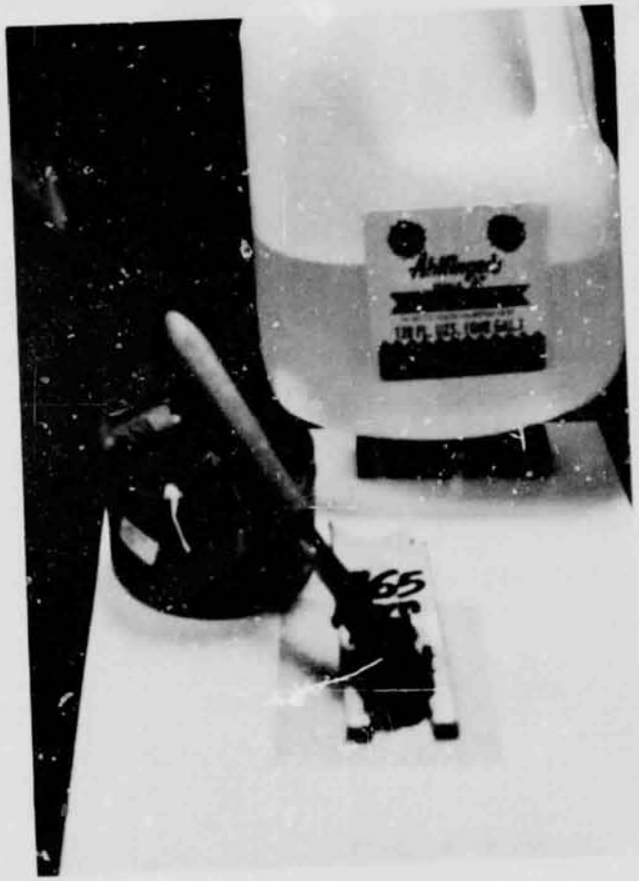

Figure B-2b. Step 2.

Figure B-3a. Step 3.

Figure B-3b. Step 4.

first step is to place the aluminum plate on a piece of paper. The second step as shown is to fill the space in the aluminum plate with clay. The third step is to compress the clay to the degree that resembles natural wet clay, and then the extra clay is leveled off with a spatula. The surface is then smoothened as shown. Then the waveguide is inserted into the clay column vertically. The fourth step, is to peal the paper away; the open surface is then further smoothened with the spatula. At the end of step four, a chunk of clay of known depth (in this case as illustrated, the clay sample would be 0.6 cm long) with two flat smooth surfaces would be placed inside the waveguide. The soil sample is then ready for dielectric constant measurements.

APPENDIX C

SKIN DEPTH AND THE "EQUIVALENT SOIL MOISTURE CONTENT"

In remote detection of soil moisture by passive microwave sensors, a knowledge of the soil skin depth and the "equivalent soil moisture content" corresponding to that skin depth is of assistance in data analysis. The skin depth provides an indication of the depth of radiation that contributes significantly to the apparent temperature measured by the sensor. The "equivalent soil moisture content" is defined as that soil moisture content that would, if constant with soil depth, produce the same skin depth as the actual soil moisture profile of the soil.

In a medium which has conductivity, the wave is attenuated by a factor $e^{-\alpha z}$ as it progresses:

$$E(z) = E_0 e^{-\alpha z} \qquad \text{(A-1)}$$

where α = attenuation constant.

The skin depth, or depth of penetration, of a medium is defined as the distance at which the electric field is attenuated by a factor of 1/e. It is apparent from equation (A-1) that skin depth is that distance which

makes αz equal to one. In terms of the electrical properties of the medium, the skin depth is

$$\delta = \frac{1}{\alpha} = \left[\omega\sqrt{\frac{\mu\varepsilon}{2}\left(\sqrt{1+\left(\frac{\sigma}{\varepsilon\omega}\right)^2}-1\right)}\right]^{-1} \qquad \text{(A-2)}$$

where ω = radian frequency

μ = magnetic permeability

ε = permittivity

σ = conductivity

From (A-2), it can be seen that the skin depth of soil is a function of frequency and the soil's permittivity. The permittivity of the soil is a function of soil moisture content (Figure IV-11). From (Figure IV-11), it should be noted that a direct calculation of skin depth using equation (A-2) is valid only if the soil has constant moisture content and essentially constant electrical properties. In reality, soil moisture usually varies as a function of depth into the soil. To obtain the skin depth for such an electrically inhomogeneous medium, special considerations and procedures are required. This is the problem examined for this study.

In dealing with the situation that the soil moisture varies as a function of depth into the soil, one is faced with the problem of continual variation of

electrical properties of soil as a function of penetration into the soil. Recall from (A-1) that skin depth is that distance which makes the product αz equal to one, therefore, the task of finding the skin depth of soil with any soil moisture profile is that of carrying out the following integration.

$$\int_0^{z=\text{SKIN DEPTH}} \alpha(z)\,dz = 1 \qquad \text{(A-3)}$$

A good approximation to the above integral is

$$\sum_{k=1}^{K} \alpha_k(z)\Delta z_k = 1 \qquad \text{(A-4)}$$

for very small increments of z, Δz's, up to that point where the summation of the product $\alpha_k(z)\Delta_k$ is to equal to one.

To facilitate the evaluation of (A-4) to obtain the skin depth, a computer program which employs the sub-routine "Polynomial Regression" (PLRG) was written [50]. This computer program calculates the skin depth and the "equivalent soil moisture content" as a function of soil

moisture profile of any soil for which the relationship between permittivity and soil moisture is known.

In this program, there are basically four steps in obtaining a value of skin depth. The first step is to obtain a fixed relationship between soil moisture and the corresponding attenuation for the soil type of interest. It is known that attenuation is related to soil moisture through the permittivity by equation [35]:

$$\alpha = \omega \sqrt{\frac{\mu \varepsilon'}{2} \left(\sqrt{1 + \left(\frac{\varepsilon_R''}{\varepsilon_R'} \right)^2} - 1 \right)} \qquad \text{(A-5)}$$

where ε_r' = real part of dielectric constant (permittivity)

ε_r'' = imaginary part of dielectric constant

$\varepsilon'' = \varepsilon_r'' \times \varepsilon_o = \varepsilon_r'' \times 8.854 \times 10^{-12}$

μ = permeability (normally equal to the permeability of free space)

A polynomial expression describing the relationship between attenuation and soil moisture is generated by means of the PLRG subroutine, this equation will be referenced as equation 1. With the functional relationship between attenuation and soil moisture known for a particular soil type, the skin depth for any soil moisture profile can be obtained with three additional steps.

The second step is to obtain an equation for

attenuation as a function of depth into the soil. This equation is obtained by first using equation 1 to calculate attenuation as a function of depth for the particular soil moisture profile of concern. Knowing these values, the PLRG program can be used to fit a polynomial equation to these points providing a functional relationship attenuation and depth for that particular soil moisture profile. This equation will be referred to as equation 2.

In the third step, equation 2 is then used to generate a table of attenuation versus depths for an arbitrarily small increment of depth.

The final and fourth step is to search the table of attenuation versus incremental depths for the value of depth that makes the summation of the product $\alpha_k(z)\Delta z_k$ equal to one. This depth is the skin depth of the soil for the particular soil moisture profile given.

Equivalent Soil Moisture

The procedures to determine the "equivalent soil moisture" are as follows. First, the depth which corresponds to the point where the summation of the product $\alpha(z)\Delta z_k$ is exactly one was determined. This skin depth is then inverted to obtain the corresponding attenuation (attenuation = 1/skin depth). This attenuation is compared to a table of attenuation versus soil moisture obtained

using equation 1. When an attenuation is found that is equal to the inverse of the skin depth, then the "equivalent soil moisture content" has been found.

Skin depth and "equivalent soil moisture content" were calculated at both L-and X-band for all the soil moisture profiles of this experiment. The results are indicated on Figures A-1 through A-6.